History of Antibiotic Adaptation Influences Evolutionary Dynamics During Subsequent Treatment in *Pseudomonas aeruginosa*

A Dissertation

presented to the faculty of the School of Engineering and Applied Science
in partial fulfillment of the requirements for the degree of

Doctor of Philosophy

by Phillip Yen

May 2017

Department of Biomedical Engineering
University of Virginia

APPROVAL SHEET

This Dissertation
is submitted in partial fulfillment of the requirements
for the degree of
Doctor of Philosophy

Author Signature: 

This Dissertation has been read and approved by the examining committee:

Advisor: Jason Papin, PhD

Committee Member: Shayn Peirce-Cottler, PhD

Committee Member: Jeff Saucerman, PhD

Committee Member: Erik Hewlett, MD

Committee Member: Peter Kasson, MD, PhD

Committee Member: _____

Accepted for the School of Engineering and Applied Science:

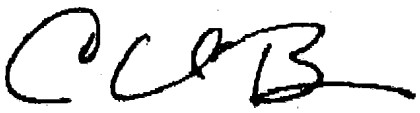

Craig H. Benson, School of Engineering and Applied Science

May 2017

Abstract

Antibiotic resistance is an increasingly serious global health problem that threatens the effective prevention and treatment of infections caused by bacterial pathogens. It is a natural phenomenon whereby bacteria are able to withstand the effects of the drugs that are meant to kill them, and these surviving bacterial populations are then able to grow and potentially disseminate the resistance phenotype around the globe. Some bacteria are able to resist multiple antibiotics of multiple classes, resulting in the threat of multidrug resistance. While there has been renewed effort in discovering new antibiotic compounds to combat these resistant bacterial pathogens, an equally important endeavor is studying how bacteria evolve to become resistant to the antibiotics that are currently available and commonly used. Having a clearer fundamental understanding of the adaptation process will allow for the development of new stewardship strategies of using the current antibiotics available in such a way that minimizes the risk of resistance evolution. Antibiotic regimens often include the sequential changing of drugs to limit development and evolution of resistance of bacterial pathogens. For example, there has been much interest in the past few years in studying collateral sensitivity of antibiotics, whereby adaptation to a drug concurrently results in the increased sensitivity to a different drug. Alternating between a reciprocally collaterally sen-

sitive pair of drugs has been proposed as a strategy for slowing down the rate of antibiotic resistance. However, rather than studying how adaptation to a drug concurrently alters the resistance or sensitivity to other drugs, an open question in the field that has not been addressed is how history of prior adaptation to one antibiotic can influence the resistance profiles when bacteria subsequently adapt to a different antibiotic. In this dissertation, we aim to characterize the effects that prior drug adaptation has on influencing the potential future evolutionary dynamics of subsequent adaptation. We experimentally evolved the model organism *Pseudomonas aeruginosa* to six two-drug sequences. We observed drug order-specific effects whereby: adaptation to the first drug can limit the rate of subsequent adaptation to the second drug, adaptation to the second drug can restore susceptibility to the first drug, or final resistance levels depend on the order of the two-drug sequence. Furthermore, we used whole-genome sequencing to determine the genetic changes that occurred during drug adaptation to better understand the molecular basis of the drug order-specific effects. This body of work demonstrates how resistance not only depends on the current drug regimen but also history of past regimens. These order-specific effects may allow for rational forecasting of the evolutionary dynamics of bacteria given knowledge of past adaptations and provide support for the need to consider history of past drug exposure when designing strategies to mitigate resistance and combat bacterial infections. This dissertation establishes a framework for a better fundamental understanding of how evolutionary historical context plays a role in antibiotic resistance evolution dynamics and how this knowledge can then hopefully be used to develop regimens that combat the development of resistance.

Acknowledgements

Thank you to my family for all your loving support over the last few years. To my mom, Ling-Mey, and my dad, Ting-Kuo, thank you for raising me and teaching me the values of hard work and diligence. Not a day goes by where I do not recognize and appreciate the enormous sacrifices you both have made when you left your homeland of Taiwan to start a new life in the United States. In doing so, you have provided me with wonderful opportunities of pursuing higher education at world-class institutions. You inspire me with your patience, love, and dedication, and I am forever grateful. To my aunt Lily, thank you for all your love and support. I have always viewed you as the matriarch of the family and your courage and encouragement have often been sources of my motivation. Thank you to my cousins Elsa and Ken, your generosity and help have made my time in Charlottesville a great one. Thank you to my girlfriend Erin, you have greatly enriched my life for the better and you have helped make the last year of my graduate studies a memorable one.

I would like to give thanks to all of my mentors in science I have had over the years, spanning from high school to graduate school. Thank you to Claudine Marcum, Raul Cachau, Marianne Engel-Stefanini, Stacey Finley, Aleksander Popel, and Matt Saunders for mentoring me at various stages of my scientific career. You have each nurtured my passion for

science in your own way and I am grateful to have been mentored by you.

Words cannot fully express how fortunate I feel to be a part of the Papin lab and the BME department at UVA. Thank you to my committee members, Shayn Peirce-Cottler, Jeff Saucerman, Erik Hewlett, and Peter Kasson for your support and guidance. I am honored to have worked with past Papin lab colleagues including Arvind, Paul, Kevin, Jennie, Edik, and Matt. You all have paved the way in defining the culture of excellence and comradery in the lab. Thank you Glynis for all the help and advice you have given me over the years, and especially for teaching me the foundations of wet-lab experimental work (I still remember when you taught me how to run my first MIC assay!). To the current graduate students in the lab: Anna, Kris, Laura, Greg, Maureen, Tom, and Bonnie, thank you for making life inside and outside the lab a blast. I cherish all the times we have exchanged advice and suggestions about lab work, as well as all the movie nights and happy hours we have had throughout the years. I wish you all the best of luck and continued success as you continue fighting the good fight that is graduate school.

Finally to my PhD advisor Jason Papin, thank you for having me as part of your team over the last few years. It has been an absolute pleasure to work with you and you have been a phenomenal mentor. Thank you for always being positive, supportive, encouraging, and always having an open door. Thank you for teaching me to be creative and granting me the freedom to pursue my own research projects and ideas. I know I will be very lucky if I ever get to have another mentor that is even half as awesome as you are!

Phillip Yen

May 2017

Contents

List of Figures

List of Tables

Chapter 1

Background and significance

1.1 Prologue

Before diving into the main contents of this dissertation, I would like to first give some context of how and why I decided to pursue the particular topic of this dissertation. I had learned early on during my tenure in the Papin lab that my advisor Jason was an advocate of having his students formulate, develop, and execute their own research ideas and projects to have them truly take ownership of the project. Around the end of my second year of graduate school, I had finished my first research project, which was done in collaboration with Jennie Bartell, on the comparative metabolic systems analysis of two species of pathogenic *Burkholderia* [1]. After completion of that project, I was then in a transition point where I needed to figure out what my "next project" would be. At that point, Jason only had one main criterion for me as I began to seek out research topics that interested me: "try to do a project related to antibiotic resistance." With that one requirement in mind, I spent a bit of time doing the research equivalent of soul-searching as I sampled the literature on

antibiotic resistance. I quickly honed in on literature studying the evolution of antibiotic resistance, and especially studies that evolved bacteria in a laboratory setting to different drugs to uncover the evolutionary dynamics of resistance development. One paper that struck a chord with me was "Use of Collateral Sensitivity networks to Design Drug Cycling Protocols That Avoid Resistance Development" by Imamovic and Sommer [2]. In this study, cultures of *Escherichia coli* were evolved to 23 different antibiotics to generate resistant mutants, and subsequently these resistant mutants were tested for differences in their drug resistance/sensitivity profiles for all the drugs to determine if adaptation to a drug led to the concurrent development of collateral resistance or collateral sensitivity to the other drugs. Based on that data, they then proposed a new treatment framework of collateral sensitivity cycling where alternation of two reciprocally collaterally sensitive drugs would select against the evolution of antibiotic resistance. What I admired about this paper was that, while the main experiments were conceptually very simple, the results were profoundly impactful both for uncovering fundamental evolutionary principles, as well as for addressing a clinically important problem. Over time, I realized that my favorite types papers tended to follow this theme of tackling big ideas using relatively simple experiments and had implications on fundamental evolutionary biology with translational aspects. I was also fascinated with the idea of being able to watch evolution in action, which is feasible when the organism of interest replicates its cells on the order of hours, which results in multiple generations of growth per day. Lastly, because the *Burkholderia* project was largely a computational modeling project, I yearned to start a new project that was more experimental ("wet-lab") in nature. That is not to say I did like or did not want to do computational work in the future, but rather, I wanted to diversify my skills and interests at this transition point in my graduate school

career. With all of these factors in mind, and with the guidance and encouragement of Jason, I formulated the research project presented in this dissertation which focuses on studying how history of past adaptation to antibiotics influences the evolutionary dynamics of subsequent drug adaptation in the bacterial pathogen *Pseudomonas aeruginosa*. As a sort of "blast from the past," Figure A.1 shows some handwritten notes during the original conception of this project.

1.2 Introduction

There is a dire need to better understand how bacteria evolve resistance to antibiotics, and in this dissertation, we used adaptive laboratory experimental approaches to study the evolutionary principles that underlie resistance adaptation. Specifically, we aimed to answer the question: how does history of past adaptation to one drug influence the evolutionary dynamics during subsequent evolution to a different drug? The outcomes of this study have important clinical implications for the rational choice of antibiotic therapy based on knowledge of the history of past therapies. As a conceptual example (Figure 1.1), if a clinician had *a priori* knowledge which suggested that treatment with Drug A first followed by Drug B would lead to high, multidrug resistance, but the reverse order would not, then perhaps the clinician would be more inclined to prescribe the latter order. Hence, knowledge of the history-dependent effects of resistance evolution can strategically be used to mitigate antibiotic resistance.

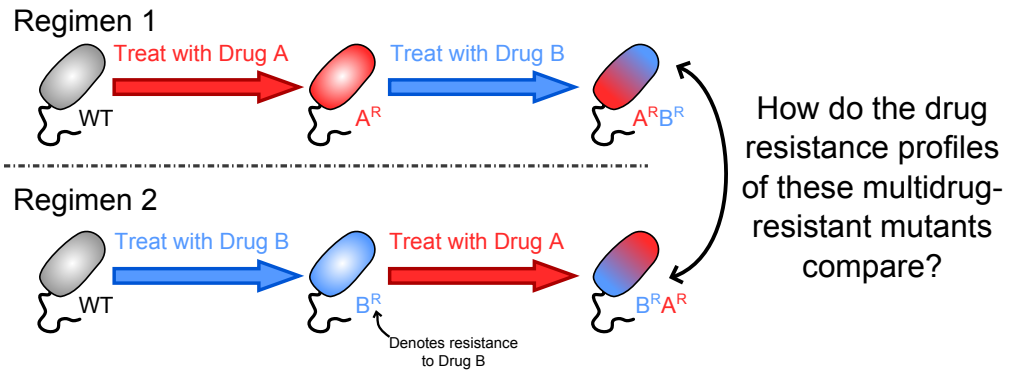

Figure 1.1: **Conceptual example of how history of antibiotic adaptation may play a role in multidrug resistance.** Suppose two different patients initially had the same bacterial infection. The first patient is prescribed with Drug A, but the bacteria develop resistance and so the patient is then switched over to Drug B. The second patient on the other hand is prescribed with Drug B first, but then when resistance develops, is switched to Drug A. Even though the bacterial populations in these two patients have both been exposed to the two drugs, the evolutionary paths that they underwent may be different, and perhaps one population is more multidrug-resistant than the other.

1.3 Antibiotic resistance is a global health concern

Antibiotic resistance is a growing healthcare concern whereby bacterial infections are increasingly difficult to eradicate due to their ability to survive antibiotic treatments [3]. There have been reported cases of resistance for nearly every antibiotic we have available [4] (Figure 1.2). Coupled with the fact that the antibiotic discovery pipeline has slowed over the past few decades [5], there is a dire need to find better treatment strategies using existing antibiotics that can slow or even reverse the development of resistance.

With over two million antibiotic-resistant infections per year in just the United States alone [7], antibiotic resistance is an ever increasing problem. Alexander Fleming first discovered penicillin in 1928, which was then mass produced for therapeutic purposes beginning in the 1940's, proving to be extremely effective in combating bacterial infections during World

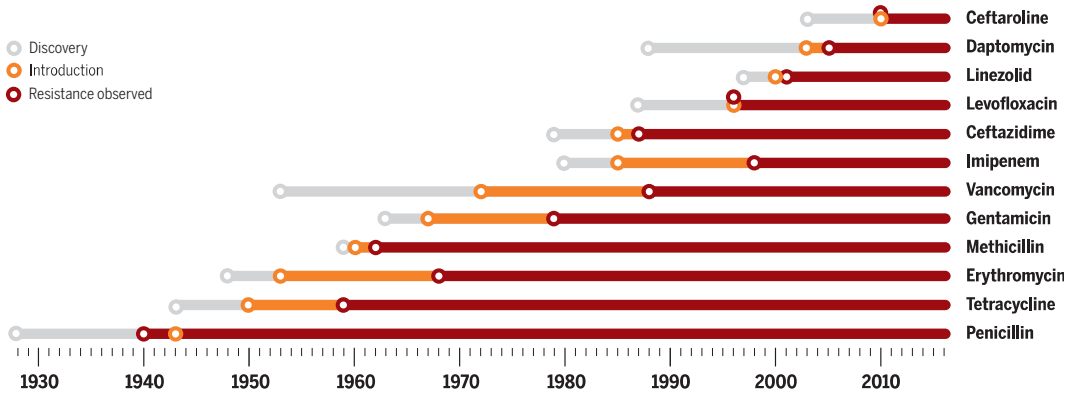

Figure 1.2: **Timeline of the development of antibiotic resistance.** Reprinted from [6], with permission from the American Association for the Advancement of Science.

War II. In his Nobel Prize speech, Fleming warned about the danger of antibiotic resistance: "There is the danger that the ignorant man may easily underdose himself and by exposing his microbes to non-lethal quantities of the drug make them resistant [8]." Indeed, penicillin-resistant strains of *Staphylococcus aureus* were identified only five years later, and we have seen resistance develop for nearly all clinically-used antibiotics since then [4]. This pattern of discovery followed by emergence of resistance repeated itself endlessly during the "golden age" of antibiotic discovery[9]. Pharmaceutical companies became less interested in investing in the discovery and development of new antibiotics because of the risk that resistance would develop and make it ineffective very quickly, or that it would be kept as a drug of last resort and thus would not generate profit [5]. It is for these reasons that we need to develop strategies to prolong the efficacy of the drugs we already have. Can we deploy antibiotics and develop regimens and therapies with existing drugs in a rational way such that we can forecast, slow down, and/or potentially even reverse resistance?

1.4 Minimum inhibitory concentration as a metric of resistance

In this section, I present the concept of the minimum inhibitory concentration (MIC) of an antimicrobial. The MIC is a measurement of antimicrobial susceptibility and is defined as the lowest concentration of an antimicrobial that will inhibit the visible growth of a microorganism after overnight incubation [10]. This measurement is the primary metric that I use in this dissertation to measure the level of susceptibility/resistance of bacterial cultures. We can determine changes in the resistance profiles as the bacteria adapt to different drugs by measuring the changes in the MICs over the time course of adaptation. That is, an increase of the MIC over time indicates the development of resistance to a drug.

There are a few standard protocols to measure the MIC, and the protocol employed in this dissertation is the broth microdilution assay [10, 11]. The premise of this assay is that a concentration gradient of the antibiotic is established across multiple wells of a microtiter plate, typically in a series of two-fold dilutions. A standardized amount of bacteria are then inoculated into the drug concentration gradient, and the microtiter plate is incubated overnight. After 24 hours of incubation, the presence or absence of growth is determined by eye, and the lowest concentration of the antibiotic that yields no visible growth is the MIC. Other common methods for determining the MIC include the E-test [12] and the macrodilultion method [11]. See Figure 1.3 for an example of the MIC assay.

There are several key parameters when performing the broth microdilution assay that can affect the measured MIC [11]. These parameters are chosen to standardize the assay between different laboratory environments, which is especially important in the clinical setting. I

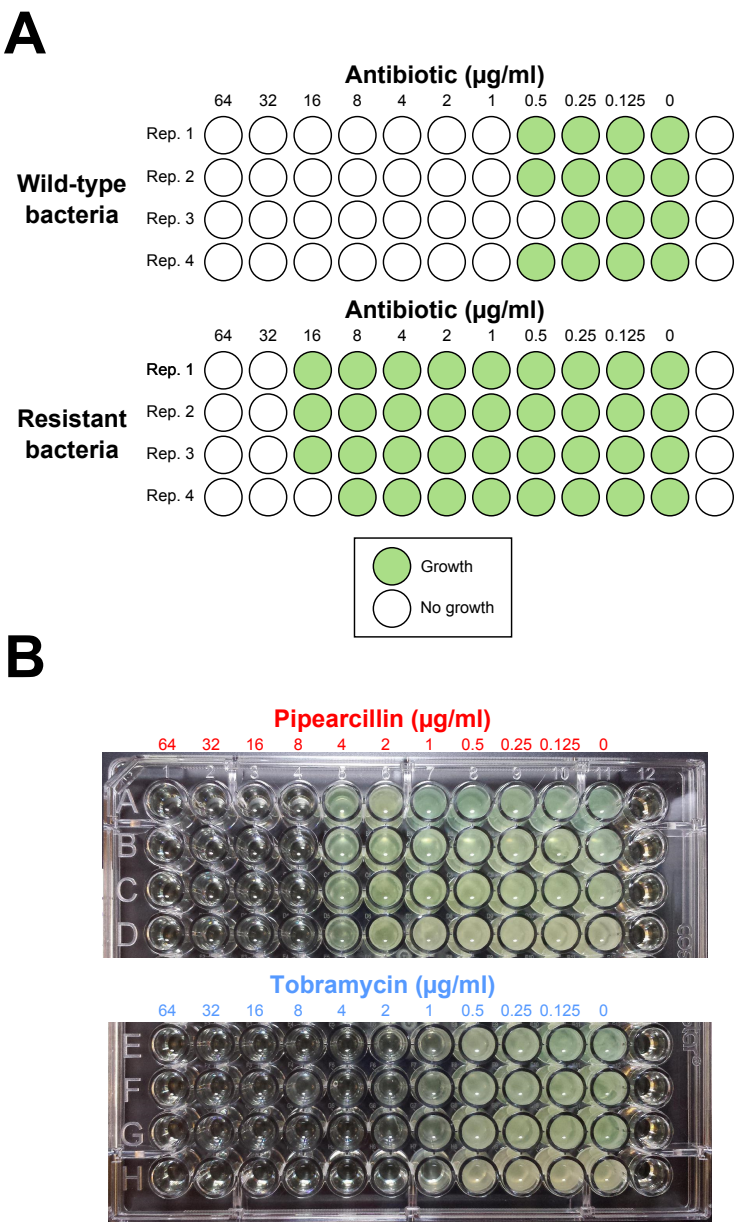

Figure 1.3: **Schematic and example of a MIC assay.** (A) This schematic represents a prototypical MIC assay as would be performed in a 96-well microtitre plate. Each row of wells is a replicate of the MIC assay. For example, in the top four rows, four replicates of the wild-type bacteria are grown in the antibiotic concentration gradient, and the MIC would be reported as approximately 1 µg/ml. In the bottom four rows, four replicates of the antibiotic resistant bacteria are grown, and the MIC would be reported as approximately 32 µg/ml. Note that it is normal to have some variability in the MICs between different replicates. (B) This representative photograph shows an actual MIC assay from the adaptive evolution experiment. Day 40 Control was grown on piperacillin (MIC is 8 µg/ml), and tobramycin (MIC is 2 µg/ml). Columns 11 and 12 are typically denoted as the "growth control" (media+no drug+bacteria) and "sterility control" (only media) wells in my MIC assays.

describe here these parameters, and the modifications we have made when we perform this assay. First, Mueller-Hinton broth is the recommended growth medium as it support the growth of a variety of non-fastidious bacteria. We chose to use LB broth instead for all experiments, as it was an alternative, commonly used, nutrient-rich growth medium. As mentioned before, the incubation period of the assay is 24 hours, and we abided to this parameter fairly consistently. Typically, the process of performing the serial propagation experiments took 1-2 hours, resulting in an incubation time of about 22-23 hours. At the end of incubation, the protocol traditionally calls for determination of growth in the wells by eye to determine the MIC. To standardize this call, we defined growth to be an OD_{600}>0.1 as measured by a spectrophotometer for all experiments. Lastly, the size of the bacterial inoculum can impact the MIC, and the standard protocol recommends a final inoculum size of $5x10^5$ colony forming units per ml. We modified this parameter such that for the daily serial propagation, the inoculum was diluted by 1/500. That is, bacteria from the well of the maximum concentration that allowed for growth (i.e. MIC/2), which has an OD_{600} of at least 0.1, was diluted by 1/500 for the next cycle of growth. These modifications were consistently used for all MIC assays performed in our study.

The MIC is an *in vitro* parameter that is used to characterize the microorganism being studied as being clinically susceptible, intermediate, or resistant to the tested drug [11]. These values are determined and published by different national organizations including the Clinical and Laboratory Standards Institute (CLSI) in the United States [13], and the European Committee on Antimicrobial Susceptibility Testing (EUCAST) [14]. For reference, the CLSI breakpoints for *P. aeruginosa* for the three drugs tested in this dissertation are presented in Table 1.1.

Table 1.1: **MICs of *P. aeruginosa* for piperacillin, tobramycin, and ciprofloxacin.** Shown are the clinical breakpoints MICs of *P. aeruginosa* to the three antibiotics used in this study according to the CLSI guidelines [13]. Values are in units of µg/ml.

	Susceptible	**Intermediate**	**Resistant**
Piperacillin	≤ 16	32-64	≥ 128
Tobramycin	≤ 4	8	≥ 16
Ciprofloxacin	≤ 1	2	≥ 4

1.5 *P. aeruginosa* as a model organism

Pseudomonas aeruginosa is a clinically important Gram-negative bacterium and is one of the six members of the ESKAPE pathogens, which are classified as pathogens that currently cause the majority of US hospital infections [15]. Recently, the World Health Organization for the first time published a list of "priority pathogens", which lists twelve families of bacteria that pose the greatest threat to human health [16]. *P. aeruginosa*, along with *Acinetobacter baumannii* and *Enterobacteriaceae* were listed as the three "Priority 1: CRITICAL" pathogens. The Center of Disease Control and Prevention reports that in the United States per year, *P. aeruginosa* is responsible for over 51,000 infections (of which 6,700 were multidrug-resistant) and 440 deaths [7]. *P. aeruginosa* can cause infections in immunocompromised patients (most notably in cystic fibrosis patients [17]), and can colonize burn wounds, implanted organs, and catheters [18]. It is a common cause of healthcare associated infections including pneumonia, bloodstream infections, urinary tract infections, and surgical site infections [7].

P. aeruginosa is an ideal model organism with a well-annotated genome for studying the evolution of multi-drug antibiotic resistance. It has several well-studied intrinsic mechanisms of resistance to several drugs and the capability of acquiring increased resistance through *de novo* mutations and horizontal gene transfer [19–22]. *P. aeruginosa* possesses

several chromosomally encoded resistance mechanisms including aminoglycoside-inactivating enzymes, multidrug efflux pumps, the AmpC beta-lactamase, and the outer membrane porins OprF and OprD [23]. Furthermore, mutations in genes both related and unrelated to these "baseline" intrinsic resistance mechanisms can lead to further increased resistance to several classes of antibiotics, including penicillins, cephalosporins, carbapenems, monobactams, aminoglycosides, fluoroquinolones, and polymyxins. For example, the expression of several of the multidrug efflux pumps are under the control of one or more negative regulators, and mutations in these regulators can lead to the overexpresion of the efflux pumps [24]. Similarly, mutations in regulators of the AmpC beta-lactamase (such as *ampD* [25]) lead to the overexpression of AmpC and consequently decreased susceptibility of penicillins and cephalosporins. Loss of the OprD porin confers resistance to imipenem and reduced susceptibility to meropenem [26]. Mutations in the DNA proofreading enzymatic machinery can result in the hypermutator phenotype and subsequent increase in the mutation rate. Resistance mutations are more likely to occur in hypermutators [11], which further increases the probability that resistance will develop. While these are examples of some of the more characterized resistance mutations in *P. aeruginosa*, there is still much to be explored of how other genes and mutations contribute to increased resistance to different antibiotics.

1.6 Adaptive laboratory evolution

Adaptive laboratory evolution is a technique that can be used to study and test evolutionary principles in a highly controlled laboratory setting [27]. Microorganisms with short generation times such as bacteria are especially amenable to adaptive laboratory evolution and

can be adapted to an environment through repeated cycles of growth in a specific media environment, dilution of the culture, and subsequent passaging into fresh media [28]. Multiple replicates for each condition can be evolved in parallel to investigate the reproducibility of evolutionary dynamics [29]. The evolutionary trajectories of the bacteria can be measured as they adapt to different nutrients and stressors over time [30]. Whole genome resequencing of the evolved strains can subsequently be used to determine the mutations that occurred that may be associated with the observed phenotypes [31, 32].

One of the most well-known ALE experiments is the ongoing "Long Term Experimental Evolution" (LTEE) experiment which was started by Richard Lenski and is maintained by his research group at Michigan State University [33]. In this experiment, 12 initially identical populations of *E. coli* were founded and grown in glucose minimal media. Each day, 1% of the population is transferred to a flask containing 9.9 ml of fresh glucose minimal media. During each dilution cycle, the populations experience approximately 6.64 doublings (generations). This experiment has been going on since 1988 and the populations have undergone more than 66,000 generations. In fact as I write this sentence, today (March 13, 2017) was the $10{,}000^{\text{th}}$ transfer. The LTEE experiment has yielded several significant findings including the deceleration of increasing fitness improvement, the increase of *E. coli* cell size, and most notably, the ability of one population to grow aerobically on citrate [33]. A defining feature of *E. coli* is its inability to aerobically grow on citrate [33].

ALE can be used to study the development of antibiotic resistance in bacterial pathogens [34]. Resistance to antibiotics is an evolutionary response of bacteria to withstand and survive the effects of the stressor. Deliberately evolving bacteria to withstand antibiotics through experimental evolution can yield insights into the evolutionary dynamics and tra-

jectories of this adaptive process [35, 36]. While the majority of ALE experiments that study the evolution of antibiotic resistance employ some variation of the daily serial propagation protocol, one study engineered a continuous culture system that continuously monitors bacterial growth and dynamically regulates the antibiotic concentration to continuously challenge the evolving populations [35]. These evolution experiments can provide a longer-term perspective which can yield information for the design of novel treatment strategies that can reduce the rate of resistance evolution or potentially even reverse the effects of resistance [2, 36, 37].

1.7 Current state of the field

I would like to end this chapter by giving an overview of what I see as the current state of the field and how the work presented in this dissertation contributes to the field of the evolutionary dynamics of antibiotic resistance. Recent studies have explored how adaptation to an antibiotic can cause bacteria to concurrently become more susceptible or more resistant to other drugs, an effect termed collateral sensitivity or collateral resistance [2, 38, 39]. Collateral sensitivities between drugs have been used to design drug cycling strategies and to explain the decreased rate of adaptation to certain antibiotics [2, 40–46]. Drug deployment strategies that exploit such collateral sensitivities between pairs of antibiotics to minimize resistance evolution have been tested *in vitro*. A recent study determined the collateral sensitivity drug interaction network in *E. coli* and demonstrated how an alternating sequential treatment of two reciprocal collaterally sensitive antibiotics can slow down the rate of resistance evolution [2]. In this drug cycling strategy, development of resistance to

one drug concurrently increases the sensitivity to the second drug, and this allows wild-type cells to outcompete the resistant cells when exposed to the second drug. In a different study, evolution experiments of alternating sequential therapies of pairs of antibiotics were performed on *Staphylococcus aureus* and the study showed that the alternating treatments slowed the rate of resistance development compared to single-drug treatments [40]. Consistent with the *E. coli* study, this study found that collateral sensitivities could explain the evolutionary constraints in the cases where alternating treatment resulted in decreased resistance development compared to the single-drug treatment.

Most of the prior studies that test the use of alternating antibiotic therapies to reduce the rate of resistance development employ an adaptive laboratory evolution scheme where the drugs are switched at daily or sub-daily intervals with the purpose of testing if rapidly changing antibiotic environments can diminish the rate of drug resistance adaptation [40, 42, 46, 47]. In this dissertation, we expand on these prior works, but we are not focused on studying the evolutionary dynamics of bacteria adapted to rapidly changing drug environments. Rather, we explore the evolutionary dynamics of sustained, longer treatments of drugs, and how development of high levels of resistance to one drug influences the subsequent dynamics of sustained adaptation to a second drug. To our knowledge, this is the first study to systematically test the evolutionary dynamics of sustained adaptation to different sequences of two drugs.

In clinical settings, when antibiotic cycling strategies are employed, they are used typically at the level of the hospital ward and the cycling of antibiotics are often done at monthly intervals [48, 49]. The rationale here is that if resistance to one drug arises after frequent use in a ward, switching to an antibiotic of a different class may allow resistance rates to the

withdrawn drug to stabilize or even fall, enabling the first drug to be efficiently re-introduced again at a later time [50]. This type of practice of cycling drugs of different classes over the course of monthly intervals is done empirically, and it remains unclear how these regimens constrain the evolutionary dynamics of antibiotic resistance development.

Here, we explore the evolutionary trajectories of bacteria as they evolve high levels of resistance to one antibiotic, and the subsequent trajectories as the selection pressure from the first drug is withdrawn and replaced with the sustained pressure of a different drug. It remains unexplored how prior adaptation to one drug environment affects the evolutionary dynamics of a bacterial population during subsequent adaptation to a second drug in terms of the amount of resistance it can potentially develop and the resistance profile of the first drug. Collateral sensitivities and collateral resistances between two drugs have been studied in the context of adaptation to single drugs [44]. However, in this study, we focus not on if bacteria become *concurrently* more resistant or sensitive to other drugs, but rather, if adaptation to one drug constrains or potentiates the evolutionary dynamics to sustained adaptation to a second drug. How does *history* of adaptation to one drug influence the *subsequent* adaptation to a second drug? If there are such historical dependencies, can we use this knowledge to design sequential therapies that slow down the evolution of resistance to the drugs used? What happens to the previously developed resistance once the drug pressure is taken away or switched to a different drug? Do compensatory adaptations sustain the high resistance, or do the bacteria revert and become susceptible again [51]? The answers to these questions are important for understanding how bacteria adapt to different antibiotic environments. Bacterial pathogens have complex evolutionary histories and elucidation of any historical dependencies of antibiotic resistance evolution would allow for rational forecasting of future

resistance development and would aid in the design of strategies for mitigating antibiotic resistance.

Chapter 2

Adaptive evolution of *P. aeruginosa*

2.1 Foreword

Antibiotic resistance of is a natural phenomenon whereby bacteria are able to resist the effects of the drugs that are meant to kill them. One way to study the evolution of antibiotic resistance is through adaptive laboratory evolution. With this technique, resistant strains can be generated in the lab starting from a susceptible, ancestral population in a highly controlled and defined setting. The focus of this dissertation was to answer the question: how does history of past drug adaptation influence the subsequent evolutionary dynamics of subsequent drug adaptation? Adaptive laboratory evolution was used as the primary method of tackling this question. By evolving bacteria to withstand increasing concentrations of antibiotics over time, we were able to track the evolutionary dynamics of the development of antibiotic resistance as the bacteria are exposed to different sequences of treatments. In this chapter, I describe the main adaptive evolution experiments that we performed to determine how prior adaptation of the pathogen *P. aeruginosa* to one drug influences the subsequent

adaptation to a second drug. Furthermore, we also tracked how adaptation to the second drug affects the resistance to the first drug.

2.2 Introduction

This chapter presents the foundational work for the remaining chapters of this dissertation. In this chapter, I detail the experiments that were performed to evolve *P. aeruginosa* to all of the different two-drug sequences of the three drugs piperacillin, tobramycin, and ciprofloxacin, as well as to LB. Initially, this project was exploratory in nature, and originally, the plan was to evolve *P. aeruginosa* to two drugs: piperacillin and tobramycin (Figure A.1). Replicate populations of *P. aeruginosa* were first evolved separately to piperacillin and tobramycin. Subsequently, the piperacillin-evolved lineages were evolved for the same amount of time to tobramycin, and, the tobramycin-evolved lineages were evolved for the same amount of time to piperacillin. A key experimental decision that I made was to measure the MICs of both drugs for all lineages during the adaptation process. For example, during the adaptation to piperacillin, the MIC was measured for tobramycin, and vice versa. In this manner, we systematically tracked the changes in MICs over time for both drugs for the lineages. This is similar to how in collateral drug sensitivity studies, the MICs of all of the other drugs are measured after a bacterial population has evolved resistance to one drug [2, 38]. However, the difference in our case was that the MIC to the other drugs was tracked on a daily basis, and not just at the endpoint. Later on, we decided to test a third drug, ciprofloxacin. With this decision, we then had to establish the ciprofloxacin-evolved lineages, as well as evolve the previously established piperacillin-evolved and tobramycin-evolved lin-

eages to ciprofloxacin. Thus, we went from two two-drug sequences (with two drugs) to six two-drug sequences (with three drugs). Consistent with before, we measured the MICs of all the drugs over time for all of the evolved lineages, which resulted in a complete set of MIC profiles for all the three drugs.

While we did not initially know what to expect in terms of the shapes of the MIC profiles over time, we did hypothesize that there would be differences in the endpoint MICs of the two-drug-evolved lineages. We suspected for example that the final MIC of piperacillin may not be the same for the lineage evolved to piperacillin first, then to tobramycin, compared to the lineage evolved to tobramycin first, then to piperacillin. Could it be possible that prior adaptation to tobramycin would result in changes to the bacterial population that would constrain the potential evolutionary paths during subsequent piperacillin adaptation? It seemed unlikely that MIC profiles would be "perfectly symmetrical" between the two two-drug sequences of adaptation. Furthermore, even if the MICs were the same between the two lineages, it would be interesting to see if the mutational paths were the same. Even if the measurable phenotype of resistance (MIC) were the same, would the mutations that occurred when piperacillin was the first drug be same or different as the mutations that occurred when piperacillin was the second drug?

The intuition, especially from a systems biology perspective, was that the interconnectedness of the nodes of underlying biochemical and genetic networks of the system would play a role in the evolutionary trajectories of the drug-evolved lineages. Epistasis is the interaction between genes, particularly, when there are mutations between the genes being compared [52–54]. Epistasis can be thought of more fundamentally as: if a mutation in gene A results in phenotype A, and separately, a mutation in gene B results in phenotype B,

what is the phenotype when the mutations in genes A and B are concurrently present? It is with this framework that we pursued the question of how the evolutionary dynamics (both phenotypically and genotypically) compared between bacterial lineages that were evolved to different "mirror image" sequences of pairs of antibiotics.

Conceptually, there has been one study that is quite thematically similar to the questions being posed here. In that study [55], different populations of the algae *Chlamydomonas reinhardtii* were evolved to become resistant to different herbicides, and these resistant mutants were then evolved to a second herbicide. The number of weeks it took for the populations to reach a certain threshold optical density was used as the metric for resistance. The study found that while evolution to two of the herbicides was largely independent of history of selection, resistance to the third herbicide developed more quickly when there was prior adaptation to either of the first two herbicides. While conceptually similar, our study is different in that it focuses on a pathogenic bacteria of clinical importance, and on the evolutionary dynamics of antibiotic resistance, which is a serious threat to public health.

2.3 Materials and methods

2.3.1 Experimental study design

We evolved in parallel four independent replicates for each evolution lineage in the primary adaptive evolution experiment, and three independent replicates for each of the clinical isolates to balance the statistical power of the conclusions with the technical feasibilities of the daily serial propagations. In the primary adaptive evolution experiment, we concluded

the single-drug evolution at the end of 20 days because the resistance levels of the evolved lineages to their respective drugs were saturated or close to saturated at that point. The clinical isolates from Figure 4.4 and from Figure 4.8 were evolved for ten and fifteen days, respectively because the similarities and differences of the drug-specific effects to those of the primary adaptive evolution experiment were readily apparent at that point.

2.3.2 Media, growth conditions, and antibiotics

MIC plates were made daily using the broth microdilution method with the standard two-fold dilution series [10]. Lysogeny broth (LB) was used as the growth medium for all experiments (1% tryptone, 0.5% yeast extract, 1% NaCl). Antibiotics tested include piperacillin sodium (referred to as piperacillin), tobramycin, and ciprofloxacin HCl (referred to as ciprofloxacin) (all from Sigma). Aliquots of 1 mg/ml and 10 mg/ml antibiotic stocks were made by diluting the antibiotic powders in LB and were stored at -20°C. New frozen drug aliquots were used on a daily basis.

2.3.3 Adaptive laboratory evolution to piperacillin and tobramycin

A frozen stock of *P. aeruginosa* PA14 was streaked on an LB agar plate and a single colony was inoculated into 4 ml of LB, which was then grown overnight at 37°C, shaking at 125 RPM. This antibiotic-susceptible culture, denoted as the Day 0 Ancestor, was diluted to an OD_{600} of 0.001 (approximately 10^6 CFU/ml), and then inoculated into three identical MIC plates consisting of concentration gradients of piperacillin and tobramycin. A sample of the ancestor was saved in 25% glycerol and stored at -80°C. The three MIC plates were used

to serially propagate cultures evolved to LB media, piperacillin, and tobramycin, with four biological replicates per condition (Figure 2.1). Wells for growth control (media+culture) and sterility control (media) were included in each MIC plate. For adaptation to LB media, bacteria were sampled from the growth control well. MIC plates were placed in a plastic container (to prevent evaporation) and incubated at 37°C with shaking at 125 RPM (Thermo Scientific MaxQ 4000). MIC plates were incubated daily for approximately 22-23 hours.

At the end of incubation, growth in the MIC plates was determined using a plate reader (Tecan Infinite M200 Pro). Growth was defined as OD_{600}>0.1 after background subtraction. We recorded the MIC of each lineage for each drug, which was defined as the lowest antibiotic concentration tested that did not show growth (Table A.1). To propagate, cultures were passaged from the highest concentration that showed growth (i.e. MIC/2) from the corresponding MIC drug gradient (Figure 2.1). For adaptation to LB, cultures were passaged from the growth control well that contained only LB without drug. For each culture to be passaged, the culture was first diluted by a factor of 1/250 in fresh LB (e.g. 20 µl of the culture was diluted in 5 ml of LB), which was then inoculated in fresh piperacillin and tobramycin drug gradients in the new day's MIC plate. Wells of the MIC plate thus contained 100 µl of double the final concentration of the antibiotic and 100 µl of the diluted culture. Hence, the cultures were diluted by a total factor of 1/500 daily. Daily samples were saved in 25% glycerol and stored at -80°C. For Day 21, the piperacillin and tobramycin evolved cultures were sub-cultured in additional MIC plates such that they could subsequently be evolved to tobramycin and piperacillin, respectively.

2.3.4 Adaptive laboratory evolution to ciprofloxacin

A similar protocol was used to establish the ciprofloxacin-evolved lineages (CIP^R). Starting with a clonal population of the Day 0 Ancestor, four replicates were established and propagated daily under ciprofloxacin treatment for 20 days. CIP^R was then sub-passaged to piperacillin and tobramycin to establish the CIP^RPIP^R and CIP^RTOB^R lineages in addition to continued ciprofloxacin evolution.

To establish the PIP^RCIP^R and TOB^RCIP^R lineages, bacteria from the frozen stocks of Day 20 PIP^R and TOB^R were revived on LB agar plates, and clonal populations were evolved to ciprofloxacin to establish these lineages. Similarly, to establish the PIP^RLB, TOB^RLB, and CIP^RLB lineages, bacteria from the frozen stocks of Day 20 PIP^R, TOB^R, and CIP^R were revived on LB agar plates, and clonal populations were evolved to LB.

Lastly, the MIC to ciprofloxacin was retrospectively measured for the Control, PIP^R, TOB^R, PIP^RTOB^R, and TOB^RPIP^R lineages. Frozen stocks were revived and plated on LB agar plates. The notation for the day numbering is such that Day X PIP^R means X days exposure to piperacillin. For consistency, stocks were revived from Days 0 (Ancestor), 5, 10, 15, 19, 20, 25, 30, 35, and 39 for Control, PIP^R, and TOB^R. One day of exposure to ciprofloxacin would yield Days 1, 6, 11, 16, 20, 21, 26, 31, 36, and 40 MICs to ciprofloxacin. For PIP^RTOB^R and TOB^RPIP^R, stocks were similarly revived from Days 20, 25, 30, 35, and 39 to and exposed to ciprofloxacin to measure Days 21, 26, 31, 36, and 40 MICs to ciprofloxacin. Table A.1 shows the MICs to piperacillin, tobramycin, and ciprofloxacin, respectively for all the lineages. Note that not all drug MICs were measured on a daily basis for all lineages.

During analysis of the mutations, we deduced that there were some cross-contaminations between replicates in a few lineages. Namely, we saw sets of mutations that were identical in two replicates. We believed that the most likely explanation was that the following seven lines were cross-contaminated sometime between Day 21 and Day 40: CIP^RPIP^R-3, CIP^RPIP^R-4, TOB^R-1 CIP^RTOB^R-1, CIP^RTOB^R-2, CIP^RTOB^R-4, and CIP^R-3, where the number denotes the replicate. To redo these lineages, the corresponding Day 20 replicate frozen stocks were revived on LB agar plates. Then clonal populations were used to redo the propagation as described before. For example, CIP^R-3 was evolved to piperacillin for 20 days to redo CIP^RPIP^R-3. We performed Sanger sequencing of replicate-specific mutations (Table 3.1) on the Day 40 mutants to confirm successful propagation of the cultures.

2.3.5 Reproducing drug history dependence in the pyomelanin phenotype during piperacillin evolution

Clonal populations of Day 0 Ancestor, Day 20 TOB^R-1, -2, -3 and -4, and Day 20 CIP^R-1, -2, -3, and -4 were grown in LB starting from the frozen samples. These cultures were diluted in LB to OD_{600} of 0.001. On Day 1, in 96-well plates, 100 µl of the diluted cultures were inoculated with 100 µl of 4 µg/ml piperacillin (to yield a final concentration of 2 µg/ml piperacillin). 92 wells were used to establish independent replicate populations exposed to piperacillin. Cultures were incubated at 37°C with shaking at 125 RPM. On Day 2, replicate populations were passaged using a 96-pin replicator tool (V&P Scientific, VP246, 100-150 µl per pin) into 200 µl of 4 µg/ml piperacillin. This protocol was continued until Day 10 with a final concentration of 20 µg/ml piperacillin. For each plate, two wells were used as sterility controls (only LB), and two wells were used as growth controls (LB with bacteria, without

drug). Photographs were taken daily, and the number of visibly brown wells was recorded.

2.3.6 Statistical significance of drug order-specific effects in MIC profiles

All statistical comparisons of MIC values were performed on the $\log_2$ transformed values. Unless noted otherwise, one-way ANOVAs were performed on the MICs of the relevant lineages. If the p-value from the ANOVA was less than 0.05, a post-hoc Tukey HSD multiple comparisons test was then performed to determine which pairs of treatments were significantly different from each other. The Tukey HSD tests report 95% confidence intervals for the true mean difference for each pairwise comparison. If the confidence interval does not contain zero, then the two groups being compared have significantly different means at the p=0.05 level. See Figure A.2 for an example calculation.

For the comparisons presented in Figure 2.7, treatments being compared consist of those listed on the x-axis of each graph in the figure. For the comparisons presented in Figure 4.4, the raw MIC values for each lineage were first normalized by subtracting the average Day 1 MIC of each of their respective lineages. For each of the three clinical isolates, a one-way ANOVA was performed on the Day 10 MIC_{PIP} values of the lineages evolved to LB, tobramycin, and ciprofloxacin (piperacillin-adapted lineages were excluded in the comparisons). The Tukey HSD test was then performed to see if the Day 10 MIC_{PIP} values of the lineages evolved to tobramycin and ciprofloxacin were significantly different from the lineages evolved to LB. See Figure A.3 for an example calculation. For the comparisons presented in Figure 4.8, the raw MIC values for each lineage were first normalized by subtracting the average Day 1 MIC of each of their respective lineages. A two-sample t-test was performed for

the Day 15 MIC_{TOB} values of the "WT" and "PM" lineages evolved to tobramycin in each of the four pairs of isolates. See Figure A.4 for an example calculation. Calculations were done in MATLAB R2016b using the functions "`anova1`" for one-way ANOVA, "`multcompare`" for Tukey HSD test, and "`ttest2`" for two-sample t-test.

2.4 Results

2.4.1 Adaptive evolution of *P. aeruginosa* to sequences of antibiotics

To test how different antibiotic resistance backgrounds affect the subsequent adaptation dynamics when evolved to a new antibiotic, we used a laboratory evolution approach to evolve *P. aeruginosa* to all two-drug sequences of the three clinically relevant drugs piperacillin, tobramycin, and ciprofloxacin. In each of the experimental sequences, *P. aeruginosa* was subjected to 20 days of adaptation to each drug by serially passaging parallel replicate cultures to increasing concentrations of the drugs followed subsequently by 20 more days of adaptation to each of the three drugs or to LB media without drug (Figure 2.1). Additional parallel replicates were adapted to LB media without drug for 40 days as a control. For each drug treatment, changes in the resistance to the other two drugs were concurrently measured (Figure 2.1B). Minimum inhibitory concentration (MIC) gradients in microtiter plates were used to simultaneously measure the drug resistance level and to propagate the bacteria daily. To adapt the bacteria to a drug, a sample is taken from the population from the well of the highest drug concentration that allowed for growth (i.e. MIC/2), and then used to inoculate a new MIC gradient. This serial dilution cycle is done daily.

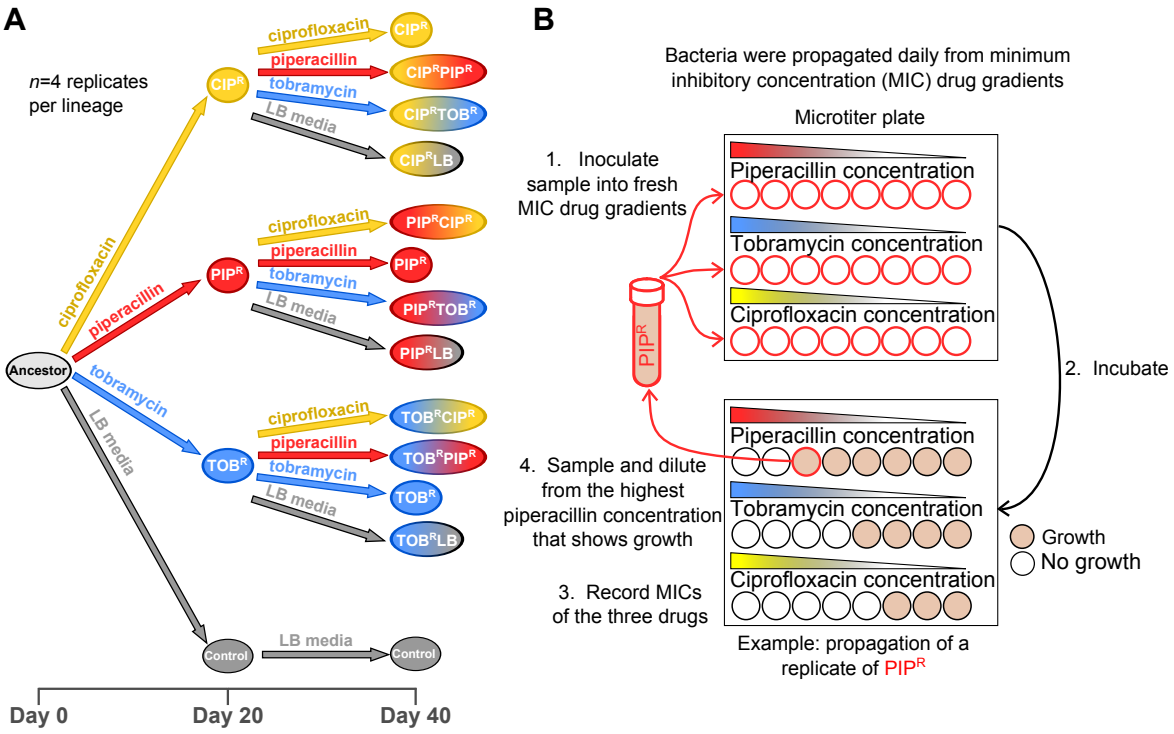

Figure 2.1: **Adaptive evolution of *P. aeruginosa* to three antibiotics.** (A) Ancestral *P. aeruginosa* PA14 was evolved daily for twenty days to piperacillin, tobramycin, ciprofloxacin, and LB media. In the following twenty days, the one-drug-resistant lineages were passaged further to the first drug, as well as sub-passaged to the other two drugs, and to LB media. (B) Bacteria were taken from the highest concentration that allowed growth (defined as OD_{600}>0.1), diluted in fresh LB, and inoculated into fresh MIC gradients, corresponding to a daily dilution factor of 1/500. After overnight incubation, the process is then repeated.

More explicitly, 20 µl of culture is sampled from the well of the highest concentration that allowed for growth, then diluted in 5 ml of fresh LB media, and then this diluted culture is used to inoculate a new MIC gradient. This dilution protocol results in a daily dilution factor of the bacterial population of 1/500 (Materials and Methods, Figure 2.1B). Figure 2.3 shows the estimated number of generations per day for the evolved lineages based on the daily measurements of the OD_{600}. For each lineage the OD_{600} values are fairly consistent from day to day (Figure 2.2), and so with a dilution factor of 1/500, the cultures undergo approximately nine generations of growth per daily dilution cycle. We used the following equation to calculate the estimated number of doublings:

$$d = \frac{log(\mathrm{OD}_n) - log(\mathrm{OD}_{n\text{-}1} \times \frac{1}{500})}{log(2)}$$

In this equation, d is the number of doublings, $\mathrm{OD_n}$ is the optical density of the population being propagated on a given day, $\mathrm{OD_{n\text{-}1}}$ is the optical density of the population from the previous day, and 1/500 denotes the dilution factor. This is derived from the equation:

$$\mathrm{OD}_n = \mathrm{OD}_{n\text{-}1} \times \frac{1}{500} \times 2^d$$

The exception is that for Day 1, the equation is:

$$d = \frac{log(\mathrm{OD}_n) - log(0.0005)}{log(2)}$$

This is because we chose an OD_{600} of 0.0005 as the initial inoculum concentration for Day 1.

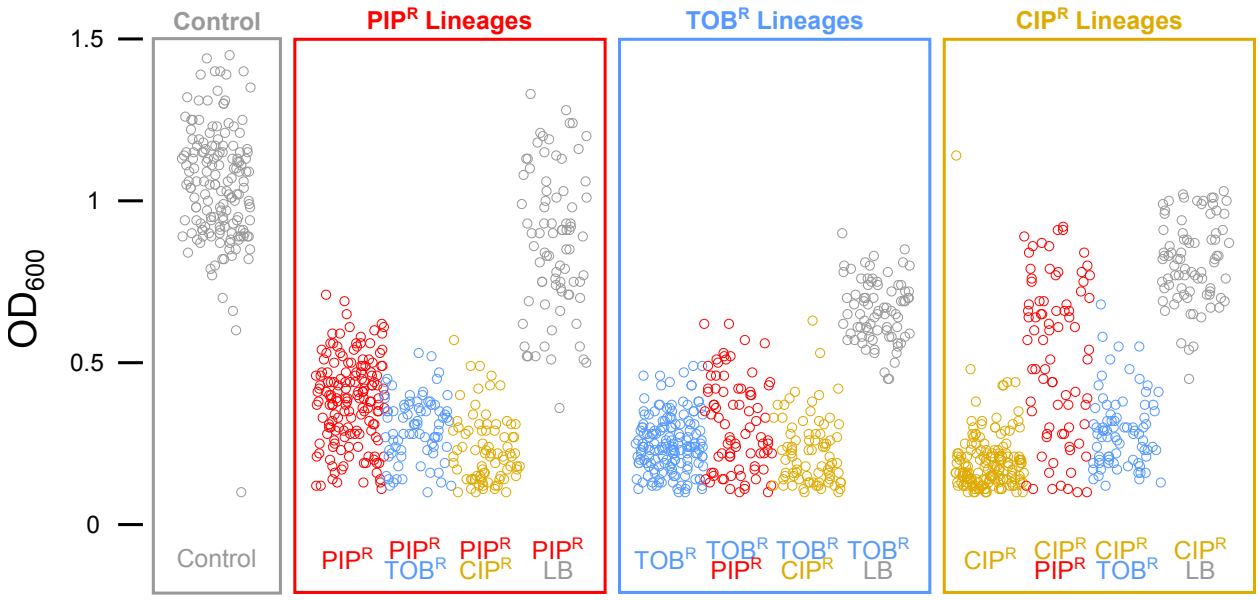

Figure 2.2: **Distribution of the optical densities of the propagated wells.** The OD_{600} values of the wells from which bacteria are sampled and propagated from are shown for each lineage. For example, "PIP^R" in the "PIP^R lineages" shows the OD_{600} values of Day 1 through Day 40 of the four replicates of PIP^R (there should be 160 data points). "PIP^RTOB^R" in the "PIP^R" lineages shows the OD_{600} values of Day 21 through Day 40 of the four replicates of PIP^RTOB^R (there should be 80 data points).

We observed differences in final resistance levels to the different drugs depending on the history of past treatments (or lack of treatments), an effect we call drug order-specific effects of adaptation. Our results show that history of past drug adaptation can affect the rate at which resistance can potentially arise when subsequently adapted to a new antibiotic. Furthermore, in some cases, adaptation to a second drug or to LB can partially or fully restore sensitivity to the first drug. These observations suggest that in order to limit the rate of development of antibiotic resistance, it is important to consider which drugs a bacterial population may have been exposed to in the past when choosing which drugs to subsequently deploy.

The three drugs tested have different mechanisms of action and are clinically used to treat *P. aeruginosa* infections [18]. Piperacillin (PIP) is a beta-lactam that inhibits cell wall

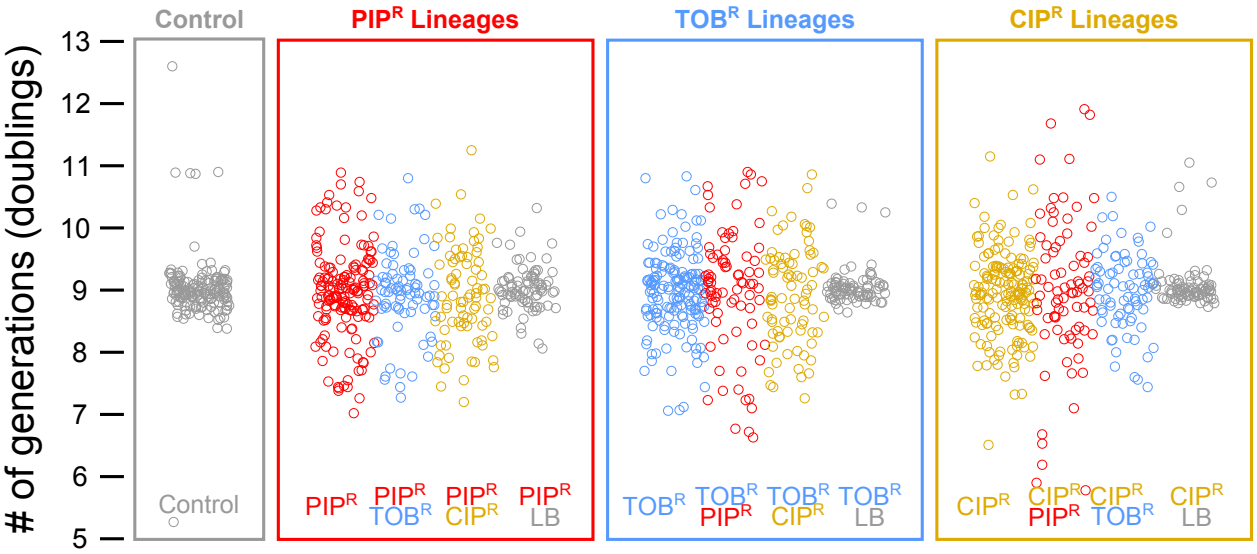

Figure 2.3: **Distribution of the calculated number of generations.** The calculated number of generations are shown for each lineage. For example, "PIP^R" in the "PIP^R lineages" shows the calculated number of doublings of Day 1 through Day 40 of the four replicates of PIP^R (there should be 160 data points). "PIP^RTOB^R" in the "PIP^R" lineages shows the calculated number of doublings of Day 21 through Day 40 of the four replicates of PIP^RTOB^R (there should be 80 data points). Because the dilution factor was chosen to be 1/500 and the fact that the OD_{600} did not vary much between days within a lineage, the calculated number of generations is very close to 9 doublings per day.

synthesis [56]; tobramycin (TOB) is an aminoglycoside that binds to the prokaryote ribosome and inhibits protein synthesis [57]; and ciprofloxacin (CIP) is a fluoroquinolone that binds DNA gyrase and inhibits DNA synthesis [58]. We chose to study these three antibiotics because of their common use in the clinical setting to treat *P. aeruginosa* infections [18], their diverse mechanisms of action, and their well-studied resistance mechanisms [19]. Adaptive evolution for 20 days to these drugs individually resulted in one-drug-resistant mutants denoted PIP^R, TOB^R, and CIP^R. Day 20 PIP^R, TOB^R and CIP^R had averages of 32-, 64-, and 64- times higher MICs to piperacillin, tobramycin, and ciprofloxacin, respectively, compared to their initial levels.

2.4.2 Drug order-specific effects

By following how the resistance to each of the three drugs changes for each of the drug sequences (Figure 2.4; Figure 2.5 and Figure 2.6 and Table A.1), we observed three types of drug order-specific effects in the MIC profiles (Figure 2.7). In the first type, prior adaptation to a first drug reduces the rate of subsequent adaptation to a second drug (such that the endpoint level of resistance to that second drug is lower compared to the amount of resistance developed when the Day 0 Ancestor is directly evolved to that second drug). We observed that evolution first to piperacillin reduces the rate of subsequent evolution to tobramycin (Figure 2.4D and 2E). That is, the MIC_{TOB} of Day 40 PIP^RTOB^R was less than that of Day 20 TOB^R (Figure 2.7B, $p<0.05$). This observation suggests that in some cases, different bacterial populations may evolve resistance to a given antibiotic at different rates depending on the history of prior adaptations that the populations have experienced. Having knowledge

of prior adaptations may then potentially be used to slow down the development of resistance to a drug if that drug is selected rationally. Interestingly, we observed no cases where prior adaptation to one drug led to enhancement in the rate of adaptation to a second drug. Note that for now, we focus on summarizing the different drug-order specific effects (as seen by the changes in drug MICs), and later we discuss several hypotheses for the underlying mechanisms of the drug-order specific effects based on analysis of the genomic mutations of the adapted lineages.

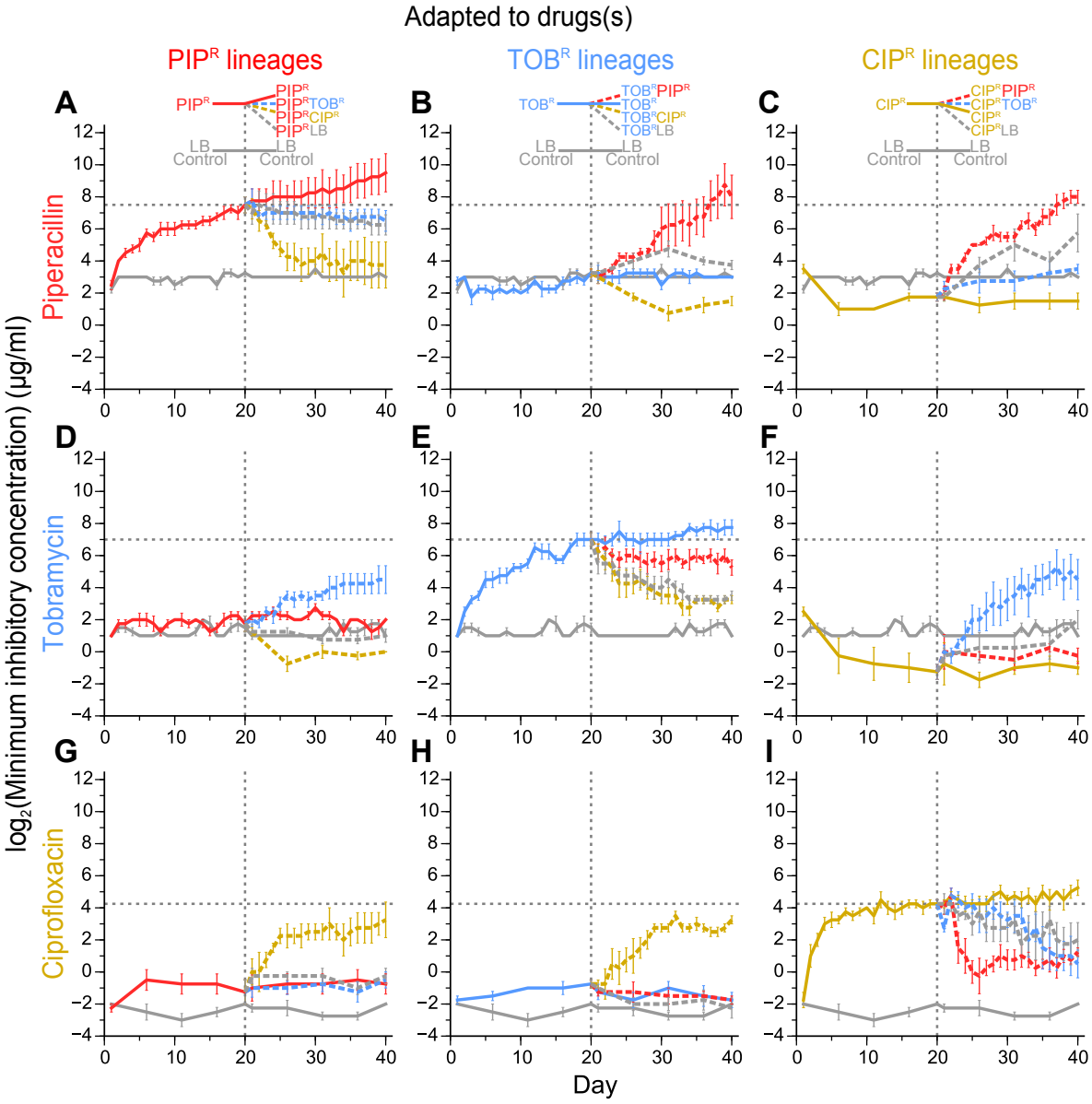

Figure 2.4: **MIC time courses of adaptive evolution.** Plots show the MICs of the treatments to the three drugs and LB over time. The top (A, B, C), middle (D, E, F), and bottom (G, H, I) rows show the MICs to piperacillin, tobramycin, and ciprofloxacin, respectively. The first, second, and third columns show the MICs of the PIP^R, TOB^R, and CIP^R lineages, respectively. The dotted black lines mark the Day 20 MICs of the three drugs (i.e. MIC_{PIP} of Day 20 PIP^R in (A), MIC_{TOB} of Day 20 TOB^R in (E), and MIC_{CIP} of Day 20 CIP^R in (I)). Error bars show SEM of four replicates per treatment.

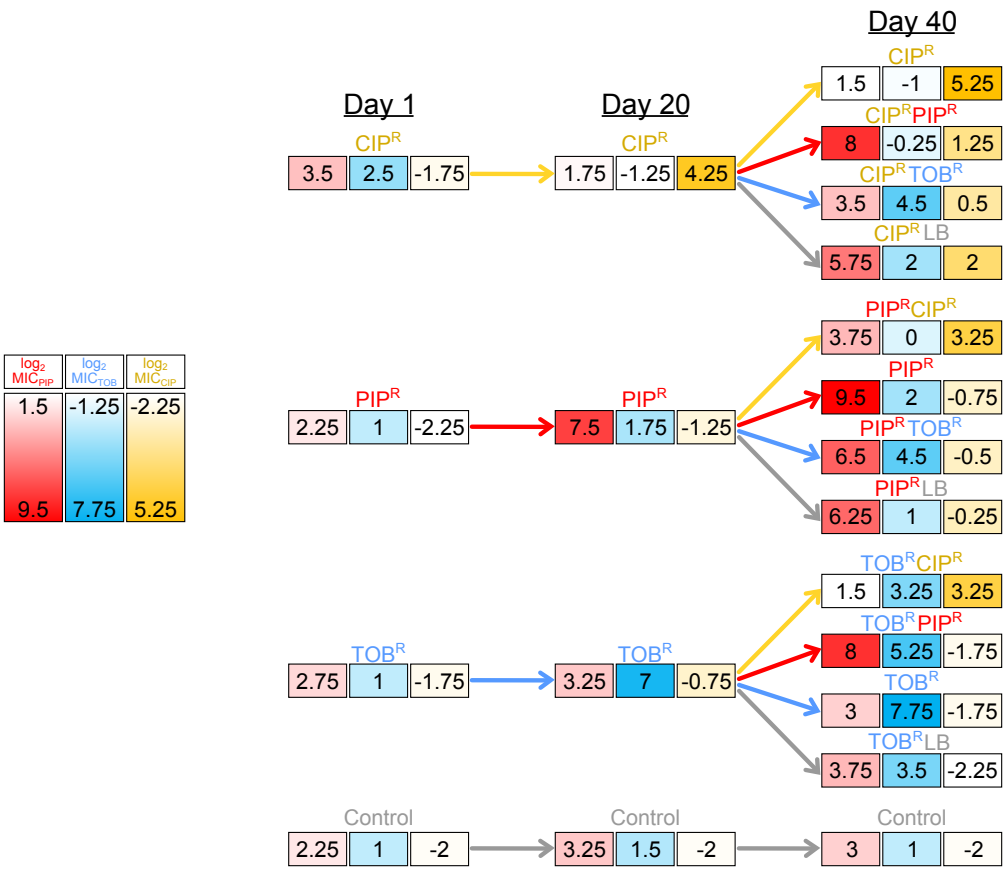

Figure 2.5: **Summary of the MIC time courses.** This figure summarizes the data presented in Figure 2.4. The Day 1, Day 20, and Day 40 $\log_2$ MIC values (µg/ml) of piperacillin, tobramycin, and ciprofloxacin are shown for all the evolved lineages of the main adaptive evolution experiment. The values are the average of four replicates per lineage (Table A.1). For each lineage, the left, middle, and right boxes denote the MIC_{PIP}, MIC_{TOB}, and MIC_{CIP}, respectively. The color intensity is normalized by the minimum and maximum MIC of each drug across all the lineages. For example, for $\log_2$ MIC_{PIP}, the lowest value is 1.5, which is seen in Day 40 CIP^{R}, and the highest $\log_2$ MIC_{PIP} is 9.5, which is seen in Day 40 PIP^{R}. The color of the arrow denotes the treatment.

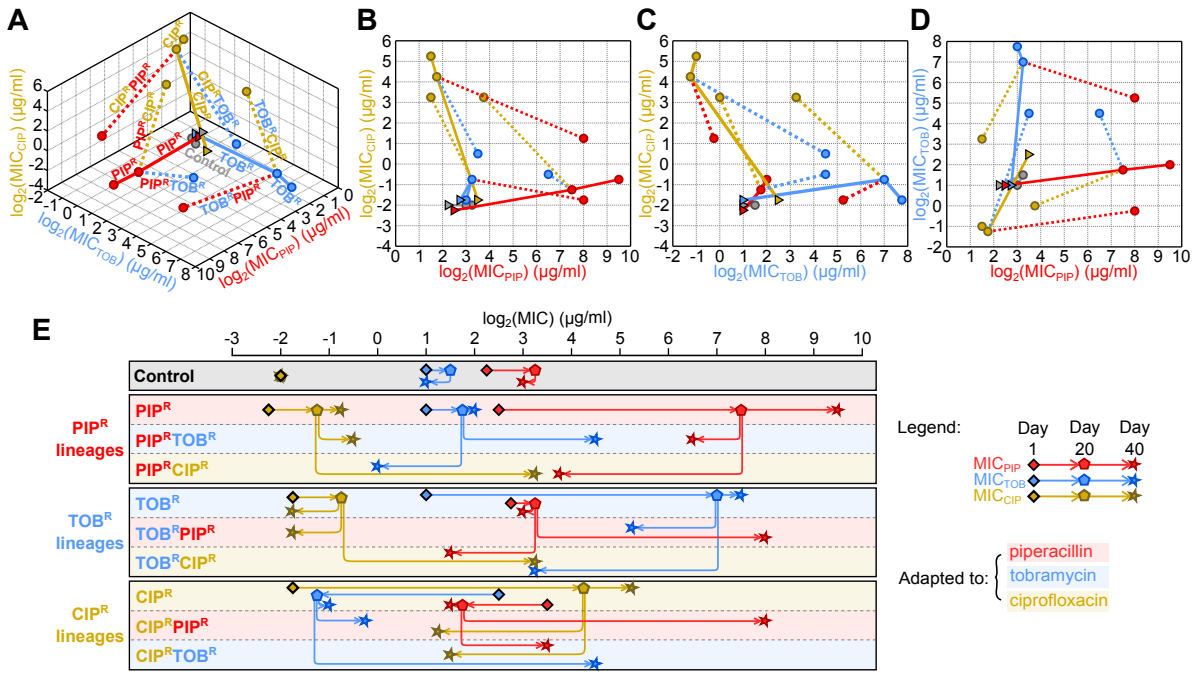

Figure 2.6: **Visualization of drug order-specific effects and quantification of the changes in MICs.** All values shown are the averages of four replicates (see Table A.1). (A) The MICs of the three drugs for Days 1, 20, and 40 for all treatments are plotted in 3D MIC space to show how the MIC profiles change over the course of adaptation. Day 1 MICs are denoted by the triangles. A "non-right angle" indicates a change in resistance to one (or more) of the other drug(s). The color/style of the line indicates the treatment, and is labeled as such. (B to D) 2D projections of (A). Labels for the lines carry over from (A). (E) Changes in average MICs for all drugs for all treatments are plotted on a single axis to better facilitate quantitative comparison. Here, red, blue, and yellow lines denote MICs to piperacillin, tobramycin, and ciprofloxacin, respectively.

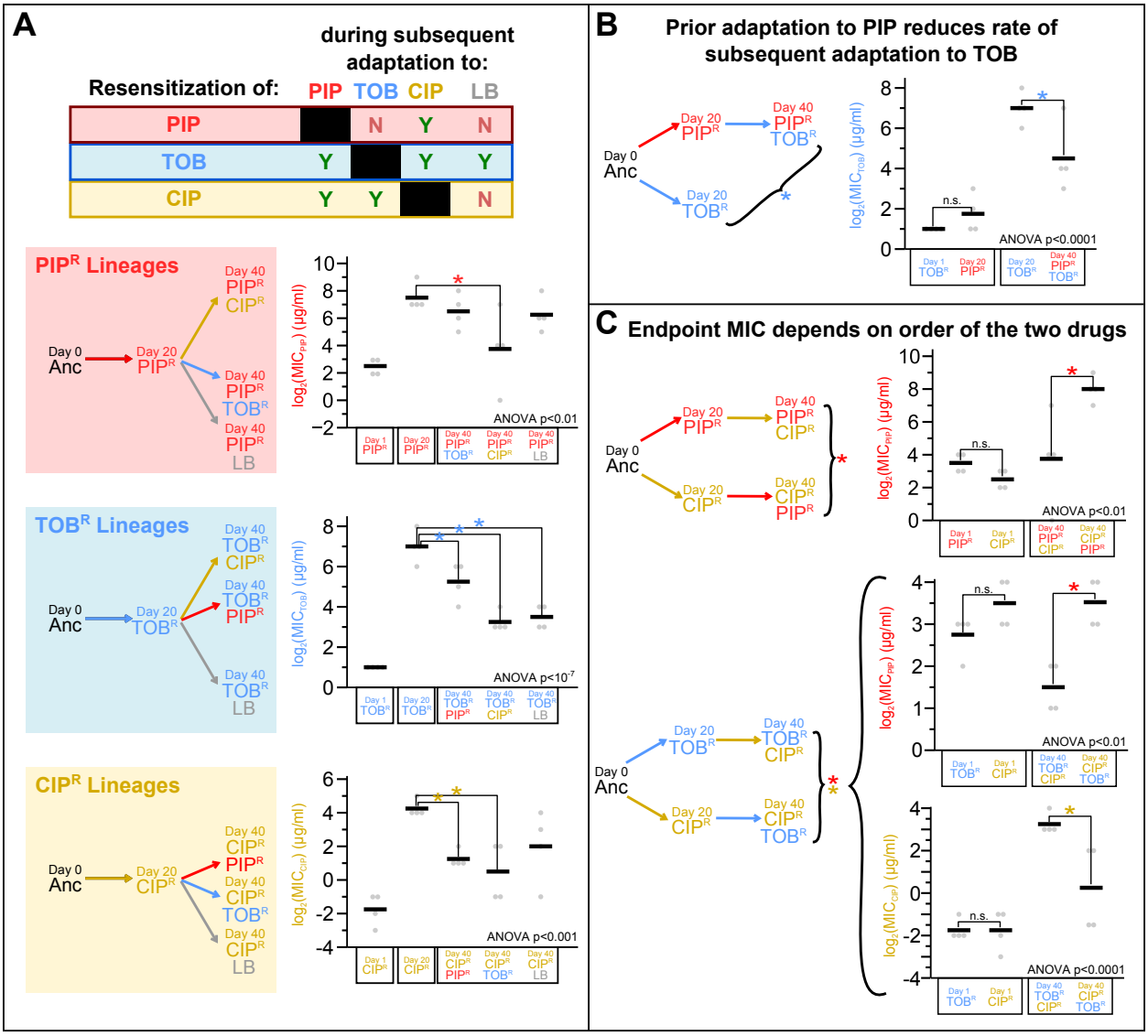

Figure 2.7: **Summary of the drug order-specific effects.** (A) The Day 20 PIP^R, TOB^R, and CIP^R lineages were partially or fully resensitized to piperacillin, tobramycin, and ciprofloxacin, respectively, during subsequent adaptation to the other two drugs and/or LB. The table above the plots summarizes which subsequent adaptations (columns) led to the resensitization of the three drugs in their respective lineages (rows). (B) The MIC_{TOB} of Day 40 PIP^RTOB^R was less than that of Day 20 TOB^R ($p<0.05$, Tukey HSD), while the MIC_{TOB} of Day 1 TOB^R and Day 20 PIP^R were comparable. (C) When bacteria are adapted to two drugs, the order of adaptation to those two drugs can lead to differences in the endpoint MICs. For example in the first plot, adaptation to ciprofloxacin followed by piperacillin led to a higher final MIC_{PIP} than the reverse order (MIC_{PIP} of Day 40 CIP^RPIP^R vs. Day 40 PIP^RCIP^R, $p<0.05$) when they had initially comparable MIC values (MIC_{PIP} of Day 1 PIP^R vs. Day 1 CIP^R). For all three panels, the asterisks denote $p<0.05$ (Tukey HSD), n.s. denotes $p>0.05$, and the color of the asterisk denotes which drug MIC is being compared. In the plots, for each lineage being shown, the black bar denotes the mean of the four individual replicate values (gray dots).

In the second type of drug order-specific effects, adaptation to a second drug or to LB restores the susceptibility to the first drug (Figure 2.7A). In these experiments, we were first interested to see if the increases in MICs of the one-drug-resistant lineages (Day 20 PIP^R, TOB^R, and CIP^R) were permanent or transient. By evolving them to LB and hence removing the selection pressure of the drug for 20 days, we observed that the high MIC_{PIP} was maintained in Day 40 PIP^RLB (Figure 2.7A (top), p=0.80; Figure 2.4A), while MIC_{TOB} declines (leading to partial resensitization) in Day 40 TOB^RLB (Figure 2.7A (middle), p<0.0001; Figure 2.4E), and MIC_{CIP} declines (although not significantly) in Day 40 CIP^RLB (Figure 2.7A (bottom), p=0.18; Figure 2.4I). Thus for these three drugs, removal of the drug pressure can maintain the high resistance or lead to resensitization in a drug-specific manner. Similar trends were seen in a recent adaptive evolution study whereby *P. aeruginosa* was evolved to tobramycin, ciprofloxacin, piperacillin/tazobactam, meropenem, and ceftazidime, followed by subsequent adaptation in the absence of the drug (growth medium only) to determine the effects of removing the drug selection pressure [59]. Similar to the patterns seen in our study, they observed that the tobramycin-resistant cultures partially resensitized, the ciprofloxacin-resistant cultures had a modest resensitization, and the three beta-lactam-evolved cultures maintained high levels of resistance.

Next we were interested to see if evolving the one-drug-resistant lineages to the other two drugs would show the same patterns seen as when evolved to LB. Interestingly, we saw unique outcomes for each of the three lineages. When Day 20 PIP^R was evolved to tobramycin, the MIC_{PIP} of Day 40 $PIP^R TOB^R$ remained high (p=0.90), similar to how the MIC_{PIP} of Day 40 PIP^RLB remained high (Figure 2.7A (top)). This result suggests that subsequent tobramycin adaptation has no role in altering the high piperacillin resistance and can then

result in multidrug-resistant *P. aeruginosa* cultures that are resistant to both piperacillin and tobramycin. On the other hand, when Day 20 PIP^R was evolved to ciprofloxacin, the resulting cultures became resensitized to piperacillin (Figure 2.7A (top), $p<0.05$) and the MIC_{PIP} declined to levels comparable to those of the initially susceptible cultures (MIC_{PIP} of Day 1 PIP^R vs. Day 40 PIP^RCIP^R, $p=0.80$), indicative of a full resensitization. Since resensitization did not occur after subsequent adaptation to tobramycin or LB, we suspect that the subsequent ciprofloxacin adaptation had an active role in the resensitization to piperacillin in such a way that tobramycin and LB did not. These results show that if a piperacillin-resistant culture (that is also sensitive to tobramycin and ciprofloxacin) is evolved to tobramycin, multidrug-resistance can occur. However if it is evolved to ciprofloxacin, despite the fact that ciprofloxacin resistance increases, the culture becomes susceptible to piperacillin again, making piperacillin a potentially rational choice for further treatment.

When Day 20 TOB^R was evolved to ciprofloxacin, partial resensitization occurred MIC_{TOB} of Day 20 TOB^R vs. Day 40 TOB^RCIP^R, $p<10^{-5}$) and the MIC_{TOB} of Day 40 TOB^RCIP^R fell to a comparable level as that of Day 40 TOB^RLB ($p=0.98$) (Figure 2.7A (middle)). This result suggests that the resensitization seen during the subsequent ciprofloxacin adaptation is not caused by the selection pressure of ciprofloxacin, but rather by the absence of the selection pressure of tobramycin. On the other hand, evolving Day 20 TOB^R to piperacillin also led to a partial resensitization (MIC_{TOB} of Day 20 TOB^R vs. Day 40 TOB^RPIP^R, $p<0.05$), but not as much as it did when Day 20 TOB^R was evolved to ciprofloxacin (MIC_{TOB} of Day 40 TOB^RPIP^R vs. Day 40 TOB^RCIP^R, $p<0.01$) and LB (MIC_{TOB} of Day 40 TOB^RPIP^R vs. Day 40 TOB^RLB, $p<0.05$). Because of this difference, we suspect that the maintenance of the comparably high tobramycin resistance is a consequence of the piperacillin selection

pressure, since we observed that adaptation to zero drug pressure in LB led to substantially greater resensitization. This case highlights how removal of all drug pressures may lead to the resensitization of the culture more than with the treatment of the culture to a new drug. In conjunction with the result that subsequent tobramycin adaptation of Day 20 PIP^R still maintained a high MIC_{PIP}, this case then also shows how regardless of the order, sequential adaptation to piperacillin and tobramycin leads to multidrug resistance of the two drugs.

Lastly, when Day 20 CIP^R was evolved to piperacillin and tobramycin, both treatments lead to a partial resensitization to ciprofloxacin (Figure 2.7A (bottom)). During subsequent tobramycin adaptation, the decrease in the MIC_{CIP} from Day 20 CIP^R to Day 40 CIP^RTOB^R ($p<0.01$) was marginally more than the decrease in the MIC_{CIP} from Day 20 CIP^R to Day 40 CIP^RPIP^R ($p<0.05$) during subsequent piperacillin adaptation. As mentioned above, subsequent adaptation of Day 20 CIP^R to LB led to a decrease in MIC_{CIP} that was not statistically significant; however, we argue that the decrease is comparable to that seen when adapted to piperacillin and tobramycin as the final MIC_{CIP} of Day 40 CIP^RLB was not significantly different than that of Day 40 CIP^RPIP^R ($p=0.93$), and that of Day 40 CIP^RTOB^R ($p=0.53$). Hence, in this case, evolution of a ciprofloxacin-resistant culture to either a different drug or to a no-drug condition led to a partial resensitization of ciprofloxacin. Interestingly, we also observed that the resensitization that occurred during subsequent piperacillin adaptation happened more quickly than the resensitization that occurred during subsequent tobramycin and LB adaptation (Figure 2.4I). After five days of subsequent piperacillin adaptation (Day 25 CIP^RPIP^R), the MIC_{CIP} was significantly different than that of Day 20 CIP^R ($p<0.001$), while this was not the case after five days of subsequent tobramycin ($p=1.00$) or LB ($p=0.57$) adaptation. These cases where partial or full resensitization to the first drug occurs after

adaptation to a second drug or LB highlight opportunities where resistance to one drug can potentially be reversed by treating with a second drug or by removing the drug pressure completely.

The last type of drug order-specific effects is when the final MIC of a drug is different after adaptation to a two-drug sequence compared to after adaptation to the opposite order of the two drugs (Figure 2.7C). This third type of drug order-specific effect exists as a consequence of the first type of effect (resensitization of the one-drug-resistant lineages during subsequent adaptations to other drugs) in addition to specific cases of collateral sensitivities during adaptation of certain lineages. First, the MIC_{PIP} was higher when piperacillin was used after ciprofloxacin (Day 40 $CIP^{R}PIP^{R}$) compared to when piperacillin was used before ciprofloxacin (Day 40 $PIP^{R}CIP^{R}$) (Figure 2.7C (top), $p<0.05$). In this case, adaptation to piperacillin first led to high levels of piperacillin resistance, and subsequent adaptation to ciprofloxacin led to the resensitization to piperacillin as discussed before (Figure 2.4A). On the other hand, even though adaptation to ciprofloxacin first led to a collateral sensitivity to piperacillin (Figure 2.8A (right), $p<0.01$), subsequent adaptation to piperacillin resulted in a final MIC_{PIP} comparable to that of Day 20 PIP^{R} (Figure 2.4C).

Next, we observed that during the adaptation to tobramycin followed by ciprofloxacin and vice versa, the final MIC values of piperacillin and ciprofloxacin were different depending on the order of adaptation to the two drugs (Figure 2.7C (bottom and middle)). With regards to the difference seen in the final MIC_{CIP} (Figure 2.7C (bottom), $p<0.05$), the partial resensitization to ciprofloxacin starting from Day 20 CIP^{R} during subsequent tobramycin adaptation (Figure 2.4I) resulted in the MIC_{CIP} to be less than adaptation to tobramycin first, followed by ciprofloxacin (Figure 2.4H). Finally, it was interesting that even though

piperacillin was not the direct selection pressure, there was a difference in the final MIC_{PIP} level whether ciprofloxacin adaptation occurred after tobramycin adaptation or vice versa (Figure 2.7C (middle), $p<0.01$). In this case, initial adaptation to tobramycin first did not affect the MIC_{PIP} (Figure 2.4B), but subsequent adaptation to ciprofloxacin resulted in a collateral sensitivity to piperacillin (Figure 2.8C, $p<0.01$). On the other hand as previously mentioned, adaptation to ciprofloxacin first initially resulted in the collateral sensitivity to piperacillin (Figure 2.8A (right), $p<0.01$); however, the MIC_{PIP} returned to baseline values during subsequent adaptation to tobramycin (Figure 2.4C). Thus, regardless if ciprofloxacin adaptation occurred before or after tobramycin adaptation, ciprofloxacin adaptation led to piperacillin collateral sensitivity. However, in order to take advantage of this collateral sensitivity, ciprofloxacin adaptation should be used after tobramycin adaptation, rather than vice versa. In a contrasting example, we also found it interesting that while ciprofloxacin adaptation also led to collateral sensitivity of tobramycin, subsequent piperacillin adaptation did not cause the MIC_{TOB} to return to baseline levels (Figure 2.4F) in the manner in which subsequent tobramycin adaptation returned the MIC_{PIP} to baseline values (Figure 2.4C). Altogether, these cases highlight how treating an infection with a sequence of two drugs can result in different resistance profiles depending on the order used.

2.4.3 Collateral sensitivities during ciprofloxacin adaptation

All the cases of collateral sensitivity that were observed occurred during ciprofloxacin treatment whereby ciprofloxacin adaptation resulted in a lower MIC of piperacillin or tobramycin compared to baseline levels (Figure 2.8). First, adaptation to ciprofloxacin starting from

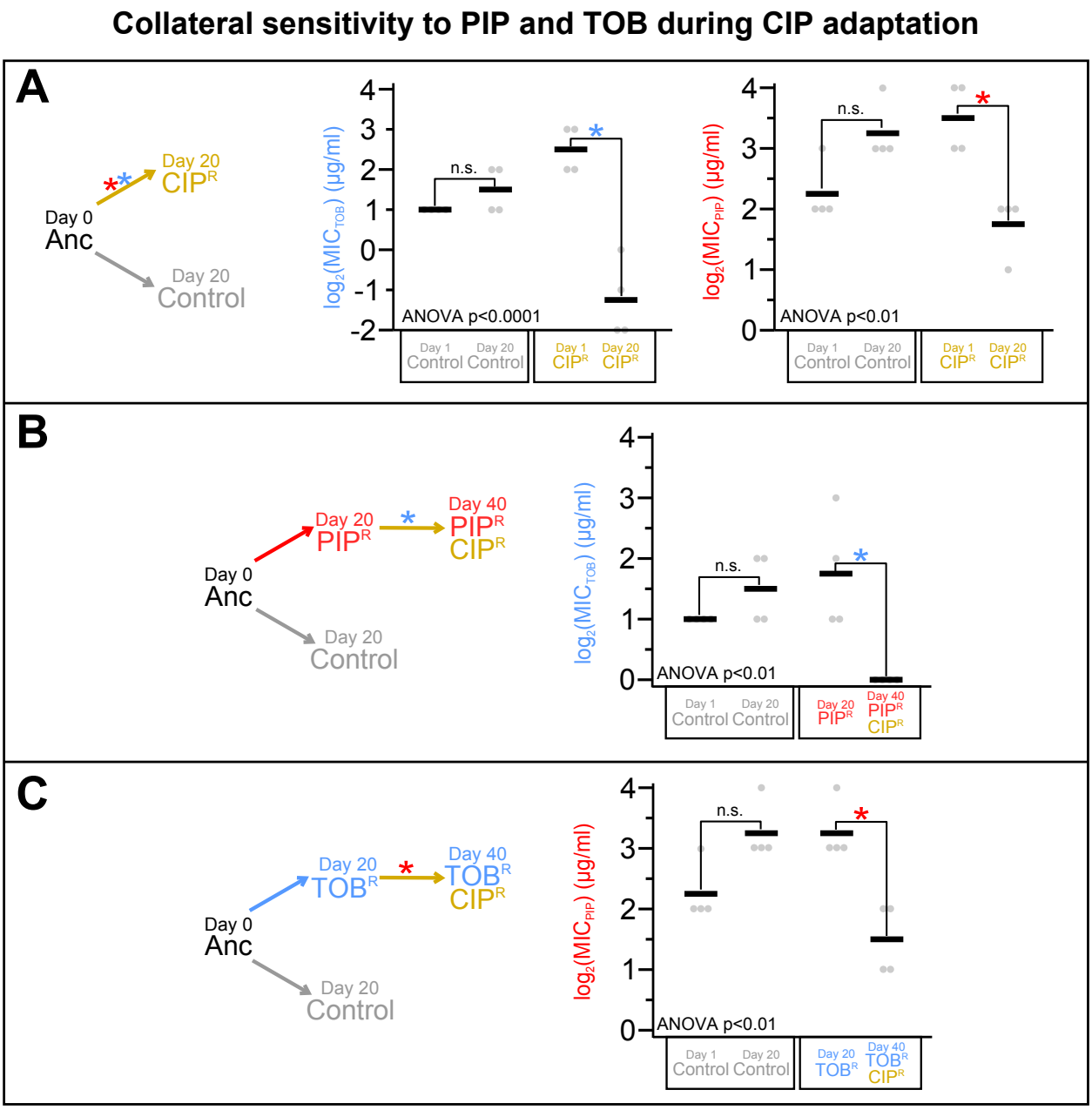

Figure 2.8: **Collateral sensitivity of piperacillin and tobramycin during ciprofloxacin adaptation.** (A) Collateral sensitivities to tobramycin (left) and piperacillin (right) were observed during the evolution starting from Day 0 Ancestor to ciprofloxacin. While there were no statistically significant changes in MIC_{TOB} and MIC_{PIP} after 20 days of evolution to LB in the Control, there were significant decreases after 20 days of evolution to ciprofloxacin. Similarly, (B) there was a significant decrease in MIC_{TOB} when Day 20 PIP^R was subsequently adapted to ciprofloxacin, (C) and in MIC_{PIP} when Day 20 TOB^R was subsequently adapted to ciprofloxacin. For all three panels, the asterisks denote $p<0.05$ (Tukey HSD), n.s. denotes $p>0.05$, and the color of the asterisk denotes which drug MIC is being compared. In the plots, for each lineage being shown, the black bar denotes the mean of the four individual replicate values (gray dots). See Figure A.2 for an example calculation of the statistical tests.

the Day 0 Ancestor resulted in collateral sensitivity to both piperacillin (Figure 2.4C; Figure 2.8A (right), $p<0.01$) and tobramycin (Figure 2.4F; Figure 2.8A (left), $p<0.0001$). Next, adaptation to ciprofloxacin starting from both the one-drug-evolved lineages Day 20 PIP^R (Figure 2.4D) and Day 20 TOB^R (Figure 2.4B) resulted in collateral sensitivity to tobramycin (Figure 2.8B, $p<0.01$) and piperacillin (Figure 2.8C, $p<0.01$), respectively. These results suggest that regardless of historical background, ciprofloxacin adaptation results in collateral sensitivity to the other two drugs. While we observed that collateral sensitivity of other drugs occurs only during ciprofloxacin adaptation, a recent study where *P. aeruginosa* ATCC 27853 was evolved to different antibiotics reported that evolution to tobramycin resulted in collateral sensitivity to piperacillin-tazobactam and ciprofloxacin, whereas we did not observe this effect [59]. Also, this study did not observe that adaptation to ciprofloxacin resulted in collateral sensitivity to piperacillin and tobramycin, as we reported here. We suspect that these inconsistences may be due to strain-specific differences in the different *P. aeruginosa* strains used (strain PA14 was used in this study).

2.4.4 Drug history dependence of pyomelanin hyperproduction

One striking mutation we observed was that three of the four replicates of Day 20 PIP^R (Day 20 PIP^R-1, -2 and -3) had large, ~400 kbp deletions (corresponding to ~6% of the genome) in a conserved region of the chromosome (Figure 3.9 (large red rectangles); Table A.6) suggestive of selective genome reduction [60–63] and have been associated with directed repeats [64] and inverted repeats [65] at the boundaries of the deletions. These large deletions were also fixed in the corresponding Day 40 PIP^RTOB^R, Day 40 PIP^RCIP^R and Day 40 PIP^RLB lineages.

Interestingly, the three PIP^R lineages with these large deletions hyperproduced the brown pigment pyomelanin during piperacillin evolution, and this visually observable phenotype also persisted when evolved to tobramycin (PIP^RTOB^R), ciprofloxacin (PIP^RCIP^R), and LB (PIP^RLB). The loss of *hmgA* as part of the large chromosomal deletions correlates exactly with the pyomelanin phenotype of these lineages. Indeed, *hmgA* mutants of *P. aeruginosa* hyperproduce pyomelanin [66]. This observation shows that evolving to piperacillin results in a high probability of sustaining large deletions spanning *hmgA* which results in the pyomelanogenic phenotype. However, when we evolved the Day 20 TOB^R and CIP^R lineages to piperacillin to yield the Day 40 TOB^RPIP^R and Day 40 CIP^RPIP^R lineages (four replicates each), none of them became pyomelanogenic, suggesting that prior history of tobramycin or ciprofloxacin adaptation leads to a lower propensity of becoming pyomelanogenic when subsequently evolved to piperacillin. Interestingly, one of the Day 20 TOB^R replicates became pyomelanogenic when subsequently evolved to ciprofloxacin (Day 40 TOB^RCIP^R-2). Hence in this study, pyomelanin hyperproduction is a consequence of piperacillin and ciprofloxacin evolution, yet the likelihood to evolve this visually striking and observable phenotype depends on the history of prior drug adaptation.

While the three PIP^R lineages that produced pyomelanin were not significantly more resistant to piperacillin than the non-pyomelanogenic PIP^R lineage, pyomelanin-producing strains have been observed clinically [60], and have been shown to be more persistent in chronic lung infection models [66]. We tested the reproducibility of this example of a phenotypic dependence on history of drug adaptation with a higher throughput approach. Starting with clonal populations of Day 0 Ancestor, Day 20 TOB^R, and Day 20 CIP^R, we seeded 92 replicate populations of each lineage into microplates and we used a 96-pin replicating

tool to serially propagate these populations and evolve them to increasing concentrations of piperacillin daily. The lineages that started from Day 0 Ancestor had the highest propensity to become pyomelanogenic (Figure 2.9A) compared to lineages starting from Day 20 TOB^R (Figure 2.9B) or Day 20 CIP^R (Figure 2.9C). Still, certain lineages starting from Day 20 TOB^R and Day 20 CIP^R did also produce pyomelanin, albeit with less propensity than starting from Day 0 Ancestor (Figure 2.9D).

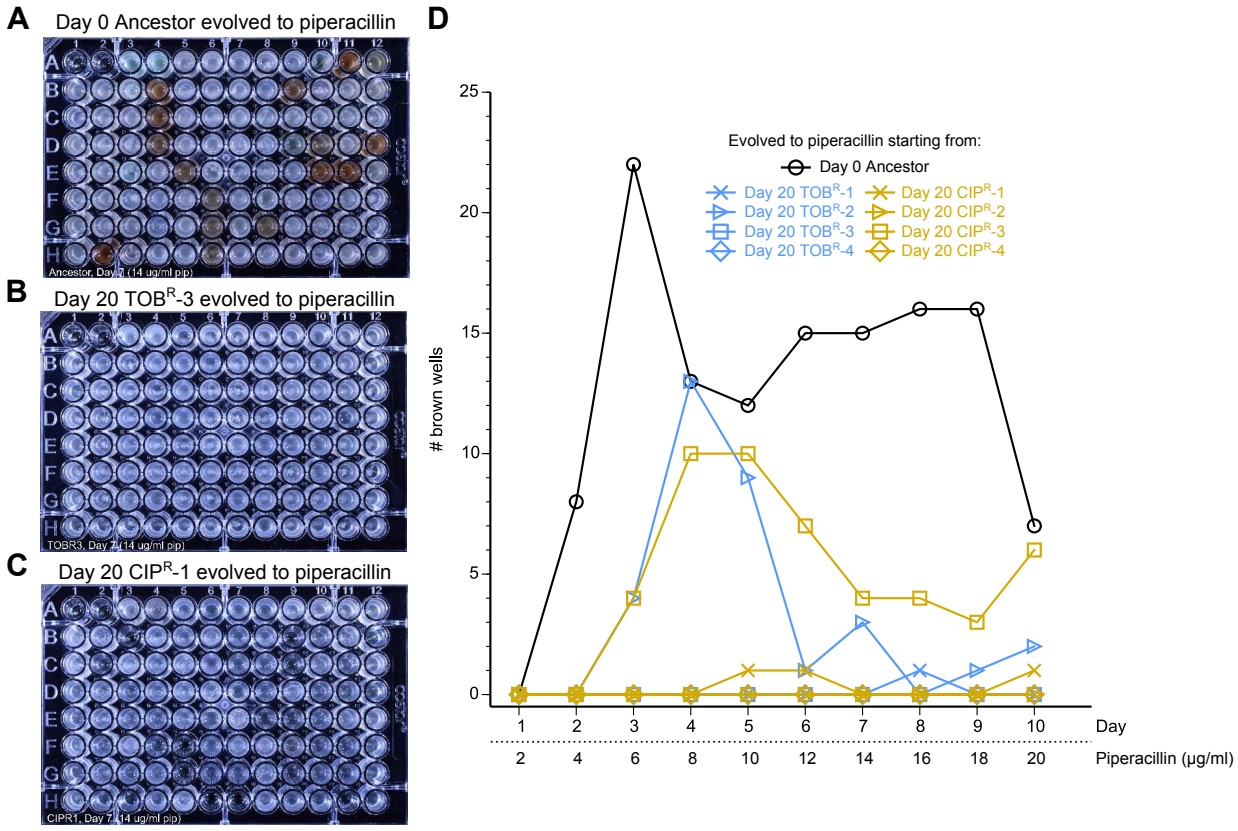

Figure 2.9: **Wild-type *P. aeruginosa* has a higher propensity to become pyomelanogenic when evolved to piperacillin compared to TOB^R and CIP^R lineages.** We tested how common it was for piperacillin adaptation to lead to pyomelanin hyperproduction under different historical backgrounds. 92 replicates of (A) Day 0 Ancestor, (B) Day 20 TOB^R-3, and (C) Day 20 CIP^R-1 were passaged daily to low, increasing concentrations of piperacillin for ten days. Photographs of Day 7 of passaging show how the Ancestor had a higher propensity of evolving the pyomelanin phenotype during piperacillin treatment compared to evolution of Day 20 TOB^R-3 and Day 20 CIP^R-1. (D) The number of visibly brown wells was tracked daily over the course of the ten days of piperacillin evolution. Overall, Day 0 Ancestor had the highest propensity to become pyomelanogenic during piperacillin evolution, followed by Day 20 CIP^R-3 and Day 20 TOB^R-2. Interestingly, the number of brown wells for these lineages did not increase monotonically over time, suggesting heterogeneity in these populations, and that non-pyomelanogenic subpopulations outcompeted the pyomelanogenic ones in the wells that transiently turned brown.

2.5 Discussion

As mentioned in the Introduction of this chapter, the adaptive laboratory evolution of *P. aeruginosa* to the different two-drug sequences and to LB was largely exploratory in nature. We were surprised to see that the MIC time courses yielded an interesting variety of similarities and differences between the evolved lineages. Initially, we had not performed the evolution of the one-drug-evolved lineages to LB (i.e. the PIP^{R}LB, TOB^{R}LB, and CIP^{R}LB lineages), and only did so near the later stages of the project. Performing this control was a worthy endeavor, as it revealed whether the effects observed during adaptation to the second drug were directly related to the second drug, or rather a result of removing the selection pressure of the first drug. Specifically, we observed two interesting cases that differed from the evolutionary dynamics of subsequent LB adaptation. First, subsequent adaptation of Day 20 PIP^{R} to ciprofloxacin resulted in full resensitization to piperacillin, while subsequent adaptation to LB led to maintenance of high MIC_{PIP}. This suggests that the ciprofloxacin adaptation actively contributed to the resensitization. Second, subsequent adaptation of Day 20 TOB^{R} to piperacillin led to maintenance of high MIC_{TOB}, while subsequent adaptation to LB led to partial resensitization to tobramycin. This suggests that piperacillin adaptation actively contributed to the maintenance of high tobramycin resistance. Taken together, these two cases show the interesting result that both adaptation to piperacillin first and tobramycin second and vice versa lead to multidrug resistance of both drugs.

We observed that prior adaptation to piperacillin limited the rate of subsequent adaptation to tobramycin. Here, the MIC_{TOB} of Day 40 $PIP^{R}TOB^{R}$ was less than of Day 20 TOB^{R}, and this difference was statistically significant. While we were careful to phrase this

effect as limiting the *rate* of subsequent adaptation, it is unclear whether or not the maximum amount of tobramycin resistance that can be developed is actually reduced. If Day 40 PIP^RTOB^R was adapted further to tobramycin, would it reach comparable levels to that of Day 20 TOB^R? In our experimental design, adaptations to each drug lasted twenty cycles of daily serial propagation in order to be comparable with each other, but it would indeed be interesting to see if the MIC_{TOB} of Day 40 PIP^RTOB^R has actually plateaued, or if it continues to increase when further adapted to tobramycin. Interestingly, we saw no cases of prior adaptation to one drug resulting to the increased rate of adaptation to a second drug, as was the case observed in a study where populations of *C. reinhardtii* were evolved to different herbicides [55].

Our results show that resistance always develops during adaptation to the second drug, and hence may not immediately be a prudent choice of an antibiotic regimen. However, we did find it interesting that while Day 20 TOB^R became resensitized during subsequent adaptation to ciprofloxacin and LB, it maintained high MIC_{TOB} during subsequent adaptation to piperacillin. In this case, this result suggests that adaptation to piperacillin would lead to *i)* an increase in MIC_{PIP}, and *ii)* maintenance of a high MIC_{TOB}. On the other hand, in this particular scenario, if Day 20 TOB^R cultures are not exposed to any drug, the culture could resensitize in the absence of any drug pressure.

It is important to note that the daily serial propagation protocol is consistent between all of the adaptive evolution experiments done in this study. This facilitates the fair comparison of the evolved lineages as the growth parameters are comparable between the lineages. It was somewhat serendipitous that the combination of dilution factor chosen (1/500), growth rate of the bacteria (doubling time of approximately 2.67 hours), and choice of optical density

threshold for growth (OD_{600}>0.1) led to a fairly consistent number of generations per day (approximately 9 doublings per day). While we eventually decided on these set of parameters for the serial propagation protocol after performing an extensive set of optimization experiments, we note that different studies that employ adaptive laboratory evolution have chosen a variety of other parameters for their serial propagation protocol [30, 40, 41, 67]. Some of these parameters include: how much bacteria is transferred daily, the culture media, the incubation time, and the metric for resistance. It is reasonable to suspect that the growth dynamics are different in all of these different conditions, but what is important is that there is internal consistency within each study such that conclusions can still be compared across studies.

While this study focuses primarily on the adaptation of bacteria to sequential therapies of antibiotics, another complementary active area of research is on the adaptation of bacteria to combination therapies of antibiotics [68]. Combination therapies can exhibit different synergistic and antagonistic drug interactions that can impact the effectiveness of the treatment and influence the evolutionary dynamics of antibiotic resistance development. Experimental and theoretical models suggest that antagonistic interactions between antibiotics can slow down the rate of resistance evolution , even though clinically, synergistic drug pairs are favored since they kill the infection with less amounts of drug [69–71]. Furthermore, recent studies have shown that collateral sensitivities and resistances between drugs are also play a role in the evolution of resistance of combination therapies [41, 43].

Chapter 3

Whole-genome sequencing of the drug-evolved lineages

3.1 Foreword

In this chapter, I describe the results of the whole genome re-sequencing of the evolved lineages that were presented in Chapter 1. We had hypothesized that studying the mutations that occurred in the evolved lineages of *P. aeruginosa* would inform us of potential genome-scale mechanistic explanations of the drug order-specific effects as well as general principles of bacterial evolution. To be frank, this endeavor was also very exploratory in nature and we were excited to see what the data from the sequencing project would yield. To my knowledge, this was the first whole genome sequencing project to be performed in the Papin lab, and we were excited to obtain and analyze this large data set. Analysis of the genes that were mutated required me to extensively pour through the literature and learn about *P. aeruginosa* genetics and their roles antibiotic resistance mechanisms. It was during this phase of the dissertation that I felt like I was learning the most about the physiology and

genetics of this organism.

I would like to mention the externship that I did as a part of the UVA Biotechnology Training Program during the first three months of 2014. I worked at a biotechnology company in San Diego, California called Sapphire Energy whose mission is to develop technologies to produce large-scale quantities of crude oil from cultivated algae. During this externship, I worked primarily on developing an RNA-seq pipeline in order to study the gene expression profiles of different algae strains of interest. I mention this experience, because the bioinformatics tools and skills that I learned during this externship were highly relevant for the work presented in this chapter. I learned how to use different tools to view and manipulate genomes, work in a UNIX environment, write scripts to process large amounts of data in bash and in Perl, and even how to perform PCR. I am fortunate to have gained all of these relevant skills, because I used all of them when I returned to UVA to work on the whole genome sequencing and bioinformatics analysis aspects of this dissertation project.

3.2 Introduction

Determining the genes that play a role in antibiotic resistance is fundamental for understanding this phenomenon. The set of all antibiotic resistance genes has been coined the "resistome" and can refer to both the wild-type alleles as well as mutated forms that confer resistance [72, 73]. Aside from directly genetically perturbing single genes of interest to determine the phenotype of the mutant, there are three primary strategies for studying the resistome of a bacterium.

The first strategy makes use of transposon mutagenesis libraries, which are a collection

of mutants of a specific bacterial strain, where each of the mutants has a single mutation in its genome [74]. The mutation is the insertion of a transposon within a gene, which presumably inactivates the gene. Then, one can screen the library by growing the mutants in the condition of interest, and measure the relevant phenotype to determine if the inactivation of specific genes alters the phenotype compared to wild-type [34]. Essentially, this method is a high throughput version of genetically perturbing single genes. Similar libraries have been made for other organisms including *E. coli* where the genes are completely removed, and hence are true, clean "knock out" mutants [75]. Rather than introducing specific mutations to single genes of interest, a transposon library theoretically contains an inactivating mutation in every non-essential gene in the genome. Transposon libraries have been created for *P. aeruginosa* [74, 76] and they have been used to determine essential genes of the genomes. With regard to probing the resistome, these libraries have been used to screen the mutants by growing them on different antibiotics to determine the MICs of the mutants. A mutant with an increased MIC compared to wild-type suggests that a mutated form of that gene leads to increased resistance, while a decreased MIC suggests increased susceptibility. Such screens of the *P. aeruginosa* transposon libraries tested against a variety of antibiotics provide an invaluable resource for understanding the genetic determinants of resistance [11, 77–79].

The second approach is to perform adaptive laboratory evolution in the presence of antibiotics and then sequence the genomes of the ancestor and the evolved lineage to determine which genes were mutated as a result of the antibiotic selection pressure. This is the approach that was taken in this dissertation. This approach more readily elucidates which genes, when mutated are involved in conferring increased antibiotic resistance, especially when mutations in the same gene are observed in multiple parallel replicates. On the

other hand, this approach can also reveal genes for which a relationship between the known function and resistance is not immediately apparent. Furthermore, if the gene is not well annotated, it can be even more of a challenge to deduce the causal link between genotype and phenotype. Nevertheless, such "evolve and resequence" studies in *P. aeruginosa* have helped elucidate the genetics of adaptation to antibiotics [59, 80]. While screening of the transposon libraries provide information of how mutated genes affect the baseline MIC, sequencing the genomes of evolved strains gives information about which genes are directly mutated during the adaptation process.

Lastly, bacterial pathogens can be studied in the context of *in vivo* human infections. *P. aeruginosa* has been well studied in the context of lung infections in patients with cystic fibrosis [81]. In this environment, the infection can colonize and persist for up to decades. During this time, the infection evolves to adapt to the lung environment. Samples of bacteria can be extracted from different patients, at different locations in the lung, and at different times during the course of the infection to map out the evolutionary trajectories of the bacterial populations [82–86]. It is likely that these populations have been exposed to different antibiotics over the course of the infection and may have evolved resistance to some of the drugs they have been exposed to, and sequencing the genomes to see which mutations occur may reveal a variety of genes that are not only related to antibiotic resistance, but also to the adaptation to the host environment. Altogether, these different, but complementary approaches allow for better understanding of the underlying genetic determinants of antibiotic resistance.

3.3 Materials and methods

Throughout this Materials and methods section, I will use the Day 20 PIP^R-1 lineage as an illustrative example of how the whole genome sequencing and analysis was performed. All of the figures are representative of this lineage and of the *dacC* mutation that was present in this lineage.

3.3.1 Whole-genome sequencing

Frozen samples of Day 0 Ancestor, Day 20 Control, PIP^R, TOB^R, CIP^R, Day 40 Control, PIP^R, TOB^R, CIP^R, PIP^RTOB^R, PIP^RCIP^R, TOB^RPIP^R, TOB^RCIP^R, CIP^RPIP^R, and CIP^RTOB^R were streaked on LB agar plates and incubated at 37°C. Agar plates were submitted to Genewiz Incorporation for sequencing service. A single colony from each plate was chosen for DNA extraction, library preparation, multiplexing, and sequencing using 101-bp paired-end reads with the Illumina HiSeq 2500 platform. Reads were aligned to the reference *P. aeruginosa* PA14 genome (NC_008463.1) with coverage ranging from 113X to 759X. This large range is due to the fact that we submitted samples for sequencing in three batches, and had different numbers of samples for each batch, but had relatively the same number of reads per batch. Nevertheless, the coverage was more than sufficient to identify the SNPs, insertions, and deletions in the genomes. The sequencing reads for Day 0 Ancestor and the 56 drug-evolved lineages are available via the NCBI SRA database (www.ncbi.nlm.nih.gov/sra), accession number SRP100674, BioProject number PRJNA376615.

```
#!/bin/sh
#SBATCH --ntasks=1
#SBATCH --time=12:00:00
#SBATCH --output=output_breseq_S06_Day20_P1
#SBATCH --mail-type=ALL
#SBATCH --mail-user=py4wg@virginia.edu
#SBATCH --partition=serial

module load R/openmpi/3.1.1

cd /scratch/py4wg/adaptive_evolution/breseq_pipeline
breseq -o S06_Day20_P1_output -r PA14_CP000438.1.gbk /scratch/py4wg/
   adaptive_evolution/reads/raw_reads/S06_Day20_P1_CGAGGCTG-
   CTCTCTAT_L001_R1_001.fastq /scratch/py4wg/adaptive_evolution/reads/
   raw_reads/S06_Day20_P1_CGAGGCTG-CTCTCTAT_L001_R2_001.fastq

```

Figure 3.1: **S06_Day20_P1.sbatch.** This is the submission script for running breseq on Day 20 PIP^{R}-1.

3.3.2 Read alignment and calling of mutations

Reads were aligned and mutations were called using the breseq pipeline [87] using default settings. The breseq pipeline mapped the sequence reads to the reference genome and identified genetic discrepancies between the sequenced reads and the reference genome (indicative of mutations). The breseq pipeline is optimized for haploid microbial-sized genomes and is intended for use on adaptive laboratory evolution experiments [87]. We implemented the breseq pipeline on the UVA Rivanna High Performance Computing cluster. Figure 3.1 shows the submission file for running the breseq pipeline for Day 20 PIP^{R}-1. The command to submit the job is: `sbatch S06_Day20_P1.sbatch`.

Because we were interested in comparing the genome of Day 20 PIP^{R}-1 to that of Day 0 Ancestor, we needed to perform a "background subtraction" of the mutations seen in the Day 0 Ancestor. Sequencing the genome of the Day 0 Ancestor revealed 234 mutations with respect to the reference genome of *P. aeruginosa* PA14 (NC_008463.1). These 234 mutations

```
gdtools SUBTRACT -o S06_Day20_P1_diff_anc.gd /scratch/py4wg/adaptive_evolution
   /breseq_pipeline/S06_Day20_P1_output/output/output.gd /scratch/py4wg/
   adaptive_evolution/breseq_pipeline/S01_Day0_Anc_output/output/output.gd
gdtools ANNOTATE -r /sfs/lustre/scratch/py4wg/adaptive_evolution/
   breseq_pipeline/PA14_CP000438.1.gbk S06_Day20_P1_diff_anc.gd
mv output.html S06_Day20_P1_diff_anc.html

```

Figure 3.2: **gdtools.** This code shows the use of gdtools to compare the mutations of Day 20 PIP^{R}-1 to those of Day 0 Ancestor.

Predicted mutations				
position	**mutation**	**annotation**	**gene**	**description**
1,046,490	C→T	A128V (GCC→GTC)	*dacC* →	D-ala-D-ala-carboxypeptidase
1,441,862	$(C)_{6\rightarrow5}$	intergenic (+32/+11)	*PA14_16820* → / ← *PA14_16830*	putative efflux transmembrane protein/conserved hypothetical protein
1,551,346	A→G	C92R (TGC→CGC)	*PA14_18080* ←	putative transcriptional regulator, TetR family
2,157,750	Δ3 bp	coding (1341-1343/1431 nt)	*dacB* ←	putative D-alanyl-D-alanine carboxypeptidase
3,176,159	Δ391,957 bp		*PA14_35720–[PA14_40040]*	***343 genes*** Show
3,923,324	G→A	G71S (GGC→AGC)	*gltA* →	citrate synthase
5,028,201	2 bp→CG	intergenic (-123/+13)	*mntH1* ← / ← *PA14_56360*	NRAMP protein MntH1/conserved hypothetical protein

Figure 3.3: **S06_Day20_P1_diff_anc.html.** This file is the output of gdtools and lists the mutations that were detected in Day 20 PIP^{R}-1 with respect to Day 0 Ancestor.

show how our Papin lab copy of the PA14 strain differs from the published genome. The genomes of all of the evolved lineages then also contain these 234 mutations in addition to the mutations that occurred during the evolution experiment. The `gdtools` function in the breseq pipeline was used to remove these 234 "baseline" mutations and then annotate the remaining mutations (Figure 3.2). Figure 3.3 shows the output of gdtools, which lists the mutations detected in Day 20 PIP^{R}-1.

All reported mutations were visually inspected by viewing the read alignments in IGV [88] (Figure 3.4) and the breseq output files, and mutations with less than 80% frequencies

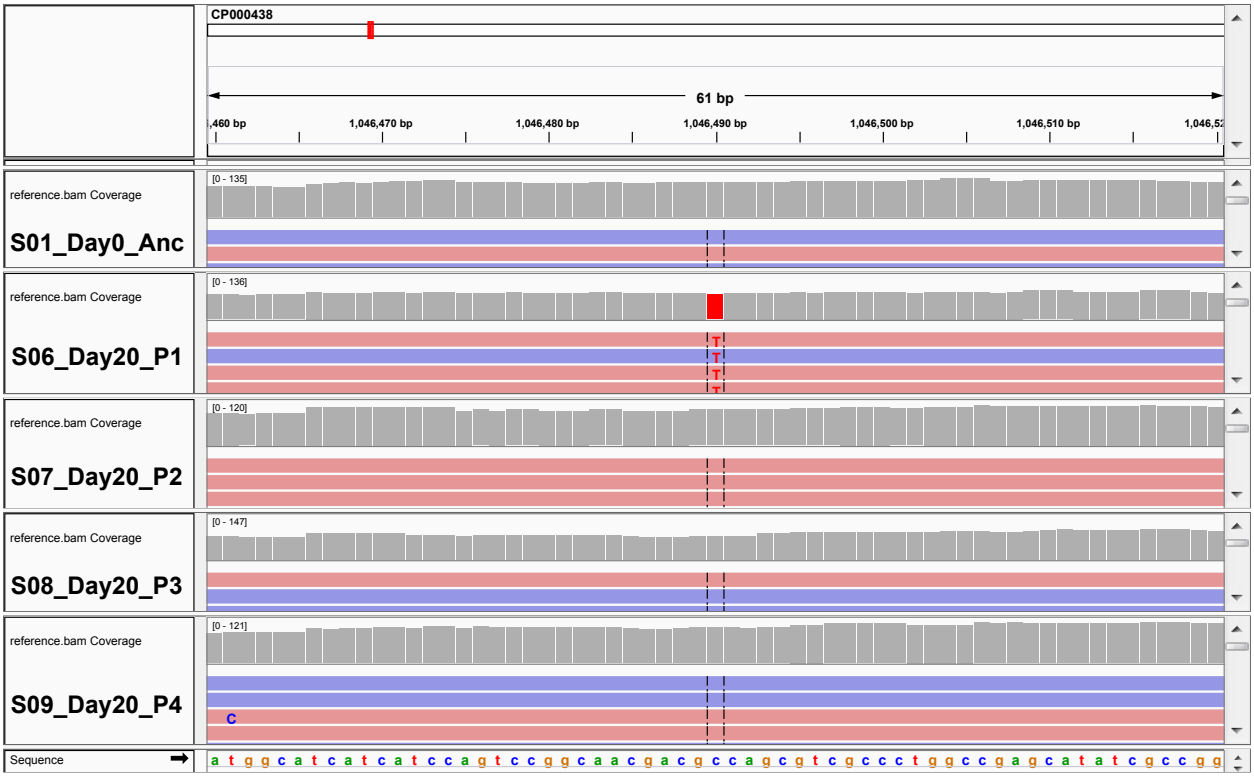

Figure 3.4: **Screenshot of IGV.** The five lanes (rows) show the mapped reads of Day 0 Ancestor, Day 20 PIP^{R}-1, -2, -3, and -4. The browser is zoomed to the area of the genome where the mutation in *dacC* is located (see first row of Figure 3.3). The "C" to "T" SNP is located at position 1,046,490 in the genome in only the Day 20 PIP^{R}-1 lineage.

were not counted. Figure 3.5 shows a similar output from the breseq pipeline. The full list of mutations is presented in Table A.4 and Table A.5. The circos software package [89] was used to plot the mutations by genomic position for Figure 3.9 and the positions of the large chromosomal deletions in Figure 4.8.

We confirmed a subset of the mutations using Sanger sequencing. For each of the Day 20 PIP^{R}, TOB^{R}, and CIP^{R} replicates, we chose one mutation each to confirm (Table 3.1). We also used these to confirm that replicates were not contaminated before submitting them for whole-genome sequencing. These mutations were also confirmed in each of the Day 40 lineages that were derived from the Day 20 PIP^{R}, TOB^{R}, and CIP^{R} replicates.

Predicted mutation

evidence	seq id	position	mutation	annotation	gene	description
RA	CP000438	1,046,490	C→T	A128V (GCC→GTC)	*dacC* →	D-ala-D-ala-carboxypeptidase

Read alignment evidence...

	seq id	position	change	freq	score	reads	annotation	genes	product
*	CP000438	1,046,490	0 C→T	100.0%	280.9	70	A128V (GCC→GTC)	*dacC*	D-ala-D-ala-carboxypeptidase

Reads supporting (aligned to +/- strand): **new** base (40/30): **ref** base (0/0): **total** (40/30)

Figure 3.5: **Output of breseq showing the mutation in *dacC*.** The breseq pipeline outputs an html for each mutation showing the evidence for the call.

Table 3.1: List of primers used in this study

Name	Lineage	Forward Primer Sequence (5'-3')	Reverse Primer Sequence (5'-3')	Position	Mutation
Paeru16SrDNA[a]	*P. aeruginosa* species	GGGGGATCTTCGGACCTCA	TCCTTAGAGTGCCCACCCG	-	-
PA_hmgA[b]	PIP^R-1, -2, -3	GCTGCCATCCACTCAAATTACG	GGGTTGGCTGGTTCATGG	3,435,343	~Δ400kbp
amrB_Tn	*P. aeruginosa* PA14	TGACCTCGATGAACCTCAGC	GAACTGGCGGTAGATGTTGC	-	-
P1_dacC	PIP^R-1	AACGCTTGTCACTGCTTGTCC	AGCGGAAGCCATAGGTCAGC	1,046,490	C → *T*
P2_orfJ	PIP^R-2	TCTGATAAAGATGGGCGAGACC	GACCTTCTCTGGCTGTTGACG	2,033,788	(G)7 → 6
P3_mexR	PIP^R-3	TTCGCCAGTAAGCGGATACC	TTCGTTGCATAGCGTTGTCC	486,113	T → *G*
P4_mucB	PIP^R-4	AGGCTCAGGTCGCTCAACG	ATCCTTCCCAACTGGCTTCC	4,824,640	G → *A*
T1_25490	TOB^R-1	TGCCGATCATTCTGAGTTCG	CCACCGAGAGTTCCAGTTGC	2,229,086	T → *C*
T2_fusA1	TOB^R-2	CGCTGGTCGAAGTGAAGTCC	CAGGCGCTTCTTGATCTGC	755,747	A → *G*
T3_rpsL	TOB^R-3	CGGGGCTTTGTCTTGACG	TGGCATCGAGAGCTTTTTCG	754,922	A → *G*
T4_nuoL	TOB^R-4	TGAATTGCAGGGTCCATTCC	ACCTTCCGCCTGATCTTCG	2,587,299	Δ1 bp
F1_aotJ	CIP^R-1	TGGCCAGGAGCATGGAAAGC	GAGTTCGACGGCCTGATCCC	4,678,735	Δ1 bp
F2_aroB	CIP^R-2	ACGGTTCGTCGCAAATGAAACC	CTTGTTGCAGAAGCCCAACCC	5,946,304	+G
F3_sucD	CIP^R-3	CGGTCTGCGGATCTTCCTGG	CATCGTGCGTTGCGACATGA	3,912,045	T → *G*
F4_aroB	CIP^R-4	GCGTCCAAGATCTCACGGGG	GGCATGACCGCAAGACTACCC	5,945,811	G → *T*

[a]Amplifies a portion of the 16S rDNA specific to *P. aeruginosa* species. Presented as the PA-SS primers in Spilker *et al.* [90]
[b]Amplifies a portion of *hmgA* in *P. aeruginosa* PA14. Failure of amplification is used as a proxy for confirming large chromosomal deletion, since *hmgA* is consistently encompassed in all large deletions.
All primers were optimized to amplify DNA with an annealing temperature of 57°C with OneTaq polymerase (New England Biolabs, M0483).

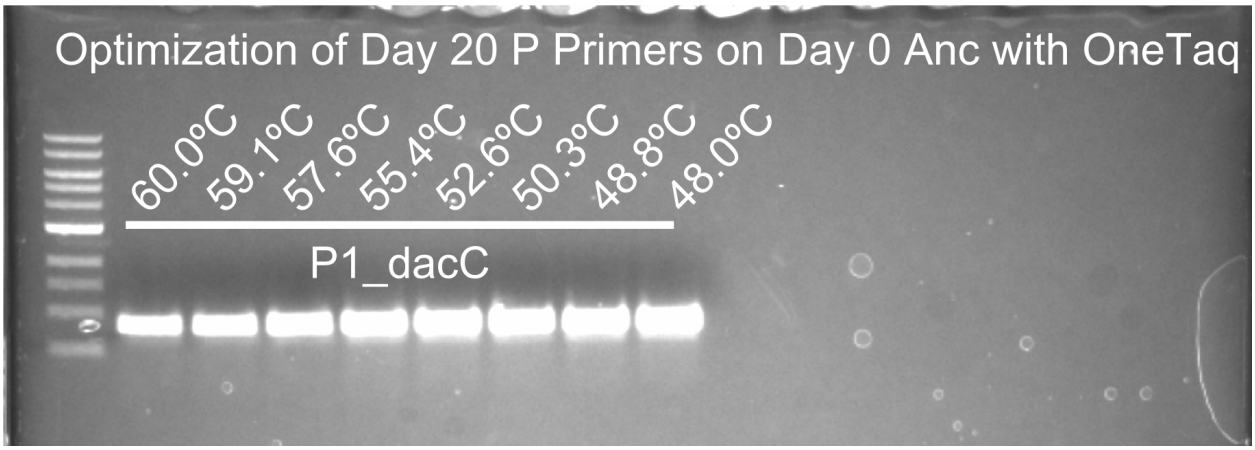

Figure 3.6: **Gradient PCR.** The pair of "P1_dacC" primers were successful at amplifying the region of DNA that encompasses the *dacC* SNP across a range of annealing temperatures.

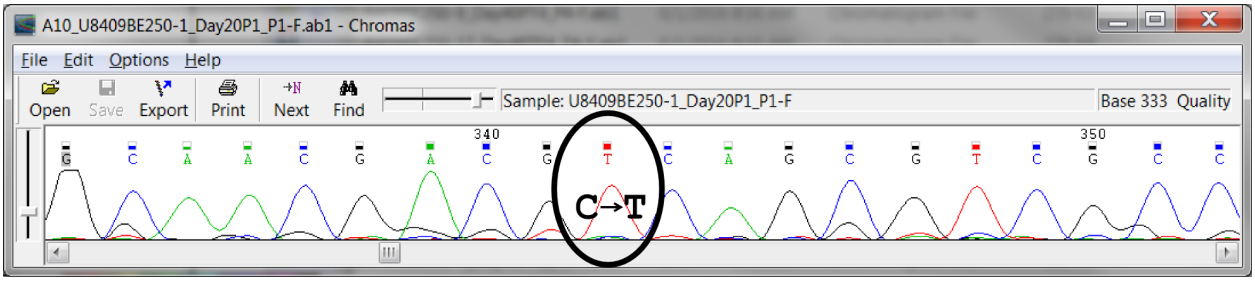

Figure 3.7: **Sanger sequencing.** This chromatogram confirms the presence of the "C" to "T" SNP in the *dacC* gene at position 1,046,490 of the genome of the PIP^{R}-1 lineage.

The primers were designed using Primer3 [91] to amplify approximately 800 bp regions centered on the mutations of interest. OneTaq polymerase (New England Biolabs, M0483) was used for all PCR amplification with an annealing temperature of 57°C. Figure 3.6 shows the gradient PCR that was performed to test the pair of primers used to amplify the region where the *dacC* mutation was located for the PIP^{R}-1 lineage. Figure 3.7 shows confirmation by subsequent Sanger sequencing of the *dacC* SNP in the Day 20 PIP^{R}-1 lineage.

3.4 Results

3.4.1 Genomic mutations of adapted lineages

We hypothesized that genomic mutations acquired during adaptive evolution contributed to the drug order-specific effects observed in the MIC profiles. We sequenced the genomes of the Day 0 Ancestor, Day 20 PIP^R, TOB^R, CIP^R and LB Control lineages and the Day 40 one-drug- and two-drug-evolved lineages, as well as the LB Control lineages. Genome sequencing of the Day 20 and Day 40 mutants revealed a total of 201 unique mutations across the 56 samples consisting of 77 SNPs, 31 insertions, and 93 deletions (Figure 3.8, Figure 3.9, Table A.4 and Table A.5). The 77 SNPs were found within 49 genes. Two SNPs were synonymous and six were intergenic.

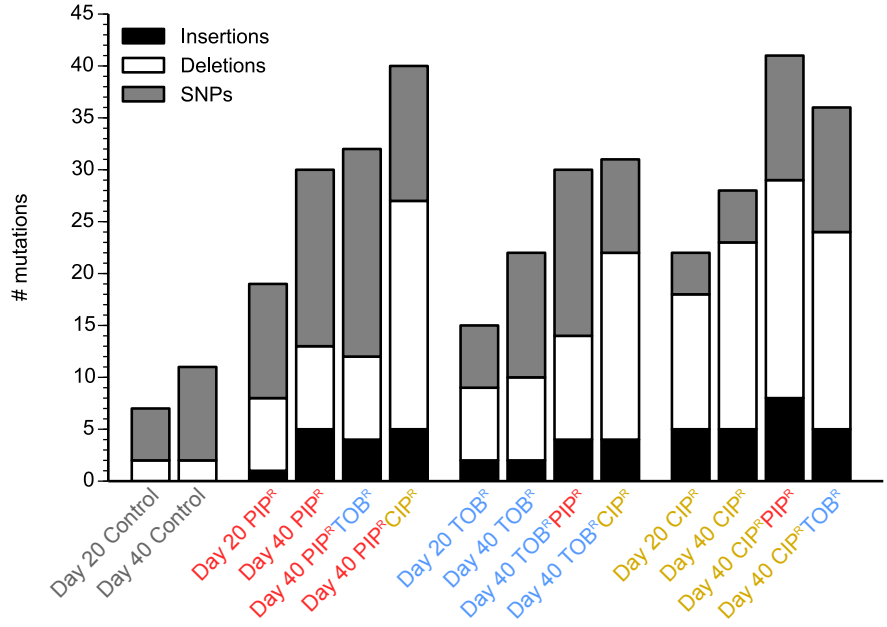

Figure 3.8: **Distribution of mutations.** Histogram of the number of mutations shows that overall, lineages that were evolved to ciprofloxacin accumulated the most mutations and had comparably more deletion mutations.

While some genes were mutated during evolution to all drugs, other mutations were drug-specific and were related to their primary mechanisms of action as would be expected (Table 3.2). Genes encoding transcriptional regulators for multidrug efflux pumps were commonly mutated during evolution to all three drugs (*mexC*, *mexR*, *mexS*, *nalC*, *nalD*, *nfxB*, *parS*) [92]. Ribosomal proteins (*rplJ*, *rplL*, *rpsL*, *rplF*) [93] and NADH dehydrogenase subunits (*nuoB*, *nuoG*, *nuoL*, and *nuoM*) [78, 94] were frequently mutated during tobramycin evolution. The most commonly mutated gene was *fusA1*, which encodes elongation factor G, and was mutated in 11 different lineages adapted to tobramycin. *fusA1* has been observed to be mutated in clinical isolates of *P. aeruginosa* [85, 95, 96] as well as in adaptive evolution studies to aminoglycosides in *P. aeruginosa* [59] and *E. coli* [38, 40, 41]. Mutations in *fusA1* may also contribute to altered intracellular (p)ppGpp levels, which may modulate virulence in *P. aeruginosa* [96]. Mutations in *gyrA* and *gyrB* were observed during ciprofloxacin evolution, but none were observed in *parC* and *parE* (the other genes of the quinolone resistance determining region [18]). Lastly, genes encoding peptidoglycan synthesis enzymes (*dacC*, *mpl*) and beta-lactamase regulators (*ampR*) were mutated during piperacillin treatment. Many of these genes have also been observed to be mutated during human host adaptation of *P. aeruginosa* [84], highlighting the importance of several of these clinical resistance determinants.

3.4.2 Role of the historical contexts in the mutation profiles

We next analyzed the genomic mutations to see how the historical context affects which mutations occur during adaptation to a drug. For example, how do the mutations that

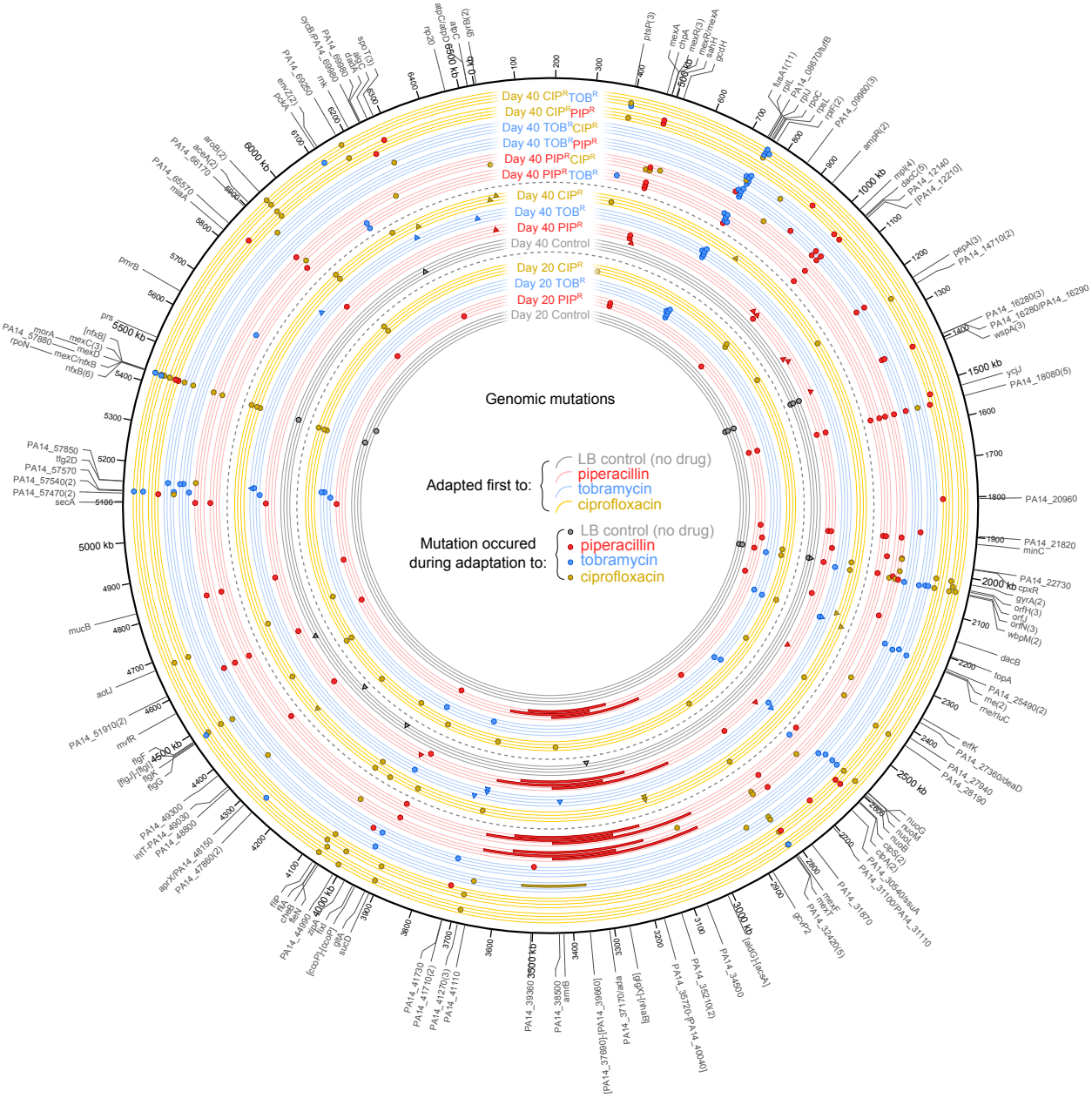

Figure 3.9: **Genomic mutations of the evolved lineages.** Mutations for the Day 20 and Day 40 mutants are plotted according to position on the chromosome. Each lineage is labeled and has four tracks for the four replicates per treatment. The inner set of tracks are the Day 20 one-drug-evolved lineages, the middle set of tracks are the Day 40 one-drug-evolved lineages, and the outer set of tracks are the Day 40 two-drug-evolved lineages. The color of the track denotes the treatment during the first 20 days. The color of the plotted mutation denotes during which treatment the mutation occurred. For example, a blue dot on a yellow track denotes a CIP^RTOB^R mutation that occurred during tobramycin adaptation. For the Day 40 one-drug-evolved lineages, circles denote mutations that occurred during the first set of 20 days, and triangles denote mutations that occurred during the second set of 20 days. Large rectangles denote large genomic deletions. Numbers in parentheses next to gene names indicate the number of unique mutations that occurred in that gene.

Table 3.2: **Frequently mutated genes.**

Category	Locus tag	Gene	Description	# of lineages that have mutations in gene			
				No drug	PIP	TOB	CIP
Multidrug efflux pumps	PA14_60850	*mexC*	multidrug efflux RND membrane fusion protein		3	2	
	PA14_05520	*mexR*	multidrug resistance operon repressor MexR		4	1	
	PA14_32420	*mexS*	putative Zn-dependent oxidoreductase				5
	PA14_16280	*nalC*	putative transcriptional regulator		4		
	PA14_18080	*nalD*	putative transcriptional regulator, TetR family		4		1
	PA14_60860	*nfxB*	transcriptional regulatory protein NfxB			2	8
	PA14_41270	*parS*	putative two-component sensor			2	1
Ribosome	PA14_08820	*fusA1*	elongation factor G			11	
	PA14_08740	*rplJ*	50S ribosomal protein L10			1	
	PA14_08750	*rplL*	50S ribosomal protein L7 / L12			1	
	PA14_08790	*rpsL*	30S ribosomal protein S12			1	
	PA14_09000	*rplF*	50S ribosomal protein L6			2	
NADH dehydrogenase	PA14_30010	*nuoB*	NADH dehydrogenase I chain B			1	
	PA14_29940	*nuoG*	NADH dehydrogenase I chain G			1	
	PA14_29880	*nuoL*	NADH dehydrogenase I chain L			1	
	PA14_29860	*nuoM*	NADH dehydrogenase I chain M			2	1
DNA and RNA	PA14_23260	*gyrA*	DNA gyrase subunit A				1
	PA14_00050	*gyrB*	DNA gyrase subunit B				2
	PA14_08780	*rpoC*	DNA-directed RNA polymerase beta* chain				1
	PA14_57940	*rpoN*	RNA polymerase sigma-54 factor				1
Flagella	PA14_23380	*orfH*	UDP-N-acetyl-D-mannosaminuronate dehydrogenase	3			
	PA14_23460	*orfN*	putative group 4 glycosyl transferase			1	3
	PA14_16430	*wspA*	putative methyl-accepting chemotaxis transducer	3			
	PA14_25490		putative tolQ-type transport protein			2	
	PA14_50440	*flgF*	flagellar basal-body rod protein FlgF				1
	PA14_50430	*flgG*	flagellar basal-body rod protein FlgG				1
	PA14_50360	*flgK*	flagellar hook-associated protein 1 FlgK				1
	PA14_45630	*fliA*	motility sigma factor FliA				1
	PA14_45770	*fliP*	flagellar biosynthetic protein FliP				1
Cell wall	PA14_12100	*dacC*	D-ala-D-ala-carboxypeptidase		5		
	PA14_11845	*mpl*	UDP-N-acetylmuramate:L-alanyl-gamma-D-glutamyl- meso-diaminopimelate ligase		4		
	PA14_10800	*ampR*	transcriptional regulator AmpR		2		
Other	PA14_38510	*hmgA*	Homogentisate 1,2-dioxygenase		3		1
	PA14_09960		putative transcriptional regulator				3
	PA14_14470	*pepA*	leucine aminopeptidase		3		
	PA14_04410	*ptsP*	phosphoenolpyruvate-protein phosphotransferase			2	1
	PA14_70470	*spoT*	guanosine-3',5'-bis(diphosphate) 3'-pyrophosphohydrolase		2		1
	PA14_66290	*aceA*	pyruvate dehydrogenase, E1 component				2

Values denote the number of different lineages that had mutations in the specified gene for the given treatment. Values are not double counted if passed on from Day 20 to Day 40, e.g. a mutation that occurs in Day 20 PIP^R that carries over to Day 40 PIP^R, PIP^RTOB^R, and PIP^RCIP^R is counted as one lineage.

occur during adaptation to piperacillin only (Day 20 PIP^R and Day 40 PIP^R) compare to the mutations that occur during piperacillin adaptation when there is a prior history of adaptation first to tobramycin (Day 40 TOB^RPIP^R) or ciprofloxacin (Day 40 CIP^RPIP^R)? To this end, we first categorized the genes in which mutations occurred into 23 broad categories based on the available literature and on the PseudoCAP functional classifications from the *Pseudomonas* Genome Database [97] (Table 3.3). Next, for each lineage, we tallied the number of times a gene in a functional category was mutated across the four biological replicates for each of the lineages (Figure 3.10). For a complete list of genes in each functional classification and descriptions of the genes, see Table A.5.

We observed several general trends in the genes mutated during adaptation to the three drugs depending on their historical context. In the lineages adapted to piperacillin, we saw history-dependent trends in the mutated genes that were related to multidrug efflux pumps (Figure 3.10, dashed-black box). While all the piperacillin-adapted lineages had mutations in genes related to the MexAB-OprM efflux pump (which is the primary efflux pump of piperacillin [98]) such as *nalD* and *mexR* (whose products repress the expression of *mexAB-oprM* [99]), the Day 40 CIP^RPIP^R lineage had additional mutations in the structural subunit genes of the other efflux pumps MexCD-OprJ (*mexC*) and MexEF-OprN (*mexF*). Lastly, no mutations in genes related to the MexXY-OprM pump were observed in any of the piperacillin-adapted lineages. With regard to adaptation to piperacillin only, most of the mutations that occurred in genes related to MexAB-OprM occurred within the first twenty days, with only a few additional mutations occurring between Day 21 and 40. Regardless of historical context, metabolic and cell wall genes tended to be frequently mutated in piperacillin-adapted lineages, whereas metabolic and cell wall genes did not seem to be con-

Table 3.3: **Functional classifications of the mutated genes.**

Cell wall	*dacC*, *mpl*
Membrane	*algC*, *aotJ*, *fixI*, *nppA1*, *secA*, *wbpM*, *ycjJ*, [PA14_12210], PA14_25490, PA14_30540/*ssuA*, PA14_34500, PA14_41710, PA14_48800, PA14_57880
Chemotaxis	*chpA*
Flagella	[*flgJ*]–[*flgI*], *cheB*, *fleN*, *flgF*, *flgG*, *flgK*, *fliA*, *fliP*, *morA*, *orfH*, *orfJ*, *orfN*, *wspA*
DNA	PA14_31100/PA14_31110
Cell division	*minC*, *zipA*
DNA/RNA synthesis	*gyrA*, *gyrB*, *rne*, *rpoC*, *rpoN*, *topA*, tRNA-Val
Ribosome	*fusA1*, *miaA*, *rne/rluC*, *rplF*, *rplJ*, *rplL*, *rpsL*, tRNA-Thr/*tufB*
MexAB-OprM	*mexA*, *mexR*, *mexR/mexA*, *nalC*, *nalD*, *nalC*/PA14_16290
MexCD-OprJ	[*nfxB*], *nfxB*, *mexC*, *mexC/nfxB*, *mexD*
MexEF-OprN	*parS*, *mexF*, *mexS*, *mexT*
MexXY-OprM	*amrB*
MuxABC	*muxA*
Metabolism	*aceA*, *aroB*, *clpA*, *clpS*, *dadA*, *gcdH*, *gcvP2*, *gltA*, *lhpE*, *pepA*, *prs*, *sahH*, PA14_20960, PA14_21820, PA14_27360/*deaD*, PA14_49300, PA14_57470, PA14_66170
Energy	[*ccoP*]-[*ccoP*], *atpC*, *atpC/atpD*, *cycB/pauR*, *pckA*, *sucD*, PA14_57540, PA14_57570
NADH dehydrogenase	*nuoB*, *nuoG*, *nuoL*, *nuoM*
Transcriptional regulation	*iscR*, *mucB*, *mvfR*, *np20*, *pauR*, *rnk*, PA14_09960, PA14_12140, PA14_35210, PA14_37170/*ada*, PA14_38500, PA14_39360
Two-component sensor	*envZ*, *cpxR*, *pmrB*, PA14_22730, PA14_27940
Beta-lactamases	*ampR*, *dacB*
Stringent response	*spoT*
Quorum sensing	*ptsP*
Large deletions	[*aldG*]–[*acsA*], [*glgX*]–[*nhaB*], *intT*–PA14_49030, PA14_35720–[PA14_40040], [PA14_37690]–[PA14_39660]
Hypothetical	*aprX*/PA14_48150, *erfK*, *ttg2D*, PA14_41730, PA14_44990, PA14_51910, PA14_57850, PA14_65570, PA14_69250

Brackets (e.g. [*gene*]) denote deletion of more than a few base pairs within a gene.
Forward slashes (e.g. *gene1*/*gene2*) denote mutations in the intergenic region between the two genes.
Hyphens (e.g. *gene1*—*gene2*) denote deletions spanning multiple genes.
For a complete list of genes in each functional classification and descriptions of the genes, see Table A.5.

sistently mutated across the tobramycin-adapted and ciprofloxacin-adapted lineages. This result is perhaps due to the fact that the primary target of piperacillin is cell wall (peptidoglycan) synthesis, which is largely a metabolic process. Interestingly, we also observed that the lineages adapted only to piperacillin (Day 20 PIP^R) sustained large chromosomal deletions that were not seen in the lineages in which there was prior tobramycin or ciprofloxacin adaptation (Day 40 TOB^RPIP^R and Day 40 CIP^RPIP^R). We discuss and explore the potential implications of these large deletions in the next Chapter.

The tobramycin-adapted lineages consistently had mutations occur in ribosomal subunit genes and other ribosomal machinery genes, regardless of historical context. In the lineages adapted only to tobramycin, mutations in genes related to the ribosome, membrane, energy, and NADH dehydrogenase tended to occur by Day 20, followed by mutations in efflux pump-related genes by Day 40. The mutations in genes related to membrane, NADH dehydrogenase, and energy likely reflect the unique requirement of the proton-motive force for the uptake of aminoglycoside antibiotics [100], and the mutations occurring during tobramycin adaptation may contribute to the resistance by reducing the proton-motive force [38]. While we observed mutations in the NADH dehydrogenase genes in the lineages adapted only to tobramycin, we saw no such mutations in the lineages where prior piperacillin or tobramycin adaptation occurred (Day 40 PIP^RTOB^R and Day 40 CIP^RTOB^R). Also, while efflux pump-related genes were mutated in the Day 40 TOB^R and Day 40 CIP^RTOB^R lineages, no such mutations were seen in the Day 40 PIP^RTOB^R lineages in which prior adaptation to piperacillin occurred (Figure 3.10, dashed-purple box).

The mutations in the ciprofloxacin-adapted lineages were fairly consistently distributed regardless of historical context. For all ciprofloxacin-adapted lineages, mutations were seen

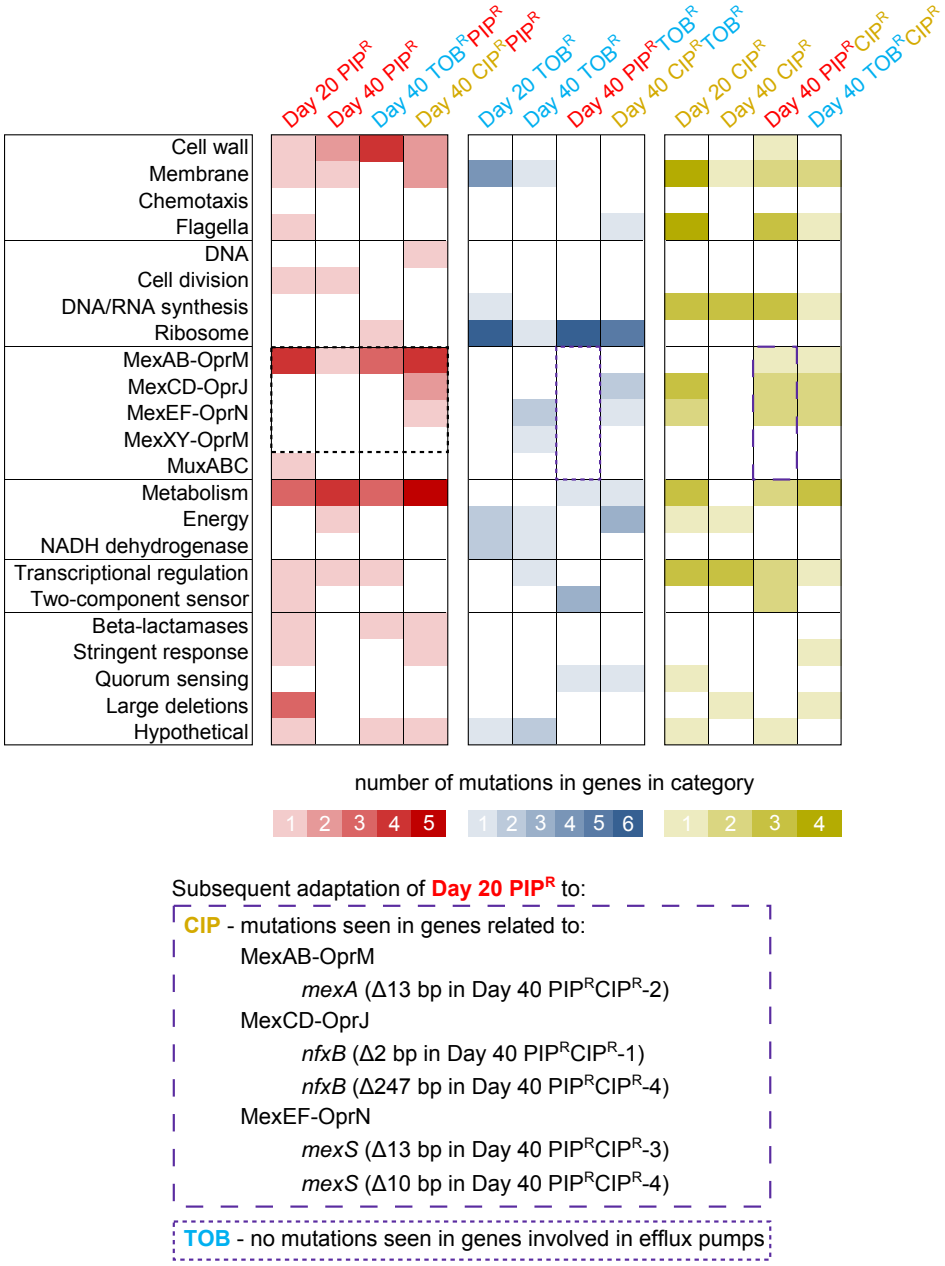

Figure 3.10: **Frequency of mutated genes during piperacillin, tobramycin, and ciprofloxacin adaptation depending the historical background.** The number of unique mutations observed in a gene in a functional class (rows) is shown based on the intensity of the color across all four biological replicates for each of the lineages (columns). The lineages are grouped according to the final (or only) drug that the lineage was adapted to in order to compare how historical context affects how often genes in the functional classes are mutated. For example, the first four columns (with red shading) correspond to the frequency of genes mutated in the lineages that were adapted to piperacillin only (Day 20 PIP^R and Day 40 PIP^R) and piperacillin after prior adaptation to a first drug (Day 40 TOB^RPIP^R and Day 40 CIP^RPIP^R). (*Continued on the following page.*)

Figure 3.10: Note that the data in the Day 40 PIP^R column correspond to additional mutations that occurred (between Day 21 and 40), and do not double count the ones from Day 20 PIP^R column. As an example of how different genes are mutated during piperacillin adaptation under different historical contexts, the cells outlined by the dashed-black box show that regardless of historical context, all lineages that underwent piperacillin adaptation had mutations in genes related to the MexAB-OprM efflux pump. However, only the lineage that had prior ciprofloxacin adaptation (Day 40 CIP^RPIP^R) had mutations in genes related to the MexCD-OprJ and MexEF-OprN efflux pumps. Lastly, none of the piperacillin-adapted lineages had mutations in genes involved in the MexXY-OprM efflux pump. The cells outlined by the dashed-purple boxes show that while subsequent adaptation of Day 20 PIP^R to ciprofloxacin (Day 40 PIP^RCIP^R) resulted in several mutations in genes involved in efflux pumps, subsequent adaptation to tobramycin (Day 40 PIP^RTOB^R) resulted in no mutations in genes involved in efflux pumps. The corresponding mutations that occurred are explicitly listed at the bottom. See main text for more details of how this difference may play a role in the resensitization to piperacillin during subsequent ciprofloxacin adaptation of Day 20 PIP^R.

in genes related to DNA/RNA synthesis as expected, as well as in genes related to membrane, flagella, efflux pumps, metabolism, and transcriptional regulators. Mutations related to the MexAB-OprM, MexCD-OprJ, and MexEF-OprN efflux pumps (mostly in genes encoding negative regulators of the pumps) are seen in the ciprofloxacin-adapted lineages, reflecting the ability these different pumps to extrude ciprofloxacin; however, no mutations were seen in genes related to MexXY-OprM, even though this pump is also known to contribute to fluoroquinolone resistance [98].

3.4.3 Role of the mutations in explaining the drug order-specific effects

Next, we sought to determine if the patterns in mutated genes could explain the mechanisms of some of the drug order-specific effects that were observed in the MIC time courses described in the previous chapter. We first discuss the cases of resensitization or maintenance of high resistance in which the one-drug-evolved lineages were subsequently adapted to the other

two drugs or to LB (Figure 2.7A). While subsequent adaptation of Day 20 PIP^R to LB and tobramycin maintained high piperacillin resistance, subsequent adaptation to ciprofloxacin led to full resensitization to piperacillin (Figure 2.7A (top)). We hypothesize that these differences stem from the different efflux pump-related genes that were mutated in these lineages (Figure 3.10, dashed-purple boxes). Evolution of the Day 0 Ancestor to piperacillin resulted in two different SNPs in *nalD*, and one SNP in *mexR* across the four biological replicates of Day 20 PIP^R, likely leading to the overexpression of the MexAB-OprM efflux pump [99]. We suspect that MIC_{PIP} remained high during subsequent adaptation to LB and tobramycin due to continued overexpression of MexAB-OprM.

However, when Day 20 PIP^R was adapted to ciprofloxacin, several mutations occurred in genes related to other efflux pumps, including one in *mexA*, two in *nfxB*, and two in *mexS* (Figure 3.10, dashed-purple boxes). In particular, *mexS* encodes a negative regulator of the expression of MexEF-OprN, and mutations in this gene likely lead to the overexpression of the pump [101]. Interestingly, expression of MexEF-OprN has been observed to correlate inversely with the expression of MexAB-OprM [101, 102]. Hence, we suspect that the resensitization to piperacillin when Day 20 PIP^R was subsequently adapted to ciprofloxacin may be have been due to a concurrent decrease in MexAB-OprM expression (leading to reduced piperacillin efflux) as MexEF-OprN expression increased. That is, it is possible that the mutations that occurred during ciprofloxacin adaptation which led to the overexpression of MexEF-OprN negated the effects of the mutations that occurred during prior piperacillin adaptation that led to overexpression of MexAB-OprM. Furthermore, we observed no mutations in efflux pump-related genes in Day 40 PIP^RTOB^R (Figure 3.10, dashed-purple boxes), which supports the notion that because no mutations occurred which would have negatively

correlated with the expression of MexAB-OprM, expression of this pump was maintained throughout the subsequent adaptation to tobramycin and hence the MIC_{PIP} stayed high.

We observed that subsequent adaptation of Day 20 TOB^R to LB and ciprofloxacin resulted in a partial resensitization to tobramycin, and that while subsequent adaptation to piperacillin also led to a significantly lower MIC_{TOB}, it was not as low as that of Day 40 TOB^RLB and $TOB^R CIP^R$ (Figure 2.7A (middle)). In this case, the partial resensitization during subsequent adaptation to LB may be attributable to adaptive resistance of aminoglycosides in *P. aeruginosa*. Adaptive resistance is a phenomenon where resistance to a drug is transiently induced in the presence of the drug and resistance recedes upon the removal of the drug [103]. In contrast to acquired resistance which is mediated through genetic mutations, adaptive resistance is explained by phenotypic alterations that allow for temporary increases in resistance. *P. aeruginosa* is known to exhibit adaptive resistance to aminoglycosides [104, 105], and it is primarily mediated through upregulation of MexXY-OprM during drug exposure, and subsequent downregulation after the removal of the drug [106]. We suspect that the partial resensitization during subsequent ciprofloxacin adaptation is also a consequence of adaptive resistance once the tobramycin selection pressure is removed. We further speculate that during the initial adaptation to tobramycin, the increase in tobramycin resistance was a combination of adaptive resistance and acquired resistance from accumulation of the mutations as seen in Day 20 TOB^R. Thus, the resensitization during subsequent LB and ciprofloxacin adaptation was not a full resensitization, but rather a partial one, perhaps reflecting the remaining contribution of the acquired resistance. Lastly, with regards to Day 40 $TOB^R PIP^R$, it is unclear how subsequent piperacillin adaptation seemingly resulted in maintenance of high MIC_{TOB} compared to that of Day 40 TOB^RLB and $TOB^R CIP^R$. We

hypothesize that the subsequent piperacillin adaptation somehow counteracted the resensitization effects of adaptive resistance even when the tobramycin selection pressure was removed.

The mechanism of ciprofloxacin resensitization is unclear when Day 20 CIP^R was subsequently adapted to LB, piperacillin, and tobramycin (Figure 2.7A (bottom)). While reversion of aminoglycoside sensitivity has been the most characterized case of adaptive resistance in *P. aeruginosa*, other studies have suggested that adaptive resistance may be prevalent in other classes of antibiotic classes as well, and that it may be mediated by epigenetic processes such as methylation and stochastic gene expression [107], particularly affecting the expression of efflux pumps [108]. It could be possible that adaptive resistance partially explains the resensitization to ciprofloxacin. We also note that qualitatively, there was much more variability in the MIC time courses between the individual replicates of the CIP^R lineages as seen by the larger error bars in Figure 2.4I, compared to that of the PIP^R (Figure 2.4A) and TOB^R (Figure 2.4E) lineages. Taken together, further investigation of the partial ciprofloxacin resensitization is needed.

While we observed clear cases of collateral sensitivity develop to piperacillin and tobramycin during the course of ciprofloxacin adaptation (Figure 2.8), other adaptive evolution studies of *P. aeruginosa* evolved to ciprofloxacin showed mixed results. In one study, adaptation of *P. aeruginosa* ATCC 27853 to ciprofloxacin showed no change in the MIC of three different beta-lactams (including piperacillin-tazobactam), nor of tobramycin [59]. In another study, while no statistical significances were assigned, adaptation of *P. aeruginosa* PAO1 to ciprofloxacin appeared to result in slight collateral sensitivities to piperacillin-tazobactam and tobramycin in some of their replicates. Nevertheless, in our study, we hypothesize that

the collateral sensitivity to piperacillin and tobramycin during ciprofloxacin adaptation is attributable to the mutations seen in *nfxB* (which encodes a transcriptional repressor that regulates MexCD-OprJ [109]) in the Day 20 CIP^R lineages. Three of the Day 20 CIP^R replicates had deletions in *nfxB* (15, 13, and 16 base pairs), likely resulting the in the inactivation of NfxB and concomitant upregulation of MexCD-OprJ and increased ciprofloxacin resistance [110]. In fact, *nfxB* mutants have been reported to be hypersusceptible to certain beta-lactams and aminoglycosides [111, 112].

Lastly, with regards to the decreased rate of tobramycin adaptation given a history of prior piperacillin adaptation (Figure 2.7B), we attribute this effect to the large chromosomal deletions that were sustained in three of the four Day 20 PIP^R replicates. The consequences of these deletions are discussed in the next chapter. In summary, based on the genomic mutations, we have presented our interpretations of potential mechanisms that contribute to the drug order-specific effects. These include how historical context can influence the frequency of mutations in certain genes, the varying contributions of adaptive and acquired resistance to total resistance, and specific cases of inverse correlation of the expression of different efflux pumps. While mutations are likely not the sole determinants of the differences [59, 113], many of the observed genomic mutations can partially explain the drug order-specific effects.

3.4.4 Extended analysis of mutations

Several of the *P. aeruginosa* multidrug efflux pumps (MexAB-OprM, MexCD-OprJ, MexEF-OprN, MexXY-OprM [114]) and their associated transcription factors were also common tar-

gets for mutations during evolution to all three drugs. The *nfxB* gene was the second most mutated gene. There were seven deletion mutations (all resulting in frameshifts) in seven separate ciprofloxacin-evolved lineages and one insertion mutation in the intergenic region between *nfxB* and *mexC* in a tobramycin-evolved sample. *nfxB* codes for a negative transcriptional regulator of the MexCD-OprJ efflux pump, and *nfxB*-type mutants overexpress the normally repressed MexCD-OprJ system [114]. *nfxB* has been observed to be mutated frequently during adaptive evolution to ciprofloxacin [80]. Inactivation of *nfxB* results in de-repression of the transcription of the MexCD-OprJ efflux pump, which contributes resistance to fluoroquinolones, macrolides, tetracycline, and some beta-lactams [114]. The one intergenic insertion occurred in the binding site of *nfxB* [109] of Day 40 $CIP^{R}TOB^{R}$-4 during the tobramycin evolution. This sample also acquired a 16 base pair deletion during the earlier ciprofloxacin evolution (Day 20 CIP^{R}-4). Thus, it seems that this sample interestingly has a non-functional NfxB protein and most likely non-functional NfxB binding site as well. Also interestingly, overexpression of the MexCD-OprJ pump has been reported to result in hypersusceptibility to beta-lactams and aminoglycosides [110, 115]. Other mutations involving the multidrug efflux pumps and their regulators include: *nalD* (PA14_18080), *mexS* (PA14_32420), *mexC* (PA14_60850), *mexR* (PA14_05520), *nalC* (PA14_16280), *parS* (PA14_41270), *amrB* (aka *mexY*, PA14_38410), *mexA* (PA14_05530), *mexD* (PA14_60830), *mexF* (PA14_32390), *mexT* (PA14_32410), and *muxA* (PA14_31870). We even saw a SNP located exactly at the predicted transcription site of PA3720-*armR* in *P. aeruginosa* PAO1 [116] (corresponding to PA14_16290-PA14_16300 in PA14), which is a possible region of a NalC binding site. NalC is a repressor of MexAB-OprM expression.

There were a few genes that were repeatedly mutated that are not very well characterized

in the literature. Three frameshift mutations occurred in PA14_09960 in three different ciprofloxacin treatments (Day 40 CIP^R-2, Day 40 PIP^RCIP^R-4, and Day 40 TOB^RCIP^R-3). This hypothetical protein has a Pfam description of being an Rrf2-like transcription regulator. Two frameshift mutations occurred in PA14_35210 in two different ciprofloxacin treatments (Day 40 CIP^R-1, and Day 40 CIP^R-2), and it is annotated as being a TetR family transcriptional regulator. Lastly, two SNPs occurred in PA14_51910 in two different piperacillin treatments (Day 20 PIP^R-3 and all progeny lineages, and Day 40 TOB^RPIP^R-2), suggesting that the hypothetical protein plays a role in piperacillin resistance.

Large deletions of the genome (>100 kbp) were observed in multiple lineages. Three of the lineages evolved to piperacillin (Day 20 PIP^R-1, -2, and -3) sustained ~400 kbp deletions (encoding ~350 genes), which subsequently fixed in their respective Day 40 PIP^R, PIP^RTOB^R, and PIP^RCIP^R lineages. These three deletions all occurred within a conserved region of the chromosome, and they overlap each other by ~190 kbp (encoding ~160 genes) (Table A.6). We also observed a ~176 kbp deletion occur in this same region during adaptation to ciprofloxacin after prior adaptation to tobramycin (TOB^RCIP^R-2), which suggests that this deletion is not specific to piperacillin adaptation in this study, but occurs during ciprofloxacin adaptation as well when the historical genomic context is suitable. When all four large deletions are compared, the overlap region is ~95 kbp (encoding ~77 genes). Bacteria are known to shed large portions of their genome as they adapt to a niche environment, suggesting that they streamline their DNA and get rid of non-essential genes that do not contribute to an enhanced fitness in the environment [61]. In pathogens such as *P. aeruginosa*, selective genome reduction has been seen in clinical isolates as bacteria adapt to the niche environment of the host [62]. It is interesting that we were able to also

recapitulate similar genomic deletions through experimental evolution. During the adaptive evolution, a visually observable phenotype was observed for all the lineages that had the large chromosomal deletion. These lineages produced the brown secreted pigment pyomelanin. The hyperproduction of pyomelanin observed here is attributed to the inactivation of the *hmgA* gene in the homogentisate pathway, which is part of the larger tyrosine catabolism pathway. hmgA codes for homogentisate-1,2-dioxygenase, which converts homogentisate to 4-maleylacetoacetate. When *hmgA* is non-functional, homogentisate gets secreted, auto-oxidizes, and self-polymerizes to form pyomelanin [66, 117]. Indeed, in all the lineages that had the large chromosomal deletion, *hmgA* was one of the genes in the deletion. Because *hmgA* is only one of many genes lost in the large deletion, it is unclear if there is an actual selective advantage for the pyomelanin phenotype, or if the pyomelanin phenotype is a "side-effect" of losing one or more genes in the deletion that actually does confer a selective advantage. There have been some studies that suggest that pyomelanin production by *P. aeruginosa* protects the bacteria against oxidative stress and contributes to increased persistence in a mouse model of chronic lung infection [66]. Clinical isolates of *P. aeruginosa* that produce pyomelanin have been well documented in the literature [118], but to the best of our knowledge, there has only been two studies that attribute the pyomelanin production in clinical isolates to loss of *hmgA* as part of a large chromosomal deletion, similar to those seen in this experimental evolution study [60, 64]. This result demonstrates how this experimental evolution study has recapitulated genotypes and phenotypes encountered clinically.

3.5 Discussion

The major challenge of analyzing the mutations after an adaptive laboratory evolution experiment is making sense of the mutations in the context of questions being asked. It is a not a trivial task to postulate what the effect of a given mutation is, let alone what the effects are in relation to each other. While some mutations are directly selected for because they allow for more optimal growth in the specific culture conditions, other "hitchhiker" mutations may have been co-selected for due to random chance [119]. Distinguishing the signal from the noise with respect to which mutations to focus our attention on was also a major challenge. The majority of the observed mutations were SNPs and small insertion/deletions, which frequently lead to frameshifts in the coding regions. While these mutations are overall non-lethal with respect to the rich media growth environment, it is unclear what the exact effects of the mutations are on the proteins that they encode. We suspect that a large number of the frameshift mutations result in a non-functional protein. In the cases where SNPs lead to amino acid substitutions, there exist algorithms to predict the potential functional implications of the substitution [120].

We observed a set of 28 mutations which were deemed anomalous and did not follow the expected patterns of inheritance based on the history of the lineages (bottom group of genes in Table A.4). For example, we expected that a mutation observed in Day 20 PIP^R-1 would also be observed in its progeny (Day 40 PIP^R-1, PIP^RCIP^R-1, and PIP^RTOB^R-1). However, there were several cases where a mutation in the Day 20 lineage was not observed in one or more of the progeny lineages. For example, while a three base pair deletion was observed in Day 20 PIP^R-1 and as well as in Day 40 PIP^R-1, and PIP^RCIP^R-1, it was not detected in

Day 40 $PIP^{R}TOB^{R}$-1. Cases like this one suggest heterogeneity in the populations during the adaptive evolution process. One caveat to mention is that we instructed Genewiz to choose a single colony from an agar streak plate for each of the samples to be sequenced, and it may also be possible that the single chosen colony was not a good representative of the population at large. Regardless, these anomalous mutations are of the minority and the majority of the mutations followed the expected patterns of inheritance, suggesting positive selection of the mutations [121].

It was interesting to see that there were 234 mutations in the Day 0 Ancestor compared to the published reference genome of *P. aeruginosa* PA14. This highlights how distribution of the laboratory strains of commonly studied bacteria between different people and institutions have likely led to the divergence of these stock "reference" strains. Put more simply, it is highly suspect that two different labs have stocks of *P. aeruginosa* PA14 that have exactly zero differences between their genomes. While usually not explicitly stated, it is important to keep in mind these potential differences with regard to commonly used laboratory reference strains of bacteria, especially when working with a reference genome. Interestingly, there has been one study that compared the genomes with several derivatives of the original PAO1 strain of *P. aeruginosa* [122]. This is noteworthy between the PAO1 strain was the first strain of *P. aeruginosa* to have its genome fully sequenced [123] and hence has been widely studied as the reference strain of *P. aeruginosa*. The study found several major differences between the PAO1 derivatives and the original strain including the lack of a large inversion and a duplication of a mobile 12 kbp prophage region in the derivative strains [122].

Chapter 4

Evolutionary forecasting of *P. aeruginosa* isolates

4.1 Foreword

Now that we have established the concept of drug order-specific effects during the evolution of *P. aeruginosa* to different sequential therapies of two drugs, we wanted to see if these effects could be recapitulated in strains of *P. aeruginosa* other than just in the laboratory PA14 strain. Analogous to how cancer studies often test different cell lines to see if the observations after a treatment are generalizable, we were interested in investigating the drug order-specific effects in the context of *P. aeruginosa* as an organism in general, regardless of the strain and origin. Because we are focused on the clinical aspects of antibiotic resistance, *P. aeruginosa* samples originating from the clinical setting were of high interest. To that end, I would like to thank Glynis Kolling and Amy Mathers for helping me collect a set of 14 clinical isolates of *P. aeruginosa* from the UVA Health System. I used a subset of these isolates to test one of the drug-order specific effects, which I present in this chapter. Also,

we came across a study where four pairs of clinical isolates of *P. aeruginosa* were collected from a hospital in France [64], and these isolates had the unique property of having large chromosomal deletions and the pyomelanin phenotype similar to the ones we observed in the PIP^R-1, -2, and -3 lineages. We thank Didier Hocquet and his research group for sharing these clinical isolates with us as we used them to try to recapitulate a different drug order-specific effect. Lastly, for the evolution of the *mexY* transposon mutant of *P. aeruginosa* PA14, I would like to thank Anna Blazier for curating the Papin lab copy of the library and teaching me how to access it.

4.2 Introduction

This chapter presents three sets of additional adaptive laboratory evolution experiments that were performed to assess the generalizability of the drug order-specific effects of resistance evolution that were presented in Chapter 2. We were interested to see if the drug order-specific effects could be recapitulated in other strains of *P. aeruginosa* with different genetic and historical backgrounds. Recapitulating these effects in different strains of *P. aeruginosa* can serve as a framework for evolutionary forecasting on the basis of genotypic and/or phenotypic similarities between the unknown strain and the evolved lineages from the main adaptive evolution experiment. More specifically by evolutionary forecasting, we aim to use the knowledge of the drug order-specific effects to predict how clinical isolates that exhibit similar genotypic and/or phenotypic characteristics as the lineages in the main adaptive evolution experiment will evolve to the three different drugs.

In the first set of experiments, we were interested to see if clinical isolates of *P. aerugi-*

nosa with high levels of piperacillin resistance could be resensitized if they were evolved to ciprofloxacin. To this end, 14 clinical isolates were obtained from the UVA Health System, and we chose to evolve three of the *P. aeruginosa* isolates that had high piperacillin resistance (and low tobramycin and ciprofloxacin resistance) to piperacillin, tobramycin, ciprofloxacin, and LB. All serial passaging protocols were consistent with those used for the main adaptive evolution experiment. This can be thought as a hybrid approach where *in vitro* evolution was performed on samples obtained from *in vivo* sources. Obviously, *in vitro* adaptation is different from what would happen the in the clinic if the patient were actually prescribed an antibiotic regimen of piperacillin, tobramycin, or ciprofloxacin. Nevertheless, our experiment attempts to narrow the gap between the conclusions from the *in vitro* studies and mitigating resistance in the clinical setting.

The second set of experiments describes how we evolved clinical isolates of *P. aeruginosa* that had large deletions and the pyomelanin phenotype, similar to those observed in our PIP^R-1, -2, and -3 lineages. These isolates were originally studied in the context of resistance to pyocins which are toxins produced by specific strains of *P. aeruginosa* [64]. There were four pairs of isolates, where each pair consisted of a non-pyomelanogenic parental ancestor and pyomelanogenic mutant that differed genetically from its corresponding parent by the presence of a large deletion. We found these pairs of isolates to be ideal candidates for testing the hypothesis that the large deletions were involved in limiting the rate of tobramycin resistance. Within each pair, the "WT" isolate would serve as the control to see if the "PM" isolate would comparably develop less tobramycin resistance when adapted to tobramycin.

Lastly, we evolved one of the mutants from the *P. aeruginosa* PA14 transposon mutant library to see if the gene that was disrupted played a role in limiting the rate of tobramycin

evolution. We chose to evolve the *mexY* (aka *amrB*) mutant because this gene was one of the genes consistently lost as part of the large deletions. It encodes a subunit of the MexXY-OprM efflux pump, which is a mechanism of aminoglycoside resistance. We hypothesized that disruption of this gene would lead to a non-functional MexXY-OprM efflux pump, and hence limit the evolutionary potential of the mutant to develop tobramycin resistance.

4.3 Materials and methods

4.3.1 Evolution of piperacillin-resistance clinical isolates of *P. aeruginosa*

A total of 14 isolates (two sets of seven) of *P. aeruginosa* were initially collected from the UVA Health System, and Figure 4.1 shows the antibiogram for the first set of seven isolates, and Figure 4.2 shows the antibiogram for the second set of seven isolates. Of these fourteen isolates, three of the isolates exhibited high piperacillin resistance and low tobramycin and ciprofloxacin resistance (Isolate ID (PY) 2-3, 2-5, and 2-7 in Figure 4.2). These three isolates are subsequently referred to as Clinical isolates #1, #2, and #3, respectively. The three isolates were evolved to the three drugs in the same manner as the main adaptive evolution experiment starting from frozen samples. They were first confirmed to be *P. aeruginosa* with PCR by using primers that specifically amplify the 16S rRNA region of *P. aeruginosa* (Paeru16SrDNA in Table 3.1) [90]. Three replicates of each isolate were evolved to each of the three drugs for ten days and their MICs to the three drugs were measured as before. In separate subsequent experiments, the three clinical isolates were evolved to LB with three replicates each. The MIC_{PIP} was measured for ten days (Table A.2). This measurement

UVA clinical *Pseudomonas aeruginosa* isolates

			Antibiotic Susceptibility Information						
source	**Isolate ID**	**Isolate ID (PY)**	**Cipro**	**Gent**	**Tob**	**Ami**	**Cef**	**Mero**	**Pip/Tazo**
catheter	1	1-1	1	≤ 1	≤ 1	4	16	4	≥ 256
catheter	2	1-2	≥ 4	≥ 16	≥ 16	8	16	≥ 16	32
BAL	3	1-3	≤ 0.25	≤ 1	≤ 1	≤ 2	2	8	24
blood	4	1-4	≤ 0.25	≤ 1	≤ 1	≤ 2	2	≤ 0.25	8
R abdomen	5	1-5	≥ 4	8	8	16	8	4	≥ 256
sputum	6	1-6	0.5	≥ 16	2	8	32	≥ 16	≥ 256
N/A	7	1-7	2	≥ 16	≥ 16	8	≥ 64	≥ 16	≥ 128

Cipro	Ciprofloxacin
Gent	Gentamicin
Tob	Tobramycin
Ami	Amikacin
Cef	Cefepime
Mero	Meropenem
Pip/Tazo	Piperacillin/Tazobactam

Figure 4.1: **Antibiogram of the first set of clinical isolates collected from the UVA Health System.** The following seven isolates were collected from the UVA Health System. MIC values are in units of µg/ml.

was done by inoculating bacteria into piperacillin concentration gradients to measure the MIC_{PIP}, but sampling and passaging was performed from the "growth control" well (LB with bacteria, without drug) to adapt to LB.

4.3.2 Evolution of the pyomelanin-producing clinical isolates with large chromosomal deletions

The four pairs of clinical isolates of *P. aeruginosa* from the Hocquet study (referred to as the "Hocquet isolates" in this dissertation) [64] were evolved to tobramycin for 15 days with three parallel replicates each, with the exception of B_{PM}, which had two replicates due to cross-contamination in the third replicate. The MICs for piperacillin and ciprofloxacin were also measured every five days (Table A.3). At the end of the 15 days of evolution, primers amplifying part of the *hmgA* gene (PA_hmgA in Table 3.1) were used to check for the presence of the gene in the "WT" isolates and the absence of the gene in the "PM" isolates.

UVA clinical *Pseudomonas aeruginosa* isolates

			Antibiotic Susceptibility Information												
Date	**Isolate ID**	**Isolate ID (PY)**	**Amp**	**Amp/Sul**	**Pip/Tazo**	**Cefaz**	**Ceftriax**	**Cefep**	**Mero**	**Amik**	**Gent**	**Tob**	**Cipro**	**Tige**	**Nitrof**	**Tri/Sulf**
8/8/2015	1	2-1	≥32	≥32	32	≥64	≥64	8	≥16	≤2	≤1	≤1	0.5	≥8	≥512	≥320
6/22/2015	2	2-2	≥32	≥32	≥128	≥64	≥64	≥64	≥16	16	8	≤1	1	≥8	256	≥320
6/19/2015	3	2-3	≥32	≥32	≥128	≥64	≥64	32	≥16	4	4	≤1	0.5	≥8	≥512	≥320
5/17/2015	4	2-4	≥32	≥32	32	≥64	≥64	16	8	4	4	≤1	≥4	≥8	≥512	≥320
5/25/2015	5	2-5	≥32	≥32	≥128	≥64	≥64	≥64	4	≤2	≤1	≤1	1	≥8	≥512	≥320
6/4/2015	6	2-6	≥32	≥32	64	≥64	≥64	8	≥16	4	4	≤1	≥4	≥8	≥512	≥320
6/3/2015	7	2-7	≥32	≥32	≥128	≥64	≥64	32	≥16	≤2	≤1	≤1	0.5	≥8	≥512	≥320

Amp	Ampicillin
Amp/Sul	Ampicillin/Sulbactam
Pip/Tazo	Piperacillin/Tazobactam
Cefaz	Cefazolin
Ceftriax	Ceftriazone
Cefep	Cefepime
Mero	Meropenem
Amik	Amikacin
Gent	Gentamicin
Tob	Tobramycin
Cipro	Ciprofloxacin
Tige	Tigecycline
Nitrof	Nitrofurantoin
Tri/Sulf	Trimethoprim/Sulfamethoxazole

Resistant
Intermediate
Sensitive

Figure 4.2: **Antibiogram of the second set of clinical isolates collected from the UVA Health System.** The following seven isolates were collected from the UVA Health System. MIC values are in units of µg/ml.

Because *hmgA* was consistently deleted as part of all of the large deletions (Table A.6), the presence or absence of *hmgA* serves as a proxy for the absence or presence of a large deletion, respectively.

4.3.3 Evolution of the *amrB* (*mexY*) transposon mutant from the *P. aeruginosa* PA14 mutant library

The *amrB* transposon mutant and PA14 wild-type strain from the *P. aeruginosa* PA14 non-redundant transposon insertion mutant set (referred to as the PA14 transposon mutant library) (Mutant ID #46235) [74] were evolved to tobramycin for 20 days with four replicates each. Because we could not locate the original wild-type PA14 strain in our Papin lab copy of the transposon library, we requested the wild-type PA14 strain from the original creators of the library, and we thank Eliana Drenkard from the Ausubel Lab for providing us the strain. We used the amrB_Tn primers (Table 3.1) to confirm the presence of the transposon insertion in *amrB*.

4.4 Results

4.4.1 Drug order-specific effects in clinical isolates

To explore the relevance of our laboratory evolution results clinically, we tested for the drug order-specific MIC evolutionary dynamics in clinical isolates of *P. aeruginosa*. We first tested the evolutionary dynamics of clinical isolates that were resistant to piperacillin but susceptible to tobramycin and ciprofloxacin. We evolved three piperacillin-resistant clinical isolates of *P. aeruginosa* to piperacillin, tobramycin and ciprofloxacin for ten days and tracked how the piperacillin resistance changed in these lineages. If the results from the adaptive evolution experiment applied to these piperacillin-resistant clinical isolates, then we would expect that evolving to tobramycin would not affect the high piperacillin resistance, but evolving to ciprofloxacin would restore susceptibility to piperacillin. As discussed in Chapter 2, evolving Day 20 PIP^R to LB did not result in a reduction of MIC_{PIP} (Figure 2.7A (top)), which suggests that the resensitization to piperacillin when Day 20 PIP^R was evolved to ciprofloxacin is a consequence of the switch to the ciprofloxacin drug pressure.

We first measured the MICs to piperacillin, tobramycin, and ciprofloxacin for the fourteen clinical isolates that were collected. Figure 4.3 shows the MICs of the drugs for these isolates normalized by the MICs of the Day 0 Ancestor by subtracting the MICs of the Day 0 Ancestor from the measurements. Based on these initial measurement of the MICs, we chose isolates 2-3, 2-5, and 2-7 for the subsequent adaptive evolution experiment because these isolates exhibited high levels of piperacillin resistance and susceptibility to tobramycin and ciprofloxacin compared to Day 0 Ancestor. Isolates 2-3, 2-5, and 2-7 are subsequently referred to as Clinical isolates #1, #2, and #3, respectively.

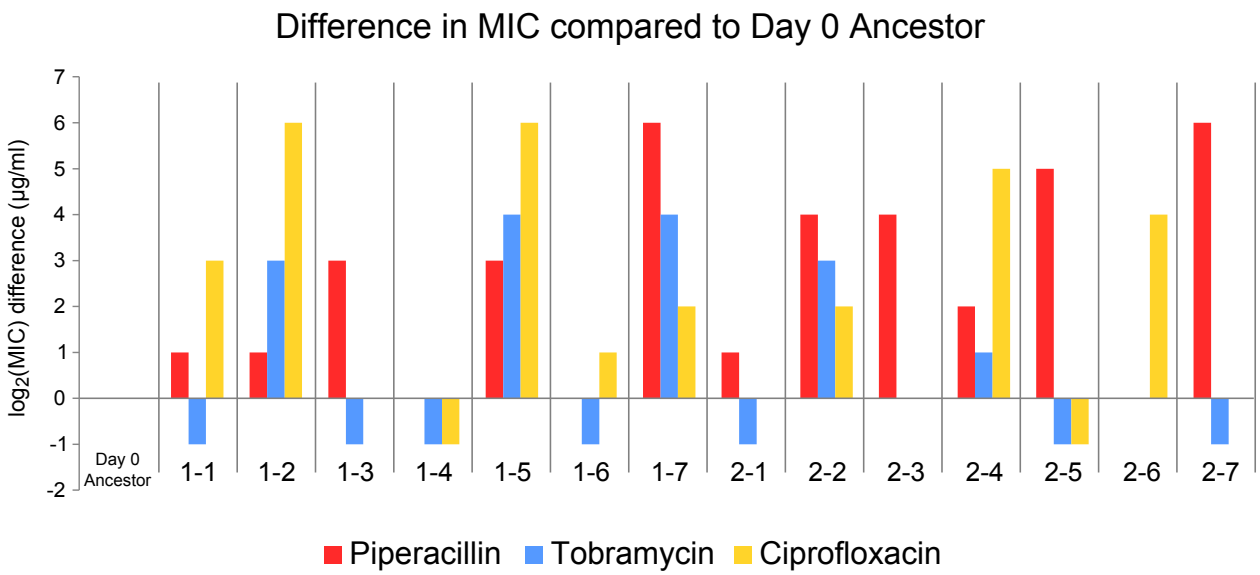

Figure 4.3: **Differences in MICs of the UVA Health System isolates.** The MICs of the 14 *P. aeruginosa* isolates obtained from the UVA Health System are normalized by the MICs of the Day 0 Ancestor from our adaptive evolution study. The notation for the isolates follow the "Isolate ID (PY)" from Figure 4.1 and Figure 4.2. For example, isolate 2-7 is the seventh isolate from the second set. n=1 for all measurements.

Of the three isolates we tested, the evolutionary dynamics of two of these isolates matched these expectations (Figure 4.4; Figure 4.5 and Table A.2). After normalizing to Day 1 MIC values, the MIC_{PIP} after ten days of ciprofloxacin adaptation was significantly less than the MIC_{PIP} after ten days of LB adaptation in isolate #2 (Figure 4.4B, $p<0.05$) and in isolate #3 (Figure 4.4C, $p<0.001$), indicating resensitization to piperacillin during ciprofloxacin adaptation. This observation suggests that this specific pattern of MIC evolutionary dynamics we observed is not limited to laboratory strains of *P. aeruginosa* and may be observed in diverse strains of *P. aeruginosa*, including those originating from human patients. Note that these three clinical isolates were isolated from different patients and their phylogenetic relatedness between each other and to the laboratory PA14 strain used in our study is untested. In isolate #1, there was no significant difference in the normalized MIC_{PIP} values after ten days of adaptation to tobramycin, ciprofloxacin, and LB (Figure 4.4A, $p=0.237$, one-way ANOVA).

Interestingly, this isolate evolved to higher levels of piperacillin and ciprofloxacin resistance than the other two isolates (Figure 4.5 and Table A.2) which suggests the possibility that adaptation to ciprofloxacin in these higher piperacillin-resistant cultures could still result in a restoration of piperacillin susceptibility.

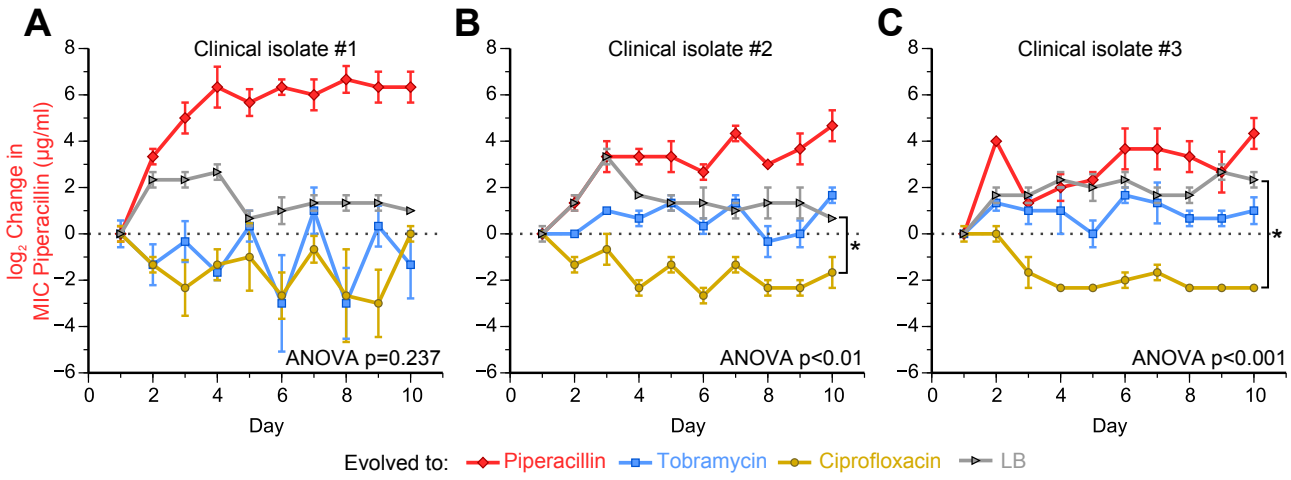

Figure 4.4: **Clinical isolates with high MIC_{PIP} become resensitized to piperacillin following adaptation to ciprofloxacin.** To see if we could recapitulate the adaptation dynamics of MIC_{PIP} when Day 20 PIP^R is evolved to tobramycin and ciprofloxacin, we evolved three piperacillin-resistant clinical isolates of *P. aeruginosa* to piperacillin, tobramycin, ciprofloxacin, and LB. (A) While the first isolate did not show restoration of piperacillin sensitivity during ciprofloxacin evolution as anticipated, (B and C) the other two isolates recapitulated this effect. In Clinical isolates #2 and #3, the relative changes in the MIC_{PIP} when the isolates were evolved to ciprofloxacin were significantly different from the relative changes when evolved to LB at Day 10 ($p<0.05$ and $p<0.001$, respectively). For each of the three isolates, a one-way ANOVA was first performed on the Day 10 MIC_{PIP} values of the lineages evolved to LB, tobramycin, and ciprofloxacin. Error bars show SEM of three replicates per treatment. See Figure A.3 for an example calculation of the statistical tests (Clinical isolate #2), and Figure 4.5 for the original, pre-normalized data.

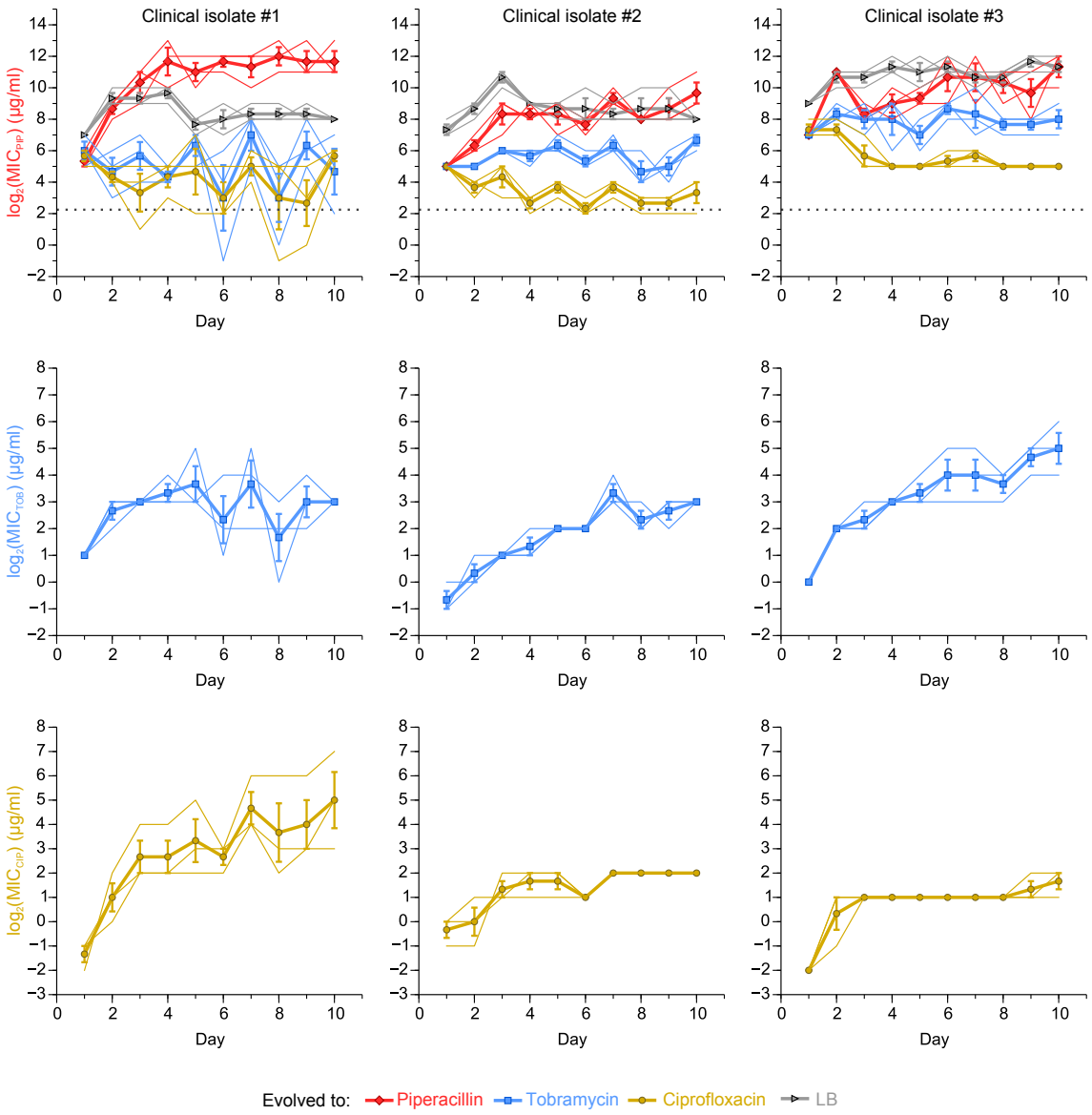

Figure 4.5: **Evolutionary dynamics in clinical isolates with high piperacillin resistance.** Three clinical isolates of *P. aeruginosa* with high piperacillin resistance were evolved to piperacillin, tobramycin, and ciprofloxacin to test if we could recapitulate the evolutionary dynamics seen in MIC_{PIP} of PIP^R, whereby evolution to ciprofloxacin would cause MIC_{PIP} to decrease while evolution to tobramycin would not. We were able to see this result recapitulated in isolate #2 and isolate #3, but not in isolate #1. Interestingly, isolate #1 was able to be evolved to higher levels of piperacillin resistance and ciprofloxacin resistance compared to the other two. Thin lines show the individual time courses of three replicates per treatment, and bold lines show their averages. The dotted line in the first row shows the mean MIC_{PIP} of Day 1 Control to emphasize that the clinical isolates are resistant to piperacillin at Day 1. Error bars show SEM for the three replicates for each lineage.

4.4.2 Role of the large chromosomal deletions in reducing the rate of tobramycin evolution

In the next set of evolution experiments, we investigated the role that the large chromosomal deletions play in a drug order-specific effect. We had observed that compared to the Day 20 PIP^R replicate that did not have a large deletion, the three Day 20 PIP^R replicates with the large deletions, when subsequently evolved to tobramycin, developed less tobramycin resistance (Figure 4.6 and Table A.1). This observation suggests that the large deletions are involved in reducing the subsequent rate of tobramycin resistance evolution given a prior history of piperacillin adaptation.

A recent study isolated four pairs of clinical isolates of *P. aeruginosa*, where each pair consisted of a pyomelanogenic isolate and a "parental wild-type" non-pyomelanogenic isolate [64]. In each of the four pairs, the only genomic difference between the pyomelanogenic (denoted A_{PM}, B_{PM}, C_{PM}, and D_{PM}) and its corresponding parental wild-type isolate (denoted A_{WT}, B_{WT}, C_{WT}, and D_{WT}) was the presence of large chromosomal deletions that overlap with parts of the deletions seen in Day 20 PIP^R-1, -2, and -3 (Figure 4.8E; Table A.6). Indeed, all of the large deletions encompass *hmgA*, whose loss accounts for the pyomelanin phenotype [66]. We used these four pairs of clinical isolates to test the hypothesis that the large deletions play a role in lowering the rate of tobramycin resistance evolution. The MICs of the four pairs of isolates were initially measured for piperacillin, tobramycin, and ciprofloxacin (Figure 4.7). We observed that within each pair, there were cases where the MIC of a drug was different between the "WT" and "PM" isolates. Most notably, B_{PM} had a much lower MIC_{TOB} than B_{WT}.

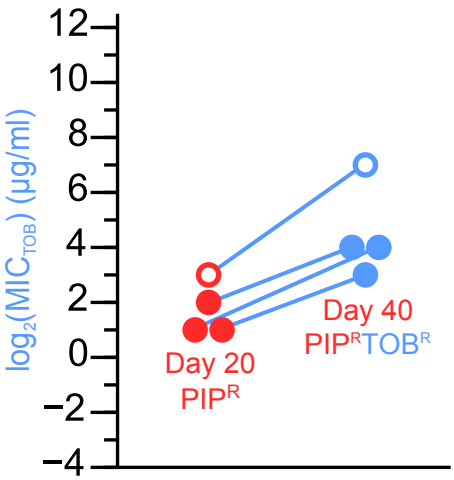

Figure 4.6: **Drug history-dependence in $\mathbf{MIC_{TOB}}$ and large deletions in $\mathbf{PIP^R}$.** The resistance levels to tobramycin for individual replicates are plotted for Day 20 PIP^R and Day 40 PIP^RTOB^R. The replicates denoted with the filled-in circles have large deletions in their genome, while the replicate denoted by the open circle does not. We see that the replicates of Day 20 PIP^R with the large chromosomal deletions develop less resistance to tobramycin than the replicate that does not have the deletion.

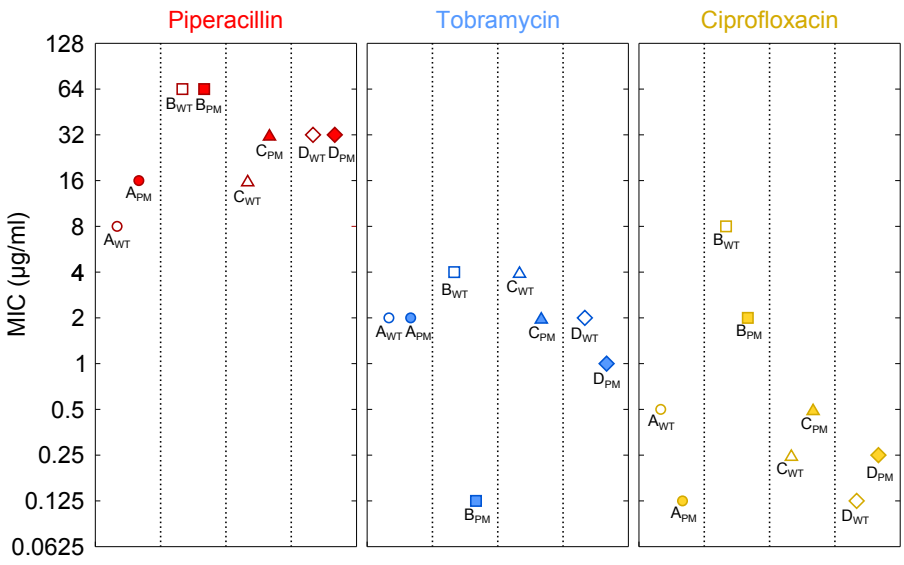

Figure 4.7: **Initial measurement of the MICs of the Hocquet isolates.** We measured the MICs of the three drugs for the eight clinical isolates (n=1 for each).

We evolved the four pairs of isolates to tobramycin using the same daily serial passaging technique used throughout this study and tracked the MICs of tobramycin, piperacillin, and ciprofloxacin over the course of 15 days (Figure 4.8; Table A.3 and Figure 4.9). At the end of the 15 days, we saw that A_{PM}, B_{PM}, and C_{PM} had lower relative increases in MIC_{TOB}, compared to A_{WT} ($p<0.01$), B_{WT} ($p<0.05$), and C_{WT} ($p<0.05$), respectively (Figure 4.8A-C).

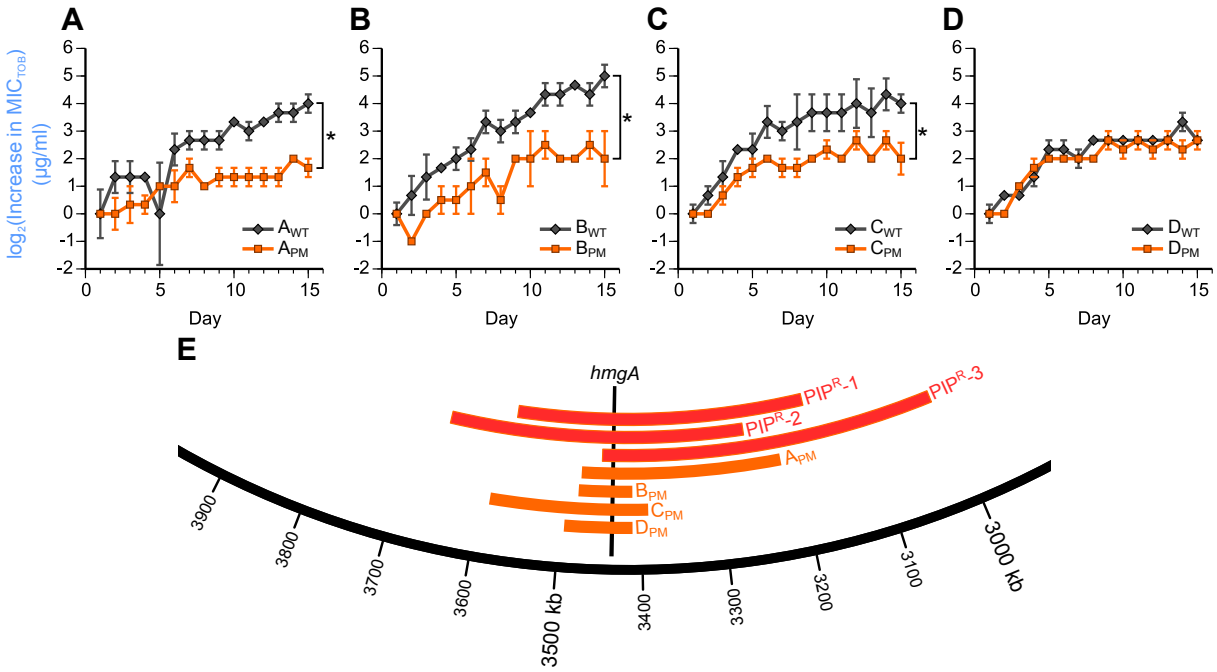

Figure 4.8: **Clinical isolates with large chromosomal deletions have lower rates of tobramycin resistance evolution.** To see if large chromosomal deletions played a role in reducing the rate of tobramycin resistance evolution, four pairs of clinical isolates were evolved to tobramycin. Each pair consisted of a pyomelanogenic isolate with a large deletion (denoted "PM") and its corresponding non-pyomelanogenic parental isolate that does not have a large deletion (denoted "WT") [64]. As anticipated, we observed that (A) A_{PM}, (B) B_{PM}, and (C) C_{PM} had lower relative increases in MIC_{TOB} compared to A_{WT}, B_{WT}, and C_{WT}, respectively. However, (D) D_{WT} and D_{PM} had comparable relative increases in MIC_{TOB}. Asterisks denote $p<0.05$ of a two-sample t-test after the raw MIC values were normalized by subtracting the average Day 1 MIC_{TOB} for each evolved lineage. See Figure A.4 for an example calculation of the statistical tests (A_{WT} vs. A_{PM}). Error bars show SEM of three replicates per treatment (except B_{PM}-2, which had two replicates). (E) The large deletions of the four "PM" isolates are located in the same region as the deletions of Day 20 PIP^R-1, -2, and -3, and all of the deletions encompass *hmgA*, whose loss causes the hyperproduction of pyomelanin.

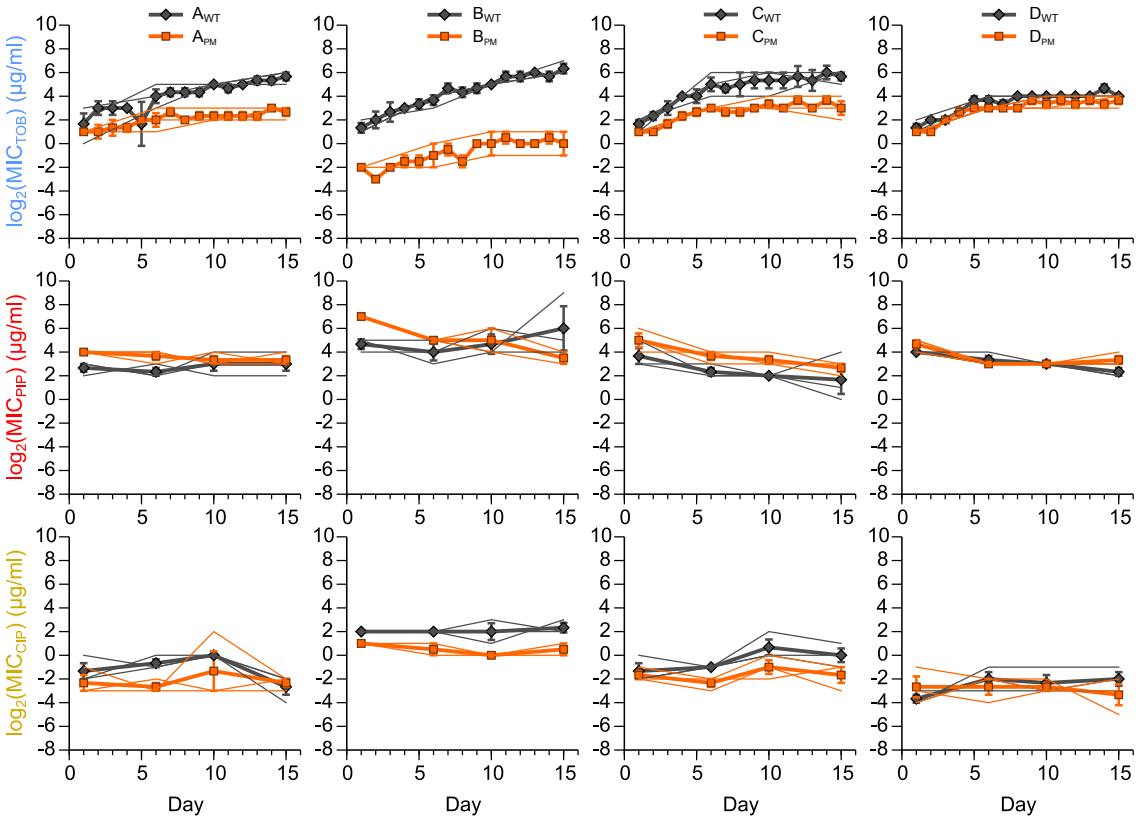

Figure 4.9: **Evolutionary dynamics in clinical isolates with large chromosomal deletions.** Four pairs of clinical isolates of *P. aeruginosa* were evolved to tobramycin. Each pair of isolates (columns) consists of a pyomelanogenic isolate (subscript PM) that has a large deletion, and a parental isolate from which the PM isolate is derived from (subscript WT). In each pair, the only genetic difference is the presence of a large chromosomal deletion in the PM isolate [64]. The top, middle, and bottom rows show the MICs of the isolates to tobramycin, piperacillin, and ciprofloxacin, respectively as they adapt to tobramycin. Thin lines show the individual time courses of three replicates per treatment (with the exception of B_{PM}, which has two replicates), and bold lines show their averages. Error bars show SEM for the three replicates (two for B_{PM}) for each lineage.

These data then provide support for the idea that the large chromosomal deletions do indeed play a role in reducing the rate of tobramycin adaptation, and potentially even in limiting the maximum level of tobramycin resistance that can be developed comparatively. In the case of the fourth pair, we saw that D_{WT} and D_{PM} had comparable increases in MIC_{TOB} over the course of the tobramycin adaptation (Figure 4.8D, p=1.00). It can be speculated that some combination of the presence or loss of specific genes in D_{PM} led to this evolutionary trajectory that is different from the other three pyomelanogenic isolates. We would also like to point out that within each pair, the "WT" and "PM" isolates vary in initial Day 1 MIC_{TOB}. The B_{PM} and B_{WT} pair was the most disparate pair, as B_{PM} had a much lower MIC_{TOB} than B_{WT} (Figure 4.9). Figure 4.10 shows that after 15 days of tobramycin evolution, the evolved "WT" lineages were still non-pyomelanogenic and the "PM" lineages were still pyomelanogenic. Furthermore, we used the PA_hmgA primers (Table 3.1) to confirm the presence of *hmgA* in the evolved "WT" lineages and absence of the gene in the "PM" lineages (Figure 4.11).

Interestingly, a recent study also observed large genomic deletions spanning *hmgA* when *P. aeruginosa* PAO1 was evolved to meropenem, which is another beta-lactam antibiotic [65]. These mutants were also pyomelanogenic. The large deletions in both our study as well as this recent study also span *mexX* and *mexY*, which encode portions of the efflux pump that is a significant determinant of aminoglycoside resistance [124]. The loss of these genes in the three PIP^R replicates may partially explain why subsequent tobramycin adaptation is limited compared to the replicate that did not sustain the large deletion.

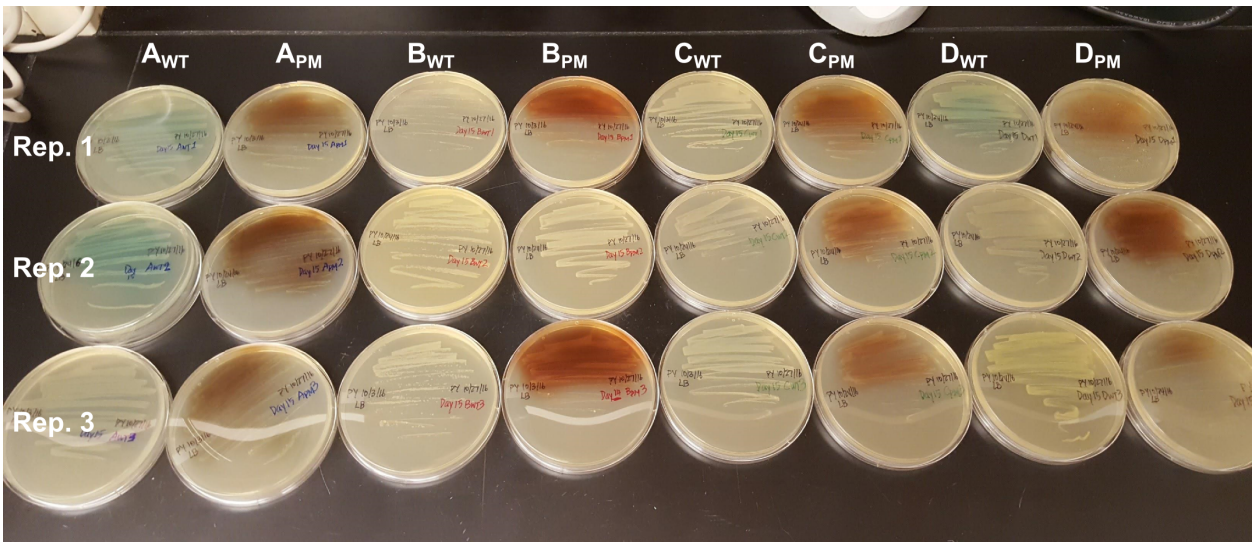

Figure 4.10: **Evolution of the Hocquet isolates to tobramycin.** This photograph shows the result of evolving the eight clinical isolates from the Hocquet study [64] to tobramycin for 15 days. The "WT" isolates maintained the "non-pyomelanin" phenotype, while the "PM" isolates maintained the pyomelanin phenotype. The exception is B_{PM}-2, which was unfortunately cross-contaminated and was discarded from any subsequent analysis.

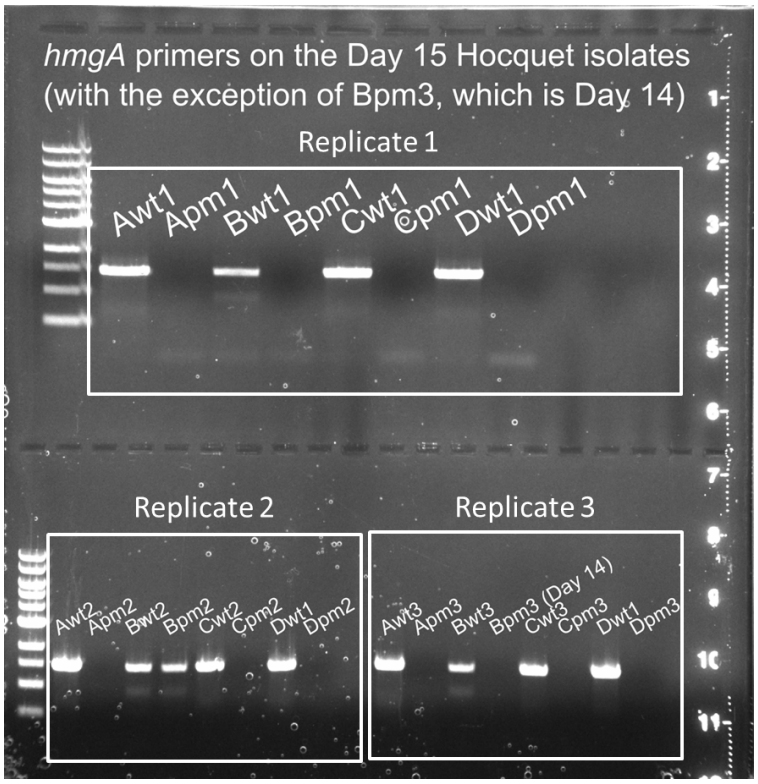

Figure 4.11: **Confirmation of the presence or absence of *hmgA* in the Hocquet isolates.** PCR was performed with the PA_hmgA primers (Table 3.1) to check for the presence of *hmgA* in the "WT" isolates (presence of a band) and the absence of *hmgA* in the "PM" isolates (absence of a band). Because *hmgA* is consistently deleted as part of the large deletions, its presence or absence serves as a proxy for the absence or presence of the large deletions, respectively. The exception is B_{PM}-2, which was cross-contaminated with one of the "WT" isolates, and hence produced a band.

4.4.3 Evolution of the *mexY* transposon mutant

To further investigate the role of the large chromosomal deletions in reducing the rate of tobramycin evolution, we attempted to determine if a specific gene that was deleted as part of the large deletions was responsible for this drug order-specific effect. The observation that the three replicates of the PIP^R lineage that had large deletions evolved less tobramycin resistance the fourth replicate, which did not have a large deletion, led us to speculate that the loss of one or more genes in the large deletions was responsible for this phenotype (Figure 4.6). The results from evolution of the Hocquet isolates in the previous section further supported this notion. To this end, we hypothesized that *amrB* was the causative gene. In the *P. aeruginosa* PA14 genome, the gene with locus tag PA14_38410 is annotated as *amrB*. This gene is orthologous to PA2018 in the *P. aeruginosa* PAO1 genome, where it is named *mexY*. Subsequently, we use *amrB* and *mexY* interchangeably.

mexY encodes the inner membrane protein subunit of the MexXY-OprM multidrug efflux pump in *P. aeruginosa*, which is a major determinant of aminoglycoside resistance [124]. *mexY* (*amrB*) was lost as part of the deletions in PIP^R-1, -2, -3, as well as all four of the "PM" Hocquet isolates (Table A.6). In a study where *P. aeruginosa* was evolved to become resistant to meropenem (a beta-lactam), the resulting mutants were also observed to have large chromosomal deletions encompassing *mexY* (as well as *hmgA*, leading to the pyomelanogenic phenotype) [65]. In these mutants, hypersusceptibility to tobramycin was also observed, and the authors speculated that the loss of *mexY* resulted in the loss of a resistance determinant for tobramycin and other aminoglycosides. Furthermore, the authors hypothesized that the mutants that had the deletion of *mexY* may have been selected for by

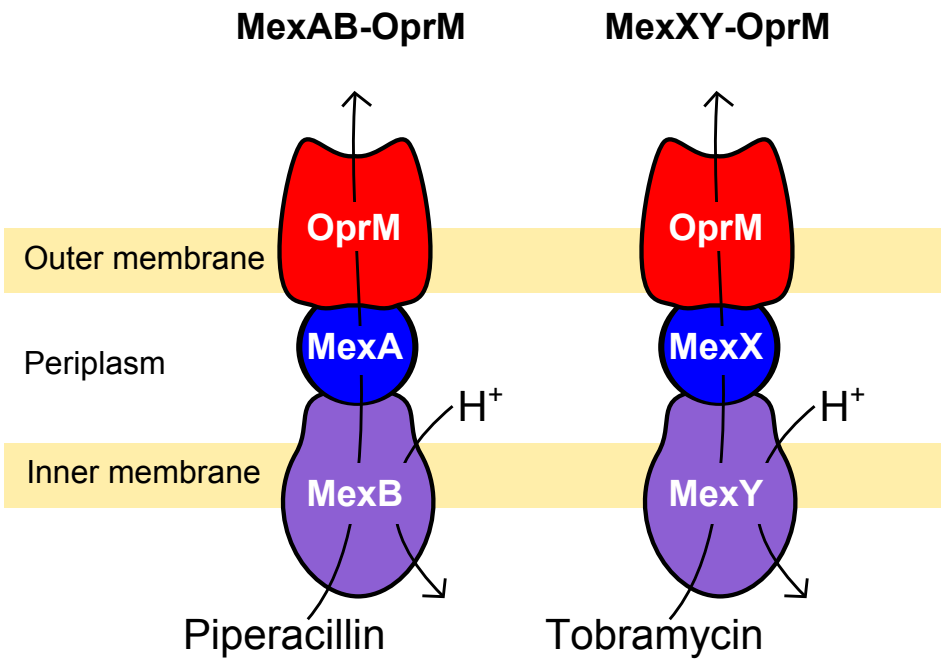

Figure 4.12: **Schematic of the MexAB-OprM and MexXY-OprM efflux pumps.** MexAB-OprM and MexXY-OprM are two of the RND-type multidrug efflux pumps found in *P. aeruginosa*. These efflux pumps consist of a three subunits: an outer membrane protein, an inner membrane protein, and a periplasmic protein. MexAB-OprM contributes to the resistance of piperacillin and other beta-lactams, while MexXY-OprM contributes to the resistance of tobramycin and other aminoglycosides. Both of these efflux pumps use OprM as the outer membrane subunit protein.

the meropenem drug pressure. Without production of the MexXY-OprM efflux pump, the OprM outer membrane subunit protein may then be used in the production of the MexAB-OprM efflux pump (which is a determinant of beta-lactam resistance) as these two efflux pumps share the same outer membrane subunit Figure 4.12.

While we did not observe hypersusceptibility to tobramycin our Day 20 PIP^R-1, -2, and -3 lineages, we nevertheless took inspiration from this study to hypothesize that perhaps the loss of *mexY* in our mutants could explain the reduced rate of tobramycin evolution. Perhaps the inability to produce the MexXY-OprM efflux pump resulted in one less evolutionary route for tobramycin resistance to develop. To test this hypothesis, we evolved the *amrB* (*mexY*) transposon mutant from the *P. aeruginosa* PA14 transposon library [74] to tobramycin using

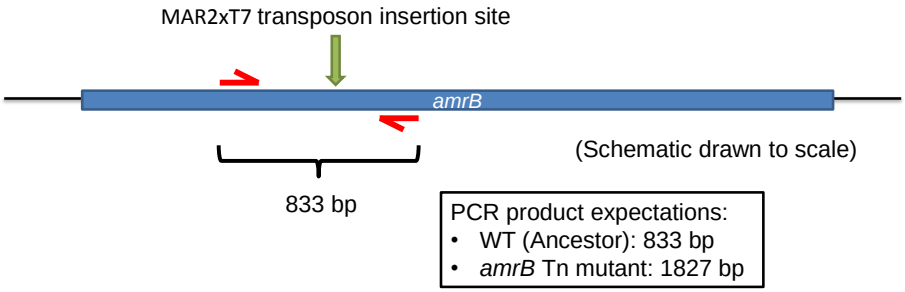

Figure 4.13: **Schematic of *amrB*.** Primers were designed to amplify a portion of *amrB* that encompassed the transposon insertion site in the *amrB* transposon mutant of *P. aeruginosa* PA14. The PCR product is 833 bp in the wild-type PA14 strain, while addition of the 994 bp MAR2xT7 transposon in the mutant leads to a PCR product of 1,827 bp.

the same daily serial passaging protocols used throughout this study. If *mexY* was indeed the causative gene, then we would expect it to evolve less tobramycin resistance compared to the PA14 wild-type strain from the transposon mutant library.

Before performing the adaptive evolution, we first wanted to confirm that the mutant indeed had the transposon inserted in the *amrB* gene. A set of primers (amrB_Tn inTable 3.1) was designed to amplify a region of *amrB* that encompassed the site of the transposon insertion (Figure 4.13). We expected that the PCR product when the primers amplified the wild-type PA14 strain would be 833 bp, while the PCR product when the primers amplified the transposon mutant would be 1,827 bp, due to the insertion of the 994 bp transposon. Indeed, PCR confirmed this difference as there was separation in the electrophoresis gel bands of approximately 1 kbp. (Figure 4.14).

Figure 4.15 shows the results of the evolution of the *amrB* mutant and PA14 wild-type strain after 20 days of tobramycin selection pressure. At first glance, it would seem that at the MIC_{TOB} time courses between the *amrB* and PA14 control lineages were comparable. This would suggest that *amrB* was not the causative gene involved in reducing the rate of

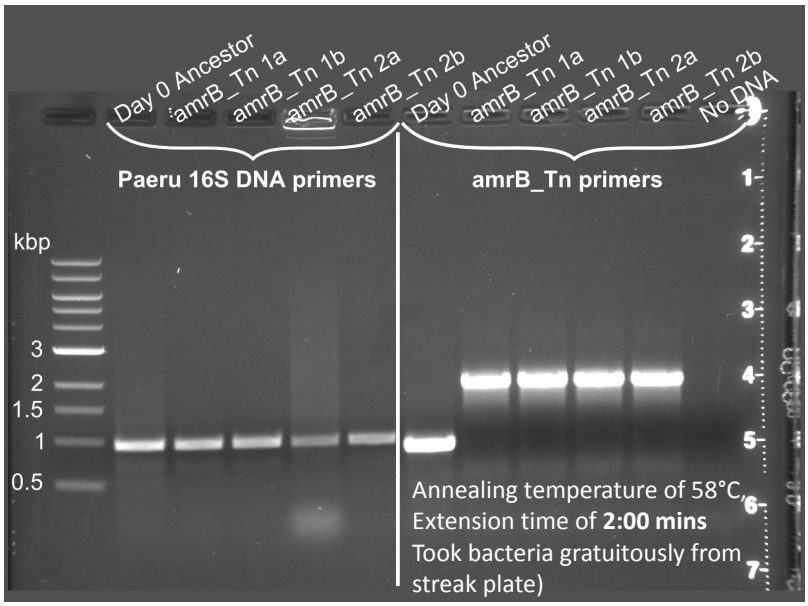

Figure 4.14: **Confirmation of the transposon insertion in the *amrB* mutant.** Primers were designed to amplify the region of *amrB* where the transposon was inserted. The amrB_Tn primers, when used to amplify the region in the Day 0 Ancestor chromosome, yielded a PCR product of 838 bases. When the primers (right) were used to amplify the region in the *amrB* transposon mutant, the PCR product was 1,827 bases, due to the insertion of the 994 bp transposon. The Paeru16SrDNA primers (left) were used to confirm that the samples were indeed from samples of *P. aeruginosa*. See Table 3.1 for the primer sequences.

tobramycin evolution. However, when we additionally plotted the time course of the TOB^R lineage from the main adaptive evolution experiment (light blue line in Figure 4.15, we saw that the final day's MIC_{TOB} was greater than that of the PA14 wild-type control. To clarify, the TOB^R lineage was founded from the Day 0 Ancestor, which itself was founded from the Papin lab's frozen stock of *P. aeruginosa* PA14. The PA14 wild-type (black line in Figure 4.15) is the wild-type control from the transposon mutant library. The frozen samples for these two "PA14" strains are different. Hence, the results from this experiment are slightly ambiguous, stemming from the variability between the time courses of two different "PA14" strains. In the future, one potential approach to attempt to resolve this discrepancy is to choose an assortment of other mutants from the transposon mutant library, and evolve them to tobramycin. If these mutants are hypothesized to have no connection with tobramycin resistance, they could serve as additional "pseudo-controls."

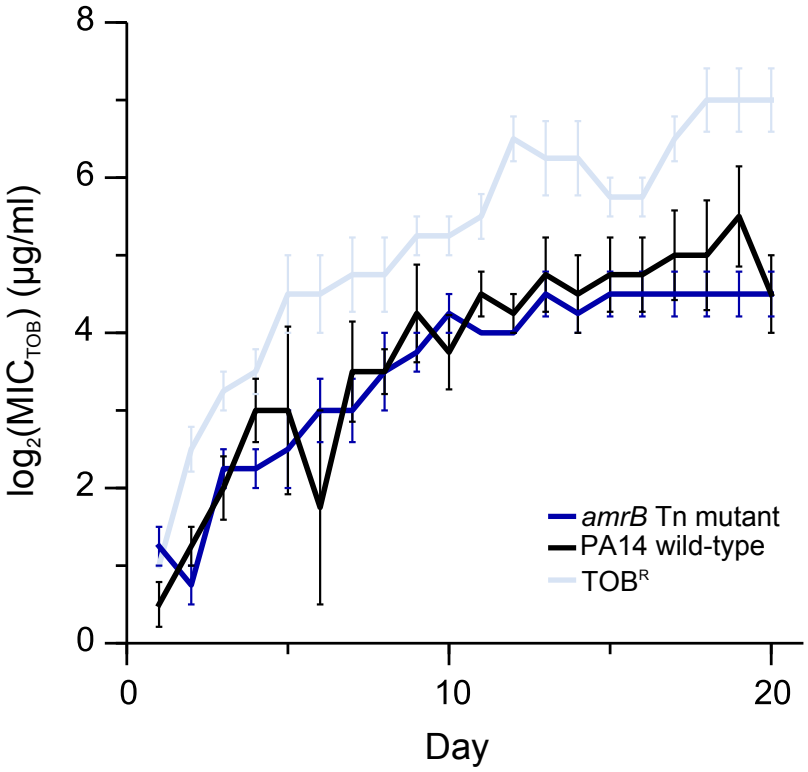

Figure 4.15: **Time course of tobramycin adaptation of the *amrB* transposon mutant.** The *amrB* transposon mutant (dark blue) and the wild-type PA14 strain (black) from the *P. aeruginosa* PA14 transposon library were evolved to tobramycin for 20 days. Shown additionally in light blue is the time course of the TOB^R lineage from the main adaptive evolution experiment (Figure 2.4E). Error bars show SEM of four replicates for each of the time courses.

4.5 Discussion

This adaptive evolution experiments presented in this chapter highlight several different aspects of how bacteria can have complex adaptation histories that can influence their evolutionary dynamics. The results also force us to carefully consider the exact definition and properties of laboratory "reference" strains of bacteria. Most laboratory studies aimed at evaluating the efficacy of different treatment protocols perform parallel evolutionary experiments starting from a "wild-type" laboratory strain; this is an arbitrary concept that ignores

that real-life bacterial pathogens have complex evolutionary histories and that this could in turn have significant consequences on how they adapt to multidrug treatments.

We chose to evolve the three clinical isolates of *P. aeruginosa* that were obtained from the UVA Health System because their antibiograms showed high resistance levels to piperacillin compared to wild-type PA14 strain, and comparably low resistances to tobramycin and ciprofloxacin. It is unclear what the actual antibiotic treatment histories were of the patients from which this isolates were obtained. These isolates have likely undergone complex *in vivo* adaptation processes in the human host that are understandably much different from the controlled laboratory settings in which the main adaptive evolution experiments were performed. We cannot assume that just because the isolates were resistant to piperacillin that at some point in time, they were exposed to piperacillin and developed resistance to the drug. It may be the case that exposure to other beta-lactams other than piperacillin resulted in the cross-resistance to piperacillin, which has been observed in other studies of clinical isolates of *P. aeruginosa* [125]. The fact that two of the three clinical isolates we tested exhibited the resensitization to piperacillin during ciprofloxacin adaptation shows that the drug order-specific effect could be recapitulated in some but not all isolates. Nevertheless we were excited to see that evolutionary forecasting may be possible based solely on the initial antibiogram, and not even necessarily on knowledge of past adaptation histories.

The evolution of the pairs of Hocquet clinical isolates support the hypothesis that the large deletions in the chromosome may contribute to the decreased rate of tobramycin adaptation. In this case, we were focused on the genotypic differences between the pyomelanin-producing and parental wild-type isolates, namely the large deletions, in explaining the drug order-specific effect. In our main adaptive evolution experiment, the large deletions were

primarily selected for during adaptation to piperacillin. However, in the Hocquet isolates, the authors reported that the patients from which the isolates were taken from were treated with other drugs, such as ceftriaxone, fosfomycin, amikacin, cotrimoxazole, co-amoxiclav, and colimycin [64]. Of these drugs, ceftriaxone is a beta-lactam and co-amoxiclav is a combination of a beta-lactam and a beta-lactamase inhibitor. It is unclear what the nature of the selective pressures was that led to the pyomelanin phenotype/large deletion genotype in these isolates. Again, nevertheless, we were excited to see that evolutionary forecasting may be possible in this case based on the pyomelanin phenotype, which correlated with the presence of the large deletion in *P. aeruginosa*.

Lastly, we attempted to identify which gene of the large deletions may contribute to limiting the rate of adaptation to tobramycin. One major caveat that we were aware of was that it could be possible that this drug order-specific effect was the result of the deletion of more than one of the genes, and that the phenotype could not be attributed to one single gene. Nevertheless, we hypothesized that the *mexXY* genes may have played a role in limiting the rate of tobramycin resistance evolution, since the MexXY-OprM efflux pump is the primary efflux pump of aminoglycosides in *P. aeruginosa* [124]. The *mexX* and *mexY* genes were consistently lost as part of the large deletions of PIP^R-1, -2, and -3, as well as in the "PM" Hocquet isolates. However, when we evolved the *mexY* transposon mutant and the wild-type strain to tobramycin, we did not observe a significant difference between their MIC_{TOB} time courses. Curiously, the wild-type strain of the transposon library, which is a separate PA14 stock than Day 0 Ancestor, did not evolve as much resistance to tobramycin as the Day 0 Ancestor. This case highlights how it is unclear what the differences are between the two "wild-type PA14" strains and the ambiguity of the appropriate choice of control

strain.

Chapter 5

Metabolic differences in drug-evolved lineages

5.1 Foreword

So far in this dissertation, we have characterized the phenotypic properties of resistance (as measured by the MIC profiles) and the genotypic determinants of resistance (genomic mutations) of the evolved lineages of *P. aeruginosa*. In this chapter, we turn our attention to characterizing the metabolic properties of the antibiotic resistance, drug-evolved lineages. Little is known about how metabolism becomes rewired during adaptation to antibiotics [126]. To better understand the role of antibiotic adaptation in influencing metabolic function, we profiled the catabolic capabilities of a subset of the one-drug-evolved lineages by measuring the growth curves of the bacteria on 190 different carbon sources. The results in this chapter describe preliminary observations of how adaptation to different antibiotics can lead to altered metabolic profiles. We also discuss our ideas of strategies to incorporate these data into the genome-scale metabolic reconstruction of *P. aeruginosa* to further investigate

how global metabolic profiles are altered by antibiotic adaptation. The work presented in this chapter has been done in collaboration with Laura Dunphy, and I am grateful to be a part of this team project with her.

5.2 Introduction

In our adaptive laboratory experiments, *P. aeruginosa* was evolved to withstand the stresses of the antibiotic selection pressures. The different antibiotic treatments influenced which genes were mutated and the mutations allowed for mechanisms of increased resistance. All of the adaptive laboratory evolution experiments were performed in LB media, which is a nutrient rich environment [127]. Hence, the media in conjunction with the antibiotic contribute to the selection pressures that drive adaptation. The mutations seen in the Day 20 and Day 40 Control lineages exemplify the genetic changes that occurred during adaptation to just the LB media.

P. aeruginosa is a hardy bacterium and is known for its ability to grow on a wide array of substrates across a broad temperature range [128]. We were interested to see if adaptation to antibiotics altered the metabolic capabilities of the bacterium and if it gained or lost the ability to grow on different substrates. The development of antibiotic resistance is often accompanied by a fitness cost that reduces the rate of bacterial proliferation [3, 47, 129, 130]. We hypothesized that adaptation to different drugs would lead to different changes in altering the metabolic capabilities. Empirically, we noticed that several of the drug-evolved lineages grew slower than the Day 0 Ancestor on LB agar media, which suggested to us that the evolution of antibiotic resistance resulted in fitness costs, even on rich media.

To investigate this question, we used Biolog Phenotype MicroArrays [131] to measure the growth of three of the one-drug-evolved lineages as well as the Day 0 Ancestor on 190 different single carbon sources. We then analyzed the growth curves to determine key parameters of growth such as growth rate, time to mid-exponential phase, and maximum growth density [132]. The differences in these growth properties highlight how antibiotic resistance evolution can affect the overall growth properties of the bacteria, and how there can be different tradeoffs between resistance and growth capabilities depending on the antibiotic.

5.3 Materials and methods

5.3.1 Carbon source utilization screen

We chose to test the Day 0 Ancestor and the one-drug evolved lineages Day 20 PIP^R-1, Day 20 TOB^R-3, and Day 20 CIP^R-4. Frozen bacterial stocks of these lineages were used to streak LB agar plates, which were then incubated at 37°C for approximately 20 hours. Cells were scraped from the lawn and incrementally added into 13 ml of IF-0 inoculating fluid to reach an inoculum density of OD_{600} of 0.07. 100 µl of the bacterial suspension was added into each of the wells for the PM1 and PM2 plates. The OD_{600} was measured at ten minute intervals with a plate reader (Tecan Infinite M200 Pro) for 48 hours with shaking. Three replicates each of lineage were used for each of the PM1 and PM2a plates [131], totaling 190 unique carbon sources and two negative controls across the two plates.

5.3.2 Automated calculation of key growth parameters

Prototypical time courses of bacteria growth (growth curves) are usually defined by three phases of growth: lag, exponential, and stationary, representing the different processes that bacterial culture undergoes during its growth in a particular media condition [133]. The dynamics and other parameters of the growth curves can vary across different media conditions, bacterial strains, and other laboratory conditions. We standardized the method by which these growth curve parameters were calculated for our set of data. We used an algorithm to automatically calculate the key growth parameters that can be inferred from curve including: growth rate, maximum growth density, and time to mid-exponential phase.

To calculate the growth rate, we implemented a sliding window algorithm adapted from [132], and added several modifications to improve the estimation of the growth parameter. Theoretically, bacterial cultures undergo a phase of exponential growth when the cells rapidly divide at a maximum rate. The first-order growth rate constant that characterizes this growth property is called the specific growth rate, or more simply the growth rate [132]. The growth rate is traditionally calculated by finding the slope of the linear region of the of the natural logarithm-transformed growth data. Here, the sliding window algorithm calculates the slope of the linear regression of the first eight consecutive natural logarithm-transformed data points (corresponding to 80 minutes). This calculated slope is stored in a vector. Next, the slope is calculated for data points two through nine and then stored. This is done iteratively until the slope is calculated for the last set of eight data points (hence, the sliding window).

The algorithm also determines the maximum natural logarithm-transformed data point

and the time at which it occurs, and we define that time to be the start of stationary phase. We decided to have the algorithm only consider windows of data points that occur before the start of stationary phase when calculating the growth rate. The window with the largest slope is identified, and then the algorithm expands the window to include any neighboring windows whose slope is at least 95% of the maximum slope. The slope of this expanded window is then the calculated growth rate. We then also stored the time of the first data point of the expanded window and defined this time to be the time to exponential phase. This time represents the duration of the lag phase, and the beginning of exponential phase.

5.4 Results

5.4.1 Carbon source utilization screens

We profiled the growth of Day 0 Ancestor, Day 20 PIP^R-1, Day 20 TOB^R-3, and Day 20 CIP^R-4 on 190 different carbon sources using the Biolog Phenotype MicroArray PM1 and PM2a plates [131] with three replicates each. The PM1 and PM2a plates each have a negative control well and 95 carbon sources. With three replicates for each of the four strains, we collected a total of 2,304 growth curves.

The Day 0 Ancestor is derived from the laboratory PA14 strain of *P. aeruginosa*, and the growth profiles for this wild-type strain matched those of other studies that have used the Biolog Phenotype MicroArray plates for screening of carbon source utilization [134–136]. In Figure 5.1, Figure 5.2, and Figure 5.3, we present example growth curves of the tested strains when grown on L-proline, L-histidine, and glycine, respectively. These three examples

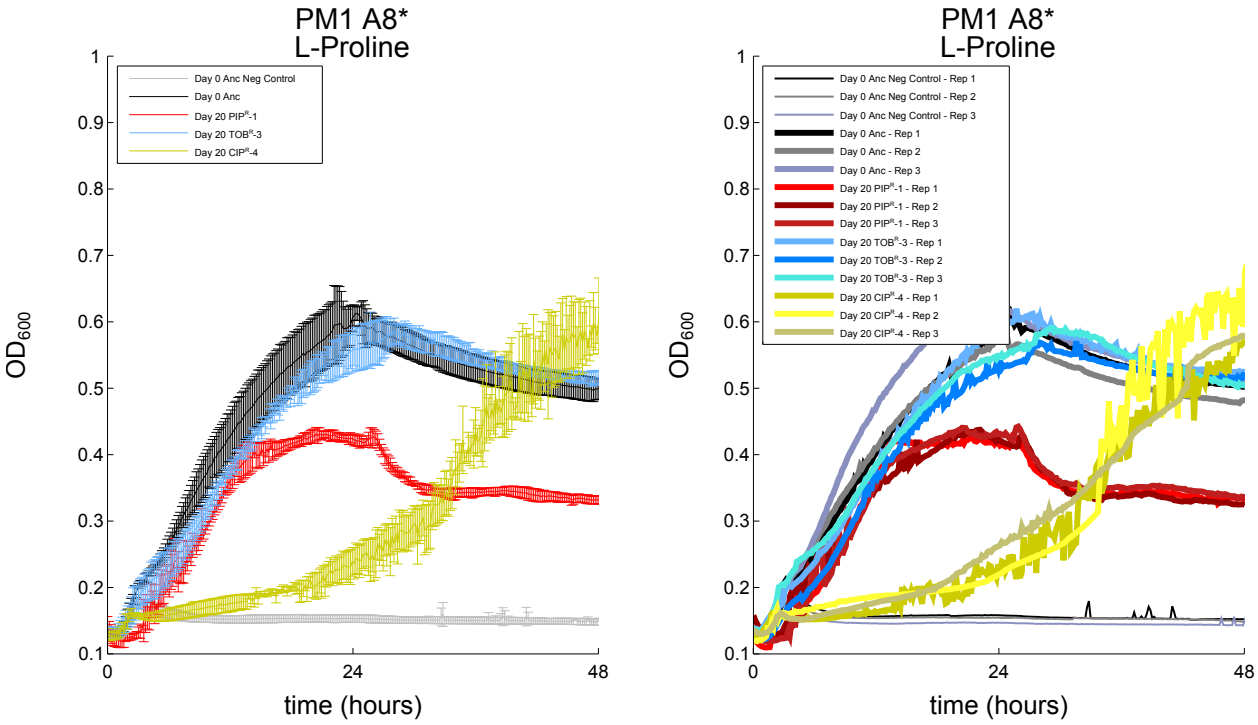

Figure 5.1: **Example of a substrate that all four strains can catabolize.** These growth curves show that all four of the tested strains can catabolize L-proline as a single carbon source. The right plot shows the time courses of the three individual replicates performed for each strain, and the left plot shows the corresponding averages and standard deviations.

highlight some of the similarities and differences in the growth dynamics for the four strains. In Figure 5.1, we see that the Day 0 Ancestor is capable of growing on L-proline as a sole carbon source. Additionally, the three antibiotic resistant strains are also able to grow on L-proline, albeit with different growth dynamics. The general shape of the growth curve of Day 20 TOB^{R}-3 matches very well with that of Day 0 Ancestor. However, while Day 20 PIP^{R}-1 is also capable of growing on L-proline, its growth curve exhibits a lower maximum cell density than that of Day 0 Ancestor and Day 20 TOB^{R}-3. Lastly, Day 20 CIP^{R}-4 reaches a comparable maximum cell density as that of Day 0 Ancestor and Day 20 TOB^{R}-3, but it has a slower growth rate, and the maximum density is only reached near the end of the 48 hour experiment.

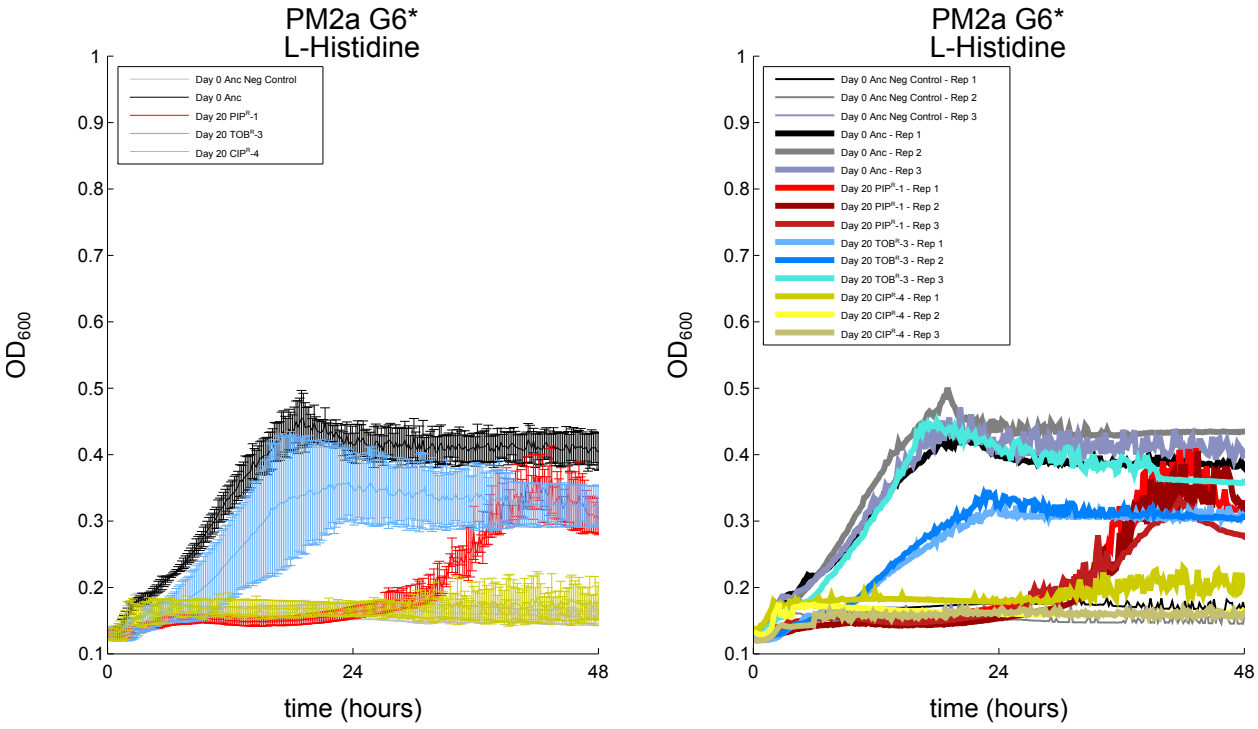

Figure 5.2: **Example of a substrate that three of the four strains can catabolize.** These growth curves show not all four of the tested strains can catabolize L-histidine as a single carbon source. The Day 20 CIP^{R}-4 lineage has lost the ability to catabolize L-histidine. The right plot shows the time courses of the three individual replicates performed for each strain, and the left plot shows the corresponding averages and standard deviations.

Figure 5.2 shows an example of a carbon source for which three of the four tested strains can catabolize. While Day 0 Ancestor, Day 20 PIP^{R}-1, and Day 20 TOB^{R}-3 can all grow on L-histidine as a sole carbons source, it appears that Day 20 CIP^{R}-4 has lost the ability to catabolize this substrate, as the growth curve for this strain showed no growth. Lastly, Figure 5.3 shows an example of a substrate for which all four strains cannot catabolize as a single carbon source. The growth curves of all four strains when grown on glycine show no signs of growth on this substrate, which is consistent with what was observed in another study [134].

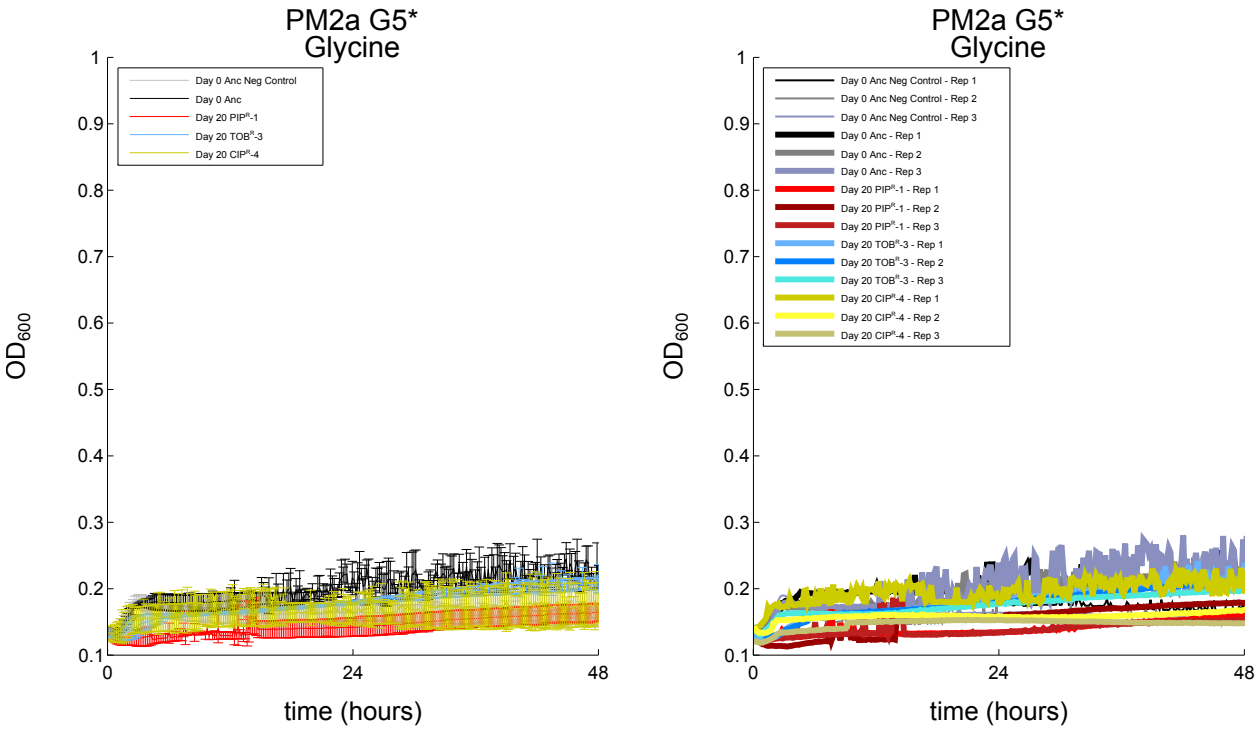

Figure 5.3: **Example of a substrate that none of the strains can catabolize.** These growth curves show that all four of the tested strains cannot catabolize glycine as a single carbon source. The right plot shows the time courses of the three individual replicates performed for each strain, and the left plot shows the corresponding averages and standard deviations.

5.4.2 Calculation of growth parameters from the growth curves

We were interested in calculating key growth parameters from the growth curves including growth rate, maximum cell growth density, and time to exponential phase [132]. Since, we had over two thousand growth curves to analyze, we sought to use an automated approach to calculate these key parameters. To that end, we implemented a sliding window algorithm based on an existing algorithm [132], and added several modifications to improve the accuracy of the calculations, especially to account for the noise in the growth curves data. Figure 5.4 shows illustrative examples of these calculations for one of the replicates runs of Day 20 TOB^R-3 grown on Tween 80 in panel (A), and tyramine in panel (B). The bottom subplots of these panels in Figure 5.4 show the original OD_{600} growth curves. The middle subplots show the natural logarithm-transformed data. The maximum growth density is identified by the algorithm is denoted by the teal line. The time at which this occurs (representative of the beginning of stationary phase) is marked by the magenta circle. The top subplot shown the slopes of the linear regressions of eight-data-point windows of the natural logarithm-transformed data. The algorithm finds the maximum slope before the start of stationary phase and then expands the corresponding eight-data-point window to include neighboring windows whose slope is 95% of this maximum slope. The slope the linear regression of the data points in this expanded window is then the calculated growth rate. The red line segment in the middle subplot shows the linear regression of the expanded window, and the slope of this regression is the calculated growth rate.

In the illustrative example shown in Figure 5.4, while growth on Tween 80 and tyramine result in comparable maximum cell growth densities (teal line), we see that this maximum

occurs at about 9 hours in Tween 80 vs 22 hours in tyramine. Furthermore, the red line segment for Tween 80 has a greater slope than that of tyramine, indicating a higher growth rate for Tween 80. Lastly, the time corresponding to the start of the red line segment occurs earlier in Tween 80 than in tyramine, indicating a shorter time to mid-exponential phase in Tween 80.

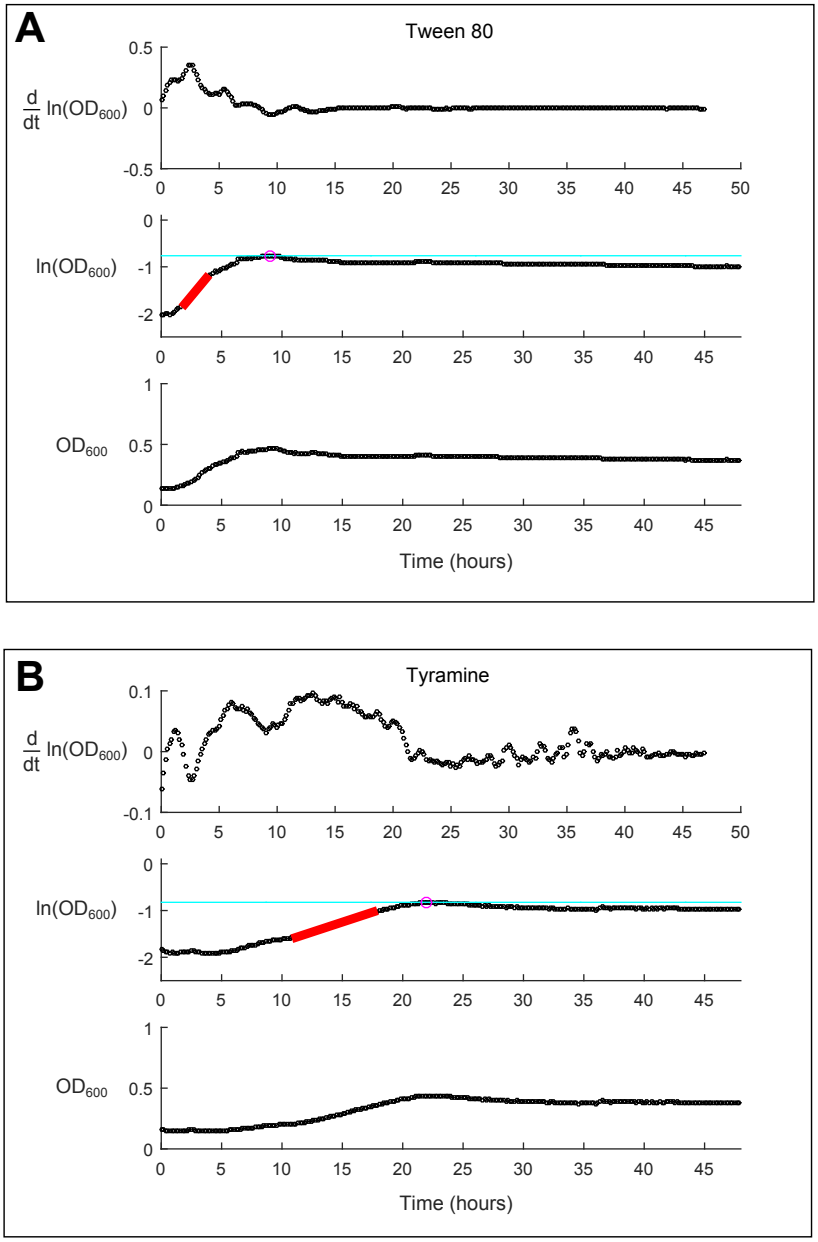

Figure 5.4: **Illustrative example of calculation of growth parameters.** (A) The bottom plot of panel (A) shows the original growth curve (OD_{600}) of one replicate of Day 20 TOB^R-3 grown on Tween 80 as single carbon source. The middle subplot shows the natural logarithm of the raw OD_{600} values. The algorithm determines the maximum natural logarithm-transformed value (teal line), and the time which it occurs (magenta circle). This time is defined as the beginning of stationary phase. The top plot shows the slope of the linear regression of the sliding windows, consisting of 8 time points each, of the data from the middle plot. The red line denotes the window for which the algorithm has identified the maximum slope, and this calculated slope is defined as the growth rate (in units of $hour^{-1}$). (B) The same analysis is done for the growth curve of one replicate of Day 20 TOB^R-3 grown on tyramine.

5.4.3 Growth versus no growth on the difference carbon sources

Next, we analyzed the calculated maximum cell growth densities of the growth curves to determine the overall growth capabilities of the four strains on the 190 different carbon sources. To do this, we computed normalized maximum cell growth densities. For each strain, six total experiments were run, where an experiment consists of either the PM1 or PM2a plate, which each consists of 96 substrates (one of which is a negative control). As an example, L-proline is found on PM1 plate. So, the maximum OD_{600} of the three PM1 negative control growth curves are first averaged. Next, the maximum OD_{600} of the three PM1 L-proline growth curves are averaged. Then the difference is calculated between these two averages, and this value is defined as the normalized maximum cell density for a given strain grown on L-proline. Figure 5.5 shows the normalized maximum cell densities of the four tested strains grown on the 190 carbon source substrates.

Next, we grouped the normalized maximum cell densities into two groups: those that were indicative of growth and those that were indicative of no growth. For this, growth was defined as a normalized maximum cell density greater than 0.1, while no growth was defined as a normalized maximum cell density less than 0.1. Figure 5.6 shows the result of this binary grouping. In total, there were 32 carbon sources that supported growth for all four tested strains, 19 carbon sources that supported growth for three of the strains, 15 carbon sources that supported growth for two of the strains, 22 carbon sources that supported growth for only one of the strains, and 102 carbon sources did not support growth on any of the strains (and additionally two negative controls). There were a few interesting cases: our calculations report that while Day 0 Ancestor did not grow on N-acetyl-D-glucosamine, the

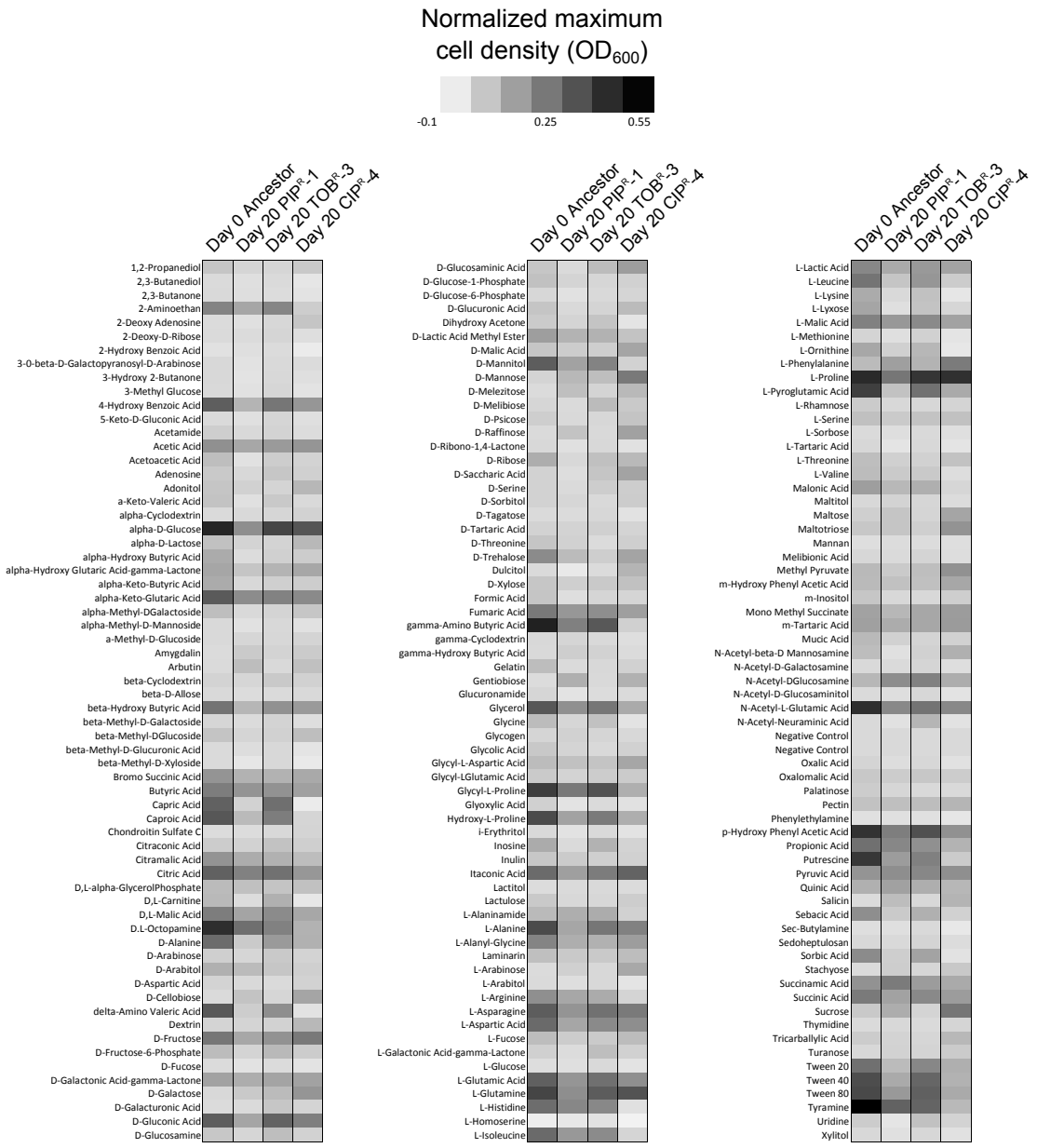

Figure 5.5: **Normalized maximum cell density.** This heatmap shows the normalized maximum OD_{600} values for each of the substrates that the four strains were grown on. For a given strain and substrate, the maximum OD_{600} was calculated for each of the three replicates and then averaged. This was also done for the negative control, which when then subtracted from the first value.

three antibiotic-evolved lineages did grow. Also, there were four carbon sources that did not support growth of the Day 0 Ancestor, but did support growth on two of the three antibiotic resistant strains. Lastly, there were fourteen substrates for which Day 20 CIP^R-4 supposedly were able to grow on that the three other tested strains could not grow on (including the Day 0 Ancestor), but I suspect that there were issues with this slow growing strain when performing the Biolog Phenotype MicroArray screens.

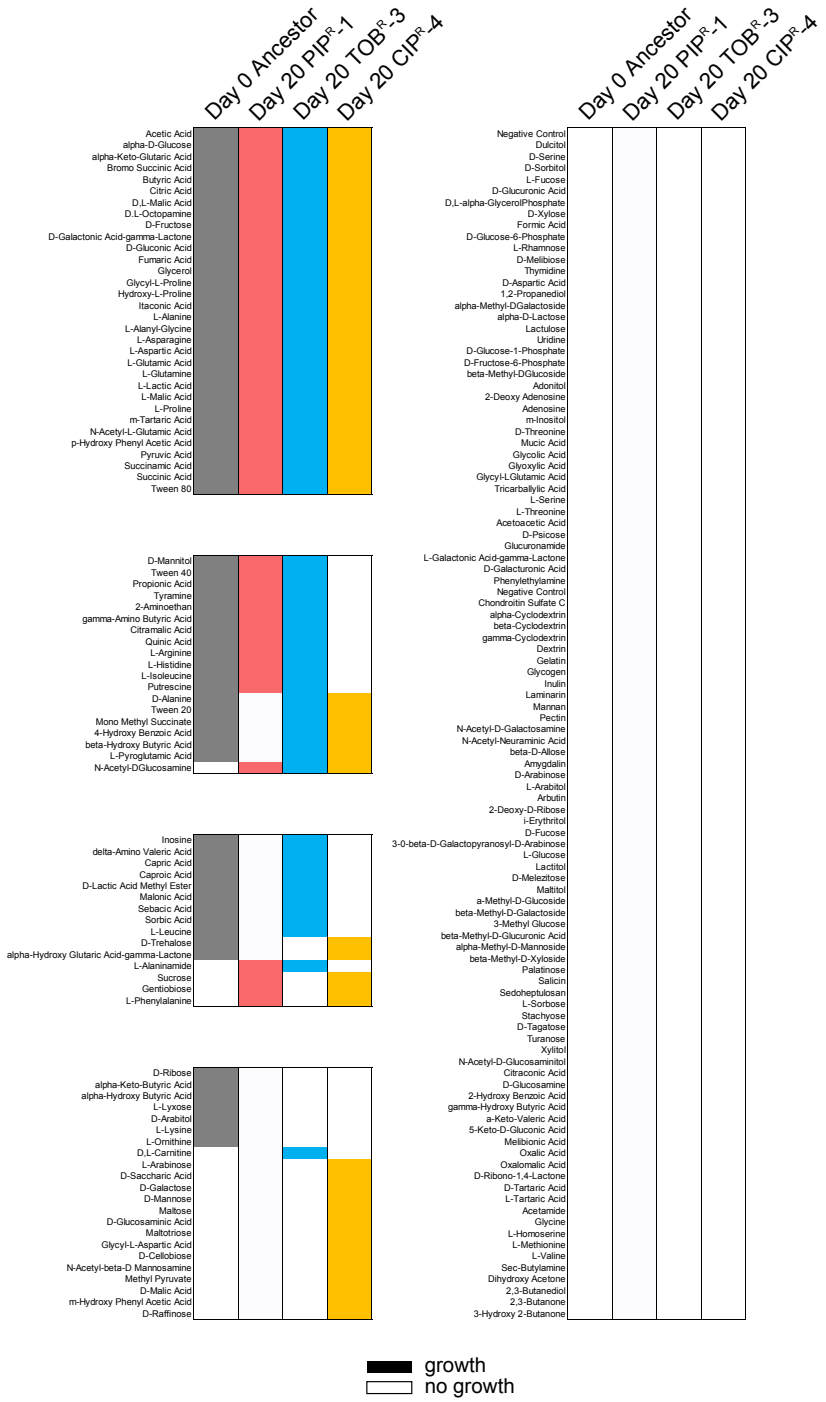

Figure 5.6: **Determination of growth or no growth on the substrates.** We took the data from Figure 5.5 and defined growth on a substrate to occur if the normalized mean cell density was greater than 0.1, and no growth to occur if the normalized mean cell density was less than 0.1. The metabolites are grouped by the number of strains for which it supports growth for. For example, the top left group shows the metabolites that support growth for all four strains, and the right group shows the metabolites that cannot support growth for any of the four strains.

5.4.4 Summary of the growth parameters for the substrates that support growth of all four strains

Finally, we focused our attention on the 32 carbon substrates that supported growth for all four of the tested strains. Figure 5.7 shows the normalized maximum cell densities, growth rates, and times to exponential phase of growth on these carbon sources. Table 5.1 summarizes these growth parameters by averaging the values across all 32 of the substrates. Overall, we observed that in general, compared to Day 0 Ancestor, the three antibiotic resistant strains had lower maximum growth densities, longer lag phases (more specifically, time to mid-exponential phase), and lower growth rates. The Day 20 PIP^{R}-1 strain had particularly longer times to mid-exponential phase. Even though all four strains could catabolize these 32 carbon sources, these reduced growth capabilities observed in the antibiotic resistant strains show that there are fitness costs to developing antibiotic resistance.

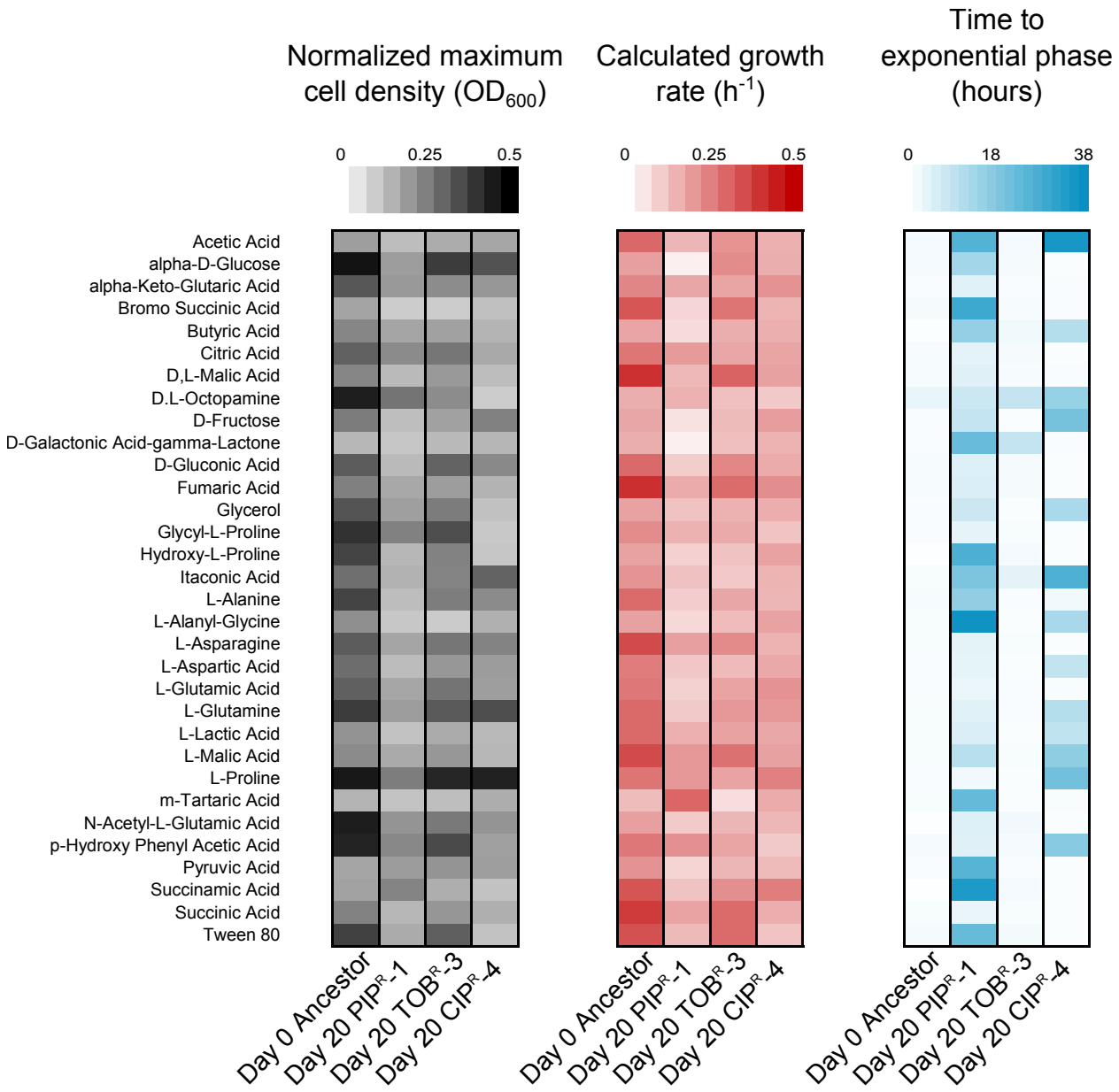

Figure 5.7: **Growth parameters for the metabolites that support growth for all four strains.** The normalized maximum cell densities, calculated growth rates, and time to exponential phase are shown for the 32 metabolites that support growth of all four strains. The parameters are calculated for each individual replicate, and the heatmap shows the average of three replicates for each strain and metabolite pair.

Table 5.1: **Average growth parameters across the 32 carbon sources that support growth of all four strains.**

Strain	Avg. max OD_{600}	Avg. lag phase (hr)	Avg. growth rate (hr^{-1})
Day 0 Ancestor	0.30	1.31	0.26
Day 20 PIP^R-1	0.17	13.22	0.13
Day 20 TOB^R-3	0.24	1.97	0.19
Day 20 CIP^R-4	0.19	7.69	0.17

5.5 Discussion

We have begun to characterize the metabolic differences in strains of *P. aeruginosa* that have been evolved to resist different antibiotics. We observed several cases where the three antibiotic resistant strains were able to grow on substrates that the Day 0 Ancestor could grow on. However, the growth rates and maximum densities were often reduced compared to that of Day 0 Ancestor. We also observed that several substrates supported growth of Day 0 Ancestor, but one or more of the evolved lineages were unable to grow. These are likely cases of fitness costs that were accrued during the adaptation to the antibiotics.

We implemented a sliding window algorithm to automatically calculate key growth parameters from a growth curve including growth rate, time to exponential phase, and maximum growth density. While prototypical "textbook" growth curves often exhibit well defined lag, exponential, and stationary phases of growth [132], we found the growth curves generated from our Biolog screens had a variety of shapes that made calculation of these parameters a non-trivial task. The algorithm attempts to calculate the key growth parameters, but it has potential pitfalls. In general, the noise in the growth time course is the major determinant of issues with the calculations. The time courses are not monotonically increasing, which would be the case for an ideal growth curve, making it particularly difficult to calculate the slopes of the logarithm-transformed data. In any case, the parameters in the algorithm are tunable

and can be altered. Naturally, the pitfall of frequently changing the algorithm parameters is that the entire analysis pipeline would need to be redone for every alteration.

There are several future directions that we plan to continue pursuing with this dataset. We plan to investigate the drug-specific similarities and differences seen in the carbon source utilization screens. For example, in the case of growth on L-histidine (Figure 5.2), which mutations that occurred during adaptation to ciprofloxacin (Day 20 CIP^R-4) resulted in the loss of the ability to catabolize L-histidine compared to the Day 0 Ancestor? What are the genetic mechanisms of this loss of catabolic potential? The Day 20 CIP^R-4 lineage only has two mutated genes: a deletion in *nfxB* (which regulates expression of the MexCD-OprJ efflux pump [109]), and a SNP in *aroB*, which encodes 3-dehydroquinate synthase (this enzyme participates in phenylalanine, tyrosine, and tryptophan biosynthesis [137]). Here, it is unclear how ciprofloxacin adaptation in this lineage led to the loss of the ability to catabolize L-histidine when considering only the genetic mutations that occurred.

One potential method to investigate the role of the antibiotic adaptation processes in altering the catabolic profiles is to use genome-scale metabolic reconstructions, which models the metabolic capabilities of an organism [138–140]. We plan to use flux sampling techniques [141] to constrain the metabolic reconstruction of *P. aeruginosa* PA14 [136] and determine which set of metabolic reactions must be inactivated to best recapitulate the results of the carbon source growth screens. Hence, three constrained models will be created for Day 20 PIP^R-1, Day 20 TOB^R-3, and Day 20 CIP^R-4, each with different sets of constrained metabolic reactions, and we plan to use these models to better understand the relationship between antibiotic adaptation and metabolism.

The interdependencies of antibiotic resistance evolution and metabolic functions are still

relatively unknown. Studies have shown that in conjunction with the primary mechanisms of actions that different antibiotics utilize to kill bacteria, antibiotics from a variety of drug classes universally induce reactive oxygen species-mediated stress in bacteria, leading to bactericidal effects [142]. The functions of multidrug efflux pumps are closely tied to energy metabolism in bacteria as several classes of these pumps depend on the proton motive force [92]. A recent study investigated how adaptation of *E. coli* growth on glycolytic versus gluconeogenic carbon sources influenced the evolutionary dynamics of antibiotic resistance to different drugs [143]. They observed condition-dependent constraints in evolution such as the shift from respiratory to fermentative metabolism of glucose when efflux pumps were overexpressed. Related to this study, it would be interesting to evolve one of the antibiotic resistant strains used in this study that developed a growth defect on a carbon source to that same carbon source to see if compensatory adaptation would restore that strain's ability to efficiently catabolize the metabolite. It would also be interesting to see if high resistance is still maintained after adaptation to the carbon source. Overall, the differences observed in the catabolic functionalities in the drug-evolved strains can yield new insight for potentially targeting metabolic functions to slow down the evolution of antibiotic resistance [144].

Chapter 6

Dissertation discussion

6.1 Discussion

This study presents evidence of how the evolutionary history of bacterial adaptation to antibiotics can complicate strategies for treating infections and for limiting the further development of multidrug resistance. Exposing bacteria to fluctuating environments have been shown to be potentially good strategies for slowing down the development of resistance [40, 42, 145]. More broadly, mechanisms of memory and history dependence in bacterial systems are being uncovered to better understand the dynamics of bacterial survival and adaptation in fluctuating environments [146–148]. For example, a recent study showed that the survival of *Caulobacter crescentus* in response to a high concentration of sodium chloride stress depended on the duration and timing of an earlier treatment of a moderate concentration of sodium chloride, and that this effect was linked to delays in cell division, which led to cell-cycle synchronization [149]. Another study described what they call response memory, which is when a gene regulatory network continues to persist after removal of its external

inducer. The study showed that in *E. coli*, *lac* induction in *E. coli* transiently continued when the environment was switched from lactose to glucose, which may be beneficial when the environment fluctuates over short timescales [150]. The results of those studies as well as the results from this study challenge the notion that bacteria respond solely to their present environment. Bacteria can encounter different stressors over time such as osmotic, oxidative, and acidic stress, and other studies have looked at how adaptation to one stressor protects the bacteria against other stressors if the environment were to change [30, 55]. Another example of bacteria adapting to changing environments is how *P. aeruginosa*, which can be found in the natural environment in the soil and water, can readily adapt to a human host under the right conditions and consequently become pathogenic [151].

There are several factors involved in the emergence of antibiotic resistance that are clinically important that are not considered in this study. We have not taken into account any of the pathogen/host interactions such as the role of the immune system. We also do not take into consideration the pharmacokinetics of the drug and the time-dependent fluctuation of drug concentration as experienced by the bacteria in a human host environment. Furthermore, the dosages of clinical regimens are typically much higher than the wild-type MIC, and the evolutionary dynamics of the bacteria under these conditions may be different from those seen in our study, where the drug pressure is slowly increased over time. We neglect to consider the role of horizontal gene transfer, which is a common mechanism of antibiotic resistance transfer, and focus rather on the role of de novo mutations acquired during adaptation. Because of the nature of the serial passaging method, we may be selecting for fast growers that may not necessarily have mutations that confer the most amount of resistance in terms of the MIC. We used a strong selection pressure in this study by propagating from

the highest concentration of drug that showed growth, but it has been shown that weak antibiotic selection pressure can greatly affect the adaptive landscape [67, 152]. Lastly, these bacteria were evolved to one antibiotic at a time and we do not know how different mutant lineages would adapt if competed against each other. It would be interesting in the future to conduct competition experiments to measure the fitness of the different lineages with respect to each other.

While adaptive evolution of clinical isolates suggests that the drug order-specific effects are clinically relevant, actual clinical studies must be performed to test the true clinical applicability of these effects. A major challenge that still needs to be addressed is how to translate the results of in vitro adaptive evolution experiments to effective therapies that can be used in an actual clinical setting [6]. For example, in this study, we saw that in vitro adaptation to piperacillin starting from wild-type *P. aeruginosa* often led to large chromosomal deletions and concomitant pyomelanin hyperproduction. However, the clinical isolates we analyzed (with data in Figure 4.4) were used to test the hypothesis that *P. aeruginosa* with high piperacillin resistance would become resensitized to piperacillin if adapted to ciprofloxacin. Yet, none of these isolates were pyomelanogenic. On the other hand, the pyomelanogenic clinical isolates from Figure 4.8 were used to test the hypothesis that *P. aeruginosa* with large chromosomal deletions would have reduced rates of tobramycin resistance evolution than their parental counterparts, yet these pyomelanin producing isolates were not more resistant to piperacillin. The evolution of these different sets of clinical isolates helped to support the concept of the drug order-specific effects that were uncovered in the main adaptive evolution experiment. However, it would seem that the former set of isolates were more phenotypically representative of Day 20 PIP^R in terms of high MIC_{PIP}, while the latter set

of isolates were more genetically representative of Day 20 PIP^R in terms of having the large chromosomal deletions. Disparities between the phenotypic and genotypic adaptations such as this will need to be studied further in terms of strain-specific differences, actual history of antibiotic exposure, and other factors that are beyond the scope of this study.

Despite these caveats, there are several key factors of this study that provide confidence in the claims made. We saw consistency in the parallel replicates for the treatment lineages. An interesting exception is Day 40 PIP^RTOB^R-4, which had a higher final tobramycin resistance compared to Day 40 PIP^RTOB^R-1, -2 and -3, which we believe is attributed to the large genomic deletions seen in the first three replicates, but not in the fourth replicate. We observed parallel evolution where several genes were mutated independently across multiple lineages, and overall there were less than 15 mutations per 20 days of evolution, and these two observations suggest positive selection. Furthermore, many of the mutated genes are observed in clinical isolates of *P. aeruginosa*, further giving credence to the clinical relevance of these mutations.

As mentioned previously, studies that have looked at alternating treatments of antibiotics have primarily looked at the effects of rapid switching, typically at daily or sub-daily intervals. One of such recent studies evaluated how *E. coli* responded to 136 different sequential treatments of sub-inhibitory concentrations of doxycycline and erythromycin, with each treatment consisting of eight "seasons" of 12 hour long adaptation periods to one of the drugs [42]. Using final optical density as an endpoint metric, the study found that five of the sequential treatments could clear the bacteria at the end of the eighth season. Interestingly, one of those five successful treatments consisted of four seasons of erythromycin, followed subsequently by four seasons of doxycycline. On the other hand, the treatment consisting

of four seasons of doxycycline followed by four seasons of erythromycin did not manage to clear the bacteria at the end of eight seasons. While the experimental setup is much different compared to that of this present study in terms of organism, antibiotics used, duration of treatment, and endpoint metric, these two treatments (four seasons of erythromycin then four seasons of doxycycline and vice versa) are quite analogous to the types of treatments tested in our present study. The fact that these authors found a difference in the outcomes of this pair of opposite sequential treatments may suggest that drug order-specific effects similar to those presented in our study may play a role in the evolutionary dynamics of their experiments.

Cycling between two drugs that exhibit collateral sensitivity to one another has been proposed and tested as a strategy to slow down the rate of resistance development [2]. The rationale here is that as a bacterial population evolves to become resistant to one drug, it concurrently becomes more susceptible to a second drug. Then, when the second drug is deployed, a wild-type subpopulation would outcompete the subpopulation that became resistant to the first drug (and hypersensitive to the second drug). Studies that have systematically tested for collateral sensitivities across a variety of antibiotics in *E. coli* have consistently discovered that when *E. coli* is adapted to drugs of the aminoglycoside class, it develops collateral sensitivity to several other drugs of different drug classes including beta-lactams, DNA synthesis inhibitors, and protein synthesis inhibitors [2, 38, 67]. In our present study, we tested one aminoglycoside (tobramycin), and we did not observe any collateral sensitivity arise to piperacillin or ciprofloxacin during adaptation to tobramycin. Instead, we saw collateral sensitivity to piperacillin and tobramycin arise as *P. aeruginosa* was adapted to ciprofloxacin, which is a DNA synthesis inhibitor. While we only tested one

drug in each of three drug classes, the dissimilarity of collateral sensitivity profiles between those studies and this present study may highlight how collateral sensitivity profiles may be organism-specific and drug-specific. Further supporting this idea, these prior studies also showed that while adaptation to drugs of the aminoglycoside class as a whole tended to lead to collateral sensitivity to other drug classes, not every aminoglycoside drug that was tested induced the same collateral sensitivity profiles.

While we did observe cases of collateral sensitivity, the main focus of our study was not to look at how resistance profiles to other drugs concurrently change during the adaptation to one drug, but rather to see how the adaptation to one drug influences the future evolutionary dynamics as the resistant population adapts to a new drug. Additionally, we wanted to see how adaptation to the second drug affects the resistance profile of the drug that the bacteria originally developed resistance to. Our sustained drug adaptation scheme can be thought of as being more akin to month-long antibiotic cycling at the level of the hospital ward, or the environments that bacteria in persistent chronic infections are exposed to. Our results show drug-specific cases where high resistance to one drug can be reversed. In some cases resensitization can occur simply from removal of the drug pressure (i.e. adaptation to LB media). In other cases, high resistance still persists when the drug pressure is removed; however, active adaptation to a second drug can lead to the resensitization of the first drug, as we saw when piperacillin-resistant lineages were subsequently adapted to ciprofloxacin. We also observed a case where removal of the drug pressure allowed for partial resensitization, yet adaptation to a second drug maintained the high resistance to the first drug (tobramycin-resistant lineages adapted to piperacillin maintained comparatively high MIC_{TOB}). Finally, we observed cases where pre-adaptation to one drug limits the rate of subsequent adaptation to a second drug

(prior piperacillin adaptation limits the rate of subsequent tobramycin adaptation). These history-dependent evolutionary dynamics highlight the complexity of bacterial adaptation to multidrug therapies, serve as a framework for forecasting evolutionary trajectories based on genetic and phenotypic signatures of past adaptation, and ultimately help to elucidate our fundamental understandings of the evolutionary forces that drive resistance adaptation.

Asymmetrical evolutionary responses in changing environments have been studied in terms of collateral sensitivity/resistance [2, 38], temperature [153], other abiotic stresses [30], and in cancer treatments [154]. Here we present the concept of drug history-specific effects in multidrug resistance adaptation, whereby history of adaptation to one antibiotic environment can influence the evolutionary dynamics during subsequent adaptation to another antibiotic environment. These history-specific effects have direct clinical implications on optimizing antibiotic treatment strategies to slow and prevent the emergence of dangerous multidrug resistant bacterial pathogens.

6.2 Future directions

There are several future directions that I can foresee this dissertation progress towards in the future. I group these future directions into ones that are immediate, medium-term, and long-term based on their goals and/or feasibility. An immediate future direction could consist of further and more rigorous characterization of the mutations revealed from the whole genome sequencing experiments. I mentioned in Chapter 3 that single colonies of the evolved lineages were chosen to be sequenced and, hence the mutations observed in those single colonies may not have been representative of the whole population. I think it would be interesting to

perform Sanger sequencing on several of the observed mutations for multiple colonies of each lineage. Throughout the adaptive evolution experiments, one major assumption was that the strong selection pressure of the antibiotics would cause certain mutations to be selected for over time and that these mutations would become fixed in the population [155]. However, this cannot be assumed to be the norm, as processes including clonal interference, bet hedging, genetic hitchhiking, and fluctuating growth environments can contribute to population heterogeneity [156]. I suspect that many of the inconsistencies in the anomalous mutations at the bottom of Table A.4 will be resolved after further investigation of the population heterogeneity.

Another relatively straightforward experiment would be to perform whole genome sequencing of the Day 40 $PIP^{R}LB$, $TOB^{R}LB$, and $CIP^{R}LB$ lineages. Because the adaptive evolution experiments for these lineages were performed as control experiments after all the other lineages were sequenced, we have not yet had a chance to sequence the genomes of these "control" lineages. I expect that doing so will help elucidate and hopefully support some of the hypothesized mechanisms of resensitization or maintenance of high resistance when the Day 20 one-drug-evolved lineages are evolved to a second drug or to LB. Sequencing these lineages would also yield information on compensatory mutations in the cases where resensitization occurred [157].

We had tested the hypothesis that the large chromosomal deletions were involved in limiting the rate of tobramycin adaptation, and specifically, we evolved the *amrB* (*mexY*) transposon mutant to see if it would develop less tobramycin resistance than the wild type PA14 strain. The result of this experiment was a bit ambiguous: the wild type strain and the mutant strain showed no notable difference in MIC_{TOB} after 20 days of tobramycin

adaptation, but the MIC_{TOB} values were comparably less than the MIC_{TOB} of Day 20 TOB^R, leading us to question whether what the appropriate "PA14 control" really is (Figure 4.15). Nevertheless, it would be interesting to obtain more mutants from the transposon library that correspond to the 160 genes that were lost in the Day 20 PIP^R-1, -2, and -3 lineages (Table A.6). Evolving these transposon mutants, perhaps in a more high throughput manner (akin to the experiment done in Figure 2.9 with the 96-pin replicator tool), could hopefully elucidate the causative gene or genes involved in this particular drug order-specific effect.

One medium-term future direction would be to artificially introduce some of the mutations we saw from the whole genome sequencing experiments into the wild type strain of *P. aeruginosa* and other relevant genetic backgrounds through allelic exchange or other methods of genetic manipulation [158]. Precisely engineering the observed mutations into the relevant genetic background strain would help elucidate the role of the mutated gene in contributing to antibiotic resistance and the drug order-specific effects. For example, to test the hypothesis that mutations in *mexS* during subsequent ciprofloxacin adaptation of Day 20 PIP^R led to the piperacillin resensitization, we could introduce the mutations into the Day 20 PIP^R lineages to see if the resulting mutant indeed had a decreased MIC_{PIP}. Similarly, this mutation could be introduced into the three piperacillin-resistant clinical isolates to see if the mutation could lead to piperacillin resensitization in these strains as well. Furthermore, it would be interesting to see if the mutation could lead to the resensitization of piperacillin in strains that were resistant to both piperacillin and tobramycin (e.g. Day 40 PIP^RTOB^R or Day 40 TOB^RPIP^R). To generalize along these lines, it would be interesting to evolve the Day 40 two-drug evolved lineages to a third drug or two one of the drugs it was already evolved to. These experiments would shed further light on the potential of antibiotic cycling

strategies in slowing resistance evolution [159].

I have described previously the hypothesis that *mexS* mutations lead to the overexpression of MexEF-OprN, which in turn leads to the resensitization of piperacillin in the Day 40 $PIP^{R}CIP^{R}$ lineages. This mutation as well as other mutations in genes related to the multidrug efflux pumps (e.g. the dashed boxes in Figure 3.10) leads me to suspect that several of the drug order-specific effects manifest as a result of differential expression of the efflux pumps in *P. aeruginosa*. Indeed, there have been studies that have shown that the expression of certain efflux pumps correlate inversely [101, 102]. I believe it would be worthwhile to measure the gene expression profiles of several efflux pump-related genes [92], (or more directly, the protein profiles via immunoblotting [160]) in the different lineages to determine if the efflux pumps indeed do play a significant role in the drug order-specific effects.

In Chapter 5, we began to uncover the differences in metabolic capabilities between the different evolved lineages, and we plan to continue characterizing these similarities and differences in catabolic functions. Specifically, we aim to determine the genetic determinants of the differences seen in the growth capabilities on the single carbon sources, and we plan to investigate the role of mutations in metabolic genes in contributing to these differences. Furthermore, genome-scale metabolic reconstructions can be employed to explore these differences with a computational systems biology perspective [161]. The genome-scale metabolic reconstruction of *P. aeruginosa* PA14 has recently been published [136] (I had a small role in the curation of this model), and we plan to develop strategies to constrain the model to recapitulate the differences in catabolic capabilities. We plan to use flux sampling techniques to explore the flux space of the model to determine the global metabolic profiles of the drug-evolved lineages [162].

These last set of ideas are long-term future directions and what I expect to see in the field of adaptive laboratory evolution applied to the problem of antibiotic resistance. First, I would like to see the experiments presented in this dissertation performed with different antibiotic drugs and with different organisms of interest. It is important to determine the generalizability of the drug order-specific effects in other organisms. We saw that even between different strains of *P. aeruginosa* that there were differences in collateral sensitivity and collateral resistance profiles [59, 65]. Furthermore, adaptive laboratory evolution studies in *E. coli* consistently reported that aminoglycoside adaptation resulted in collateral sensitivity to different drugs [2, 38]. In our case however, we saw no collateral sensitivity develop to piperacillin or ciprofloxacin during adaptation to tobramycin, which is the aminoglycoside that we tested in our study. These observations suggest that drug order-specific effects may be strain-specific as well as organism-specific, and further investigation of these effects are needed in order to better understand the generalizability of the evolutionary dynamics of antibiotic resistance evolution.

One important open question that has not been addressed yet is the relationship between collateral sensitivity and resensitization of an already antibiotic-resistance strain. Both of these processes involve the decrease in MIC of drug. In the former, it is the decrease in MIC relative to the wild type baseline value. In the latter case, it is the decrease in MIC relative to the high MIC in an already resistant strain. It is unclear whether the mechanisms of "lowering the MIC" are the same or different in these cases. We observed that ciprofloxacin adaptation resulted in collateral sensitivities to piperacillin and tobramycin, and that subsequent ciprofloxacin adaptation in Day 20 PIP^R and Day 20 TOB^R led to resensitization of piperacillin and tobramycin, respectively. It would be interesting to test the hypothesis

that the mutations responsible for the collateral sensitivity are the same mutations responsible for the resensitization. To do this, one could use genome engineering to introduce the mutation(s) of interest into the wild-type Day 0 Ancestor, and Day 20 one-drug-evolved lineages, and measure the MICs of the resulting mutants. If introduction of the mutation into the Day 0 Ancestor leads to collateral sensitivity and introduction of the mutation into the Day 20 one-drug-evolved lineages leads to resensitization, one could posit that the genetic mechanisms underlying these two processes are related.

We saw that evolution of two of three clinical isolates of *P. aeruginosa* with high piperacillin resistance recapitulated the drug order-specific effect of resensitization to piperacillin when adapted to ciprofloxacin, suggesting that the drug order-specific effects could be used as a means of evolutionary forecasting, based on MIC profile of isolates. I would like to see this idea investigated more thoroughly, and see if evolutionary trajectories can be forecasted based solely on a set of MIC profiles for a panel of drugs for a given isolate or strain of bacteria. Can an antibiogram serve as a surrogate for the history of adaptation that the bacterial population has undergone? Can we use the antibiogram in conjunction with knowledge of the drug order-specific effects to predict how the bacteria will evolve when treated with a certain antibiotic? In a related question, can we predict when genes are mutated based on history of adaptation that is deduced from the antibiogram? Can we then also predict which genes will likely be mutated during subsequent drug adaptation given the constraints of the drug order-specific effects? Investigation of these questions will move the field towards a state where it may one day be possible to predict the precise evolutionary trajectories a bacterial population based on minimal initial screening of the properties of the bacteria. In this scenario, bacterial populations could then be steered to follow paths along the adaptive

landscape that minimize the development of resistance [152, 163].

I believe advances in the field of adaptive laboratory evolution will allow this technique to become an even more powerful tool for studying the evolution of antibiotic resistance. The daily serial passaging protocol that I have employed in this study is fundamentally very simple: bacteria is grown, then sampled, and then transferred into fresh media, and the process continues for as many cycles as you choose. This protocol is extremely simple in theory, but it very tedious in practice and is also low throughput in terms of the number of parallel replicates that can be performed for each tested condition. Parallel replicates are typically located physically next to each other on a 96-well microtiter plate, and daily serial propagation can easily be prone to human error, leading to cross-contamination of wells and/or samples, as I had experienced on a few occasions. With only at most four replicates per treatment in my adaptive laboratory evolution experiments, statistical power is limited. Furthermore, it would be interesting to see if there would be a higher degree of parallel evolution in terms of the genes that were mutated if there were more replicates per treatment.

While daily serial passaging is a tried and true method of evolving bacteria in the lab, I am excited to see what new innovative methods can be developed to quickly evolve bacteria to become antibiotic resistant in a more automated fashion. One promising approach is the use of the morbidostat, which is a continuous culture device that has been engineered to automatically monitor the density of a liquid bacterial culture and dynamically challenge the population with increasing concentrations of antibiotics [35]. The feedback loops in the device are implemented such that it automatically tunes the drug concentration to maintain constant growth inhibition. The resistance to trimethoprim in *E. coli* increased approxi-

mately 1,680 fold using this system. Another promising system is the evolution of bacteria on solid media. The same group that developed the morbidostat has recently developed what is essentially a giant agar petri dish with a concentration gradient of antibiotics embedded within the agar. This device, which is named the microbial evolution and growth arena (or MEGA plate), is 120 cm x 60 cm and can be used to visualize the evolution of the bacteria as it grows and migrates along the agar surface to higher concentration of nutrients, but concurrently traverses an increasing concentration gradient of the antibiotic [164]. Using this adaptive laboratory evolution platform, one can visually see the emergence and decline of distinct evolutionary lineages as they compete for resources, and bacteria from different lineages can be sampled to have their genomes sequenced. Innovative new platforms for adaptive laboratory evolution such as the morbidostat and MEGA plate will allow for the automation of adaptive laboratory evolution, which will in turn allow for higher throughput and lower the risk of human error.

Lastly, there is currently a striking disconnect between the theories developed from *in vitro* experiments and mathematical models of resistance evolution versus the clinical practices and decisions of antibiotic deployment. It is often difficult to test evolutionary theories of antibiotic resistance in humans, as the main goal of the clinician is to typically prescribe the antibiotics that will most quickly clear the infection, especially when the infection is life threatening [6]. The dosing practices used by clinicians are often empirical in nature. "Evolutionary medicine" or "Darwinian medicine" is the application of evolutionary theory in understanding health and disease [165]. The field of evolutionary medicine will flourish when more physicians and evolutionary biologists realize that they must collaborate in order to synergistically develop new ways of using antibiotics that slows down the rate of resistance

evolution. I think it would be of great value for researchers studying antibiotic resistance evolution to collaborate with physicians and immerse themselves in the clinic to understand how antibiotics are actually used in practice [166]. Only then can the gap between theory and practice of antibiotic deployment strategies that mitigate the development of resistance begin to close.

The evolved lineages of *P. aeruginosa* that I have generated from the adaptive laboratory evolution experiments will serve as a useful collection of antibiotic resistant mutants that can be used to further investigate the different facets of the evolutionary dynamics of resistance development. Frozen samples of the bacteria were saved after every daily serial passage, resulting in a "frozen fossil record" [167]. Bacterial samples can be revived from any point in the evolution experiment, which means that the evolutionary dynamics can be studied at a finer time resolution. In our whole genome sequencing experiments, we determined the mutations that occurred in the lineages at Day 20 and Day 40. If we wanted to investigate the order that the mutations appeared in a Day 20 lineage for example, the genomes could be sequenced at Day 5, 10, and 15. Because we saved the sample daily, this type of investigation is possible.

Already, my collection of evolved lineages has served as a valuable resource for other members in the Papin lab in their own projects. While most of these projects are in the early preliminary phases, I am excited to see that others have found my evolved bacterial lineages useful and are being used to explore questions that diverge from the original goals of this dissertation. For example, Laura has plans to study the gene expression profile changes of antibiotic resistant bacteria [94] using the TOB^R mutants, and has begun to characterize the growth properties of these mutants when exposed to different concentrations of tobramycin.

Laura has also used my evolved strains to investigate drug synergy in combination drug therapies [168]. Anna has ideas to explore the role of persistence in antibiotic resistant strains compared to the wild-type strain [169], and has plans to perform kill-curve experiments to explore possible differences in persistence. During initial prototyping phases of his co-culture device, Tom used one of my mutants that hyperproduced the pyomelanin pigment to test the properties of the membrane that is used to confine the bacteria to their separate chambers, but allow the diffusion of metabolites. Lastly, John from Nathan Swami's laboratory at UVA has recently been using my evolved lineages of *P. aeruginosa* to test the applicability of using the deielectrophoresis technology developed in the Swami to rapidly distinguish between susceptible and resistance bacteria [170]. I look forward to seeing the developments of all of these projects, and am excited to see what other creative and innovative projects my evolved lineages (and my dissertation as a whole) will help inspire.

6.3 Conclusions

Antibiotic resistance is truly a serious threat to public health. It is quite understandable that at the scope of a single patient presented with a bacterial infection, the goal of the physician is prescribe a regiment that quickly and effectively clears the infection. However, if antibiotic resistance develops in any single patient, this threat may be transmitted to the population at large and disseminated across the globe [171]. While there was been much renewed attention in the past few years in developing new technologies to screen large compound libraries for antimicrobial properties [172], it is not enough of a solution to discover new antibiotics, because invariably, resistance to these compounds will arise based on the patterns we have

witnessed for all the existing antibiotics. We must study the mechanisms by which bacteria evolve to withstand the effects these drugs and use this knowledge to rationally design drug therapies that mitigate the development of resistance. Here, we have investigated the role of adaptation history in influencing the evolutionary dynamics of resistance development in the pathogenic model organism *P. aeruginosa*. In conclusion, this dissertation serves as a framework for advancing our fundamental understanding of how the history of adaptations that bacterial populations experience plays a role in the development of multidrug antibiotic resistance.

Bibliography

[1] J. A. Bartell et al. "Comparative metabolic systems analysis of pathogenic Burkholderia." In: *Journal of Bacteriology* 196.2 (Jan. 2014), pp. 210–226. DOI: 10.1128/JB.00997-13 (cit. on p. 1).

[2] L. Imamovic and M. O. A. Sommer. "Use of Collateral Sensitivity Networks to Design Drug Cycling Protocols That Avoid Resistance Development". In: *Science Translational Medicine* 5.204 (Sept. 2013), pp. 132–204. DOI: 10.1126/scitranslmed.3006609 (cit. on pp. 2, 12, 17, 130, 132, 136).

[3] D. I. Andersson and D. Hughes. "Antibiotic resistance and its cost: is it possible to reverse resistance?" In: *Nature Reviews Microbiology* 8.4 (Apr. 2010), pp. 260–271. DOI: 10.1038/nrmicro2319 (cit. on pp. 4, 107).

[4] L. L. Ling et al. "A new antibiotic kills pathogens without detectable resistance". In: *Nature* 517.7535 (2015), pp. 455–459. DOI: 10.1038/nature14098 (cit. on pp. 4, 5).

[5] M. A. Cooper and D. Shlaes. "Fix the antibiotics pipeline." In: *Nature* 472.7341 (2011), p. 32. DOI: 10.1038/472032a (cit. on pp. 4, 5).

[6] K. Kupferschmidt. "Resistance fighters". In: *Science* 352.6287 (2016), pp. 758–61. DOI: 10.1126/science.352.6287.758 (cit. on pp. 5, 128, 139).

[7] US Department of Health and Human Services. *Antibiotic Resistance Threats in the United States, 2013*. Tech. rep. Atlanta: Centers for Disease Control and Prevention, 2013 (cit. on pp. 4, 9).

[8] A. Fleming. "Nobel Lecture, December 11, 1945". In: *Nobel Lectures, Physiology or Medicine 1942-1962* (1964), pp. 83–93 (cit. on p. 5).

[9] I. M. Gould. "Antibiotic resistance: the perfect storm". In: *International Journal of Antimicrobial Agents* 34.SUPPL. 3 (2009), S2–S5. DOI: 10.1016/S0924-8579(09)70549-7 (cit. on p. 5).

[10] J. M. Andrews. "Determination of minimum inhibitory concentrations". In: *The Journal of Antimicrobial Chemotherapy* 48 Suppl 1 (July 2001), pp. 5–16. DOI: 10.1093/jac/48.suppl{_}1.5 (cit. on pp. 6, 20).

[11] I. Wiegand et al. "Mutator genes giving rise to decreased antibiotic susceptibility in Pseudomonas aeruginosa". In: *Antimicrobial Agents and Chemotherapy* 52.10 (2008), pp. 3810–3813. DOI: 10.1128/AAC.00233-08 (cit. on pp. 6, 8, 10, 51).

[12] D. J. Biedenbach, I. H. Schermer, and R. N. Jones. "Validation of Etest for seven antimicrobial agents using regulatory criteria for the assessment of antimicrobial susceptibility devices." In: *Diagnostic Microbiology and Infectious Disease* 27.1-2 (1997), pp. 1–5 (cit. on p. 6).

[13] Clinical and Laboratory Standards Institute. "Performance Standards for Antimicrobial Susceptibility Testing: Twenty-third Informational Supplement M100-S23." In: *CLSI* (2013) (cit. on pp. 8, 9).

[14] H. Ericsson et al. "Determination of minimum inhibitory concentrations (MICs) of antibacterial agents by broth dilution". In: *Clinical Microbiology and Infection* 9.8 (Aug. 2003), pp. ix–xv. DOI: 10.1046/j.1469-0691.2003.00790.x (cit. on p. 8).

[15] H. W. Boucher et al. "Bad bugs, no drugs: no ESKAPE! An update from the Infectious Diseases Society of America." In: *Clinical Infectious Diseases* 48.1 (Jan. 2009), pp. 1–12. DOI: 10.1086/595011 (cit. on p. 9).

[16] World Health Organization. *WHO publishes list of bacteria for which new antibiotics are urgently needed*. 2017 (cit. on p. 9).

[17] N. Cramer et al. "Microevolution of the major common Pseudomonas aeruginosa clones C and PA14 in cystic fibrosis lungs". In: *Environmental Microbiology* 13.7 (2011), pp. 1690–1704. DOI: 10.1111/j.1462-2920.2011.02483.x (cit. on p. 9).

[18] P. D. Lister, D. J. Wolter, and N. D. Hanson. "Antibacterial-Resistant Pseudomonas aeruginosa: Clinical Impact and Complex Regulation of Chromosomally Encoded Resistance Mechanisms". In: *Clinical Microbiology Reviews* 22.4 (Oct. 2009), pp. 582–610. DOI: 10.1128/CMR.00040-09 (cit. on pp. 9, 28, 30, 61).

[19] M. Chatterjee et al. "Antibiotic resistance in Pseudomonas aeruginosa and alternative therapeutic options". In: *International Journal of Medical Microbiology* 306.1 (2016), pp. 48–58. DOI: 10.1016/j.ijmm.2015.11.004 (cit. on pp. 9, 30).

[20] A. A. El Solh and A. Alhajhusain. "Update on the treatment of Pseudomonas aeruginosa pneumonia." In: *The Journal of Antimicrobial Chemotherapy* 64.2 (Aug. 2009), pp. 229–38. DOI: 10.1093/jac/dkp201 (cit. on p. 9).

[21] N. Mesaros et al. "Pseudomonas aeruginosa: resistance and therapeutic options at the turn of the new millennium." In: *Clinical Microbiology and Infection* 13.6 (June 2007), pp. 560–78. DOI: 10.1111/j.1469-0691.2007.01681.x (cit. on p. 9).

[22] J. B. Bulitta et al. "Two Mechanisms of Killing of Pseudomonas aeruginosa by Tobramycin Assessed at Multiple Inocula via Mechanism-Based Modeling". In: *Antimicrobial Agents and Chemotherapy* 59.4 (2015), pp. 2315–2327. DOI: 10.1128/AAC.04099-14 (cit. on p. 9).

[23] D. M. Livermore. "Multiple Mechanisms of Antimicrobial Resistance in Pseudomonas aeruginosa: Our Worst Nightmare?" In: *Clinical Infectious Diseases* 34.5 (Mar. 2002), pp. 634–640. DOI: 10.1086/338782 (cit. on p. 10).

[24] E. B. M. Breidenstein, C. de la Fuente-Núñez, and R. E. W. Hancock. "Pseudomonas aeruginosa: all roads lead to resistance". In: *Trends in Microbiology* 19.8 (Aug. 2011), pp. 419–26. DOI: 10.1016/j.tim.2011.04.005 (cit. on p. 10).

[25] N. Bagge et al. "Constitutive high expression of chromosomal beta-lactamase in Pseudomonas aeruginosa caused by a new insertion sequence (IS1669) located in ampD." In: *Antimicrobial Agents and Chemotherapy* 46.11 (Nov. 2002), pp. 3406–11. DOI: 10.1128/AAC.46.11.3406-3411.2002 (cit. on p. 10).

[26] A. A. Ocampo-Sosa et al. "Alterations of OprD in carbapenem-intermediate and -susceptible strains of Pseudomonas aeruginosa isolated from patients with bacteremia in a Spanish multicenter study". In: *Antimicrobial Agents and Chemotherapy* 56.4 (Apr. 2012), pp. 1703–13. DOI: 10.1128/AAC.05451-11 (cit. on p. 10).

[27] T. M. Conrad, N. E. Lewis, and B. Ø. Palsson. "Microbial laboratory evolution in the era of genome-scale science." In: *Molecular Systems Biology* 7.509 (Jan. 2011), p. 509. DOI: 10.1038/msb.2011.42 (cit. on p. 10).

[28] J. P. Adams and F. Rosenzweig. "Experimental Microbial Evolution: History and Conceptual underpinnings". In: *Genomics* 104.6 (Oct. 2014), pp. 393–398. DOI: 10.1016/j.ygeno.2014.10.004 (cit. on p. 11).

[29] S. F. Elena and R. E. Lenski. "Evolution experiments with microorganisms: the dynamics and genetic bases of adaptation". In: *Nature Reviews Genetics* 4.6 (June 2003), pp. 457–69. DOI: 10.1038/nrg1088 (cit. on p. 11).

[30] M. Dragosits et al. "Evolutionary potential, cross-stress behavior and the genetic basis of acquired stress resistance in Escherichia coli." In: *Molecular Systems Biology* 9.1 (Mar. 2013), p. 643. DOI: 10.1038/msb.2012.76 (cit. on pp. 11, 48, 127, 132).

[31] A. Long et al. "Elucidating the molecular architecture of adaptation via evolve and resequence experiments". In: *Nature Reviews Genetics* 16.10 (Sept. 2015), pp. 567–582. DOI: 10.1038/nrg3937 (cit. on p. 11).

[32] G. I. Lang and M. M. Desai. "The spectrum of adaptive mutations in experimental evolution". In: *Genomics* 104.6 (Dec. 2014), pp. 412–416. DOI: 10.1016/j.ygeno.2014.09.011 (cit. on p. 11).

[33] Z. D. Blount, C. Z. Borland, and R. E. Lenski. "Historical contingency and the evolution of a key innovation in an experimental population of Escherichia coli." In: *Proceedings of the National Academy of Sciences* 105.23 (June 2008), pp. 7899–906. DOI: 10.1073/pnas.0803151105 (cit. on p. 11).

[34] A. C. Palmer and R. Kishony. "Understanding, predicting and manipulating the genotypic evolution of antibiotic resistance". In: *Nature Reviews Genetics* 14.4 (Feb. 2013), pp. 243–248. DOI: 10.1038/nrg3351 (cit. on pp. 11, 51).

[35] E. Toprak et al. "Evolutionary paths to antibiotic resistance under dynamically sustained drug selection". In: *Nature Genetics* 44.1 (Jan. 2012), pp. 101–5. DOI: 10.1038/ng.1034 (cit. on pp. 12, 138).

[36] G. Jansen, C. Barbosa, and H. Schulenburg. "Experimental evolution as an efficient tool to dissect adaptive paths to antibiotic resistance". In: *Drug Resistance Updates* 16.6 (Dec. 2013), pp. 96–107. DOI: 10.1016/j.drup.2014.02.002 (cit. on p. 12).

[37] M. Baym, L. K. Stone, and R. Kishony. "Multidrug evolutionary strategies to reverse antibiotic resistance". In: *Science* 351.6268 (2016), aad3292–aad3292. DOI: 10.1126/science.aad3292 (cit. on p. 12).

[38] V. Lázár et al. "Bacterial evolution of antibiotic hypersensitivity." In: *Molecular Systems Biology* 9.700 (Oct. 2013), p. 700. DOI: 10.1038/msb.2013.57 (cit. on pp. 12, 17, 61, 66, 130, 132, 136).

[39] W. Szybalski and V. Bryson. "Genetic studies on microbial cross resistance to toxic agents. I. Cross resistance of Escherichia coli to fifteen antibiotics". In: *Journal of Bacteriology* 64.4 (1952), pp. 489–499 (cit. on p. 12).

[40] S. Kim, T. D. Lieberman, and R. Kishony. "Alternating antibiotic treatments constrain evolutionary paths to multidrug resistance". In: *Proceedings of the National Academy of Sciences* 111.40 (Sept. 2014), pp. 14494–14499. DOI: 10.1073/pnas.1409800111 (cit. on pp. 12, 13, 48, 61, 126).

[41] C. Munck et al. "Prediction of resistance development against drug combinations by collateral responses to component drugs". In: *Science Translational Medicine* 6.262 (Nov. 2014), 262ra156. DOI: 10.1126/scitranslmed.3009940 (cit. on pp. 12, 48, 61).

[42] A. Fuentes-Hernandez et al. "Using a Sequential Regimen to Eliminate Bacteria at Sublethal Antibiotic Dosages". In: *PLoS Biology* 13.4 (2015), e1002104. DOI: 10.1371/journal.pbio.1002104 (cit. on pp. 12, 13, 126, 129).

[43] M. Rodriguez de Evgrafov et al. "Collateral Resistance and Sensitivity Modulate Evolution of High-Level Resistance to Drug Combination Treatment in Staphylococcus aureus". In: *Molecular Biology and Evolution* 32.5 (2015), pp. 1175–1185. DOI: 10.1093/molbev/msv006 (cit. on pp. 12, 48).

[44] C. Pál, B. Papp, and V. Lázár. "Collateral sensitivity of antibiotic-resistant microbes". In: *Trends in Microbiology* 23.7 (2015), pp. 401–407. DOI: 10.1016/j.tim.2015.02.009 (cit. on pp. 12, 14).

[45] V. Lázár et al. "Genome-wide analysis captures the determinants of the antibiotic cross-resistance interaction network." In: *Nature Communications* 5 (July 2014), p. 4352. DOI: 10.1038/ncomms5352 (cit. on p. 12).

[46] R. Roemhild et al. "Temporal variation in antibiotic environments slows down resistance evolution in pathogenic Pseudomonas aeruginosa". In: *Evolutionary Applications* 8.10 (2015), pp. 945–955. DOI: 10.1111/eva.12330 (cit. on pp. 12, 13).

[47] G. G. Perron, A. Gonzalez, and A. Buckling. "Source–sink dynamics shape the evolution of antibiotic resistance and its pleiotropic fitness cost". In: *Proceedings of the Royal Society B* 274.1623 (2007), pp. 2351–2356. DOI: 10.1098/rspb.2007.0640 (cit. on pp. 13, 107).

[48] S. Sarraf-Yazdi et al. "A 9-year retrospective review of antibiotic cycling in a surgical intensive care unit". In: *Journal of Surgical Research* 176.2 (2012), e73–e78. DOI: 10.1016/j.jss.2011.12.014 (cit. on p. 13).

[49] P. Abel zur Wiesch et al. "Cycling Empirical Antibiotic Therapy in Hospitals: Meta-Analysis and Models". In: *PLoS Pathogens* 10.6 (June 2014). Ed. by C. O. Wilke, e1004225. DOI: 10.1371/journal.ppat.1004225 (cit. on p. 13).

[50] E. M. Brown and D. Nathwani. "Antibiotic cycling or rotation: A systematic review of the evidence of efficacy". In: *Journal of Antimicrobial Chemotherapy* 55.1 (2005), pp. 6–9. DOI: 10.1093/jac/dkh482 (cit. on p. 14).

[51] D. R. Gifford and R. C. Maclean. "Evolutionary Reversals Of Antibiotic Resistance In Experimental Populations Of Pseudomonas Aeruginosa". In: *Evolution* 67.10 (June 2013), pp. 2973–2981. DOI: 10.1111/evo.12158 (cit. on p. 14).

[52] D. M. Weinreich et al. "Should evolutionary geneticists worry about higher-order epistasis?" In: *Current Opinion in Genetics & Development* 23.6 (Nov. 2013), pp. 700–707. DOI: 10.1016/j.gde.2013.10.007 (cit. on p. 18).

[53] H.-H. Chou et al. "Diminishing returns epistasis among beneficial mutations decelerates adaptation." In: *Science* 332.6034 (June 2011), pp. 1190–2. DOI: 10.1126/science.1203799 (cit. on p. 18).

[54] M. F. Schenk et al. "Patterns of Epistasis between beneficial mutations in an antibiotic resistance gene." In: *Molecular Biology and Evolution* 30.8 (Aug. 2013), pp. 1779–87. DOI: 10.1093/molbev/mst096 (cit. on p. 18).

[55] M. Lagator, N. Colegrave, and P. Neve. "Selection history and epistatic interactions impact dynamics of adaptation to novel environmental stresses". In: *Proceedings of the Royal Society of London B: Biological Sciences* 281.1794 (2014), p. 20141679. DOI: 10.1098/rspb.2014.1679 (cit. on pp. 19, 47, 127).

[56] T. P. Lodise, B. Lomaestro, and G. L. Drusano. "Piperacillin-tazobactam for Pseudomonas aeruginosa infection: Clinical Implications of an Extended-Infusion Dosing Strategy." In: *Clinical Infectious Diseases* 44.3 (2007), pp. 357–363. DOI: 10.1016/S0734-3299(08)70539-2 (cit. on p. 30).

[57] R. M. Shawar et al. "Activities of Tobramycin and Six Other Antibiotics against Pseudomonas aeruginosa Isolates from Patients with Cystic Fibrosis." In: *Antimicrobial Agents and Chemotherapy* 43.12 (1999), pp. 2877–2880 (cit. on p. 30).

[58] N. A. Chaudhry et al. "Emerging Ciprofloxacin-Resistant Pseudomonas aeruginosa". In: *American Journal of Ophthalmology* 128.4 (1999), pp. 509–510. DOI: 10.1016/S0002-9394(99)00196-8 (cit. on p. 30).

[59] Y. Feng et al. "Dynamics of Mutations during Development of Resistance by Pseudomonas aeruginosa against Five A ntibiotics". In: *Antimicrobial Agents and Chemotherapy* 60.7 (2016), pp. 4229–4236. DOI: 10.1128/AAC.00434-16 (cit. on pp. 36, 42, 52, 61, 71, 72, 136).

[60] R. K. Ernst et al. "Genome mosaicism is conserved but not unique in Pseudomonas aeruginosa isolates from the airways of young children with cystic fibrosis". In: *Environmental Microbiology* 5.12 (2003), pp. 1341–1349. DOI: 10.1111/j.1462-2920.2003.00518.x (cit. on pp. 42, 43, 75).

[61] N. A. Moran. "Microbial Minimalism: Genome Reduction in Bacterial Pathogens". In: *Cell* 108.5 (2002), pp. 583–586. DOI: 10.1016/S0092-8674(02)00665-7 (cit. on pp. 42, 74).

[62] M. H. Rau et al. "Deletion and acquisition of genomic content during early stage adaptation of Pseudomonas aeruginosa to a human host environment". In: *Environmental Microbiology* 14.8 (2012), pp. 2200–2211. DOI: 10.1111/j.1462-2920.2012.02795.x (cit. on pp. 42, 74).

[63] M. C. Lee and C. J. Marx. "Repeated, Selection-Driven Genome Reduction of Accessory Genes in Experimental Populations". In: *PLoS Genetics* 8.5 (2012), pp. 2–9. DOI: 10.1371/journal.pgen.1002651 (cit. on p. 42).

[64] D. Hocquet et al. "Pyomelanin-producing Pseudomonas aeruginosa selected during chronic infections have a large chromosomal deletion which confers resistance to pyocins". In: *Environmental Microbiology* 18 (2016), pp. 3482–3493. DOI: 10.1111/1462-2920.13336 (cit. on pp. 42, 75, 79, 80, 82, 89, 92, 93, 95, 104).

[65] G. Cabot et al. "Evolution of Pseudomonas aeruginosa Antimicrobial Resistance and Fitness under Low and High Mutation Rates". In: *Antimicrobial Agents and Chemotherapy* 60.3 (2016), pp. 1767–1778. DOI: 10.1128/AAC.02676-15 (cit. on pp. 42, 94, 97, 136).

[66] A. Rodríguez-Rojas et al. "Inactivation of the hmgA gene of Pseudomonas aeruginosa leads to pyomelanin hyperproduction, stress resistance and increased persistence in chronic lung infection". In: *Microbiology* 155.4 (Apr. 2009), pp. 1050–1057. DOI: 10.1099/mic.0.024745-0 (cit. on pp. 43, 75, 89).

[67] T. Oz et al. "Strength of Selection Pressure Is an Important Parameter Contributing to the Complexity of Antibiotic Resistance Evolution". In: *Molecular Biology and Evolution* 31.9 (June 2014), pp. 2387–2401. DOI: 10.1093/molbev/msu191 (cit. on pp. 48, 128, 130).

[68] P. J. Yeh et al. "Drug interactions and the evolution of antibiotic resistance." In: *Nature Reviews Microbiology* 7.6 (2009), pp. 460–6. DOI: 10.1038/nrmicro2133 (cit. on p. 48).

[69] J. P. Torella, R. Chait, and R. Kishony. "Optimal drug synergy in antimicrobial treatments." In: *PLoS Computational Biology* 6.6 (June 2010), e1000796. DOI: 10.1371/journal.pcbi.1000796 (cit. on p. 48).

[70] M. Hegreness et al. "Accelerated evolution of resistance in multidrug environments." In: *Proceedings of the National Academy of Sciences of the United States of America* 105.37 (Sept. 2008), pp. 13977–81. DOI: 10.1073/pnas.0805965105 (cit. on p. 48).

[71] R. Chait, A. Craney, and R. Kishony. "Antibiotic interactions that select against resistance." In: *Nature* 446.7136 (Apr. 2007), pp. 668–71. DOI: 10.1038/nature05685 (cit. on p. 48).

[72] V. Kos et al. "The Resistome of Pseudomonas aeruginosa in Relationship to Phenotypic Susceptibility". In: *Antimicrobial Agents and Chemotherapy* 59.1 (2015), pp. 427–436. DOI: 10.1128/AAC.03954-14 (cit. on p. 50).

[73] A. Fajardo et al. "The neglected intrinsic resistome of bacterial pathogens." In: *PloS One* 3.2 (Jan. 2008), e1619. DOI: 10.1371/journal.pone.0001619 (cit. on p. 50).

[74] N. T. Liberati et al. "An ordered, nonredundant library of Pseudomonas aeruginosa strain PA14 transposon insertion mutants." In: *Proceedings of the National Academy of Sciences of the United States of America* 103.8 (Feb. 2006), pp. 2833–8. DOI: 10.1073/pnas.0511100103 (cit. on pp. 51, 83, 98).

[75] T. Baba et al. "Construction of Escherichia coli K-12 in-frame, single-gene knockout mutants: the Keio collection." In: *Molecular Systems Biology* 2 (2006), p. 2006.0008. DOI: 10.1038/msb4100050 (cit. on p. 51).

[76] M. A. Jacobs et al. "Comprehensive transposon mutant library of Pseudomonas aeruginosa." In: *Proceedings of the National Academy of Sciences of the United States of America* 100.24 (Nov. 2003), pp. 14339–44. DOI: 10.1073/pnas.2036282100 (cit. on p. 51).

[77] A. Dötsch et al. "Genomewide identification of genetic determinants of antimicrobial drug resistance in Pseudomonas aeruginosa." In: *Antimicrobial Agents and Chemotherapy* 53.6 (June 2009), pp. 2522–31. DOI: 10.1128/AAC.00035-09 (cit. on p. 51).

[78] K. N. Schurek et al. "Novel Genetic Determinants of Low-Level Aminoglycoside Resistance in Pseudomonas aeruginosa". In: *Antimicrobial Agents and Chemotherapy* 52.12 (Dec. 2008), pp. 4213–9. DOI: 10.1128/AAC.00507-08 (cit. on pp. 51, 61).

[79] E. B. M. Breidenstein et al. "Complex ciprofloxacin resistome revealed by screening a Pseudomonas aeruginosa mutant library for altered susceptibility." In: *Antimicrobial Agents and Chemotherapy* 52.12 (Dec. 2008), pp. 4486–91. DOI: 10.1128/AAC.00222-08 (cit. on p. 51).

[80] A. Wong, N. Rodrigue, and R. Kassen. "Genomics of Adaptation during Experimental Evolution of the Opportunistic Pathogen Pseudomonas aeruginosa". In: *PLoS Genetics* 8.9 (Sept. 2012), e1002928. DOI: 10.1371/journal.pgen.1002928 (cit. on pp. 52, 73).

[81] A. Folkesson et al. "Adaptation of Pseudomonas aeruginosa to the cystic fibrosis airway: an evolutionary perspective." In: *Nature Reviews Microbiology* 10.12 (Dec. 2012), pp. 841–51. DOI: 10.1038/nrmicro2907 (cit. on p. 52).

[82] T. D. Lieberman et al. "Genetic variation of a bacterial pathogen within individuals with cystic fibrosis provides a record of selective pressures." In: *Nature Genetics* December (Dec. 2013), pp. 1–7. DOI: 10.1038/ng.2848 (cit. on p. 52).

[83] T. D. Lieberman et al. "Parallel bacterial evolution within multiple patients identifies candidate pathogenicity genes." In: *Nature Genetics* 43.12 (Dec. 2011), pp. 1275–80. DOI: 10.1038/ng.997 (cit. on p. 52).

[84] R. L. Marvig et al. "Convergent evolution and adaptation of Pseudomonas aeruginosa within patients with cystic fibrosis". In: *Nature Genetics* 47.1 (Nov. 2015), pp. 57–64. DOI: 10.1038/ng.3148 (cit. on pp. 52, 61).

[85] T. Markussen et al. "Environmental Heterogeneity Drives Within-Host Diversification and Evolution of Pseudomonas aeruginosa". In: *mBio* 5.5 (2014), pp. 1–10. DOI: 10.1128/mBio.01592-14.Editor (cit. on pp. 52, 61).

[86] R. L. Marvig et al. "Genome Analysis of a Transmissible Lineage of Pseudomonas aeruginosa Reveals Pathoadaptive Mutations and Distinct Evolutionary Paths of Hypermutators". In: *PLoS Genetics* 9.9 (2013). DOI: 10.1371/journal.pgen.1003741 (cit. on p. 52).

[87] D. E. Deatherage et al. "Detecting rare structural variation in evolving microbial populations from new sequence junctions using breseq". In: *Frontiers in Genetics* 5.JAN (2015), pp. 1–16. DOI: 10.3389/fgene.2014.00468 (cit. on p. 54).

[88] J. T. Robinson et al. "Integrative genomics viewer". In: *Nature Biotechnology* 29.1 (Jan. 2011), pp. 24–26. DOI: 10.1038/nbt.1754 (cit. on p. 55).

[89] M. Krzywinski et al. "Circos: an Information Aesthetic for Comparative Genomics". In: *Genome Research* 19.604 (2009), pp. 1639–1645. DOI: 10.1101/gr.092759.109 (cit. on p. 56).

[90] T. Spilker et al. "PCR-Based Assay for Differentiation of Pseudomonas aeruginosa from Other Pseudomonas Species Recovered from Cystic Fibrosis Patients". In: *Journal of Clinical Microbiology* 42.5 (May 2004), pp. 2074–2079. DOI: 10.1128/JCM.42.5.2074-2079.2004 (cit. on pp. 57, 81).

[91] A. Untergasser et al. "Primer3–new capabilities and interfaces." In: *Nucleic Acids Research* 40.15 (Aug. 2012), e115. DOI: 10.1093/nar/gks596 (cit. on p. 58).

[92] H. A. Terzi, C. Kulah, and I. H. Ciftci. "The effects of active efflux pumps on antibiotic resistance in Pseudomonas aeruginosa." In: *World Journal of Microbiology & Biotechnology* 30 (2014), pp. 2681–2687. DOI: 10.1007/s11274-014-1692-2 (cit. on pp. 61, 125, 135).

[93] K. Hosokawa et al. "Streptomycin-resistant (rpsL) or rifampicin-resistant (rpoB) mutation in Pseudomonas putida KH146-2 confers enhanced tolerance to organic chemicals". In: *Environmental Microbiology* 4.11 (2002), pp. 703–712. DOI: 10.1046/j.1462-2920.2002.00348.x (cit. on p. 61).

[94] S. Suzuki, T. Horinouchi, and C. Furusawa. "Prediction of antibiotic resistance by gene expression profiles". In: *Nature Communications* 5 (Dec. 2014), p. 5792. DOI: 10.1038/ncomms6792 (cit. on pp. 61, 140).

[95] S. Feliziani et al. "Coexistence and Within-Host Evolution of Diversified Lineages of Hypermutable Pseudomonas aeruginosa in Long-term Cystic Fibrosis Infections". In: *PLoS Genetics* 10.10 (2014). DOI: 10.1371/journal.pgen.1004651 (cit. on p. 61).

[96] J. C. S. Chung et al. "Genomic Variation among Contemporary Pseudomonas aeruginosa Isolates from Chronically Infected Cystic Fibrosis Patients". In: *Journal of Bacteriology* 194.18 (2012), pp. 4857–4866. DOI: 10.1128/JB.01050-12 (cit. on p. 61).

[97] G. L. Winsor et al. "Pseudomonas Genome Database: improved comparative analysis and population genomics capability for Pseudomonas genomes." In: *Nucleic Acids Research* 39.Database issue (Jan. 2011), pp. 596–600. DOI: 10.1093/nar/gkq869 (cit. on p. 64).

[98] J. R. Aeschlimann. "The Role of Multidrug Efflux Pumps in the Antibiotic Resistance of Pseudomonas aeruginosa and Other Gram-Negative Bacteria". In: *Pharmacotherapy* 23.7 (2003), pp. 916–924. DOI: 10.1592/phco.23.7.916.32722 (cit. on pp. 64, 68).

[99] Y. Morita et al. "nalD encodes a second repressor of the mexAB-oprM multidrug efflux operon of Pseudomonas aeruginosa". In: *Journal of Bacteriology* 188.24 (2006), pp. 8649–8654. DOI: 10.1128/JB.01342-06 (cit. on pp. 64, 69).

[100] J. A. Karlowsky et al. "In Vitro Characterization of Aminoglycoside Adaptive Resistance in Pseudomonas aeruginosa". In: *Antimicrobial Agents and Chemotherapy* 40.6 (1996), pp. 1387–1393 (cit. on p. 66).

[101] M. L. Sobel, S. Neshat, and K. Poole. "Mutations in PA2491 (mexS) Promote MexT-Dependent mexEF-oprN Expression and Multidrug Resistance in a Clinical Strain of Pseudomonas aeruginosa". In: *Journal of Bacteriology* 187.4 (2005), pp. 1246–1253. DOI: 10.1128/JB.187.4.1246 (cit. on pp. 69, 135).

[102] H. Maseda et al. "Enhancement of the mexAB - oprM Efflux Pump Expression by a Quorum-Sensing Autoinducer and Its Cancellation by a Regulator , MexT , of the mexEF-oprN Efflux Pump Operon in Pseudomonas aeruginosa". In: *Antimicrobial Agents and Chemotherapy* 48.4 (2004), pp. 1320–1328. DOI: 10.1128/AAC.48.4.1320 (cit. on pp. 69, 135).

[103] L. Fernández, E. B. Breidenstein, and R. E. Hancock. "Creeping baselines and adaptive resistance to antibiotics". In: *Drug Resistance Updates* 14.1 (Feb. 2011), pp. 1–21. DOI: 10.1016/j.drup.2011.01.001 (cit. on p. 70).

[104] A. Skiada et al. "Adaptive resistance to cationic compounds in Pseudomonas aeruginosa". In: *International Journal of Antimicrobial Agents* 37.3 (2011), pp. 187–193. DOI: 10.1016/j.ijantimicag.2010.11.019 (cit. on p. 70).

[105] F. El'Garch et al. "Cumulative Effects of Several Nonenzymatic Mechanisms on the Resistance of Pseudomonas aeruginosa to aminoglycosides". In: *Antimicrobial Agents and Chemotherapy* 51.3 (Mar. 2007), pp. 1016–21. DOI: 10.1128/AAC.00704-06 (cit. on p. 70).

[106] D. Hocquet et al. "MexXY-OprM Efflux Pump Is Necessary for Adaptive Resistance of Pseudomonas aeruginosa to Aminoglycosides". In: *Antimicrobial Agents and Chemotherapy* 47.4 (2003), pp. 1371–1375. DOI: 10.1128/AAC.47.4.1371 (cit. on p. 70).

[107] M. Adam et al. "Epigenetic inheritance based evolution of antibiotic resistance in bacteria". In: *BMC Evolutionary Biology* 8.52 (2008). DOI: 10.1186/1471-2148-8-52 (cit. on p. 71).

[108] S. S. Motta, P. Cluzel, and M. Aldana. "Adaptive Resistance in Bacteria Requires Epigenetic Inheritance, Genetic Noise, and Cost of Efflux Pumps". In: *PLoS ONE* 10.3 (2015). DOI: 10.1371/journal.pone.0118464 (cit. on p. 71).

[109] A. Purssell and K. Poole. "Functional characterization of the NfxB repressor of the mexCD-oprJ multidrug efflux operon of Pseudomonas aeruginosa." In: *Microbiology* 159.Pt 10 (2013), pp. 2058–2073. DOI: 10.1099/mic.0.069286-0 (cit. on pp. 72, 73, 124).

[110] K. Poole et al. "Overexpression of the mexC-mexD-oprJ efflux operon in nfxB-type multidrug-resistant strains of Pseudomonas aeruginosa". In: *Molecular Microbiology* 21.4 (1996), pp. 713–724. DOI: Doi10.1046/J.1365-2958.1996.281397.X (cit. on pp. 72, 73).

[111] N. Masuda et al. "Hypersusceptibility of the Pseudomonas aeruginosa nfxB Mutant to beta-Lactams Due to Reduced Expression of the AmpC beta-Lactamase." In: *Antimicrobial Agents and Chemotherapy* 45.4 (2001), pp. 1284–6. DOI: 10.1128/AAC.45.4.1284-1286.2001 (cit. on p. 72).

[112] N. Masuda et al. "Quantitative Correlation between Susceptibility and OprJ Production in NfxB Mutants of Pseudomonas aeruginosa". In: *Antimicrobial Agents and Chemotherapy* 40.4 (1996), pp. 909–913 (cit. on p. 72).

[113] J. Plucain et al. "Contrasting effects of historical contingency on phenotypic and genomic trajectories during a two-step evolution experiment with bacteria." In: *BMC Evolutionary Biology* 16.86 (2016), pp. 1–11. DOI: 10.1186/s12862-016-0662-8 (cit. on p. 72).

[114] Y. Morita et al. "Induction of mexCD-oprJ operon for a multidrug efflux pump by disinfectants in wild-type Pseudomonas aeruginosa PAO1". In: *Journal of Antimicrobial Chemotherapy* 51.4 (2003), pp. 991–994. DOI: 10.1093/jac/dkg173 (cit. on pp. 72, 73).

[115] K. Hirai et al. "Mutations producing resistance to norfloxacin in Pseudomonas aeruginosa". In: *Antimicrobial Agents and Chemotherapy* 31.4 (1987), pp. 582–586. DOI: 10.1128/AAC.31.4.582 (cit. on p. 73).

[116] L. M. Starr, M. Fruci, and K. Poole. "Pentachlorophenol Induction of the Pseudomonas aeruginosa mexAB-oprM Efflux Operon: Involvement of Repressors NalC and MexR and the Antirepressor ArmR". In: *PLoS ONE* 7.2 (2012), pp. 1–9. DOI: 10.1371/journal.pone.0032684 (cit. on p. 73).

[117] L. M. Ketelboeter, V. Y. Potharla, and S. L. Bardy. "NTBC Treatment of the Pyomelanogenic Pseudomonas aeruginosa Clinical Isolate PA1111 Inhibits Pigment Production and Increases Sensitivity to Oxidative Stress". In: *Current Microbiology* 69.3 (Sept. 2014), pp. 343–348. DOI: 10.1007/s00284-014-0593-9 (cit. on p. 75).

[118] E. Yabuuchi and A. Ohyama. "Characterization of "Pyomelanin" -Producing Strains of Pseudomonas aeruginosa". In: *International Journal of Systematic Bacteriology* 22.2 (1972), pp. 53–64. DOI: 10.1099/00207713-22-2-53 (cit. on p. 75).

[119] G. I. Lang et al. "Pervasive genetic hitchhiking and clonal interference in forty evolving yeast populations." In: *Nature* 500.7464 (July 2013), pp. 571–574. DOI: 10.1038/nature12344 (cit. on p. 76).

[120] P. Kumar, S. Henikoff, and P. C. Ng. "Predicting the effects of coding non-synonymous variants on protein function using the SIFT algorithm." In: *Nature Protocols* 4.7 (2009), pp. 1073–1081. DOI: 10.1038/nprot.2009.86 (cit. on p. 76).

[121] M. R. Farhat et al. "Genomic analysis identifies targets of convergent positive selection in drug-resistant Mycobacterium tuberculosis". In: *Nature Genetics* September (Sept. 2013), pp. 1–9. DOI: 10.1038/ng.2747 (cit. on p. 77).

[122] J. Klockgether et al. "Genome diversity of Pseudomonas aeruginosa PAO1 laboratory strains." In: *Journal of Bacteriology* 192.4 (Feb. 2010), pp. 1113–21. DOI: 10.1128/JB.01515-09 (cit. on p. 77).

[123] C. K. Stover et al. "Complete genome sequence of Pseudomonas aeruginosa PAO1, an opportunisticpathogen". In: *Nature* 406.6799 (Aug. 2000), pp. 959–964. DOI: 10.1038/35023079 (cit. on p. 77).

[124] Y. Morita, J. Tomida, and Y. Kawamura. "MexXY multidrug efflux system of Pseudomonas aeruginosa". In: *Frontiers in Microbiology* 3.408 (2012), pp. 1–13. DOI: 10.3389/fmicb.2012.00408 (cit. on pp. 94, 97, 104).

[125] E. Mokaddas and S. Sanyal. "Resistance Patterns of Pseudomonas aeruginosa to Carbapenems and Piperacillin/Tazobactam". In: *Journal of Chemotherapy* 11.2 (Jan. 1999), pp. 93–96. DOI: 10.1179/joc.1999.11.2.93 (cit. on p. 103).

[126] J. L. Martínez and F. Rojo. "Metabolic regulation of antibiotic resistance." In: *FEMS Microbiology Reviews* 35.5 (Sept. 2011), pp. 768–89. DOI: 10.1111/j.1574-6976.2011.00282.x (cit. on p. 106).

[127] "LB (Luria-Bertani) liquid medium". In: *Cold Spring Harbor Protocols* 2006.1 (June 2006), pdb.rec8141. DOI: 10.1101/pdb.rec8141 (cit. on p. 107).

[128] A. E. LaBauve and M. J. Wargo. "Growth and laboratory maintenance of Pseudomonas aeruginosa." In: *Current Protocols in Microbiology* Chapter 6 (May 2012), Unit 6E.1. DOI: 10.1002/9780471729259.mc06e01s25 (cit. on p. 107).

[129] Q. Qi, G. Preston, and R. MacLean. "Linking System-Wide Impacts of RNA Polymerase Mutations to the Fitness Cost of Rifampin Resistance in Pseudomonas aeruginosa". In: *mBio* 5.6 (2014), pp. 1–12. DOI: 10.1128/mBio.01562-14.Editor (cit. on p. 107).

[130] D. I. Andersson. "The biological cost of mutational antibiotic resistance: any practical conclusions?" In: *Current Opinion in Microbiology* 9.5 (Oct. 2006), pp. 461–5. DOI: 10.1016/j.mib.2006.07.002 (cit. on p. 107).

[131] B. R. Bochner. "Phenotype MicroArrays for High-Throughput Phenotypic Testing and Assay of Gene Function". In: *Genome Research* 11.7 (2001), pp. 1246–1255. DOI: 10.1101/gr.186501 (cit. on pp. 108, 110).

[132] B. G. Hall et al. "Growth rates made easy". In: *Molecular Biology and Evolution* 31.1 (2014), pp. 232–238. DOI: 10.1093/molbev/mst187 (cit. on pp. 108, 109, 114, 123).

[133] M. H. Zwietering et al. "Modeling of the Bacterial Growth Curve". In: *Applied and Environmental Microbiology* 56.6 (June 1990), pp. 1875–1881 (cit. on p. 109).

[134] D. A. Johnson et al. "High-throughput phenotypic characterization of Pseudomonas aeruginosa membrane transport genes". In: *PLoS Genetics* 4.10 (2008). DOI: 10.1371/journal.pgen.1000211 (cit. on pp. 110, 112).

[135] M. A. Oberhardt et al. "Genome-scale metabolic network analysis of the opportunistic pathogen Pseudomonas aeruginosa PAO1." In: *Journal of Bacteriology* 190.8 (Apr. 2008), pp. 2790–803. DOI: 10.1128/JB.01583-07 (cit. on p. 110).

[136] J. A. Bartell et al. "Reconstruction of the metabolic network of Pseudomonas aeruginosa to interrogate virulence factor synthesis". In: *Nature Communications* 8 (Mar. 2017), p. 14631. DOI: 10.1038/ncomms14631 (cit. on pp. 110, 124, 135).

[137] G. Millar and J. R. Coggins. "The complete amino acid sequence of 3-dehydroquinate synthase of Escherichia coli K12." eng. In: *FEBS letters* 200.1 (May 1986), pp. 11–17 (cit. on p. 124).

[138] J. D. Orth, I. Thiele, and B. Ø. Palsson. "What is flux balance analysis?" In: *Nature Biotechnology* 28.3 (Mar. 2010), pp. 245–8. DOI: 10.1038/nbt.1614 (cit. on p. 124).

[139] I. Thiele and B. Ø. Palsson. "A protocol for generating a high-quality genome-scale metabolic reconstruction." In: *Nature Protocols* 5.1 (Jan. 2010), pp. 93–121. DOI: 10.1038/nprot.2009.203 (cit. on p. 124).

[140] C. R. Haggart et al. "Whole-genome metabolic network reconstruction and constraint-based modeling." In: *Methods in Enzymology* 500 (Jan. 2011), pp. 411–33. DOI: 10.1016/B978-0-12-385118-5.00021-9 (cit. on p. 124).

[141] J. Schellenberger and B. Ø. Palsson. "Use of Randomized Sampling for Analysis of Metabolic Networks". In: *Journal of Biological Chemistry* 284.9 (Feb. 2009), pp. 5457–5461. DOI: 10.1074/jbc.R800048200 (cit. on p. 124).

[142] P. Bhargava and J. J. Collins. "Boosting bacterial metabolism to combat antibiotic resistance". In: *Cell Metabolism* 21.2 (2015), pp. 154–155. DOI: 10.1016/j.cmet.2015.01.012 (cit. on p. 125).

[143] M. Zampieri et al. "Metabolic constraints on the evolution of antibiotic resistance". In: *Molecular Systems Biology* 13 (2017). DOI: 10.15252/msb (cit. on p. 125).

[144] B. Peng et al. "Exogenous Alanine and / or Glucose plus Kanamycin Kills Antibiotic-Resistant Bacteria Article Exogenous Alanine and / or Glucose plus Kanamycin Kills Antibiotic-Resistant Bacteria". In: *Cell Metabolism* 21.2 (2015), pp. 249–261. DOI: 10.1016/j.cmet.2015.01.008 (cit. on p. 125).

[145] D. Nichol et al. "Steering Evolution with Sequential Therapy to Prevent the Emergence of Bacterial Antibiotic Resistance". In: *PLoS Computational Biology* 11.9 (2015), pp. 1–19. DOI: 10.1371/journal.pcbi.1004493 (cit. on p. 126).

[146] J. Casadesús and R. D'Ari. "Memory in bacteria and phage". In: *BioEssays* 24.6 (2002), pp. 512–518. DOI: 10.1002/bies.10102 (cit. on p. 126).

[147] G. Lambert and E. Kussell. "Quantifying Selective Pressures Driving Bacterial Evolution Using Lineage Analysis". In: *Physical Review X* 011016.5 (2015), pp. 1–10. DOI: 10.1103/PhysRevX.5.011016 (cit. on p. 126).

[148] D. M. Wolf et al. "Memory in Microbes: Quantifying History-Dependent Behavior in a Bacterium". In: *PLoS ONE* 3.2 (2008). DOI: 10.1371/journal.pone.0001700 (cit. on p. 126).

[149] R. Mathis and M. Ackermann. "Response of single bacterial cells to stress gives rise to complex history-dependence at the population level". In: *Proceedings of the National Academy of Sciences* 113.15 (2016), pp. 4224–4229. DOI: 10.1073/pnas.1511509113 (cit. on p. 126).

[150] G. Lambert and E. Kussel. "Memory and Fitness Optimization of Bacteria under Fluctuating Environments". In: *PLoS Genetics* 10.9 (2014). DOI: 10.1371/journal.pgen.1004556 (cit. on p. 127).

[151] J. B. Lyczak, C. L. Cannon, and G. B. Pier. "Establishment of Pseudomonas aeruginosa infection: Lessons from a versatile opportunist". In: *Microbes and Infection* 2.9 (2000), pp. 1051–1060. DOI: 10.1016/S1286-4579(00)01259-4 (cit. on p. 127).

[152] P. M. Mira et al. "Adaptive Landscapes of Resistance Genes Change as Antibiotic Concentrations Change". In: *Molecular Biology and Evolution* 32.10 (2015), pp. 2707–2715. DOI: 10.1093/molbev/msv146 (cit. on pp. 128, 138).

[153] J. A. Mongold, A. F. Bennett, and R. E. Lenski. "Evolutionary adaptation to temperature. IV. Adaptation of Escherichia coli at a niche boundary". In: *Evolution* 50.1 (1996), p. 493. DOI: 10.2307/2410825 (cit. on p. 132).

[154] M. J. Lee et al. "Sequential Application of Anticancer Drugs Enhances Cell Death by Rewiring Apoptotic Signaling Networks". In: *Cell* 149.4 (May 2012), pp. 780–794. DOI: 10.1016/j.cell.2012.03.031 (cit. on p. 132).

[155] L. A. Magdanova and N. V. Golyasnaya. "Heterogeneity as an adaptive trait of microbial populations". In: *Microbiology* 82.1 (2013), pp. 1–10. DOI: 10.1134/S0026261713010074 (cit. on p. 133).

[156] M. Dragosits and D. Mattanovich. "Adaptive laboratory evolution – principles and applications for biotechnology". In: *Microbial Cell Factories* 12.1 (2013), p. 64. DOI: 10.1186/1475-2859-12-64 (cit. on p. 133).

[157] B. Levin, V. Perrot, and N. Walker. "Compensatory mutations, antibiotic resistance and the population genetics of adaptive evolution in bacteria". In: *Genetics* 154.3 (2000), pp. 958–997 (cit. on p. 133).

[158] L. R. Hmelo et al. "Precision-engineering the Pseudomonas aeruginosa genome with two-step allelic exchange". In: *Nature Protocols* 10.11 (2015), pp. 1820–41. DOI: 10.1038/nprot.2015.115 (cit. on p. 134).

[159] C. P. Goulart et al. "Designing antibiotic cycling strategies by determining and understanding local adaptive landscapes." In: *PloS ONE* 8.2 (Jan. 2013), e56040. DOI: 10.1371/journal.pone.0056040 (cit. on p. 135).

[160] T. H. Kiser et al. "Efflux pump contribution to multidrug resistance in clinical isolates of Pseudomonas aeruginosa." eng. In: *Pharmacotherapy* 30.7 (July 2010), pp. 632–638. DOI: 10.1592/phco.30.7.632 (cit. on p. 135).

[161] M. A. Oberhardt, B. Ø. Palsson, and J. A. Papin. "Applications of genome-scale metabolic reconstructions." In: *Molecular Systems Biology* 5.320 (Jan. 2009), p. 320. DOI: 10.1038/msb.2009.77 (cit. on p. 135).

[162] J. Schellenberger et al. "Quantitative prediction of cellular metabolism with constraint-based models: the COBRA Toolbox v2.0." In: *Nature Protocols* 6.9 (Sept. 2011), pp. 1290–307. DOI: 10.1038/nprot.2011.308 (cit. on p. 135).

[163] B. Szamecz et al. "The Genomic Landscape of Compensatory Evolution." In: *PLoS Biology* 12.8 (Aug. 2014), e1001935. DOI: 10.1371/journal.pbio.1001935 (cit. on p. 138).

[164] M. Baym et al. "Spatiotemporal microbial evolution on antibiotic landscapes". In: *Science* 353.6304 (Sept. 2016), 1147 LP - 1151 (cit. on p. 139).

[165] R. M. Nesse. "How is Darwinian medicine useful?" In: *Western Journal of Medicine* 174.5 (May 2001), pp. 358–360 (cit. on p. 139).

[166] E. Dolgin. "Inner Workings: Taking evolution to the clinic". In: *Proceedings of the National Academy of Sciences* 112.44 (Nov. 2015), pp. 13421–13422. DOI: 10.1073/pnas.1516954112 (cit. on p. 140).

[167] J. E. Barrick and R. E. Lenski. "Genome dynamics during experimental evolution." In: *Nature Reviews Genetics* October (Oct. 2013). DOI: 10.1038/nrg3564 (cit. on p. 140).

[168] S. Chandrasekaran et al. "Chemogenomics and orthology-based design of antibiotic combination therapies". In: *Molecular Systems Biology* 12.5 (May 2016) (cit. on p. 141).

[169] A. Brauner et al. "Distinguishing between resistance, tolerance and persistence to antibiotic treatment". In: *Nature Reviews Microbiology* 14.5 (May 2016), pp. 320–330 (cit. on p. 141).

[170] Y.-H. Su et al. "Dielectrophoretic Monitoring and Interstrain Separation of Intact Clostridium difficile Based on Their S(Surface)-Layers". In: *Analytical Chemistry* 86.21 (Nov. 2014), pp. 10855–10863. DOI: 10.1021/ac5029837 (cit. on p. 141).

[171] N. Woodford and A. P. Johnson. "Global spread of antibiotic resistance: the example of New Delhi metallo-β-lactamase (NDM)-mediated carbapenem resistance". In: *Journal of Medical Microbiology* 62.4 (Apr. 2013), pp. 499–513. DOI: 10.1099/jmm.0.052555-0 (cit. on p. 141).

[172] K. Lewis. "Platforms for antibiotic discovery". In: *Nature Reviews Drug Discovery* 12.5 (Apr. 2013), pp. 371–387. DOI: 10.1038/nrd3975 (cit. on p. 141).

List of publications

(*denotes equal contribution)

P. Yen.*, L. J. Dunphy*, J. A. Papin. "Profiling Catabolic Capabilities of Antibiotic Resistant *Pseudomonas aeruginosa*." In preparation. (March 2017)

P. Yen and J. A. Papin. "History of Antibiotic Adaptation Influences Microbial Evolutionary Dynamics During Subsequent Treatment." Revision under review at: *PLOS Biology* (March 2017)

J. A. Bartell*, A. S. Blazier*, **P. Yen**, J. C. Thøgersen, L. J. Jelsbak, J. B. Goldberg, J. A. Papin. "Reconstruction of the metabolic network of Pseudomonas aeruginosa to interrogate virulence factor synthesis." In: *Nature Communications* 8 (March 2017), p. 14631. doi: doi:10.1038/ncomms14631.

J. A. Bartell*, **P. Yen***, J. J. Varga, J. B. Goldberg, J. A. Papin."Comparative metabolic systems analysis of pathogenic Burkholderia." In: *Journal of Bacteriology* 196.2 (January 2013), pp. 210-226. doi: 10.1128/JB. 00997-13. ***Cover Illustration.***

H. N. Hayenga, B. C. Thorne, **P. Yen**, J. A. Papin, S. M. Peirce, J. D. Humphrey. "Multiscale Computational Modeling in Vascular Biology: From Molecular Mechanisms to Tissue-Level Structure and Function." Springer-Verlag Berlin Heidelberg. Series 8415. In: *Studies in Mechanobiology, Tissue Engineering, and Biomaterials* (September 2012). pp. 209-240. doi:10.1007/8415_2012_147

P. Yen*, S. D. Finley*, M. O. Engel-Stefanini, A. S. Popel. "A Two-Compartment Model of VEGF Distribution in the Mouse." In: *PLoS ONE* 6.11 (November 2011). p. e27514. doi:10.1371/ journal.pone.0027514.

Appendix A

Supplementary figures and tables

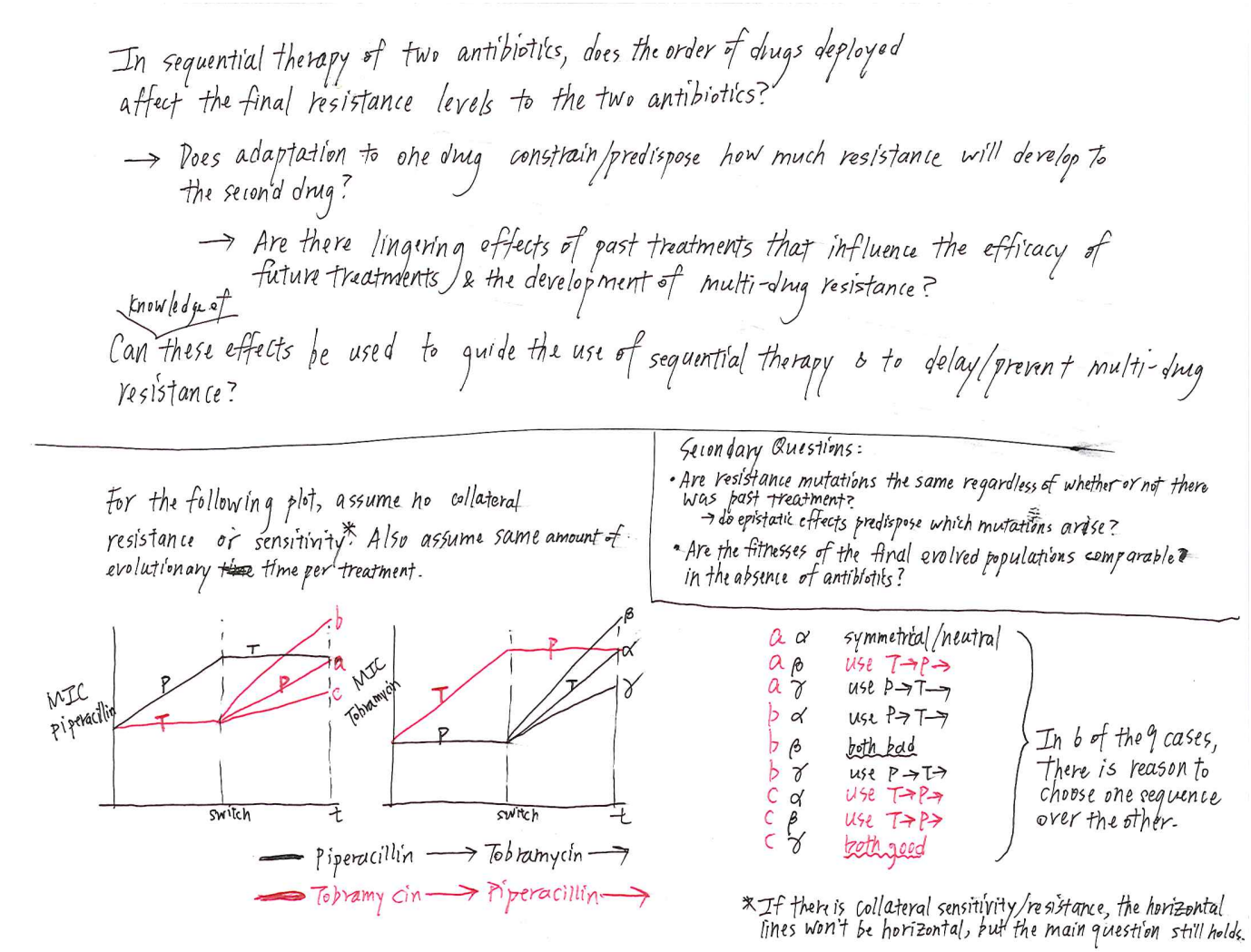

Figure A.1: **Early conception of the project.**

Table A.1: **MICs of main adaptive evolution experiment.**

$\log_2$(MIC Piperacillin) (µg/ml)

	Control				PIP^R				TOB^R				CIP^R				PIP^RTOB^R				TOB^RPIP^R				PIP^RCIP^R				TOB^RCIP^R				CIP^RTOB^R				CIP^RPIP^R				PIP^RLB				TOB^RLB				CIP^RLB			
Day	1	2	3	4	1	2	3	4	1	2	3	4	1	2	3	4	1	2	3	4	1	2	3	4	1	2	3	4	1	2	3	4	1	2	3	4	1	2	3	4	1	2	3	4	1	2	3	4	1	2	3	4
1	2	3	2	2	2	3	3	2	3	3	2	3	3	4	3	4																																				
2	3	3	3	3	4	4	4	4	3	3	3	3																																						
3	3	3	3	3	4	5	5	4	1	1	3	2																																						
4	3	3	3	3	5	5	5	4	2	2	2	3																																						
5	3	3	3	3	5	6	5	4	2	2	2	3																																						
6	3	3	3	3	6	6	6	5	2	2	1	3	2	0	1	1																																		
7	2	3	3	3	6	6	5	5	2	2	2	3																																						
8	2	3	3	3	6	7	6	5	2	2	2	2																																						
9	3	3	3	3	6	7	6	5	2	3	2	2																																						
10	2	3	3	2	6	7	6	5	2	2	2	2																																						
11	2	3	3	3	6	7	6	6	2	2	2	3	1	1	1	1																																		
12	3	3	3	3	6	7	6	6	3	2	3	3																																						
13	3	3	3	3	6	7	6	6	3	2	1	3																																						
14	3	3	3	3	7	7	6	6	2	2	2	3																																						
15	3	3	3	3	7	7	6	6	2	2	2	3																																						
16	2	3	3	2	7	7	6	7	3	3	2	3	2	1	2	2																																		
17	3	3	4	3	8	7	6	7	3	3	2	3																																						
18	3	3	4	3	8	7	7	7	3	3	2	4																																						
19	3	3	3	3	8	7	6	7	3	3	2	3																																						
20	3	3	4	3	9	7	7	7	3	3	3	4	2	2	1	2																																		
21	3	3	3	3	10	7	7	7	4	3	2	4	2	2	1	2	10	7	7	7	3	3	2	4	9	6	7	7	3	2	3	4	3	2	1	3	2	2	1	3	9	6	7	6	3	2	4	4	2	1	2	2
22	3	3	3	3	10	7	7	7	3	3	2	4					7	7	6	7	3	3	3	4	8	5	7	6													4	3	3	4	10	6	7	7								
23	3	3	3	3	10	7	7	7	3	3	2	4					8	7	6	7	3	4	3	4	6	6	7	6													4	3	3	4	10	6	7	6								
24	3	3	3	3	11	7	7	7	3	2	3	4					8	7	6	7	4	5	4	4	6	5	4	6													5	4	4	4	10	6	7	6								
25	3	3	3	3	11	7	7	7	3	3	3	4					8	7	6	7	4	5	4	4	6	4	4	5													5	5	5	5	9	6	7	6								
26	3	3	3	3	10	7	7	8	3	3	3	4	2	1	0	2	8	7	6	7	4	5	4	4	6	2	4	5	1	2	2	2	2	4	1	4	5	5	5	5	9	6	7	6	4	3	4	5	4	3	5	3
27	3	3	3	3	11	7	7	7	3	3	3	4					8	7	6	7	4	5	5	4	6	2	4	5													5	6	5	5	9	6	7	6								
28	3	3	3	3	11	7	7	7	3	3	3	4					8	7	6	7	4	5	5	4	6	1	4	4													6	7	5	5	9	6	6	6								
29	3	3	3	3	11	7	7	8	3	3	3	4					8	7	6	7	5	7	5	4	6	2	4	4													6	6	5	5	9	6	6	6								
30	4	4	3	3	11	7	7	8	3	2	2	3					8	7	6	7	5	10	5	4	6	2	4	4													6	6	5	5	9	6	6	6								
31	3	3	3	3	12	7	7	8	3	3	3	3	2	2	0	2	8	6	6	7	6	10	5	4	6	2	7	3	1	0	0	2	3	3	1	4	6	6	5	5	9	6	6	6	4	4	4	7	4	4	8	4
32	3	3	3	3	11	7	7	8	3	3	3	4					8	7	6	7	6	10	5	4	6	1	4	4													7	6	6	6	9	6	6	6								
33	3	3	3	3	12	7	7	8	3	3	3	4					8	7	6	6	6	10	6	4	7	1	4	4													8	6	6	6	8	6	6	6								
34	3	3	3	3	11	7	8	8	3	3	2	4					8	7	6	6	6	10	5	4	6	-1	4	4													7	6	5	6	8	6	6	6								
35	3	3	3	3	12	7	8	8	3	3	3	4					8	7	6	5	6	10	6	5	7	1	4	4													8	6	6	7	8	6	6	6								
36	3	3	3	3	12	7	9	8	3	3	3	3	2	2	0	2	8	7	6	6	7	10	6	4	7	1	4	4	1	2	0	2	2	4	2	5	8	7	6	6	8	6	6	6	4	4	4	4	3	3	5	5
37	3	3	3	3	12	7	9	8	3	3	3	3					8	7	6	6	8	11	7	5	7	0	5	4													9	7	6	8	8	6	6	6								
38	3	3	3	3	12	7	10	8	3	3	3	3					8	7	6	6	9	10	9	4	7	0	4	4													9	7	7	8	8	6	5	6								
39	4	3	3	3	12	7	10	8	3	3	3	3					8	7	6	6	9	11	10	5	7	0	4	4													9	7	8	8	8	6	5	6								
40	3	3	3	3	12	7	11	8	3	3	3	3	2	2	0	2	8	7	6	5	9	10	9	4	7	0	4	4	1	2	1	2	3	4	3	4	9	7	8	8	8	6	5	6	4	3	4	4	4	4	9	6

$\log_2$(MIC Tobramycin) (µg/ml)

	Control				PIP^R				TOB^R				CIP^R				PIP^RTOB^R				TOB^RPIP^R				PIP^RCIP^R				TOB^RCIP^R				CIP^RTOB^R				CIP^RPIP^R				PIP^RLB				TOB^RLB				CIP^RLB			
Day	1	2	3	4	1	2	3	4	1	2	3	4	1	2	3	4	1	2	3	4	1	2	3	4	1	2	3	4	1	2	3	4	1	2	3	4	1	2	3	4	1	2	3	4	1	2	3	4	1	2	3	4
1	1	1	1	1	1	1	1	1	1	1	1	1	2	3	3	2																																				
2	1	2	1	2	2	2	1	2	3	3	2	2																																						
3	1	2	1	2	1	2	2	2	3	4	3	3																																						
4	2	1	1	1	2	2	2	2	4	4	3	3																																						
5	1	1	1	1	1	2	2	3	6	4	4	4																																						
6	1	1	1	1	1	2	2	3	6	4	4	4	1	-3	2	-1																																		
7	1	1	1	1	2	1	1	3	6	4	4	5																																						
8	1	1	2	1	1	1	1	2	6	4	4	5																																						
9	1	1	1	1	2	1	2	2	6	5	5	5																																						
10	1	1	1	1	2	2	2	2	6	5	5	5																																						
11	1	1	1	1	2	2	1	3	6	5	5	6	1	-2	1	-3																																		
12	1	1	1	1	2	2	1	2	7	6	6	7																																						
13	1	2	1	1	2	2	2	2	7	5	6	7																																						
14	2	2	2	2	2	2	1	2	7	5	7	6																																						
15	1	1	2	3	1	1	1	2	6	5	6	6																																						
16	1	1	1	1	1	1	2	2	6	5	6	6	0	-3	1	-2																																		
17	1	1	1	1	2	1	2	3	7	6	7	6																																						
18	1	2	2	1	2	2	2	3	7	6	8	7																																						
19	1	3	2	1	2	2	2	3	7	6	8	7																																						
20	1	1	2	2	1	1	2	3	7	6	8	7	-1	-2	0	-2																																		
21	1	1	1	1	2	2	2	3	7	6	8	7	-1	-2	3	-3	2	1	2	3	6	5	7	7	1	1	1	2	6	5	7	7	1	-1	0	0	-1	-2	3	0	1	0	2	2	5	4	7	6	0	-1	1	-1
22	1	1	1	1	2	2	2	3	6	6	8	7					1	2	2	2	6	5	8	7					6	4	7	6	0	-1	1	-1									5	4	7	6				
23	1	1	1	1	2	2	2	3	6	7	8	7					3	2	2	3	6	5	7	6					5	6	3	7	1	0	1	0									5	4	7	6				
24	1	1	1	1	2	2	3	3	6	7	9	8					3	1	2	3	6	5	5	7					5	4	2	6	2	-1	3	0									5	4	4	6				
25	1	1	1	1	2	2	2	3	6	7	8	7					3	2	3	4	6	5	7	6					4	5	2	6	3	1	4	0									5	4	4	6				
26	1	1	1	1	2	2	2	3	6	7	8	7	-1	-3	-1	-2	4	3	3	4	6	5	6	7	0	-2	-1	0	4	4	3	6	2	1	4	1	0	-1	0	0	1	1	2	1	5	4	4	6	0	-1	3	-1
27	1	1	1	1	2	2	2	2	5	7	8	7					4	2	3	4	6	5	5	7					4	5	3	6	2	1	6	1									4	4	4	6				
28	1	1	1	1	2	2	2	2	6	7	8	7					4	3	3	4	6	5	4	7					4	3	3	6	2	1	7	2									4	3	4	6				
29	1	1	1	1	2	2	2	3	6	7	8	7					4	2	3	4	6	5	5	7					3	4	3	5	2	2	6	1									4	3	3	6				
30	1	1	1	1	2	3	3	3	6	7	8	7					4	3	3	4	5	5	5	7					3	3	3	5	3	1	7	2									4	3	3	6				
31	1	1	1	1	2	2	2	3	6	7	8	7	-1	-1	0	-2	4	3	3	4	6	6	4	7	0	-1	1	0	3	3	3	5	3	2	7	2	1	-2	0	-1	1	0	1	1	4	4	4	6	0	-1	3	-1
32	1	2	2	1	2	2	2	3	7	7	8	7					4	3	3	6	6	6	5	7					3	3	3	5	4	3	7	3									4	3	4	5				
33	1	1	1	1	2	2	2	2	7	7	8	7					4	3	3	6	6	5	5	6					2	3	2	4	4	2	7	1									4	3	3	5				
34	1	2	2	2	1	1	1	2	7	8	8	8					4	3	4	6	6	6	4	7					2	2	3	4	4	4	7	3									4	3	3	3				
35	1	1	2	1	2	2	2	2	7	7	8	8					4	3	4	6	6	6	5	7					3	3	3	4	5	3	7	3									4	3	3	3				
36	1	1	2	1	2	2	2	2	7	8	8	8	0	-1	0	-2	4	3	4	6	6	6	5	6	0	-1	0	0	3	3	3	4	5	4	7	3	1	0	0	0	1	0	1	1	4	3	3	3	1	-1	3	-1
37	1	1	3	1	2	2	1	2	7	7	9	8					4	3	4	6	6	6	5	7					3	3	3	4	6	4	8	3									4	3	3	3				
38	1	2	2	2	2	1	0	2	7	7	9	7					4	3	4	6	5	6	4	7					3	2	3	3	4	4	8	2									4	3	3	3				
39	1	2	2	2	2	2	0	2	7	7	9	8					4	3	4	7	6	6	5	7					3	3	3	4	5	4	8	3									4	3	3	3				
40	1	1	1	1	2	2	2	2	7	7	9	8	0	-1	-1	-2	4	3	4	7	5	6	4	6	0	0	0	0	3	3	3	4	4	4	8	2	1	-1	-1	0	1	0	1	2	4	3	3	4	1	3	3	1

	$\log_2$(MIC Ciprofloxacin) (μg/ml)																																							
	Control				PIP^R				TOB^R				CIP^R				PIP^RTOB^R				TOB^RPIP^R				PIP^RCIP^R				TOB^RCIP^R				CIP^RTOB^R				CIP^RPIP^R				PIP^RLB				TOB^RLB				CIP^RLB			
	1	2	3	4	1	2	3	4	1	2	3	4	1	2	3	4	1	2	3	4	1	2	3	4	1	2	3	4	1	2	3	4	1	2	3	4	1	2	3	4	1	2	3	4	1	2	3	4	1	2	3	4
Day																																																		
1	-2	-2	-2	-2	-3	-2	-2	-2	-1	-2	-2	-2	-1	-2	-3	-1																																				
2													1	2	-1	2																																				
3													2	2	1	3																																		
4													3	3	2	4																																		
5													2	4	3	4																																		
6	-3	-1	-3	-3	0	1	-2	-1	-1	-2	-2	-1	3	3	3	4																																		
7													4	4	3	4																																		
8													4	3	3	4																																		
9													4	4	3	4																																		
10													4	4	4	4																																		
11	-3	-3	-2	-4	-1	1	-2	-1	-1	-1	-1	-1	5	3	3	3																																		
12													6	4	4	4																																		
13													5	3	4	4																																		
14													5	3	3	4																																		
15													5	4	4	3																																		
16	-3	-2	-2	-3	-1	1	-2	-1	-1	-1	0	-2	5	4	4	4																																		
17													5	4	4	4																																		
18													5	3	4	4																																		
19													5	4	4	4																																		
20	-2	-2	-2	-2	-2	1	-2	-2	-1	-1	-1	0	5	4	4	4																																		
21	-3	-2	-2	-2	-1	1	-3	-1	-2	-1	-2	0	5	4	4	4	0	0	-2	-2	-1	-1	-2	-1	0	2	-2	0	-1	0	-1	-1	3	3	3	2	5	4	4	3	0	1	-1	-1	-1	-1	-1	-1	6	4	3	4
22													5	5	5	4									3	1	-2	-2	-1	-2	2	-2	6	4	4	5	6	4	5	4									5	5	4	3
23													5	4	4	5									2	1	0	0	1	-1	3	-1	6	4	4	4	0	4	0	2									4	4	3	3
24													5	4	3	5									2	2	1	1	2	-2	2	-1	5	3	4	4	0	4	1	-1									5	4	3	3
25													5	4	4	4									3	3	1	2	2	-1	2	0	6	3	4	4	0	-1	2	-1									2	5	2	3
26	-1	-2	-3	-3	-1	1	-2	-1	-1	-1	-2	-3	5	4	3	5	-1	0	-2	-1	0	-1	-3	-1	3	3	0	3	2	-2	3	1	6	4	1	3	2	-3	1	-1	0	0	-1	0	-2	-2	-3	-1	4	5	2	4
27													5	5	3	4									2	3	1	3	2	0	3	1	6	3	1	4	1	0	1	-1									2	5	1	3
28													5	5	4	5									3	3	0	3	3	1	3	1	5	4	2	5	1	1	1	-1									2	5	1	3
29													6	5	4	5									3	3	1	3	3	3	3	2	5	4	1	4	2	1	2	-1									2	5	1	3
30													5	5	4	4									3	3	1	3	3	3	3	2	4	3	2	4	2	1	1	-1									2	5	1	3
31	-3	-3	-2	-3	-1	1	-2	-1	-1	0	-1	-2	5	5	4	5	0	0	-2	-1	-1	-3	-1	-1	3	3	1	3	3	3	3	2	6	3	1	4	2	1	1	-1	-1	1	-1	0	-2	-3	-1	-2	3	5	1	4
32													5	5	3	5									4	4	0	4	4	3	4	3	4	4	2	4	2	1	2	-1									2	3	-1	3
33													6	5	4	4									3	3	1	3	3	3	3	2	4	3	2	-1	0	1	2	0									2	5	-1	3
34													5	5	3	4									3	3	-1	3	3	3	3	2	5	3	2	1	0	1	1	-1									3	5	-2	3
35													6	5	4	5									3	3	0	4	4	3	3	2	5	-1	2	0	0	1	1	0									3	5	-2	3
36	-3	-2	-3	-3	-1	1	-2	0	-1	0	-2	-3	6	5	3	4	-1	-1	-3	0	-1	-2	-2	-1	4	3	0	4	3	2	3	3	4	-1	2	0	0	2	2	-1	-2	0	-1	-1	-2	-2	0	-3	4	5	1	3
37													5	5	5	5									4	3	0	4	3	2	3	2	3	-1	2	0	0	0	2	-1									2	4	-1	3
38													6	5	3	4									4	3	0	4	3	2	3	2	3	-1	2	0	1	0	2	1									2	4	-1	2
39													6	5	4	5									4	3	1	4	3	3	2	3	4	-1	2	-1	0	1	1	1									3	4	-2	2
40	-2	-2	-2	-2	-1	1	-2	-1	-1	-1	-2	-3	6	5	4	6	0	0	-2	0	-1	-2	-2	-2	4	4	0	5	4	3	3	3	2	-1	2	-1	1	1	2	1	0	1	-1	-1	-4	-1	-2	-2	3	4	-1	2

Table A.2: **MICs of the evolution of the piperacillin-resistant clinical isolates.**

Raw $\log_2$(MIC Piperacillin) (μg/ml)

	Clinical Isolate 1									Clinical Isolate 2									Clinical Isolate 3								
	Evolved to piperacillin			Evolved to tobramycin			Evolved to ciprofloxacin			Evolved to LB			Evolved to piperacillin			Evolved to tobramycin			Evolved to ciprofloxacin			Evolved to LB			Evolved to piperacillin			Evolved to tobramycin			Evolved to ciprofloxacin			Evolved to LB		
	1	2	3	1	2	3	1	2	3	1	2	3	1	2	3	1	2	3	1	2	3	1	2	3	1	2	3	1	2	3	1	2	3	1	2	3
Day																																				
1	5	5	6	6	7	5	6	5	6	7	7	7	5	5	5	5	5	5	5	5	5	8	7	7	7	7	7	7	7	7	8	7	7	9	9	9
2	8	9	9	3	5	6	4	5	4	9	9	10	7	6	6	5	5	5	4	4	3	9	8	9	11	11	11	9	8	8	8	7	7	11	11	10
3	9	11	11	4	6	7	1	5	4	9	9	10	9	7	9	6	6	6	5	3	5	11	10	11	8	9	8	8	7	9	7	5	5	11	11	10
4	12	10	13	4	4	5	3	5	5	9	10	10	8	9	8	5	6	6	2	3	3	9	9	9	9	8	10	9	9	6	5	5	5	12	11	11
5	12	11	10	7	7	5	2	5	7	7	8	8	9	7	9	7	6	6	3	4	4	9	8	9	10	9	9	6	7	8	5	5	5	11	10	12
6	12	11	12	-1	4	6	2	5	2	8	7	9	7	8	8	6	5	5	2	2	3	8	8	10	11	9	12	8	9	9	5	6	5	12	11	11
7	12	10	12	5	8	8	4	5	6	9	8	8	9	9	10	6	6	7	3	4	4	8	8	9	11	12	9	8	7	10	6	6	5	11	10	11
8	13	11	12	0	5	4	-1	5	5	9	8	8	8	8	8	6	4	4	2	3	3	8	8	10	11	9	11	7	8	8	5	5	5	11	11	10
9	11	11	13	5	6	8	0	5	3	8	8	9	8	8	10	4	5	6	2	3	3	8	8	10	11	10	8	7	8	8	5	5	5	12	12	11
10	13	11	11	2	7	5	5	6	6	8	8	8	9	9	11	7	6	7	2	4	4	8	8	8	12	10	12	7	8	9	5	5	5	12	11	11

Normalized (for plotting Fig 7) $\log_2$(MIC Piperacillin) (μg/ml)

	Clinical Isolate 1									Clinical Isolate 2									Clinical Isolate 3								
	Evolved to piperacillin			Evolved to tobramycin			Evolved to ciprofloxacin			Evolved to LB			Evolved to piperacillin			Evolved to tobramycin			Evolved to ciprofloxacin			Evolved to LB			Evolved to piperacillin			Evolved to tobramycin			Evolved to ciprofloxacin			Evolved to LB		
	1	2	3	1	2	3	1	2	3	1	2	3	1	2	3	1	2	3	1	2	3	1	2	3	1	2	3	1	2	3	1	2	3	1	2	3
Day																																				
1	-0.333	-0.333	0.6667	0	1	-1	0.3333	-0.667	0.3333	0	0	0	0	0	0	0	0	0	0	0	0	0.6667	-0.333	-0.333	0	0	0	0	0	0	0.6667	-0.333	-0.333	0	0	0
2	2.6667	3.6667	3.6667	-3	-1	0	-1.667	-0.667	-1.667	2	2	3	2	1	1	0	0	0	-1	-1	-2	1.6667	0.6667	1.6667	4	4	4	2	1	1	0.6667	-0.333	-0.333	2	2	1
3	3.6667	5.6667	5.6667	-2	0	1	-4.667	-0.667	-1.667	2	2	3	4	2	4	1	1	1	0	-2	0	3.6667	2.6667	3.6667	1	2	1	1	0	2	-0.333	-2.333	-2.333	2	2	1
4	6.6667	4.6667	7.6667	-2	-2	-1	-2.667	-0.667	-0.667	2	3	3	3	4	3	0	1	1	-3	-2	-2	1.6667	1.6667	1.6667	2	1	3	2	2	-1	-2.333	-2.333	-2.333	3	2	2
5	6.6667	5.6667	4.6667	1	1	-1	-3.667	-0.667	1.3333	0	1	1	4	2	4	2	1	1	-2	-1	-1	1.6667	0.6667	1.6667	3	2	2	-1	0	1	-2.333	-2.333	-2.333	2	1	3
6	6.6667	5.6667	6.6667	-7	-2	0	-3.667	-0.667	-3.667	1	0	2	2	3	3	1	0	0	-3	-3	-2	0.6667	0.6667	2.6667	4	2	5	1	2	2	-2.333	-1.333	-2.333	3	2	2
7	6.6667	4.6667	6.6667	-1	2	2	-1.667	-0.667	0.3333	2	1	1	4	4	5	1	1	2	-2	-1	-1	0.6667	0.6667	1.6667	4	5	2	1	0	3	-1.333	-1.333	-2.333	2	1	2
8	7.6667	5.6667	6.6667	-6	-1	-2	-6.667	-0.667	-0.667	2	1	1	3	3	3	1	-1	-1	-3	-2	-2	0.6667	0.6667	2.6667	4	2	4	0	1	1	-2.333	-2.333	-2.333	2	2	1
9	5.6667	5.6667	7.6667	-1	0	2	-5.667	-0.667	-2.667	1	1	2	3	3	5	-1	0	1	-3	-2	-2	0.6667	0.6667	2.6667	4	3	1	0	1	1	-2.333	-2.333	-2.333	3	3	2
10	7.6667	5.6667	5.6667	-4	1	-1	-0.667	0.3333	0.3333	1	1	1	4	4	6	2	1	2	-3	-1	-1	0.6667	0.6667	0.6667	5	3	5	0	1	2	-2.333	-2.333	-2.333	3	2	2

Raw $\log_2$(MIC Tobramycin) (μg/ml)

	Clinical Isolate 1									Clinical Isolate 2									Clinical Isolate 3								
	Evolved to piperacillin			Evolved to tobramycin			Evolved to ciprofloxacin			Evolved to LB			Evolved to piperacillin			Evolved to tobramycin			Evolved to ciprofloxacin			Evolved to LB			Evolved to piperacillin			Evolved to tobramycin			Evolved to ciprofloxacin			Evolved to LB		
	1	2	3	1	2	3	1	2	3	1	2	3	1	2	3	1	2	3	1	2	3	1	2	3	1	2	3	1	2	3	1	2	3	1	2	3
Day																																				
1				1	1	1										-1	-1	0										0	0	0						
2				2	3	3										1	0	0										2	2	2						
3				3	3	3										1	1	1										2	3	2						
4				3	4	3										2	1	1										3	3	3						
5				5	3	3										2	2	2										4	3	3						
6				1	2	4										2	2	2										5	4	3						
7				5	2	4										3	4	3										5	4	3						
8				0	2	3										3	2	2										4	4	3						
9				3	2	4										2	3	3										5	5	4						
10				3	3	3										3	3	3										5	6	4						

Raw $\log_2$(MIC Ciprofloxacin) (μg/ml)

	Clinical Isolate 1									Clinical Isolate 2									Clinical Isolate 3								
	Evolved to piperacillin			Evolved to tobramycin			Evolved to ciprofloxacin			Evolved to LB			Evolved to piperacillin			Evolved to tobramycin			Evolved to ciprofloxacin			Evolved to LB			Evolved to piperacillin			Evolved to tobramycin			Evolved to ciprofloxacin			Evolved to LB		
	1	2	3	1	2	3	1	2	3	1	2	3	1	2	3	1	2	3	1	2	3	1	2	3	1	2	3	1	2	3	1	2	3	1	2	3
Day																																				
1							-1	-1	-2										0	0	-1										-2	-2	-2			
2							1	0	2										0	1	-1										-1	1	1			
3							2	2	4										1	1	2										1	1	1			
4							2	2	4										1	2	2										1	1	1			
5							2	3	5										1	2	2										1	1	1			
6							2	3	3										1	1	1										1	1	1			
7							4	4	6										2	2	2										1	1	1			
8							2	3	6										2	2	2										1	1	1			
9							3	3	6										2	2	2										1	1	2			
10							3	5	7										2	2	2										2	1	2			

Table A.3: **MICs of the evolution of the Hocquet isolates.**

	Raw $\log_2$(MIC Piperacillin) (µg/ml)																							
	A_{WT}			A_{PM}			B_{WT}			B_{PM}			C_{WT}			C_{PM}			D_{WT}			D_{PM}		
	1	2	3	1	2	3	1	2	3	1	2	3	1	2	3	1	2	3	1	2	3	1	2	3
Day																								
1	3	2	3	4	4	4	5	5	4	7		7	3	5	3	5	6	4	4	4	4	5	5	4
2																								
3																								
4																								
5																								
6	2	3	2	3	4	4	5	3	4	5		5	2	2	3	3	4	4	3	3	4	3	3	3
7																								
8																								
9																								
10	4	2	3	4	3	3	4	4	6	4		6	2	2	2	3	3	4	3	3	3	3	3	3
11																								
12																								
13																								
14																								
15	4	2	3	3	3	4	9	4	5	3		4	0	4	1	2	3	3	2	3	2	3	3	4

	Raw $\log_2$(MIC Tobramycin) (µg/ml)																							
	A_{WT}			A_{PM}			B_{WT}			B_{PM}			C_{WT}			C_{PM}			D_{WT}			D_{PM}		
	1	2	3	1	2	3	1	2	3	1	2	3	1	2	3	1	2	3	1	2	3	1	2	3
Day																								
1	0	2	3	1	1	1	1	2	1	-2		-2	1	2	2	1	1	1	1	1	2	1	1	1
2	2	4	3	1	2	0	1	2	3	-3		-3	2	3	2	1	1	1	2	2	2	1	1	1
3	4	3	2	2	0	2	2	2	4	-2		-2	3	2	4	2	1	2	2	2	2	2	2	2
4	3	3	3	2	1	1	3	3	3	-2		-1	4	4	4	2	2	3	3	3	2	3	2	3
5	3	4	-2	2	2	2	3	3	4	-1		-2	5	3	4	3	2	3	4	4	3	3	3	3
6	3	5	4	1	2	3	4	3	4	-2		0	6	4	5	3	3	3	3	4	4	3	3	3
7	4	5	4	3	2	3	5	4	5	-1		0	5	4	5	2	3	3	3	4	3	3	3	3
8	4	5	4	2	2	2	5	4	4	-2		-1	6	3	6	3	2	3	4	4	4	3	3	3
9	4	5	4	2	2	3	5	4	5	0		0	6	4	6	3	3	3	4	4	4	4	3	4
10	5	5	5	2	2	3	5	5	5	-1		1	6	4	6	3	3	4	4	4	4	4	3	3
11	5	5	4	2	2	3	6	6	5	0		1	6	4	6	3	3	3	4	4	4	4	3	4
12	5	5	5	2	2	3	6	5	6	0		0	6	4	7	4	3	4	4	4	4	4	3	3
13	5	6	5	2	2	3	6	6	6	0		0	5	4	7	3	3	3	4	4	4	4	3	4
14	5	6	5	3	3	3	6	5	6	1		0	6	5	7	4	3	4	5	4	5	4	3	3
15	6	6	5	3	2	3	6	6	7	-1		1	5	6	6	2	3	4	4	4	4	4	3	4

	Normalized log_2(MIC Tobramycin) (µg/ml)																					
	A_{WT}			A_{PM}			B_{WT}			B_{PM}			C_{WT}			C_{PM}			D_{WT}			D_{PM}		
	1	2	3	1	2	3	1	2	3	1	2	3	1	2	3	1	2	3	1	2	3	1	2	3
Day																								
1	-1.7	0.33	1.33	0	0	0	-0.3	0.67	-0.3	0		0	-0.7	0.33	0.33	0	0	0	-0.3	-0.3	0.67	0	0	0
2	0.33	2.33	1.33	0	1	-1	-0.3	0.67	1.67	-1		-1	0.33	1.33	0.33	0	0	0	0.67	0.67	0.67	0	0	0
3	2.33	1.33	0.33	1	-1	1	0.67	0.67	2.67	0		0	1.33	0.33	2.33	1	0	1	0.67	0.67	0.67	1	1	1
4	1.33	1.33	1.33	1	0	0	1.67	1.67	1.67	0		1	2.33	2.33	2.33	1	1	2	1.67	1.67	0.67	2	1	2
5	1.33	2.33	-3.7	1	1	1	1.67	1.67	2.67	1		0	3.33	1.33	2.33	2	1	2	2.67	2.67	1.67	2	2	2
6	1.33	3.33	2.33	0	1	2	2.67	1.67	2.67	0		2	4.33	2.33	3.33	2	2	2	1.67	2.67	2.67	2	2	2
7	2.33	3.33	2.33	2	1	2	3.67	2.67	3.67	1		2	3.33	2.33	3.33	1	2	2	1.67	2.67	1.67	2	2	2
8	2.33	3.33	2.33	1	1	1	3.67	2.67	2.67	0		1	4.33	1.33	4.33	2	1	2	2.67	2.67	2.67	2	2	2
9	2.33	3.33	2.33	1	1	2	3.67	2.67	3.67	2		2	4.33	2.33	4.33	2	2	2	2.67	2.67	2.67	3	2	3
10	3.33	3.33	3.33	1	1	2	3.67	3.67	3.67	1		3	4.33	2.33	4.33	2	2	3	2.67	2.67	2.67	3	2	2
11	3.33	3.33	2.33	1	1	2	4.67	4.67	3.67	2		3	4.33	2.33	4.33	2	2	2	2.67	2.67	2.67	3	2	3
12	3.33	3.33	3.33	1	1	2	4.67	3.67	4.67	2		2	4.33	2.33	5.33	3	2	3	2.67	2.67	2.67	3	2	2
13	3.33	4.33	3.33	1	1	2	4.67	4.67	4.67	2		2	3.33	2.33	5.33	2	2	2	2.67	2.67	2.67	3	2	3
14	3.33	4.33	3.33	2	2	2	4.67	3.67	4.67	3		2	4.33	3.33	5.33	3	2	3	3.67	2.67	3.67	3	2	2
15	4.33	4.33	3.33	2	1	2	4.67	4.67	5.67	1		3	3.33	4.33	4.33	1	2	3	2.67	2.67	2.67	3	2	3

	Raw log_2(MIC Ciprofloxacin) (µg/ml)																					
	A_{WT}			A_{PM}			B_{WT}			B_{PM}			C_{WT}			C_{PM}			D_{WT}			D_{PM}		
	1	2	3	1	2	3	1	2	3	1	2	3	1	2	3	1	2	3	1	2	3	1	2	3
Day																								
1	-2	0	-2	-3	-1	-3	2	2	2	1		1	-2	0	-2	-2	-2	-1	-4	-3	-4	-3	-4	-1
2																								
3																								
4																								
5																								
6	-1	-1	0	-3	-3	-2	2	2	2	0		1	-1	-1	-1	-3	-2	-2	-2	-3	-1	-4	-2	-2
7																								
8																								
9																								
10	0	0	0	-3	2	-3	2	3	1	0		0	0	2	0	-1	0	-2	-3	-3	-1	-3	-3	-2
11																								
12																								
13																								
14																								
15	-4	-2	-2	-2	-2	-3	2	2	3	0		1	-1	1	0	-3	-1	-1	-3	-2	-1	-3	-2	-5

$\log_2$ MIC_{PIP} of:	Replicate			
	1	**2**	**3**	**4**
Day 1 PIP^R	2	3	3	2
Day 20 PIP^R	9	7	7	7
Day 40 PIP^RLB	8	6	5	6
Day 40 $PIP^R$$TOB^R$	8	7	6	5
Day 40 $PIP^R$$CIP^R$	7	0	4	4

A one-way ANOVA is performed (`anova1` in MATLAB) on the $\log_2$ MIC_{PIP} values of these lineages:

ANOVA Table

Source	SS	df	MS	F	Prob>F
Columns	69.7	4	17.425	6.79	0.0025
Error	38.5	15	2.5667		
Total	108.2	19			

With an **ANOVA p-value of 0.0025**, the treatments are significantly different at the alpha=0.05 level, and we continue with multiple comparisons testing with the Tukey HSD test (`multcompare` in MATLAB).

$\log_2$ MIC_{PIP} of:		lower bound	difference between means	upper bound	Tukey HSD p-value
Day 1 PIP^R	Day 20 PIP^R	-8.50	-5.00	-1.50	0.0039
Day 1 PIP^R	Day 40 PIP^RLB	-7.25	-3.75	-0.25	0.0329
Day 1 PIP^R	Day 40 $PIP^R$$TOB^R$	-7.50	-4.00	-0.50	0.0216
Day 1 PIP^R	**Day 40 $PIP^R$$CIP^R$**	**-4.75**	**-1.25**	**2.25**	**0.8022**
Day 20 PIP^R	**Day 40 PIP^RLB**	**-2.25**	**1.25**	**4.75**	**0.8022**
Day 20 PIP^R	**Day 40 $PIP^R$$TOB^R$**	**-2.50**	**1.00**	**4.50**	**0.8989**
Day 20 PIP^R	**Day 40 $PIP^R$$CIP^R$**	**0.25**	**3.75**	**7.25**	**0.0329**
Day 40 PIP^RLB	Day 40 $PIP^R$$TOB^R$	-3.75	-0.25	3.25	0.9994
Day 40 PIP^RLB	Day 40 $PIP^R$$CIP^R$	-1.00	2.50	6.00	0.2296
Day 40 $PIP^R$$TOB^R$	Day 40 $PIP^R$$CIP^R$	-0.75	2.75	6.25	0.1612

Figure A.2: **Example of the statistical test for resensitization of the PIP^R lineages.**

Clinical Isolate #2

Raw values									
log_2(MIC Piperacillin) (µg/ml)									
Clinical Isolate 2									
	Evolved to tobramycin			Evolved to ciprofloxacin			Evolved to LB		
	1	2	3	1	2	3	1	2	3
Day									
1	5	5	5	5	5	5	8	7	7
10	7	6	7	2	4	4	8	8	8

Normalized values									
log_2(MIC Piperacillin) (µg/ml)									
Clinical Isolate 2									
	Evolved to tobramycin			Evolved to ciprofloxacin			Evolved to LB		
	1	2	3	1	2	3	1	2	3
Day									
1	0.00	0.00	0.00	0.00	0.00	0.00	0.67	-0.33	-0.33
10	2.00	1.00	2.00	-3.00	-1.00	-1.00	0.67	0.67	0.67

A one-way ANOVA is performed (`anova1` in MATLAB) on the normalized Day 10 log_2 MIC_{PIP} values:

ANOVA Table

Source	SS	df	MS	F	Prob>F
Columns	17.5556	2	8.77778	15.8	0.0041
Error	3.3333	6	0.55556		
Total	20.8889	8			

With an **ANOVA p-value of 0.0041**, the treatments are significantly different at the alpha=0.05 level, and we continue with multiple comparisons testing with the Tukey HSD test (`multcompare` in MATLAB).

Day 10 log_2 MIC_{PIP} of Clinical Isolate #2		lower bound	difference between means	upper bound	Tukey HSD p-value
Evolved to tobramycin	Evolved to ciprofloxacin	1.47	3.33	5.20	0.0037
Evolved to tobramycin	Evolved to LB	-0.87	1.00	2.87	0.3000
Evolved to ciprofloxacin	**Evolved to LB**	**-4.20**	**-2.33**	**-0.47**	**0.0202**

Figure A.3: **Example of the statistical test for the evolution of the piperacillin-resistant clinical isolates.**

A_{WT} vs. A_{PM}

Raw values

	log_2(MIC Tobramycin) (µg/ml)					
	A_{WT}			A_{PM}		
	1	2	3	1	2	3
Day						
1	0	2	3	1	1	1
15	6	6	5	3	2	3

Normalized values

	log_2(MIC Tobramycin) (µg/ml)					
	A_{WT}			A_{PM}		
	1	2	3	1	2	3
Day						
1	-1.67	0.33	1.33	0.00	0.00	0.00
15	4.33	4.33	3.33	2.00	1.00	2.00

The normalized values are calculated by subtracting the average of the Day 1 $\log_2$ MIC_{TOB} values from the raw values. More explicitly,

Normalized $\log_2$ MIC_{TOB} of Day 1 A_{WT}:
`[0 2 3] - mean([0 2 3]) = [-1.67 0.33 1.33]`

Normalized $\log_2$ MIC_{TOB} of Day 1 A_{PM}:
`[1 1 1] - mean([1 1 1]) = [0 0 0]`

Normalized $\log_2$ MIC_{TOB} of Day 15 A_{WT}:
`[6 6 5] - mean([0 2 3]) = [4.33 4.33 3.33]`

Normalized $\log_2$ MIC_{TOB} of Day 15 A_{PM}:
`[3 2 3] - mean([1 1 1]) = [2 1 2]`

A two-sample t-test is (`ttest2` in MATLAB) then performed on the normalized $\log_2$ MIC_{TOB} values of Day 15 A_{WT} vs. Day 15 A_{PM} and yields **p= 0.0078.**

Similar calculations are done for the B, C, and D pairs of clinical isolates.

Figure A.4: **Example of the statistical test for the evolution of the Hocquet clinical isolates.**

Table A.4: **Complete list of mutations.** 1's and 0's denote the presence and absence of mutations, respectively. The two mutations highlighted in green denote synonymous SNPs.

					Day 20 Control	Day 20 PIP^R	Day 20 TOB^R	Day 20 CIP^R	Day 40 Control	Day 40 PIP^R	Day 40 TOB^R	Day 40 CIP^R	Day 40 PIP^{R}TOB^R	Day 40 PIP^{R}CIP^R	Day 40 TOB^{R}PIP^R	Day 40 TOB^{R}CIP^R	Day 40 CIP^{R}PIP^R	Day 40 CIP^{R}TOB^R
Position	Mutation	Type	Condition	Gene	1 2 3 4	1 2 3 4	1 2 3 4	1 2 3 4	1 2 3 4	1 2 3 4	1 2 3 4	1 2 3 4	1 2 3 4	1 2 3 4	1 2 3 4	1 2 3 4	1 2 3 4	1 2 3 4
1406909	C→T	SNP	LB	wspA	1 0 0 0	0 0 0 0	0 0 0 0	0 0 0 0	1 0 0 0	0 0 0 0	0 0 0 0	0 0 0 0	0 0 0 0	0 0 0 0	0 0 0 0	0 0 0 0	0 0 0 0	0 0 0 0
1406482	G→A	SNP	LB	wspA	0 1 0 0	0 0 0 0	0 0 0 0	0 0 0 0	0 1 0 0	0 0 0 0	0 0 0 0	0 0 0 0	0 0 0 0	0 0 0 0	0 0 0 0	0 0 0 0	0 0 0 0	0 0 0 0
5432004	G→A	SNP	LB	morA	0 0 1 0	0 0 0 0	0 0 0 0	0 0 0 0	0 0 1 0	0 0 0 0	0 0 0 0	0 0 0 0	0 0 0 0	0 0 0 0	0 0 0 0	0 0 0 0	0 0 0 0	0 0 0 0
1407064	G→C	SNP	LB	wspA	0 0 0 1	0 0 0 0	0 0 0 0	0 0 0 0	0 0 0 1	0 0 0 0	0 0 0 0	0 0 0 0	0 0 0 0	0 0 0 0	0 0 0 0	0 0 0 0	0 0 0 0	0 0 0 0
1046490	C→T	SNP	pip	dacC	0 0 0 0	1 0 0 0	0 0 0 0	0 0 0 0	0 0 0 0	1 0 0 0	0 0 0 0	0 0 0 0	1 0 0 0	1 0 0 0	0 0 0 0	0 0 0 0	0 0 0 0	0 0 0 0
1551346	A→G	SNP	pip	PA14_18080	0 0 0 0	1 0 0 0	0 0 0 0	0 0 0 0	0 0 0 0	1 0 0 0	0 0 0 0	0 0 0 0	1 0 0 0	1 0 0 0	0 0 0 0	0 0 0 0	0 0 0 0	0 0 0 0
3176159	Δ391,957 bp	DEL	pip	PA14_35720–[PA14_40040]	0 0 0 0	1 0 0 0	0 0 0 0	0 0 0 0	0 0 0 0	1 0 0 0	0 0 0 0	0 0 0 0	1 0 0 0	1 0 0 0	0 0 0 0	0 0 0 0	0 0 0 0	0 0 0 0
3923324	G→A	SNP	pip	gltA	0 0 0 0	1 0 0 0	0 0 0 0	0 0 0 0	0 0 0 0	1 0 0 0	0 0 0 0	0 0 0 0	1 0 0 0	1 0 0 0	0 0 0 0	0 0 0 0	0 0 0 0	0 0 0 0
2033788	(G)7→6	DEL	pip	orfJ	0 0 0 0	0 1 0 0	0 0 0 0	0 0 0 0	0 0 0 0	0 1 0 0	0 0 0 0	0 0 0 0	0 1 0 0	0 1 0 0	0 0 0 0	0 0 0 0	0 0 0 0	0 0 0 0
3262305	Δ393,493 bp	DEL	pip	[glgX]–[nhaB]	0 0 0 0	0 1 0 0	0 0 0 0	0 0 0 0	0 0 0 0	0 1 0 0	0 0 0 0	0 0 0 0	0 1 0 0	0 1 0 0	0 0 0 0	0 0 0 0	0 0 0 0	0 0 0 0
486113	T→G	SNP	pip	mexR	0 0 0 0	0 1 0 0	0 0 0 0	0 0 0 0	0 0 0 0	0 1 0 0	0 0 0 0	0 0 0 0	0 1 0 0	0 1 0 0	0 0 0 0	0 0 0 0	0 0 0 0	0 0 0 0
3011430	Δ438,816 bp	DEL	pip	[aldG]–[acsA]	0 0 0 0	0 1 0 0	0 0 0 0	0 0 0 0	0 0 0 0	0 1 0 0	0 0 0 0	0 0 0 0	0 1 0 0	0 1 0 0	0 0 0 0	0 0 0 0	0 0 0 0	0 0 0 0
4610061	T→C	SNP	pip	PA14_51910	0 0 0 0	0 1 0 0	0 0 0 0	0 0 0 0	0 0 0 0	0 1 0 0	0 0 0 0	0 0 0 0	0 1 0 0	0 1 0 0	0 0 0 0	0 0 0 0	0 0 0 0	0 0 0 0
1551588	G→T	SNP	pip	PA14_18080	0 0 0 0	0 0 0 1	0 0 0 0	0 0 0 0	0 0 0 0	0 0 0 1	0 0 0 0	0 0 0 0	0 0 0 1	0 0 0 1	0 0 0 0	0 0 0 0	0 0 0 0	0 0 0 0
1977251	A→T	SNP	pip	PA14_22730	0 0 0 0	0 0 0 1	0 0 0 0	0 0 0 0	0 0 0 0	0 0 0 1	0 0 0 0	0 0 0 0	0 0 0 1	0 0 0 1	0 0 0 0	0 0 0 0	0 0 0 0	0 0 0 0
2772547	Δ28 bp	DEL	pip	PA14_31870	0 0 0 0	0 0 0 1	0 0 0 0	0 0 0 0	0 0 0 0	0 0 0 1	0 0 0 0	0 0 0 0	0 0 0 1	0 0 0 1	0 0 0 0	0 0 0 0	0 0 0 0	0 0 0 0
4824640	G→A	SNP	pip	mucB	0 0 0 0	0 0 0 1	0 0 0 0	0 0 0 0	0 0 0 0	0 0 0 1	0 0 0 0	0 0 0 0	0 0 0 1	0 0 0 1	0 0 0 0	0 0 0 0	0 0 0 0	0 0 0 0
5098481	C→A	SNP	pip	secA	0 0 0 0	0 0 0 1	0 0 0 0	0 0 0 0	0 0 0 0	0 0 0 1	0 0 0 0	0 0 0 0	0 0 0 1	0 0 0 1	0 0 0 0	0 0 0 0	0 0 0 0	0 0 0 0
5895714	C→A	SNP	pip	PA14_66170	0 0 0 0	0 0 0 1	0 0 0 0	0 0 0 0	0 0 0 0	0 0 0 1	0 0 0 0	0 0 0 0	0 0 0 1	0 0 0 1	0 0 0 0	0 0 0 0	0 0 0 0	0 0 0 0
757307	T→C	SNP	tob	fusA1	0 0 0 0	0 0 0 0	1 0 0 0	0 0 0 0	0 0 0 0	0 0 0 0	1 0 0 0	0 0 0 0	0 0 0 0	0 0 0 0	1 0 0 0	1 0 0 0	0 0 0 0	0 0 0 0
2043232	Δ243 bp	DEL	tob	wbpM	0 0 0 0	0 0 0 0	1 0 0 0	0 0 0 0	0 0 0 0	0 0 0 0	1 0 0 0	0 0 0 0	0 0 0 0	0 0 0 0	1 0 0 0	1 0 0 0	0 0 0 0	0 0 0 0
2229086	T→C	SNP	tob	PA14_25490	0 0 0 0	0 0 0 0	1 0 0 0	0 0 0 0	0 0 0 0	0 0 0 0	1 0 0 0	0 0 0 0	0 0 0 0	0 0 0 0	1 0 0 0	1 0 0 0	0 0 0 0	0 0 0 0
5128248	Δ1 bp	DEL	tob	PA14_57570	0 0 0 0	0 0 0 0	1 0 0 0	0 0 0 0	0 0 0 0	0 0 0 0	1 0 0 0	0 0 0 0	0 0 0 0	0 0 0 0	1 0 0 0	1 0 0 0	0 0 0 0	0 0 0 0
755747	A→G	SNP	tob	fusA1	0 0 0 0	0 0 0 0	0 1 0 0	0 0 0 0	0 0 0 0	0 0 0 0	0 1 0 0	0 0 0 0	0 0 0 0	0 0 0 0	0 1 0 0	0 1 0 0	0 0 0 0	0 0 0 0
745732	(ACCGCTGCTGCCGCTACCGTT)1→2	IN	tob	rplL	0 0 0 0	0 0 0 0	0 1 0 0	0 0 0 0	0 0 0 0	0 0 0 0	0 1 0 0	0 0 0 0	0 0 0 0	0 0 0 0	0 1 0 0	0 1 0 0	0 0 0 0	0 0 0 0
754922	A→G	SNP	tob	rpsL	0 0 0 0	0 0 0 0	0 1 0 0	0 0 0 0	0 0 0 0	0 0 0 0	0 1 0 0	0 0 0 0	0 0 0 0	0 0 0 0	0 1 0 0	0 1 0 0	0 0 0 0	0 0 0 0
5151959	T→G	SNP	tob	PA14_57880	0 0 0 0	0 0 0 0	0 1 0 0	0 0 0 0	0 0 0 0	0 0 0 0	0 1 0 0	0 0 0 0	0 0 0 0	0 0 0 0	0 1 0 0	0 1 0 0	0 0 0 0	0 0 0 0
3950174	Δ3,558 bp	DEL	tob	[ccoP]-[ccoP]	0 0 0 0	0 0 0 0	0 1 0 0	0 0 0 0	0 0 0 0	0 0 0 0	0 1 0 0	0 0 0 0	0 0 0 0	0 0 0 0	0 1 0 0	0 1 0 0	0 0 0 0	0 0 0 0
756775	C→T	SNP	tob	fusA1	0 0 0 0	0 0 0 0	0 0 1 0	0 0 0 0	0 0 0 0	0 0 0 0	0 0 1 0	0 0 0 0	0 0 0 0	0 0 0 0	0 0 1 0	0 0 1 0	0 0 0 0	0 0 0 0
2015766	T→A	SNP	cip	gyrA	0 0 0 0	0 0 0 0	0 0 0 0	1 0 0 0	0 0 0 0	0 0 0 0	0 0 0 0	1 0 0 0	0 0 0 0	0 0 0 0	0 0 0 0	0 0 0 0	1 0 0 0	1 0 0 0
2042146	Δ10 bp	DEL	cip	wbpM	0 0 0 0	0 0 0 0	0 0 0 0	1 0 0 0	0 0 0 0	0 0 0 0	0 0 0 0	1 0 0 0	0 0 0 0	0 0 0 0	0 0 0 0	0 0 0 0	1 0 0 0	1 0 0 0
2440786	G→C	SNP	cip	PA14_28190	0 0 0 0	0 0 0 0	0 0 0 0	1 0 0 0	0 0 0 0	0 0 0 0	0 0 0 0	1 0 0 0	0 0 0 0	0 0 0 0	0 0 0 0	0 0 0 0	1 0 0 0	1 0 0 0
4059298	Δ10 bp	DEL	cip	fliA	0 0 0 0	0 0 0 0	0 0 0 0	1 0 0 0	0 0 0 0	0 0 0 0	0 0 0 0	1 0 0 0	0 0 0 0	0 0 0 0	0 0 0 0	0 0 0 0	1 0 0 0	1 0 0 0
4678735	Δ1 bp	DEL	cip	aotJ	0 0 0 0	0 0 0 0	0 0 0 0	1 0 0 0	0 0 0 0	0 0 0 0	0 0 0 0	1 0 0 0	0 0 0 0	0 0 0 0	0 0 0 0	0 0 0 0	1 0 0 0	1 0 0 0
5428203	Δ15 bp	DEL	cip	nfxB	0 0 0 0	0 0 0 0	0 0 0 0	1 0 0 0	0 0 0 0	0 0 0 0	0 0 0 0	1 0 0 0	0 0 0 0	0 0 0 0	0 0 0 0	0 0 0 0	1 0 0 0	1 0 0 0
393006	(CTGGTCGGC)2→3	IN	cip	ptsP	0 0 0 0	0 0 0 0	0 0 0 0	1 0 0 0	0 0 0 0	0 0 0 0	0 0 0 0	1 0 0 0	0 0 0 0	0 0 0 0	0 0 0 0	0 0 0 0	1 0 0 0	1 0 0 0
4481804	(TCTTC)1→2	IN	cip	flgF	0 0 0 0	0 0 0 0	0 0 0 0	1 0 0 0	0 0 0 0	0 0 0 0	0 0 0 0	1 0 0 0	0 0 0 0	0 0 0 0	0 0 0 0	0 0 0 0	1 0 0 0	1 0 0 0
5428385	Δ13 bp	DEL	cip	nfxB	0 0 0 0	0 0 0 0	0 0 0 0	1 0 0 0	0 0 0 0	0 0 0 0	0 0 0 0	1 0 0 0	0 0 0 0	0 0 0 0	0 0 0 0	0 0 0 0	1 0 0 0	1 0 0 0
5946304	+G	IN	cip	aroB	0 0 0 0	0 0 0 0	0 0 0 0	1 0 0 0	0 0 0 0	0 0 0 0	0 0 0 0	1 0 0 0	0 0 0 0	0 0 0 0	0 0 0 0	0 0 0 0	1 0 0 0	1 0 0 0
2820800	Δ11 bp	DEL	cip	PA14_32420	0 0 0 0	0 0 0 0	0 0 0 0	0 1 0 0	0 0 0 0	0 0 0 0	0 0 0 0	0 0 0 1	0 0 0 0	0 0 0 0	0 0 0 0	0 0 0 0	0 1 0 0	0 1 0 0
3684101	Δ3 bp	DEL	cip	PA14_41270	0 0 0 0	0 0 0 0	0 0 0 0	0 1 0 0	0 0 0 0	0 0 0 0	0 0 0 0	0 0 0 1	0 0 0 0	0 0 0 0	0 0 0 0	0 0 0 0	0 1 0 0	0 1 0 0
3912045	T→G	SNP	cip	sucD	0 0 0 0	0 0 0 0	0 0 0 0	0 1 0 0	0 0 0 0	0 0 0 0	0 0 0 0	0 0 0 1	0 0 0 0	0 0 0 0	0 0 0 0	0 0 0 0	0 1 0 0	0 1 0 0
5428368	Δ16 bp	DEL	cip	nfxB	0 0 0 0	0 0 0 0	0 0 0 0	0 0 0 1	0 0 0 0	0 0 0 0	0 0 0 0	0 0 0 1	0 0 0 0	0 0 0 0	0 0 0 0	0 0 0 0	0 0 0 1	0 0 0 1
5945811	G→T	SNP	cip	aroB	0 0 0 0	0 0 0 0	0 0 0 0	0 0 0 1	0 0 0 0	0 0 0 0	0 0 0 0	0 0 0 1	0 0 0 0	0 0 0 0	0 0 0 0	0 0 0 0	0 0 0 1	0 0 0 1
3312140	Δ149 bp	DEL	LB	PA14_37170/ada	0 0 0 0	0 0 0 0	0 0 0 0	0 0 0 0	1 0 0 0	0 0 0 0	0 0 0 0	0 0 0 0	0 0 0 0	0 0 0 0	0 0 0 0	0 0 0 0	0 0 0 0	0 0 0 0
4286155	A→C	SNP	LB	aprX/PA14_48150	0 0 0 0	0 0 0 0	0 0 0 0	0 0 0 0	1 0 0 0	0 0 0 0	0 0 0 0	0 0 0 0	0 0 0 0	0 0 0 0	0 0 0 0	0 0 0 0	0 0 0 0	0 0 0 0
4059804	T→C	SNP	LB	fleN	0 0 0 0	0 0 0 0	0 0 0 0	0 0 0 0	0 1 0 0	0 0 0 0	0 0 0 0	0 0 0 0	0 0 0 0	0 0 0 0	0 0 0 0	0 0 0 0	0 0 0 0	0 0 0 0
2029960	C→A	SNP	LB	orfH	0 0 0 0	0 0 0 0	0 0 0 0	0 0 0 0	0 0 0 1	0 0 0 0	0 0 0 0	0 0 0 0	0 0 0 0	0 0 0 0	0 0 0 0	0 0 0 0	0 0 0 0	0 0 0 0
6213317	Δ12 bp	DEL	LB	rnk	0 0 0 0	0 0 0 0	0 0 0 0	0 0 0 0	0 0 1 0	0 0 0 0	0 0 0 0	0 0 0 0	0 0 0 0	0 0 0 0	0 0 0 0	0 0 0 0	0 0 0 0	0 0 0 0
4563212	C→G	SNP	LB	mvfR	0 0 0 0	0 0 0 0	0 0 0 0	0 0 0 0	0 0 0 1	0 0 0 0	0 0 0 0	0 0 0 0	0 0 0 0	0 0 0 0	0 0 0 0	0 0 0 0	0 0 0 0	0 0 0 0
497970	(ACGTTG)2→3	IN	pip	sahH	0 0 0 0	0 0 0 0	0 0 0 0	0 0 0 0	0 0 0 0	1 0 0 0	0 0 0 0	0 0 0 0	0 0 0 0	0 0 0 0	0 0 0 0	0 0 0 0	0 0 0 0	0 0 0 0
1236756	(TGGCGC)2→1	DEL	pip	pepA	0 0 0 0	0 0 0 0	0 0 0 0	0 0 0 0	0 0 0 0	1 0 0 0	0 0 0 0	0 0 0 0	0 0 0 0	0 0 0 0	0 0 0 0	0 0 0 0	0 0 0 0	0 0 0 0
2373793	T→G	SNP	pip	PA14_27360/deaD	0 0 0 0	0 0 0 0	0 0 0 0	0 0 0 0	0 0 0 0	1 0 0 0	0 0 0 0	0 0 0 0	0 0 0 0	0 0 0 0	0 0 0 0	0 0 0 0	0 0 0 0	0 0 0 0
1253908	C→T	SNP	pip	PA14_14710	0 0 0 0	0 0 0 0	0 0 0 0	0 0 0 0	0 0 0 0	1 0 0 0	0 0 0 0	0 0 0 0	0 0 0 0	0 0 0 0	0 0 0 0	0 0 0 0	0 0 0 0	0 0 0 0
1026776	T→G	SNP	pip	mpl	0 0 0 0	0 0 0 0	0 0 0 0	0 0 0 0	0 0 0 0	0 1 0 0	0 0 0 0	0 0 0 0	0 0 0 0	0 0 0 0	0 0 0 0	0 0 0 0	0 0 0 0	0 0 0 0
1046883	Δ1 bp	DEL	pip	dacC	0 0 0 0	0 0 0 0	0 0 0 0	0 0 0 0	0 0 0 0	0 1 0 0	0 0 0 0	0 0 0 0	0 0 0 0	0 0 0 0	0 0 0 0	0 0 0 0	0 0 0 0	0 0 0 0
3956160	(C)6→7	IN	pip	fixl	0 0 0 0	0 0 0 0	0 0 0 0	0 0 0 0	0 0 0 0	0 1 0 0	0 0 0 0	0 0 0 0	0 0 0 0	0 0 0 0	0 0 0 0	0 0 0 0	0 0 0 0	0 0 0 0
6521525	(CGGGC)1→2	IN	pip	atpC/atpD	0 0 0 0	0 0 0 0	0 0 0 0	0 0 0 0	0 0 0 0	0 1 0 0	0 0 0 0	0 0 0 0	0 0 0 0	0 0 0 0	0 0 0 0	0 0 0 0	0 0 0 0	0 0 0 0
1391629	A→G	SNP	pip	PA14_16280/PA14_16290	0 0 0 0	0 0 0 0	0 0 0 0	0 0 0 0	0 0 0 0	0 0 0 1	0 0 0 0	0 0 0 0	0 0 0 0	0 0 0 0	0 0 0 0	0 0 0 0	0 0 0 0	0 0 0 0
2617021	+C	IN	pip	clpS	0 0 0 0	0 0 0 0	0 0 0 0	0 0 0 0	0 0 0 0	0 0 0 1	0 0 0 0	0 0 0 0	0 0 0 0	0 0 0 0	0 0 0 0	0 0 0 0	0 0 0 0	0 0 0 0
3683615	A→G	SNP	tob	PA14_41270	0 0 0 0	0 0 0 0	0 0 0 0	0 0 0 0	0 0 0 0	0 0 0 0	1 0 0 0	0 0 0 0	0 0 0 0	0 0 0 0	0 0 0 0	0 0 0 0	0 0 0 0	0 0 0 0
2228651	(CCGCCA)2→3	IN	tob	PA14_25490	0 0 0 0	0 0 0 0	0 0 0 0	0 0 0 0	0 0 0 0	0 0 0 0	0 1 0 0	0 0 0 0	0 0 0 0	0 0 0 0	0 0 0 0	0 0 0 0	0 0 0 0	0 0 0 0
3683159	Δ9 bp	DEL	tob	PA14_41270	0 0 0 0	0 0 0 0	0 0 0 0	0 0 0 0	0 0 0 0	0 0 0 0	1 0 0 0	0 0 0 0	0 0 0 0	0 0 0 0	0 0 0 0	0 0 0 0	0 0 0 0	0 0 0 0
3423759	G→T	SNP	tob	amrB	0 0 0 0	0 0 0 0	0 0 0 0	0 0 0 0	0 0 0 0	0 0 0 0	0 1 0 0	0 0 0 0	0 0 0 0	0 0 0 0	0 0 0 0	0 0 0 0	0 0 0 0	0 0 0 0
6465641	Δ5 bp	DEL	tob	np20	0 0 0 0	0 0 0 0	0 0 0 0	0 0 0 0	0 0 0 0	0 0 0 0	0 1 0 0	0 0 0 0	0 0 0 0	0 0 0 0	0 0 0 0	0 0 0 0	0 0 0 0	0 0 0 0
2593980	T→G	SNP	tob	nuoG	0 0 0 0	0 0 0 0	0 0 0 0	0 0 0 0	0 0 0 0	0 0 0 0	0 0 1 0	0 0 0 0	0 0 0 0	0 0 0 0	0 0 0 0	0 0 0 0	0 0 0 0	0 0 0 0
3724012	Δ10 bp	DEL	tob	PA14_41730	0 0 0 0	0 0 0 0	0 0 0 0	0 0 0 0	0 0 0 0	0 0 0 0	0 0 1 0	0 0 0 0	0 0 0 0	0 0 0 0	0 0 0 0	0 0 0 0	0 0 0 0	0 0 0 0
5150240	Δ21 bp	DEL	tob	ttg2D	0 0 0 0	0 0 0 0	0 0 0 0	0 0 0 0	0 0 0 0	0 0 0 0	0 0 1 0	0 0 0 0	0 0 0 0	0 0 0 0	0 0 0 0	0 0 0 0	0 0 0 0	0 0 0 0
5820352	G→A	SNP	tob	miaA	0 0 0 0	0 0 0 0	0 0 0 0	0 0 0 0	0 0 0 0	0 0 0 0	0 0 1 0	0 0 0 0	0 0 0 0	0 0 0 0	0 0 0 0	0 0 0 0	0 0 0 0	0 0 0 0
6243031	A→C	SNP	tob	cycB/PA14_69980	0 0 0 0	0 0 0 0	0 0 0 0	0 0 0 0	0 0 0 0	0 0 0 0	0 0 1 0	0 0 0 0	0 0 0 0	0 0 0 0	0 0 0 0	0 0 0 0	0 0 0 0	0 0 0 0
2196877	T→C	SNP	cip	topA	0 0 0 0	0 0 0 0	0 0 0 0	0 0 0 0	0 0 0 0	0 0 0 0	0 0 0 0	1 0 0 0	0 0 0 0	0 0 0 0	0 0 0 0	0 0 0 0	0 0 0 0	0 0 0 0
3132243	Δ2 bp	DEL	cip	PA14_35210	0 0 0 0	0 0 0 0	0 0 0 0	0 0 0 0	0 0 0 0	0 0 0 0	0 0 0 0	1 0 0 0	0 0 0 0	0 0 0 0	0 0 0 0	0 0 0 0	0 0 0 0	0 0 0 0
856330	Δ10 bp	DEL	cip	PA14_09960	0 0 0 0	0 0 0 0	0 0 0 0	0 0 0 0	0 0 0 0	0 0 0 0	0 0 0 0	0 1 0 0	0 0 0 0	0 0 0 0	0 0 0 0	0 0 0 0	0 0 0 0	0 0 0 0
3132316	Δ4 bp	DEL	cip	PA14_35210	0 0 0 0	0 0 0 0	0 0 0 0	0 0 0 0	0 0 0 0	0 0 0 0	0 0 0 0	1 0 0 0	0 0 0 0	0 0 0 0	0 0 0 0	0 0 0 0	0 0 0 0	0 0 0 0
4345136	Δ10,665 bp	DEL	cip	intT–PA14_49030	0 0 0 0	0 0 0 0	0 0 0 0	0 0 0 0	0 0 0 0	0 0 0 0	0 0 0 0	1 0 0 0	0 0 0 0	0 0 0 0	0 0 0 0	0 0 0 0	0 0 0 0	0 0 0 0
6264430	Δ1 bp	DEL	cip	algC	0 0 0 0	0 0 0 0	0 0 0 0	0 0 0 0	0 0 0 0	0 0 0 0	0 0 0 0	1 0 0 0	0 0 0 0	0 0 0 0	0 0 0 0	0 0 0 0	0 0 0 0	0 0 0 0
6521405	57 bp x 2	IN	cip	atpC	0 0 0 0	0 0 0 0	0 0 0 0	0 0 0 0	0 0 0 0	0 0 0 0	0 0 0 0	0 0 0 1	0 0 0 0	0 0 0 0	0 0 0 0	0 0 0 0	0 0 0 0	0 0 0 0
5735	Δ9 bp	DEL	cip	gyrB	0 0 0 0	0 0 0 0	0 0 0 0	0 0 0 0	0 0 0 0	0 0 0 0	0 0 0 0	0 0 0 1	0 0 0 0	0 0 0 0	0 0 0 0	0 0 0 0	0 0 0 0	0 0 0 0
2233990	Δ14 bp	DEL	cip	rne	0 0 0 0	0 0 0 0	0 0 0 0	0 0 0 0	0 0 0 0	0 0 0 0	0 0 0 0	0 0 0 1	0 0 0 0	0 0 0 0	0 0 0 0	0 0 0 0	0 0 0 0	0 0 0 0
2617087	Δ8 bp	DEL	tob	clpS	0 0 0 0	0 0 0 0	0 0 0 0	0 0 0 0	0 0 0 0	0 0 0 0	0 0 0 0	0 0 0 0	1 0 0 0	0 0 0 0	0 0 0 0	0 0 0 0	0 0 0 0	0 0 0 0
6124478	(ATCTGC)2→3	IN	tob	envZ	0 0 0 0	0 0 0 0	0 0 0 0	0 0 0 0	0 0 0 0	0 0 0 0	0 0 0 0	0 0 0 0	1 0 0 0	0 0 0 0	0 0 0 0	0 0 0 0	0 0 0 0	0 0 0 0
757517	C→T	SNP	tob	fusA1	0 0 0 0	0 0 0 0	0 0 0 0	0 0 0 0	0 0 0 0	0 0 0 0	0 0 0 0	0 0 0 0	0 1 0 0	0 0 0 0	0 0 0 0	0 0 0 0	0 0 0 0	0 0 0 0

					Day 20 Control	Day 20 PIP^R	Day 20 TOB^R	Day 20 CIP^R	Day 40 Control	Day 40 PIP^R	Day 40 TOB^R	Day 40 CIP^R	Day 40 PIP^{R}TOB^R	Day 40 PIP^{R}CIP^R	Day 40 TOB^{R}PIP^R	Day 40 TOB^{R}CIP^R	Day 40 CIP^{R}PIP^R	Day 40 CIP^{R}TOB^R
Position	Mutation	Type	Condition	Gene	1 2 3 4	1 2 3 4	1 2 3 4	1 2 3 4	1 2 3 4	1 2 3 4	1 2 3 4	1 2 3 4	1 2 3 4	1 2 3 4	1 2 3 4	1 2 3 4	1 2 3 4	1 2 3 4
766635	A→C	SNP	tob	rplF	0 0 0 0	0 0 0 0	0 0 0 0	0 0 0 0	0 0 0 0	0 0 0 0	0 0 0 0	0 0 0 0	1 0	0 0 0 0	0 0 0 0	0 0 0 0	0 0 0 0	0 0 0 0
393535	+A	IN	tob	ptsP	0 0 0 0	0 0 0 0	0 0 0 0	0 0 0 0	0 0 0 0	0 0 0 0	0 0 0 0	0 0 0 0	0 1 0	0 0 0 0	0 0 0 0	0 0 0 0	0 0 0 0	0 0 0 0
755840	G→A	SNP	tob	fusA1	0 0 0 0	0 0 0 0	0 0 0 0	0 0 0 0	0 0 0 0	0 0 0 0	0 0 0 0	0 0 0 0	0 1 0	0 0 0 0	0 0 0 0	0 0 0 0	0 0 0 0	0 0 0 0
6124696	A→G	SNP	tob	envZ	0 0 0 0	0 0 0 0	0 0 0 0	0 0 0 0	0 0 0 0	0 0 0 0	0 0 0 0	0 0 0 0	0 1 0	0 0 0 0	0 0 0 0	0 0 0 0	0 0 0 0	0 0 0 0
745178	Δ6 bp	DEL	tob	rplJ	0 0 0 0	0 0 0 0	0 0 0 0	0 0 0 0	0 0 0 0	0 0 0 0	0 0 0 0	0 0 0 0	0 0 0 1	0 0 0 0	0 0 0 0	0 0 0 0	0 0 0 0	0 0 0 0
756515	A→G	SNP	tob	fusA1	0 0 0 0	0 0 0 0	0 0 0 0	0 0 0 0	0 0 0 0	0 0 0 0	0 0 0 0	0 0 0 0	0 0 0 1	0 0 0 0	0 0 0 0	0 0 0 0	0 0 0 0	0 0 0 0
5637003	T→C	SNP	tob	pmrB	0 0 0 0	0 0 0 0	0 0 0 0	0 0 0 0	0 0 0 0	0 0 0 0	0 0 0 0	0 0 0 0	0 0 0 1	0 0 0 0	0 0 0 0	0 0 0 0	0 0 0 0	0 0 0 0
5454	A→G	SNP	cip	gyrB	0 0 0 0	0 0 0 0	0 0 0 0	0 0 0 0	0 0 0 0	0 0 0 0	0 0 0 0	0 0 0 0	0 0 0 0	1 0 0 0	0 0 0 0	0 0 0 0	0 0 0 0	0 0 0 0
2040296	(G)10→11	IN	cip	orfN	0 0 0 0	0 0 0 0	0 0 0 0	0 0 0 0	0 0 0 0	0 0 0 0	0 0 0 0	0 0 0 0	0 0 0 0	1 0 0 0	0 0 0 0	0 0 0 0	0 0 0 0	0 0 0 0
2362007	+G	IN	cip	erfK	0 0 0 0	0 0 0 0	0 0 0 0	0 0 0 0	0 0 0 0	0 0 0 0	0 0 0 0	0 0 0 0	0 0 0 0	1 0 0 0	0 0 0 0	0 0 0 0	0 0 0 0	0 0 0 0
3066665	Δ18 bp	DEL	cip	PA14_34500	0 0 0 0	0 0 0 0	0 0 0 0	0 0 0 0	0 0 0 0	0 0 0 0	0 0 0 0	0 0 0 0	0 0 0 0	1 0 0 0	0 0 0 0	0 0 0 0	0 0 0 0	0 0 0 0
5428450	Δ2 bp	DEL	cip	nfxB	0 0 0 0	0 0 0 0	0 0 0 0	0 0 0 0	0 0 0 0	0 0 0 0	0 0 0 0	0 0 0 0	0 0 0 0	1 0 0 0	0 0 0 0	0 0 0 0	0 0 0 0	0 0 0 0
5909393	Δ17 bp	DEL	cip	aceA	0 0 0 0	0 0 0 0	0 0 0 0	0 0 0 0	0 0 0 0	0 0 0 0	0 0 0 0	0 0 0 0	0 0 0 0	1 0 0 0	0 0 0 0	0 0 0 0	0 0 0 0	0 0 0 0
6243372	Δ12 bp	DEL	cip	PA14_60980	0 0 0 0	0 0 0 0	0 0 0 0	0 0 0 0	0 0 0 0	0 0 0 0	0 0 0 0	0 0 0 0	0 0 0 0	1 0 0 0	0 0 0 0	0 0 0 0	0 0 0 0	0 0 0 0
474355	Δ1 bp	DEL	cip	chpA	0 0 0 0	0 0 0 0	0 0 0 0	0 0 0 0	0 0 0 0	0 0 0 0	0 0 0 0	0 0 0 0	0 0 0 0	0 1 0 0	0 0 0 0	0 0 0 0	0 0 0 0	0 0 0 0
487154	Δ13 bp	DEL	cip	mexA	0 0 0 0	0 0 0 0	0 0 0 0	0 0 0 0	0 0 0 0	0 0 0 0	0 0 0 0	0 0 0 0	0 0 0 0	0 1 0 0	0 0 0 0	0 0 0 0	0 0 0 0	0 0 0 0
2418615	+GCG	IN	cip	PA14_27940	0 0 0 0	0 0 0 0	0 0 0 0	0 0 0 0	0 0 0 0	0 0 0 0	0 0 0 0	0 0 0 0	0 0 0 0	0 1 0 0	0 0 0 0	0 0 0 0	0 0 0 0	0 0 0 0
2644419	(TCCGT)6→5	DEL	cip	PA14_30540/ssuA	0 0 0 0	0 0 0 0	0 0 0 0	0 0 0 0	0 0 0 0	0 0 0 0	0 0 0 0	0 0 0 0	0 0 0 0	0 1 0 0	0 0 0 0	0 0 0 0	0 0 0 0	0 0 0 0
2820054	Δ10 bp	DEL	cip	PA14_32420	0 0 0 0	0 0 0 0	0 0 0 0	0 0 0 0	0 0 0 0	0 0 0 0	0 0 0 0	0 0 0 0	0 0 0 0	0 1 0 0	0 0 0 0	0 0 0 0	0 0 0 0	0 0 0 0
4053882	Δ9 bp	DEL	cip	cheB	0 0 0 0	0 0 0 0	0 0 0 0	0 0 0 0	0 0 0 0	0 0 0 0	0 0 0 0	0 0 0 0	0 0 0 0	0 1 0 0	0 0 0 0	0 0 0 0	0 0 0 0	0 0 0 0
516356	Δ15 bp	DEL	cip	gcdH	0 0 0 0	0 0 0 0	0 0 0 0	0 0 0 0	0 0 0 0	0 0 0 0	0 0 0 0	0 0 0 0	0 0 0 0	0 0 1 0	0 0 0 0	0 0 0 0	0 0 0 0	0 0 0 0
2040296	(G)10→12	IN	cip	orfN	0 0 0 0	0 0 0 0	0 0 0 0	0 0 0 0	0 0 0 0	0 0 0 0	0 0 0 0	0 0 0 0	0 0 0 0	0 0 1 0	0 0 0 0	0 0 0 0	0 0 0 0	0 0 0 0
2820287	Δ13 bp	DEL	cip	PA14_32420	0 0 0 0	0 0 0 0	0 0 0 0	0 0 0 0	0 0 0 0	0 0 0 0	0 0 0 0	0 0 0 0	0 0 0 0	0 0 1 0	0 0 0 0	0 0 0 0	0 0 0 0	0 0 0 0
856350	Δ1 bp	DEL	cip	PA14_09960	0 0 0 0	0 0 0 0	0 0 0 0	0 0 0 0	0 0 0 0	0 0 0 0	0 0 0 0	0 0 0 0	0 0 0 0	0 0 0 1	0 0 0 0	0 0 0 0	0 0 0 0	0 0 0 0
1978813	Δ13 bp	DEL	cip	cpxR	0 0 0 0	0 0 0 0	0 0 0 0	0 0 0 0	0 0 0 0	0 0 0 0	0 0 0 0	0 0 0 0	0 0 0 0	0 0 0 1	0 0 0 0	0 0 0 0	0 0 0 0	0 0 0 0
2014994	G→T	SNP	cip	gyrA	0 0 0 0	0 0 0 0	0 0 0 0	0 0 0 0	0 0 0 0	0 0 0 0	0 0 0 0	0 0 0 0	0 0 0 0	0 0 0 1	0 0 0 0	0 0 0 0	0 0 0 0	0 0 0 0
5156856	Δ16 bp	DEL	cip	rpoN	0 0 0 0	0 0 0 0	0 0 0 0	0 0 0 0	0 0 0 0	0 0 0 0	0 0 0 0	0 0 0 0	0 0 0 0	0 0 0 1	0 0 0 0	0 0 0 0	0 0 0 0	0 0 0 0
5428368	Δ247 bp	DEL	cip	[nfxB]	0 0 0 0	0 0 0 0	0 0 0 0	0 0 0 0	0 0 0 0	0 0 0 0	0 0 0 0	0 0 0 0	0 0 0 0	0 0 0 1	0 0 0 0	0 0 0 0	0 0 0 0	0 0 0 0
1026532	C→T	SNP	pip	mpl	0 0 0 0	0 0 0 0	0 0 0 0	0 0 0 0	0 0 0 0	0 0 0 0	0 0 0 0	0 0 0 0	0 0 0 0	0 0 0 0	1 0 0 0	0 0 0 0	0 0 0 0	0 0 0 0
1046345	+G	IN	pip	dacC	0 0 0 0	0 0 0 0	0 0 0 0	0 0 0 0	0 0 0 0	0 0 0 0	0 0 0 0	0 0 0 0	0 0 0 0	0 0 0 0	1 0 0 0	0 0 0 0	0 0 0 0	0 0 0 0
1235954	C→T	SNP	pip	pepA	0 0 0 0	0 0 0 0	0 0 0 0	0 0 0 0	0 0 0 0	0 0 0 0	0 0 0 0	0 0 0 0	0 0 0 0	0 0 0 0	1 0 0 0	0 0 0 0	0 0 0 0	0 0 0 0
1391338	T→C	SNP	pip	PA14_16280	0 0 0 0	0 0 0 0	0 0 0 0	0 0 0 0	0 0 0 0	0 0 0 0	0 0 0 0	0 0 0 0	0 0 0 0	0 0 0 0	1 0 0 0	0 0 0 0	0 0 0 0	0 0 0 0
3503834	G→A	SNP	pip	PA14_39360	0 0 0 0	0 0 0 0	0 0 0 0	0 0 0 0	0 0 0 0	0 0 0 0	0 0 0 0	0 0 0 0	0 0 0 0	0 0 0 0	1 0 0 0	0 0 0 0	0 0 0 0	0 0 0 0
741273	A→G	SNP	pip	PA14_08670/tufB	0 0 0 0	0 0 0 0	0 0 0 0	0 0 0 0	0 0 0 0	0 0 0 0	0 0 0 0	0 0 0 0	0 0 0 0	0 0 0 0	0 1 0 0	0 0 0 0	0 0 0 0	0 0 0 0
934375	G→A	SNP	pip	ampR	0 0 0 0	0 0 0 0	0 0 0 0	0 0 0 0	0 0 0 0	0 0 0 0	0 0 0 0	0 0 0 0	0 0 0 0	0 0 0 0	0 1 0 0	0 0 0 0	0 0 0 0	0 0 0 0
1391472	(G)6→5	DEL	pip	PA14_16280	0 0 0 0	0 0 0 0	0 0 0 0	0 0 0 0	0 0 0 0	0 0 0 0	0 0 0 0	0 0 0 0	0 0 0 0	0 0 0 0	0 1 0 0	0 0 0 0	0 0 0 0	0 0 0 0
4610124	T→C	SNP	pip	PA14_51910	0 0 0 0	0 0 0 0	0 0 0 0	0 0 0 0	0 0 0 0	0 0 0 0	0 0 0 0	0 0 0 0	0 0 0 0	0 0 0 0	0 1 0 0	0 0 0 0	0 0 0 0	0 0 0 0
1026516	(C)7→6	DEL	pip	mpl	0 0 0 0	0 0 0 0	0 0 0 0	0 0 0 0	0 0 0 0	0 0 0 0	0 0 0 0	0 0 0 0	0 0 0 0	0 0 0 0	0 1 0 0	0 0 0 0	0 0 0 0	0 0 0 0
1046789	(TCGACGGCCTGAAGACCG)1→2	IN	pip	dacC	0 0 0 0	0 0 0 0	0 0 0 0	0 0 0 0	0 0 0 0	0 0 0 0	0 0 0 0	0 0 0 0	0 0 0 0	0 0 0 0	0 1 0 0	0 0 0 0	0 0 0 0	0 0 0 0
1551039	A→G	SNP	pip	PA14_18080	0 0 0 0	0 0 0 0	0 0 0 0	0 0 0 0	0 0 0 0	0 0 0 0	0 0 0 0	0 0 0 0	0 0 0 0	0 0 0 0	0 1 0 0	0 0 0 0	0 0 0 0	0 0 0 0
3979085	G→A	SNP	pip	zipA	0 0 0 0	0 0 0 0	0 0 0 0	0 0 0 0	0 0 0 0	0 0 0 0	0 0 0 0	0 0 0 0	0 0 0 0	0 0 0 0	0 1 0 0	0 0 0 0	0 0 0 0	0 0 0 0
1235955	C→T	SNP	pip	pepA	0 0 0 0	0 0 0 0	0 0 0 0	0 0 0 0	0 0 0 0	0 0 0 0	0 0 0 0	0 0 0 0	0 0 0 0	0 0 0 0	0 0 1 0	0 0 0 0	0 0 0 0	0 0 0 0
1896987	Δ2 bp	DEL	pip	PA14_21820	0 0 0 0	0 0 0 0	0 0 0 0	0 0 0 0	0 0 0 0	0 0 0 0	0 0 0 0	0 0 0 0	0 0 0 0	0 0 0 0	0 0 1 0	0 0 0 0	0 0 0 0	0 0 0 0
2888067	Δ14 bp	DEL	cip	gcvP2	0 0 0 0	0 0 0 0	0 0 0 0	0 0 0 0	0 0 0 0	0 0 0 0	0 0 0 0	0 0 0 0	0 0 0 0	0 0 0 0	0 0 0 0	1 0 0 0	0 0 0 0	0 0 0 0
4338224	+CTTG	IN	cip	PA14_48800	0 0 0 0	0 0 0 0	0 0 0 0	0 0 0 0	0 0 0 0	0 0 0 0	0 0 0 0	0 0 0 0	0 0 0 0	0 0 0 0	0 0 0 0	1 0 0 0	0 0 0 0	0 0 0 0
5121114	+CGCC	IN	cip	PA14_57470	0 0 0 0	0 0 0 0	0 0 0 0	0 0 0 0	0 0 0 0	0 0 0 0	0 0 0 0	0 0 0 0	0 0 0 0	0 0 0 0	0 0 0 0	1 0 0 0	0 0 0 0	0 0 0 0
5428132	Δ23 bp	DEL	cip	nfxB	0 0 0 0	0 0 0 0	0 0 0 0	0 0 0 0	0 0 0 0	0 0 0 0	0 0 0 0	0 0 0 0	0 0 0 0	0 0 0 0	0 0 0 0	1 0 0 0	0 0 0 0	0 0 0 0
6280243	Δ7 bp	SNP	cip	spoT	0 0 0 0	0 0 0 0	0 0 0 0	0 0 0 0	0 0 0 0	0 0 0 0	0 0 0 0	0 0 0 0	0 0 0 0	0 0 0 0	0 0 0 0	1 0 0 0	0 0 0 0	0 0 0 0
750702	C→T	SNP	cip	rpoC	0 0 0 0	0 0 0 0	0 0 0 0	0 0 0 0	0 0 0 0	0 0 0 0	0 0 0 0	0 0 0 0	0 0 0 0	0 0 0 0	0 0 0 0	0 1 0 0	0 0 0 0	0 0 0 0
1551015	Δ11 bp	DEL	cip	PA14_18080	0 0 0 0	0 0 0 0	0 0 0 0	0 0 0 0	0 0 0 0	0 0 0 0	0 0 0 0	0 0 0 0	0 0 0 0	0 0 0 0	0 0 0 0	0 1 0 0	0 0 0 0	0 0 0 0
2820833	Δ11 bp	DEL	cip	PA14_32420	0 0 0 0	0 0 0 0	0 0 0 0	0 0 0 0	0 0 0 0	0 0 0 0	0 0 0 0	0 0 0 0	0 0 0 0	0 0 0 0	0 0 0 0	0 1 0 0	0 0 0 0	0 0 0 0
3359401	Δ176,012 bp	DEL	cip	[PA14_37690]–[PA14_39660]	0 0 0 0	0 0 0 0	0 0 0 0	0 0 0 0	0 0 0 0	0 0 0 0	0 0 0 0	0 0 0 0	0 0 0 0	0 0 0 0	0 0 0 0	0 1 0 0	0 0 0 0	0 0 0 0
856310	+CCTG	IN	cip	PA14_09960	0 0 0 0	0 0 0 0	0 0 0 0	0 0 0 0	0 0 0 0	0 0 0 0	0 0 0 0	0 0 0 0	0 0 0 0	0 0 0 0	0 0 0 0	0 0 1 0	0 0 0 0	0 0 0 0
2820879	Δ90 bp	DEL	cip	PA14_32420	0 0 0 0	0 0 0 0	0 0 0 0	0 0 0 0	0 0 0 0	0 0 0 0	0 0 0 0	0 0 0 0	0 0 0 0	0 0 0 0	0 0 0 0	0 1 0 0	0 0 0 0	0 0 0 0
3665795	Δ1 bp	DEL	cip	PA14_41110	0 0 0 0	0 0 0 0	0 0 0 0	0 0 0 0	0 0 0 0	0 0 0 0	0 0 0 0	0 0 0 0	0 0 0 0	0 0 0 0	0 0 0 0	0 1 0 0	0 0 0 0	0 0 0 0
4475830	Δ12 bp	DEL	cip	flgK	0 0 0 0	0 0 0 0	0 0 0 0	0 0 0 0	0 0 0 0	0 0 0 0	0 0 0 0	0 0 0 0	0 0 0 0	0 0 0 0	0 0 0 0	0 1 0 0	0 0 0 0	0 0 0 0
5428401	Δ13 bp	DEL	cip	nfxB	0 0 0 0	0 0 0 0	0 0 0 0	0 0 0 0	0 0 0 0	0 0 0 0	0 0 0 0	0 0 0 0	0 0 0 0	0 0 0 0	0 0 0 0	0 0 0 1	0 0 0 0	0 0 0 0
5907665	Δ1 bp	DEL	cip	aceA	0 0 0 0	0 0 0 0	0 0 0 0	0 0 0 0	0 0 0 0	0 0 0 0	0 0 0 0	0 0 0 0	0 0 0 0	0 0 0 0	0 0 0 0	0 0 0 1	0 0 0 0	0 0 0 0
1027591	Δ1 bp	DEL	pip	mpl	0 0 0 0	0 0 0 0	0 0 0 0	0 0 0 0	0 0 0 0	0 0 0 0	0 0 0 0	0 0 0 0	0 0 0 0	0 0 0 0	0 0 0 0	0 0 0 0	1 0 0 0	0 0 0 0
1047169	+GC	IN	pip	dacC	0 0 0 0	0 0 0 0	0 0 0 0	0 0 0 0	0 0 0 0	0 0 0 0	0 0 0 0	0 0 0 0	0 0 0 0	0 0 0 0	0 0 0 0	0 0 0 0	1 0 0 0	0 0 0 0
1551511	C→T	SNP	pip	PA14_18080	0 0 0 0	0 0 0 0	0 0 0 0	0 0 0 0	0 0 0 0	0 0 0 0	0 0 0 0	0 0 0 0	0 0 0 0	0 0 0 0	0 0 0 0	0 0 0 0	1 0 0 0	0 0 0 0
1804651	Δ1 bp	DEL	pip	PA14_20960	0 0 0 0	0 0 0 0	0 0 0 0	0 0 0 0	0 0 0 0	0 0 0 0	0 0 0 0	0 0 0 0	0 0 0 0	0 0 0 0	0 0 0 0	0 0 0 0	1 0 0 0	0 0 0 0
2705834	Δ23 bp	DEL	pip	PA14_31100/PA14_31110	0 0 0 0	0 0 0 0	0 0 0 0	0 0 0 0	0 0 0 0	0 0 0 0	0 0 0 0	0 0 0 0	0 0 0 0	0 0 0 0	0 0 0 0	0 0 0 0	1 0 0 0	0 0 0 0
3722786	A→C	SNP	pip	PA14_41710	0 0 0 0	0 0 0 0	0 0 0 0	0 0 0 0	0 0 0 0	0 0 0 0	0 0 0 0	0 0 0 0	0 0 0 0	0 0 0 0	0 0 0 0	0 0 0 0	1 0 0 0	0 0 0 0
5120919	(C)8→9	IN	pip	PA14_57470	0 0 0 0	0 0 0 0	0 0 0 0	0 0 0 0	0 0 0 0	0 0 0 0	0 0 0 0	0 0 0 0	0 0 0 0	0 0 0 0	0 0 0 0	0 0 0 0	1 0 0 0	0 0 0 0
5426859	(GCATG)1→2	IN	pip	mexC	0 0 0 0	0 0 0 0	0 0 0 0	0 0 0 0	0 0 0 0	0 0 0 0	0 0 0 0	0 0 0 0	0 0 0 0	0 0 0 0	0 0 0 0	0 0 0 0	1 0 0 0	0 0 0 0
6246268	T→C	SNP	pip	dadA	0 0 0 0	0 0 0 0	0 0 0 0	0 0 0 0	0 0 0 0	0 0 0 0	0 0 0 0	0 0 0 0	0 0 0 0	0 0 0 0	0 0 0 0	0 0 0 0	1 0 0 0	0 0 0 0
1391446	Δ12 bp	DEL	pip	PA14_16280	0 0 0 0	0 0 0 0	0 0 0 0	0 0 0 0	0 0 0 0	0 0 0 0	0 0 0 0	0 0 0 0	0 0 0 0	0 0 0 0	0 0 0 0	0 0 0 0	0 1 0 0	0 0 0 0
1524881	C→T	SNP	pip	ycjJ	0 0 0 0	0 0 0 0	0 0 0 0	0 0 0 0	0 0 0 0	0 0 0 0	0 0 0 0	0 0 0 0	0 0 0 0	0 0 0 0	0 0 0 0	0 0 0 0	0 1 0 0	0 0 0 0
2618989	Δ6 bp	DEL	pip	clpA	0 0 0 0	0 0 0 0	0 0 0 0	0 0 0 0	0 0 0 0	0 0 0 0	0 0 0 0	0 0 0 0	0 0 0 0	0 0 0 0	0 0 0 0	0 0 0 0	0 1 0 0	0 0 0 0
5427510	Δ1 bp	DEL	pip	mexC	0 0 0 0	0 0 0 0	0 0 0 0	0 0 0 0	0 0 0 0	0 0 0 0	0 0 0 0	0 0 0 0	0 0 0 0	0 0 0 0	0 0 0 0	0 0 0 0	0 1 0 0	0 0 0 0
486577	A→G	SNP	pip	mexR/mexA	0 0 0 0	0 0 0 0	0 0 0 0	0 0 0 0	0 0 0 0	0 0 0 0	0 0 0 0	0 0 0 0	0 0 0 0	0 0 0 0	0 0 0 0	0 0 0 0	0 0 1 0	0 0 0 0
934377	C→A	SNP	pip	ampR	0 0 0 0	0 0 0 0	0 0 0 0	0 0 0 0	0 0 0 0	0 0 0 0	0 0 0 0	0 0 0 0	0 0 0 0	0 0 0 0	0 0 0 0	0 0 0 0	0 0 1 0	0 0 0 0
2814657	Δ1 bp	DEL	pip	mexF	0 0 0 0	0 0 0 0	0 0 0 0	0 0 0 0	0 0 0 0	0 0 0 0	0 0 0 0	0 0 0 0	0 0 0 0	0 0 0 0	0 0 0 0	0 0 0 0	0 0 1 0	0 0 0 0
486229	Δ12 bp	DEL	pip	mexR	0 0 0 0	0 0 0 0	0 0 0 0	0 0 0 0	0 0 0 0	0 0 0 0	0 0 0 0	0 0 0 0	0 0 0 0	0 0 0 0	0 0 0 0	0 0 0 0	0 0 0 1	0 0 0 0
2618434	(CCTCAAGGG)2→3	IN	pip	clpA	0 0 0 0	0 0 0 0	0 0 0 0	0 0 0 0	0 0 0 0	0 0 0 0	0 0 0 0	0 0 0 0	0 0 0 0	0 0 0 0	0 0 0 0	0 0 0 0	0 0 0 1	0 0 0 0
5840488	G→A	SNP	pip	PA14_65570	0 0 0 0	0 0 0 0	0 0 0 0	0 0 0 0	0 0 0 0	0 0 0 0	0 0 0 0	0 0 0 0	0 0 0 0	0 0 0 0	0 0 0 0	0 0 0 0	0 0 0 1	0 0 0 0
6280741	G→T	SNP	pip	spoT	0 0 0 0	0 0 0 0	0 0 0 0	0 0 0 0	0 0 0 0	0 0 0 0	0 0 0 0	0 0 0 0	0 0 0 0	0 0 0 0	0 0 0 0	0 0 0 0	0 0 0 1	0 0 0 0
394599	C→G	SNP	tob	ptsP	0 0 0 0	0 0 0 0	0 0 0 0	0 0 0 0	0 0 0 0	0 0 0 0	0 0 0 0	0 0 0 0	0 0 0 0	0 0 0 0	0 0 0 0	0 0 0 0	0 0 0 0	1 0 0 0
4258923	Δ13 bp	DEL	tob	PA14_47860	0 0 0 0	0 0 0 0	0 0 0 0	0 0 0 0	0 0 0 0	0 0 0 0	0 0 0 0	0 0 0 0	0 0 0 0	0 0 0 0	0 0 0 0	0 0 0 0	0 0 0 0	1 0 0 0
5126485	Δ2 bp	DEL	tob	PA14_57540	0 0 0 0	0 0 0 0	0 0 0 0	0 0 0 0	0 0 0 0	0 0 0 0	0 0 0 0	0 0 0 0	0 0 0 0	0 0 0 0	0 0 0 0	0 0 0 0	0 0 0 0	1 0 0 0
757036	Δ3 bp	DEL	tob	fusA1	0 0 0 0	0 0 0 0	0 0 0 0	0 0 0 0	0 0 0 0	0 0 0 0	0 0 0 0	0 0 0 0	0 0 0 0	0 0 0 0	0 0 0 0	0 0 0 0	0 0 0 0	0 1 0 0

					Day 20 Control	Day 20 PIP^R	Day 20 TOB^R	Day 20 CIP^R	Day 40 Control	Day 40 PIP^R	Day 40 TOB^R	Day 40 CIP^R	Day 40 PIP^{R}TOB^R	Day 40 PIP^{R}CIP^R	Day 40 TOB^{R}PIP^R	Day 40 TOB^{R}CIP^R	Day 40 CIP^{R}PIP^R	Day 40 CIP^{R}TOB^R
Position	Mutation	Type	Condition	Gene	1 2 3 4	1 2 3 4	1 2 3 4	1 2 3 4	1 2 3 4	1 2 3 4	1 2 3 4	1 2 3 4	1 2 3 4	1 2 3 4	1 2 3 4	1 2 3 4	1 2 3 4	1 2 3 4
5426321	G→A	SNP	tob	mexD	0 0 0 0	0 0 0 0	0 0 0 0	0 0 0 0	0 0 0 0	0 0 0 0	0 0 0 0	0 0 0 0	0 0 0 0	0 0 0 0	0 0 0 0	0 0 0 0	0 0 0 0	0 1 0 0
6118176	+G	IN	tob	pckA	0 0 0 0	0 0 0 0	0 0 0 0	0 0 0 0	0 0 0 0	0 0 0 0	0 0 0 0	0 0 0 0	0 0 0 0	0 0 0 0	0 0 0 0	0 0 0 0	0 0 0 0	0 1 0 0
757553	A→G	SNP	tob	fusA1	0 0 0 0	0 0 0 0	0 0 0 0	0 0 0 0	0 0 0 0	0 0 0 0	0 0 0 0	0 0 0 0	0 0 0 0	0 0 0 0	0 0 0 0	0 0 0 0	0 0 0 0	0 0 1 0
766633	A→G	SNP	tob	rplF	0 0 0 0	0 0 0 0	0 0 0 0	0 0 0 0	0 0 0 0	0 0 0 0	0 0 0 0	0 0 0 0	0 0 0 0	0 0 0 0	0 0 0 0	0 0 0 0	0 0 0 0	0 0 1 0
2819101	C→T	SNP	tob	mexT	0 0 0 0	0 0 0 0	0 0 0 0	0 0 0 0	0 0 0 0	0 0 0 0	0 0 0 0	0 0 0 0	0 0 0 0	0 0 0 0	0 0 0 0	0 0 0 0	0 0 0 0	0 0 1 0
4478532	Δ1,122 bp	DEL	tob	[flgJ]–[flgI]	0 0 0 0	0 0 0 0	0 0 0 0	0 0 0 0	0 0 0 0	0 0 0 0	0 0 0 0	0 0 0 0	0 0 0 0	0 0 0 0	0 0 0 0	0 0 0 0	0 0 0 0	0 0 1 0
757030	A→G	SNP	tob	fusA1	0 0 0 0	0 0 0 0	0 0 0 0	0 0 0 0	0 0 0 0	0 0 0 0	0 0 0 0	0 0 0 0	0 0 0 0	0 0 0 0	0 0 0 0	0 0 0 0	0 0 0 0	0 0 0 1
5125962	Δ1 bp	DEL	tob	PA14_57540	0 0 0 0	0 0 0 0	0 0 0 0	0 0 0 0	0 0 0 0	0 0 0 0	0 0 0 0	0 0 0 0	0 0 0 0	0 0 0 0	0 0 0 0	0 0 0 0	0 0 0 0	0 0 0 1
5427906	+GG	IN	tob	mexC/nfxB	0 0 0 0	0 0 0 0	0 0 0 0	0 0 0 0	0 0 0 0	0 0 0 0	0 0 0 0	0 0 0 0	0 0 0 0	0 0 0 0	0 0 0 0	0 0 0 0	0 0 0 0	0 0 0 1
5511288	Δ1 bp	DEL	LB	prs	1 0 0 0	0 0 0 0	0 0 0 0	0 0 0 0	0 0 0 0	0 0 0 0	0 0 0 0	0 0 0 0	0 0 0 0	0 0 0 0	0 0 0 0	0 0 0 0	0 0 0 0	0 0 0 0
2030092	(G)7→6	DEL	LB	orfH	0 1 0 0	0 0 0 0	0 0 0 0	0 0 0 0	0 0 0 0	0 0 0 0	0 0 0 0	0 0 0 0	0 0 0 0	0 0 0 0	0 0 0 0	0 0 0 0	0 0 0 0	0 0 0 0
2029395	T→G	SNP	LB	orfH	0 0 1 0	0 0 0 0	0 0 0 0	0 0 0 0	0 1 0 0	0 0 0 0	0 0 0 0	0 0 0 0	0 0 0 0	0 0 0 0	0 0 0 0	0 0 0 0	0 0 0 0	0 1 0 0
2157750	Δ3 bp	DEL	pip	dacB	0 0 0 0	1 0 0 0	0 0 0 0	0 0 0 0	0 0 0 0	1 0 0 0	0 0 0 0	0 0 0 0	0 0 0 0	1 0 0 0	0 0 0 0	0 0 0 0	0 0 0 0	0 0 0 0
486420	+A	IN	pip,tob	mexR	0 0 0 0	0 1 0 0	0 0 0 0	0 0 0 0	0 0 0 0	0 1 0 0	0 0 0 0	0 0 0 0	1 1 0 0	0 1 0 0	0 0 0 0	0 0 0 0	0 0 0 0	0 0 0 0
6279525	(ATGGCC)3→2	DEL	pip	spoT	0 0 0 0	0 1 0 0	0 0 0 0	0 0 0 0	0 0 0 0	0 0 0 0	0 0 0 0	0 0 0 0	0 0 0 0	0 0 0 0	0 0 0 0	0 0 0 0	0 0 0 0	0 0 0 0
1916308	T→G	SNP	pip	minC	0 0 0 0	0 0 1 0	0 0 0 0	0 0 0 0	0 0 0 0	0 1 1 0	0 0 0 0	0 0 0 0	0 1 1 0	0 0 1 0	0 0 0 0	0 0 0 0	0 0 0 0	0 0 0 0
2598246	Δ6 bp	DEL	tob	nuoB	0 0 0 0	0 0 0 0	0 1 0 0	0 0 0 0	0 0 0 0	0 0 0 0	0 0 0 0	0 0 0 0	0 0 0 0	0 0 0 0	0 1 0 0	0 0 0 0	0 0 0 0	0 0 0 0
3722917	(C)5→4	DEL	tob	PA14_41710	0 0 0 0	0 0 0 0	0 1 0 0	0 0 0 0	0 0 0 0	0 0 0 0	0 0 0 0	0 0 0 0	0 0 0 0	0 0 0 0	0 1 0 0	0 0 0 0	0 0 0 0	0 0 0 0
2236742	Δ1 bp	DEL	tob	rne/rluC	0 0 0 0	0 0 0 0	0 0 0 1	0 0 0 0	0 0 0 0	0 0 0 0	0 0 0 0	0 0 0 0	0 0 0 0	0 0 0 0	0 0 0 1	0 0 0 1	0 0 0 0	0 0 0 0
2587299	Δ1 bp	DEL	tob	nuoL	0 0 0 0	0 0 0 0	0 0 0 1	0 0 0 0	0 0 0 0	0 0 0 0	0 0 0 0	0 0 0 0	0 0 0 0	0 0 0 0	0 0 0 1	0 0 0 1	0 0 0 0	0 0 0 0
5150824	(CAACAGGGCCAGCAG)1→2	IN	tob	PA14_57850	0 0 0 0	0 0 0 0	0 0 0 1	0 0 0 0	0 0 0 0	0 0 0 0	0 0 0 0	0 0 0 0	0 0 0 0	0 0 0 0	0 0 0 1	0 0 0 0	0 0 0 0	0 0 0 0
1054708	Δ14 bp	DEL	cip	[PA14_12210]	0 0 0 0	0 0 0 0	0 0 0 0	1 0 0 0	0 0 0 0	0 0 0 0	0 0 0 0	0 0 0 0	0 0 0 0	0 0 0 0	0 0 0 0	0 0 0 0	0 0 0 0	0 0 0 0
1049864	Δ5 bp	DEL	cip	PA14_12140	0 0 0 0	0 0 0 0	0 0 0 0	0 1 0 0	0 0 0 0	0 0 0 0	0 0 0 0	0 0 0 0	0 0 0 0	0 0 0 0	0 0 0 0	0 0 0 0	0 0 0 0	0 0 0 0
1254015	(GCGGC)1→2	IN	cip	PA14_14710	0 0 0 0	0 0 0 0	0 0 0 0	0 0 1 0	0 0 0 0	0 0 0 0	0 0 0 0	0 1 0 0	0 0 0 0	0 0 0 0	0 0 0 0	0 0 0 0	0 0 1 0	0 0 0 0
3434712	Δ17 bp	DEL	cip	PA14_38500	0 0 0 0	0 0 0 0	0 0 0 0	0 0 1 0	0 0 0 0	0 0 0 0	0 0 0 0	0 0 0 0	0 0 0 0	0 0 0 0	0 0 0 0	0 0 0 0	0 0 0 0	0 0 0 0
4259404	Δ1 bp	DEL	cip	PA14_47860	0 0 0 0	0 0 0 0	0 0 0 0	0 0 1 0	0 0 0 0	0 0 0 0	0 0 0 0	0 0 0 0	0 0 0 0	0 0 0 0	0 0 0 0	0 0 0 0	0 0 0 0	0 0 0 0
2233591	Δ14 bp	DEL	cip	rne	0 0 0 0	0 0 0 0	0 0 0 0	0 0 0 1	0 0 0 0	0 0 0 0	0 0 0 0	0 0 0 0	0 0 0 0	0 0 0 0	0 0 0 0	0 0 0 0	0 0 0 0	0 0 0 0
4481546	+G	IN	cip	flgG	0 0 0 0	0 0 0 0	0 0 0 0	0 0 0 1	0 0 0 0	0 0 0 0	0 0 0 0	0 0 0 0	0 0 0 0	0 0 0 0	0 0 0 0	0 0 0 0	0 0 0 0	0 0 0 0
4381158	T→G	SNP	pip	PA14_49300	0 0 0 0	0 0 0 0	0 0 0 0	0 0 0 0	0 0 0 0	0 1 0 0	0 0 0 0	0 0 0 0	0 1 0 0	0 0 0 0	0 0 0 0	0 0 0 0	0 0 0 0	0 0 0 0
2586758	Δ3 bp	DEL	pip,tob,cip	nuoM	0 0 0 0	0 0 0 0	0 0 0 0	0 0 0 0	0 0 0 0	0 0 0 0	0 1 0 0	0 0 0 0	1 0 0 0	0 0 0 0	0 0 0 0	0 1 0 0	0 1 0 0	0 1 0 0
757697	A→G	SNP	tob	fusA1	0 0 0 0	0 0 0 0	0 0 0 0	0 0 0 0	0 0 0 0	0 0 0 0	0 1 0 0	0 0 0 0	0 0 0 0	0 0 0 0	0 0 0 0	0 1 0 0	0 0 0 0	0 0 0 0
4011474	Δ12 bp	DEL	cip	PA14_44990	0 0 0 0	0 0 0 0	0 0 0 0	0 0 0 0	0 0 0 0	0 0 0 0	0 0 0 0	0 0 0 1	0 0 0 0	0 0 0 0	0 0 0 0	0 0 0 0	0 0 1 0	0 0 0 1
4069309	Δ11 bp	DEL	cip	fliP	0 0 0 0	0 0 0 0	0 0 0 0	0 0 0 0	0 0 0 0	0 0 0 0	0 0 0 0	0 0 0 1	0 0 0 0	0 0 0 0	0 0 0 0	0 0 0 0	0 0 1 0	0 0 0 1
6178492	Δ11 bp	DEL	cip	PA14_69250	0 0 0 0	0 0 0 0	0 0 0 0	0 0 0 0	0 0 0 0	0 0 0 0	0 0 0 0	0 0 0 1	0 0 0 0	0 0 0 0	0 0 0 0	0 0 0 0	0 0 1 0	0 0 0 1
757697	A→T	SNP	tob	fusA1	0 0 0 0	0 0 0 0	0 0 0 0	0 0 0 0	0 0 0 0	0 0 0 0	0 0 0 0	0 0 0 0	0 0 0 1	0 0 0 0	0 0 0 0	0 0 0 0	0 0 0 1	0 0 0 0
2040296	(G)10→9	DEL	tob,cip	orfN	0 0 0 0	0 0 0 0	0 0 0 0	0 0 0 0	0 0 0 0	0 0 0 0	0 0 0 0	0 0 0 0	0 0 0 0	0 0 0 1	0 0 0 0	0 1 1 0	0 0 0 0	0 0 1 0
5427671	Δ2 bp	DEL	pip,tob	mexC	0 0 0 0	0 0 0 0	0 0 0 0	0 0 0 0	0 0 0 0	0 0 0 0	0 0 0 0	0 0 0 0	0 0 0 0	0 0 0 0	0 0 0 0	0 0 0 0	0 0 0 1	1 0 0 0

Table A.5: **Description of mutated genes.**

Gene	Locus tag	Functional class	Description
[*aldG*]–[*acsA*]	[PA14_33890]-[PA14_38690]	Large deletions	380 genes
[*ccoP*]-[*ccoP*]	[PA14_44360]-[PA14_44400]	Energy	5 genes
[*flgJ*]–[*flgI*]	[PA14_50380]-[PA14_50410]	Flagella	[*flgJ*], [*flgI*]
[*glgX*]–[*nhaB*]	[PA14_36630]-[PA14_41000]	Large deletions	341 genes
[*nfxB*]	[PA14_60860]	MexCD-OprJ	[*nfxB*]
[PA14_12210]	[PA14_12210]	Membrane	[PA14_12210]
[PA14_37690]–[PA14_39660]	[PA14_37690]–[PA14_39660]	Large deletions	151 genes
aceA	PA14_66290	Metabolism	pyruvate dehydrogenase, E1 component
algC	PA14_70270	Membrane	phosphomannomutase AlgC
ampR	PA14_10800	Beta-lactamases	transcriptional regulator AmpR
amrB	PA14_38410	MexXY-OprM	RND multidrug efflux transporter
aotJ	PA14_52790	Membrane	arginine/ornithine binding protein AotJ
aprX/PA14_48150	PA14_48140/PA14_48150	Hypothetical	conserved hypothetical protein/hypothetical protein
aroB	PA14_66600	Metabolism	3-dehydroquinate synthase
atpC	PA14_73230	Energy	ATP synthase epsilon chain
atpC/atpD	PA14_73230/PA14_73240	Energy	ATP synthase epsilon chain/ATP synthase beta chain
cheB	PA14_45580	Flagella	putative chemotaxis methylesterase
chpA	PA14_05390	Chemotaxis	ChpA
clpA	PA14_30230	Metabolism	ATP-dependent clp protease, ATP-binding subunit ClpA
clpS	PA14_30210	Metabolism	ATP-dependent Clp protease adaptor protein clpS
cpxR	PA14_22760	Two-component sensor	putative transcriptional regulator in 2-component system
cycB/pauR	PA14_69970/PA14_69980	Energy	cytochrome c5/putative transcriptional regulator
dacB	PA14_24690	Beta-lactamases	putative D-alanyl-D-alanine carboxypeptidase
dacC	PA14_12100	Cell wall	D-ala-D-ala-carboxypeptidase
dadA	PA14_70040	Metabolism	D-amino acid dehydrogenase, small subunit
envZ	PA14_68680	Two-component sensor	two-component sensor EnvZ
erfK	PA14_27180	Hypothetical	putative ErfK/YbiS/YcfS/YnhG family protein
fixI	PA14_44440	Membrane	putative cation-transporting P-type ATPase
fleN	PA14_45640	Flagella	flagellar synthesis regulator FleN
flgF	PA14_50440	Flagella	flagellar basal-body rod protein FlgF
flgG	PA14_50430	Flagella	flagellar basal-body rod protein FlgG
flgK	PA14_50360	Flagella	flagellar hook-associated protein 1 FlgK
fliA	PA14_45630	Flagella	motility sigma factor FliA
fliP	PA14_45770	Flagella	flagellar biosynthetic protein FliP
fusA1	PA14_08820	Ribosome	elongation factor G
gcdH	PA14_05840	Metabolism	glutaryl-CoA dehydrogenase
gcvP2	PA14_33000	Metabolism	glycine cleavage system protein P2
gltA	PA14_44070	Metabolism	citrate synthase
gyrA	PA14_23260	DNA/RNA synthesis	DNA gyrase subunit A
gyrB	PA14_00050	DNA/RNA synthesis	DNA gyrase subunit B
intT–PA14_49030	PA14_48880–PA14_49030	Large deletions	16 genes
iscR	PA14_14710	Transcriptional regulation	putative Rrf2 family protein
lhpE	PA14_47860	Metabolism	putative oxidoreductase
mexA	PA14_05530	MexAB-OprM	RND multidrug efflux membrane fusion protein MexA precursor
mexC	PA14_60850	MexCD-OprJ	multidrug efflux RND membrane fusion protein
mexC/nfxB	PA14_60850/PA14_60860	MexCD-OprJ	multidrug efflux RND membrane fusion protein/transcriptional regulatory protein NfxB
mexD	PA14_60830	MexCD-OprJ	multidrug efflux RND transporter MexD
mexF	PA14_32390	MexEF-OprN	RND multidrug efflux transporter MexF
mexR	PA14_05520	MexAB-OprM	multidrug resistance operon repressor MexR
mexR/mexA	PA14_05520/PA14_05530	MexAB-OprM	multidrug resistance operon repressor MexR/RND multidrug efflux membrane fusion protein MexA precursor
mexS	PA14_32420	MexEF-OprN	putative Zn-dependent oxidoreductase
mexT	PA14_32410	MexEF-OprN	transcriptional regulator MexT
miaA	PA14_65320	Ribosome	delta 2-isopentenylpyrophosphate transferase

Gene	Locus tag	Functional class	Description
minC	PA14_22040	Cell division	cell division inhibitor MinC
morA	PA14_60870	Flagella	motility regulator
mpl	PA14_11845	Cell wall	UDP-N-acetylmuramate:L-alanyl-gamma-D-glutamyl- meso-diaminopimelate ligase
mucB	PA14_54410	Transcriptional regulation	negative regulator for alginate biosynthesis MucB
muxA	PA14_31870	MuxABC	putative RND efflux membrane fusion protein precursor
mvfR	PA14_51340	Transcriptional regulation	Transcriptional regulator MvfR
nalC	PA14_16280	MexAB-OprM	putative transcriptional regulator
nalC/PA14_16290	PA14_16280/PA14_16290	MexAB-OprM	putative transcriptional regulator/conserved hypothetical protein
nalD	PA14_18080	MexAB-OprM	putative transcriptional regulator, TetR family
nfxB	PA14_60860	MexCD-OprJ	transcriptional regulatory protein NfxB
np20	PA14_72560	Transcriptional regulation	transcriptional regulator np20
nppA1	PA14_41110	Membrane	putative solute-binding protein
nuoB	PA14_30010	NADH dehydrogenase	NADH dehydrogenase I chain B
nuoG	PA14_29940	NADH dehydrogenase	NADH dehydrogenase I chain G
nuoL	PA14_29880	NADH dehydrogenase	NADH dehydrogenase I chain L
nuoM	PA14_29860	NADH dehydrogenase	NADH dehydrogenase I chain M
orfH	PA14_23380	Flagella	UDP-N-acetyl-D-mannosaminuronate dehydrogenase
orfJ	PA14_23410	Flagella	putative glycosyl transferase
orfN	PA14_23460	Flagella	putative group 4 glycosyl transferase
PA14_09960	PA14_09960	Transcriptional regulation	putative transcriptional regulator
PA14_12140	PA14_12140	Transcriptional regulation	putative transcriptional regulator
PA14_20960	PA14_20960	Metabolism	putative isomerase
PA14_21820	PA14_21820	Metabolism	putative peptidyl-prolyl cis-trans isomerase, FkbP-type
PA14_22730	PA14_22730	Two-component sensor	putative two component sensor histidine kinase protein
PA14_25490	PA14_25490	Membrane	putative tolQ-type transport protein
PA14_27360/*deaD*	PA14_27360/PA14_27370	Metabolism	putative enoyl-CoA hydratase/putative ATP-dependent RNA helicase, DEAD box family
PA14_27940	PA14_27940	Two-component sensor	putative two-component response regulator
PA14_30540/*ssuA*	PA14_30540/PA14_30550	Membrane	putative periplasmic aliphatic sulfonate-binding protein/putative periplasmic aliphatic sulfonate-binding protein
PA14_31100/PA14_31110	PA14_31100/PA14_31110	DNA	putative plasmid partitioning protein/putative replication initiator and transcriptional repressor protein
PA14_34500	PA14_34500	Membrane	putative ATP-binding component of ABC transporter
PA14_35210	PA14_35210	Transcriptional regulation	putative transcriptional regulator, TetR family
PA14_35720–[PA14_40040]	PA14_35720–[PA14_40040]	Large deletions	343 genes
PA14_37170/*ada*	PA14_37170/PA14_37190	Transcriptional regulation	conserved hypothetical protein/O6-methylguanine-DNA methyltransferase
PA14_38500	PA14_38500	Transcriptional regulation	putative transcriptional regulator, IclR family
PA14_39360	PA14_39360	Transcriptional regulation	putative sigma-54 dependent transcriptional regulator
PA14_41710	PA14_41710	Membrane	putative membrane protein
PA14_41730	PA14_41730	Hypothetical	conserved hypothetical protein
PA14_44990	PA14_44990	Hypothetical	conserved hypothetical protein
PA14_48800	PA14_48800	Membrane	putative lipoprotein
PA14_49300	PA14_49300	Metabolism	probable lipoxygenase
PA14_51910	PA14_51910	Hypothetical	hypothetical protein
PA14_57470	PA14_57470	Metabolism	putative methyltransferases
PA14_57540	PA14_57540	Energy	putative cytochrome c1 precursor
PA14_57570	PA14_57570	Energy	putative cytochrome c reductase, iron-sulfur subunit
PA14_57850	PA14_57850	Hypothetical	conserved hypothetical protein
PA14_57880	PA14_57880	Membrane	putative toluene tolerance ABC efflux transporter
PA14_65570	PA14_65570	Hypothetical	conserved hypothetical protein
PA14_66170	PA14_66170	Metabolism	putative carbamoyltransferase
PA14_69250	PA14_69250	Hypothetical	putative membrane-associated protein
parS	PA14_41270	MexEF-OprN	putative two-component sensor
pauR	PA14_69980	Transcriptional regulation	putative transcriptional regulator
pckA	PA14_68580	Energy	phosphoenolpyruvate carboxykinase
pepA	PA14_14470	Metabolism	leucine aminopeptidase

Gene	Locus tag	Functional class	Description
pmrB	PA14_63160	Two-component sensor	two-component sensor
prs	PA14_61770	Metabolism	ribose-phosphate pyrophosphokinase
ptsP	PA14_04410	Quorum sensing	phosphoenolpyruvate-protein phosphotransferase
rne	PA14_25560	DNA/RNA synthesis	ribonuclease E
rne/rluC	PA14_25560/PA14_25580	Ribosome	ribonuclease E/ribosomal large subunit pseudouridine synthase C
rnk	PA14_69630	Transcriptional regulation	nucleoside diphosphate kinase regulator
rplF	PA14_09000	Ribosome	50S ribosomal protein L6
rplJ	PA14_08740	Ribosome	50S ribosomal protein L10
rplL	PA14_08750	Ribosome	50S ribosomal protein L7 / L12
rpoC	PA14_08780	DNA/RNA synthesis	DNA-directed RNA polymerase beta* chain
rpoN	PA14_57940	DNA/RNA synthesis	RNA polymerase sigma-54 factor
rpsL	PA14_08790	Ribosome	30S ribosomal protein S12
sahH	PA14_05620	Metabolism	S-adenosyl-L-homocysteine hydrolase
secA	PA14_57220	Membrane	preprotein translocase, SecA subunit
spoT	PA14_70470	Stringent response	guanosine-3',5'-bis(diphosphate) 3'-pyrophosphohydrolase
sucD	PA14_43940	Energy	succinyl-CoA synthetase alpha chain
topA	PA14_25110	DNA/RNA synthesis	DNA topoisomerase I
tRNA-Thr/*tufB*	PA14_08670/PA14_08680	Ribosome	tRNA-Thr/elongation factor Tu
tRNA-Val	PA14_28190	DNA/RNA synthesis	tRNA-Val
ttg2D	PA14_57840	Hypothetical	putative toluene tolerance protein
wbpM	PA14_23470	Membrane	nucleotide sugar epimerase/dehydratase WbpM
wspA	PA14_16430	Flagella	putative methyl-accepting chemotaxis transducer
ycjJ	PA14_17740	Membrane	putative amino acid/amine transport protein
zipA	PA14_44670	Cell division	cell division protein ZipA

Table A.6: **Genes in large deletions.** This table lists the genes and their relevant information of the large chromosomal deletions of PIP^R-1, PIP^R-2, PIP^R-3, A_{PM}, B_{PM}, C_{PM}, and D_{PM}

Start	End	Strand	Length	Gene	Locus	Protein Product	Product	PIP^R-1	PIP^R-2	PIP^R-3	A_{PM}	B_{PM}	C_{PM}	D_{PM}
3011096	3011566	+	471	*aldG*	PA14_33890	YP_790863.1	putative oxidoreductase							
3011563	3013878	+	2316		PA14_33900	YP_790864.1	putative aldehyde dehydrogenase							
3014295	3015569	-	1275		PA14_33910	YP_790865.1	putative ABC-type transport protein, periplasmic component							
3015701	3016342	-	642		PA14_33920	YP_790866.1	putative transcriptional regulator							
3016619	3017014	+	396		PA14_33930	YP_790867.1	hypothetical protein							
3017037	3017573	-	537		PA14_33940	YP_790868.1	conserved hypothetical protein							
3017584	3019590	-	2007		PA14_33960	YP_790869.1	conserved hypothetical protein							
3019627	3020694	-	1068		PA14_33970	YP_790870.1	hypothetical protein							
3020733	3021266	-	534		PA14_33980	YP_790871.1	hypothetical protein							
3021340	3023889	-	2550		PA14_33990	YP_790872.1	probable ClpA/B-type protease							
3023891	3024907	-	1017		PA14_34000	YP_790873.1	conserved hypothetical protein							
3024871	3026664	-	1794		PA14_34010	YP_790874.1	conserved hypothetical protein							
3026648	3027073	-	426		PA14_34020	YP_790875.1	conserved hypothetical protein							
3027086	3027583	-	498		PA14_34030	YP_790876.1	conserved hypothetical protein							
3027657	3029141	-	1485		PA14_34050	YP_790877.1	conserved hypothetical protein							
3029164	3029709	-	546		PA14_34070	YP_790878.1	conserved hypothetical protein							
3029917	3030393	+	477		PA14_34080	YP_790879.1	hypothetical protein							
3030453	3031784	+	1332		PA14_34100	YP_790880.1	hypothetical protein							
3031802	3032560	+	759		PA14_34110	YP_790881.1	conserved hypothetical protein							
3032557	3036372	+	3816		PA14_34130	YP_790882.1	conserved hypothetical protein							
3036369	3037469	+	1101		PA14_34140	YP_790883.1	conserved hypothetical protein							
3037579	3038664	+	1086	*sfnR*	PA14_34150	YP_790884.1	putative sigma54-dependent transcriptional regulator							
3038777	3039166	+	390		PA14_34170	YP_790885.1	hypothetical protein							
3039326	3039886	+	561	*msuE*	PA14_34180	YP_790886.1	NADH-dependent FMN reductase							
3039896	3041041	+	1146	*msuD*	PA14_34190	YP_790887.1	FMNH2-dependent methanesulfonate sulfonatase							
3041071	3042255	+	1185	*msuC*	PA14_34200	YP_790888.1	putative FMNH2-dependent monooxygenase							
3042252	3043382	+	1131	*sfnR*	PA14_34210	YP_790889.1	putative transcriptional regulator							
3043554	3044708	+	1155		PA14_34230	YP_790890.1	putative ATPase							
3044774	3045901	-	1128		PA14_34250	YP_790891.1	putative glycerophosphoryl diester phosphodiesterase							
3046079	3046732	-	654	*metI-1*	PA14_34260	YP_790892.1	putative permease of ABC transporter							
3046716	3047825	-	1110	*metN-1*	PA14_34270	YP_790893.1	putative ATP-binding component of ABC transporter							
3047822	3048616	-	795	*metQ-1*	PA14_34280	YP_790894.1	putative ABC transporter, periplasmic binding protein							
3048648	3050036	-	1389		PA14_34290	YP_790895.1	putative monooxygenase, DszA family							
3050054	3051271	-	1218		PA14_34300	YP_790896.1	putative monooxygenase, DszC family							
3051282	3052517	-	1236		PA14_34320	YP_790897.1	putative monooxygenase, DszC family							
3052936	3054171	+	1236		PA14_34330	YP_790898.1	putative transmembrane protein							
3054202	3055134	-	933	*mtlZ*	PA14_34340	YP_790899.1	fructokinase							
3055176	3056684	-	1509	*mtlY*	PA14_34350	YP_790900.1	xylulose kinase							
3056681	3058156	-	1476	*mtlD*	PA14_34360	YP_790901.1	mannitol dehydrogenase							
3058179	3059291	-	1113	*mtlk*	PA14_34370	YP_790902.1	putative ATP-binding component of ABC maltose/mannitol transporter							
3059331	3060164	-	834	*mtlG*	PA14_34390	YP_790903.1	putative binding-protein-dependent maltose/mannitol transport protein							
3060175	3061107	-	933	*mtlF*	PA14_34410	YP_790904.1	putative binding-protein-dependent maltose/mannitol transport protein							
3061183	3062493	-	1311	*mtlE*	PA14_34420	YP_790905.1	putative binding protein component of ABC maltose/mannitol transporter							
3062651	3063556	-	906	*mtlR*	PA14_34440	YP_790906.1	transcriptional regulator MtlR							
3063779	3064684	-	906		PA14_34450	YP_790907.1	putative transcriptional regulator, AraC family							
3064789	3065349	+	561		PA14_34460	YP_790908.1	putative alkylhydroperoxidase							
3065399	3066466	+	1068		PA14_34490	YP_790909.1	putative acyl-CoA dehydrogenase							
3066463	3067299	+	837		PA14_34500	YP_790910.1	putative ATP-binding component of ABC transporter							
3067265	3068464	+	1200	*srpL*	PA14_34510	YP_790911.1	putative sulfonate ABC transporter, periplasmic sulfonate-binding protein							
3068461	3069225	+	765	*srpM*	PA14_34520	YP_790912.1	putative sulfonate ABC transporter, permease protein							
3069451	3070860	+	1410		PA14_34540	YP_790913.1	putative xenobiotic compound monooxygenase, DszA family							
3070920	3072155	-	1236		PA14_34550	YP_790914.1	putative flavin reductase dependent enzyme							
3072186	3073445	-	1260		PA14_34580	YP_790915.1	putative flavin reductase dependent enzyme							
3073663	3075288	-	1626	*gapB*	PA14_34600	YP_790916.1	putative glyceraldehyde-3-phosphate dehydrogenase							
3075453	3075596	-	144		PA14_34610	YP_790917.1	hypothetical protein							
3075622	3076974	-	1353	*gnuT*	PA14_34630	YP_790918.1	gluconate permease							
3077071	3077592	-	522	*gntK*	PA14_34640	YP_790919.1	gluconokinase							
3077787	3078818	+	1032	*gntR*	PA14_34660	YP_790920.1	transcriptional regulator GntR							
3079172	3079537	-	366		PA14_34670	YP_790921.1	putative enzyme of the cupin superfamily							
3079570	3080868	-	1299		PA14_34680	YP_790922.1	putative amino acid oxidase							
3080972	3081865	-	894		PA14_34690	YP_790923.1	putative transcriptional regulator, LysR family							
3081983	3083158	+	1176		PA14_34700	YP_790924.1	putative beta lactamase							
3083158	3084411	+	1254		PA14_34710	YP_790925.1	putative major facilitator family transporter							
3084472	3085272	-	801		PA14_34720	YP_790926.1	hypothetical protein							
3085289	3085870	-	582		PA14_34730	YP_790927.1	putative transcriptional regulator, XRE family							
3085925	3086083	-	159		PA14_34740	YP_790928.1	hypothetical protein							
3086373	3087260	+	888	*tauD*	PA14_34750	YP_790929.1	putative taurine catabolism dioxygenase							
3087301	3088323	+	1023		PA14_34770	YP_790930.1	putative ABC transporter, periplasmic binding protein							
3088331	3089179	+	849		PA14_34780	YP_790931.1	putative ABC transporter ATP-binding component							
3089196	3090062	+	867		PA14_34790	YP_790932.1	putative permease of ABC transporter							
3090172	3090789	+	618		PA14_34800	YP_790933.1	putative transporter, LysE family							
3090885	3094634	+	3750	*mxaA*	PA14_34810	YP_790934.1	putative non-ribosomal peptide synthetase							
3094663	3095751	+	1089		PA14_34820	YP_790935.1	putative regulatory protein							
3095748	3096767	+	1020		PA14_34830	YP_790936.1	putative regulatory protein							
3096787	3103164	+	6378		PA14_34840	YP_790937.1	putative non-ribosomal peptide synthetase							
3103232	3103774	+	543		PA14_34850	YP_790938.1	putative tRNA synthase							
3103993	3105444	+	1452	*chiC*	PA14_34870	YP_790939.1	chitinase							
3105621	3106370	+	750		PA14_34880	YP_790940.1	putative transcriptional regulator, GntR family							
3106367	3108091	+	1725		PA14_34900	YP_790941.1	pucconate dehydrogenase							
3108177	3108422	+	246		PA14_34920	YP_790942.1	putative ferredoxin							
3108760	3109725	+	966		PA14_34930	YP_790943.1	putative phycobiliprotein							
3109722	3110003	+	282		PA14_34940	YP_790944.1	conserved hypothetical protein							
3110344	3111702	+	1359	*opbA*	PA14_34960	YP_790945.1	probable glucose-sensitive porin							
3111856	3114267	+	2412	*gcd*	PA14_34970	YP_790946.1	glucose dehydrogenase							
3114399	3116519	+	2121		PA14_34990	YP_790947.1	putative TonB-dependent receptor							
3116640	3116927	+	288		PA14_35000	YP_790948.1	conserved hypothetical protein							
3116940	3117575	-	636		PA14_35010	YP_790949.1	hypothetical protein							
3117562	3119106	-	1545		PA14_35020	YP_790950.1	hypothetical protein							
3119107	3119769	-	663		PA14_35030	YP_790951.1	hypothetical protein							
3119766	3120437	-	672		PA14_35040	YP_790952.1	hypothetical protein							
3120434	3121891	-	1458		PA14_35050	YP_790953.1	putative protease							
3121898	3122326	-	429		PA14_35060	YP_790954.1	conserved hypothetical protein							
3122614	3123468	+	855		PA14_35070	YP_790955.1	putative transcriptional regulator, AraC family							
3123481	3124173	-	693	*arsH*	PA14_35080	YP_790956.1	putative arsenical resistance protein							
3124185	3124655	-	471	*arsC*	PA14_35100	YP_790957.1	arsenate reductase							
3124687	3125970	-	1284	*arsB*	PA14_35110	YP_790958.1	arsenical pump membrane protein							
3125984	3126334	-	351	*arsR*	PA14_35130	YP_790959.1	arsenic resistance transcriptional regulator							
3126413	3127303	-	891		PA14_35140	YP_790960.1	putative transcriptional regulator, AraC family							
3127512	3128573	+	1062		PA14_35150	YP_790961.1	putative Zn-dependent alcohol dehydrogenase							
3128598	3128975	-	378		PA14_35160	YP_790962.1	hypothetical protein							
3129053	3129523	+	471	*soxR*	PA14_35170	YP_790963.1	putative redox-sensing activator of soxS							
3129531	3131228	-	1698	*pbpC*	PA14_35190	YP_790964.1	penicillin-binding protein 3A							
3131350	3131865	-	516		PA14_35200	YP_790965.1	putative acetyltransferase							
3131873	3132463	-	591		PA14_35210	YP_790966.1	putative transcriptional regulator, TetR family							
3132610	3133815	+	1206		PA14_35230	YP_790967.1	putative efflux protein							
3133779	3134849	-	1071		PA14_35240	YP_790968.1	conserved hypothetical protein							
3134936	3135832	+	897		PA14_35250	YP_790969.1	putative transcriptional regulator, LysR family							
3135932	3137251	-	1320		PA14_35270	YP_790970.1	putative cytochrome c precursor							
3137263	3139038	-	1776	*gnd*	PA14_35290	YP_790971.1	gluconate dehydrogenase							
3139041	3139757	-	717		PA14_35300	YP_790972.1	conserved hypothetical protein							
3139925	3140911	-	987	*kguD*	PA14_35320	YP_790973.1	2-ketogluconate 6-phosphate reductase							
3140930	3142237	-	1308	*kguT*	PA14_35330	YP_790974.1	putative 2-ketogluconate transporter							
3142300	3143250	-	951	*kguK*	PA14_35340	YP_790975.1	putative 2-ketogluconate kinase							
3143243	3144025	-	783	*kguE*	PA14_35360	YP_790976.1	putative putative epimerase							
3144097	3145119	-	1023	*ptxS*	PA14_35370	YP_790977.1	transcriptional regulator PtxS							
3145681	3146619	+	939	*ptxR*	PA14_35380	YP_790978.1	transcriptional regulator PtxR							
3146722	3147369	-	648	*pvcD*	PA14_35390	YP_790979.1	pyoverdine biosynthesis protein PvcD							
3147362	3148864	-	1503	*pvcC*	PA14_35400	YP_790980.1	pyoverdine biosynthesis protein PvcC							
3148916	3149791	-	876	*pvcB*	PA14_35420	YP_790981.1	pyoverdine biosynthesis protein PvcB							
3149809	3150795	-	987	*pvcA*	PA14_35430	YP_790982.1	pyoverdine biosynthesis protein PvcA							
3151011	3151997	-	987	*ansA*	PA14_35440	YP_790983.1	L-asparaginase I							
3152097	3153542	-	1446		PA14_35460	YP_790984.1	putative sodium/alanine symporter							
3153711	3154529	+	819		PA14_35470	YP_790985.1	hypothetical protein							
3154662	3156056	-	1395	*lpdV*	PA14_35490	YP_790986.1	lipoamide dehydrogenase-Val							
3156060	3157346	-	1287	*bkdB*	PA14_35500	YP_790987.1	lipoamide acyltransferase component of branched-chain alpha-keto acid dehydrogenase complex E2							
3157347	3158399	-	1053	*bkdA2*	PA14_35520	YP_790988.1	2-oxoisovalerate dehydrogenase, beta subunit'							
3158396	3159628	-	1233	*bkdA1*	PA14_35530	YP_790989.1	2-oxoisovalerate dehydrogenase (alpha subunit)							
3159938	3160399	+	462	*bkdR*	PA14_35540	YP_790990.1	transcriptional regulator BkdR							
3160432	3160737	-	306	*pslO*	PA14_35550	YP_790991.1	hypothetical protein							
3160765	3161766	-	1002	*pslN*	PA14_35570	YP_790992.1	putative DNA topoisomerase							
3161822	3163555	-	1734	*pslM*	PA14_35590	YP_790993.1	possible succinate dehydrogenase, flavoprotein subunit							
3163743	3164810	-	1068	*pslL*	PA14_35600	YP_790994.1	possible acetyltransferase							
3164893	3166302	-	1410	*pslK*	PA14_35620	YP_790995.1	hypothetical protein							
3166304	3167740	-	1437	*pslJ*	PA14_35630	YP_790996.1	conserved hypothetical protein							

Start	End	Strand	Length	Gene	Locus	Protein Product	Product
3167743	3168846	-	1104	*pslI*	PA14_35640	YP_790997.1	putative glycosyltransferase
3168837	3170045	-	1209	*pslH*	PA14_35650	YP_790998.1	possible glycosyltransferase
3170054	3171382	-	1329	*pslG*	PA14_35670	YP_790999.1	putative glycosyl hydrolase
3171372	3172559	-	1188	*pslF*	PA14_35680	YP_791000.1	possible glycosyl transferase
3172559	3174547	-	1989	*pslE*	PA14_35690	YP_791001.1	hypothetical protein
3174603	3175307	+	705		PA14_35700	YP_791002.1	hypothetical protein
3175803	3176147	-	345		PA14_35710	YP_791003.1	hypothetical protein
3176214	3176615	-	402		PA14_35720	YP_791004.1	hypothetical protein
3176984	3177358	-	375		PA14_35730	YP_791005.1	hypothetical protein
3177507	3180521	+	3015	*tpnA*	PA14_35740	YP_791006.1	putative transposase
3180518	3180880	+	363	*tpnC*	PA14_35750	YP_791007.1	putative tpnA repressor protein
3181060	3181524	-	465		PA14_35760	YP_791008.1	hypothetical protein
3181532	3182437	-	906		PA14_35770	YP_791009.1	hypothetical protein
3182434	3183162	-	729		PA14_35780	YP_791010.1	hypothetical protein
3183178	3184587	-	1410		PA14_35790	YP_791011.1	Putative homospermidine synthase
3184999	3186315	-	1317		PA14_35800	YP_791012.1	conserved hypothetical protein
3186337	3187047	-	711		PA14_35810	YP_791013.1	conserved hypothetical protein
3187110	3188081	-	972	*tnpS*	PA14_35820	YP_791014.1	Cointegrate resolution protein S
3188265	3189263	+	999	*tnpT*	PA14_35830	YP_791015.1	Cointegrate resolution protein T
3189302	3189946	+	645		PA14_35840	YP_791016.1	conserved hypothetical protein
3189927	3190406	+	480		PA14_35850	YP_791017.1	conserved hypothetical protein
3190988	3192292	+	1305		PA14_35860	YP_791018.1	Probable amino acid permease
3192356	3193795	+	1440		PA14_35880	YP_791019.2	Probable aldehyde dehydrogenase
3193841	3195094	+	1254		PA14_35890	YP_791020.1	Putative aminotransferase
3195183	3196103	+	921		PA14_35900	YP_791021.1	Putative dehydrogenase
3196396	3198054	-	1659		PA14_35920	YP_791022.1	Predicted symporter
3198051	3198149	-	99		PA14_35930	YP_791023.1	hypothetical protein
3198432	3200078	-	1647		PA14_35940	YP_791024.1	Putative Acyl-CoA synthetase
3200165	3200932	-	768		PA14_35950	YP_791025.1	Putative Dehydrogenase
3200932	3202104	-	1173		PA14_35970	YP_791026.1	Probable Acyl-CoA dehydrogenase
3202155	3202511	-	357		PA14_35980	YP_791027.1	putative acyl-CoA dehydrogenase
3202508	3203704	-	1197		PA14_35990	YP_791028.1	FadE36, possible aminoglycoside phosphotransferase
3204291	3205712	+	1422	*prpR*	PA14_36000	YP_791029.1	Probable propionate catabolism operon regulator
3205778	3206281	-	504		PA14_36010	YP_791030.1	hypothetical protein
3206340	3208643	-	2304		PA14_36020	YP_791031.1	paraquat-inducible protein B
3208636	3209256	-	621		PA14_36030	YP_791032.1	paraquat-inducible protein A
3209914	3211497	-	1584		PA14_36050	YP_791033.1	Probable NAD-dependent aldehyde dehydrogenase
3211626	3212621	-	996		PA14_36060	YP_791034.1	conserved hypothetical protein
3212649	3213824	-	1176		PA14_36070	YP_791035.1	putative enzyme
3213855	3215177	-	1323	*yfoV*	PA14_36080	YP_791036.1	putative MFS transporter
3215363	3216613	-	1251	*opdG*	PA14_36090	YP_791037.1	putative porin
3216786	3217799	-	1014		PA14_36100	YP_791038.1	putative pyridoxal phosphate biosynthesis protein
3217796	3218755	-	960		PA14_36110	YP_791039.1	putative hydrolase
3218748	3220073	-	1326		PA14_36120	YP_791040.1	putative MFS transporter
3220256	3221353	+	1098		PA14_36130	YP_791041.1	conserved hypothetical protein
3221381	3221911	+	531		PA14_36150	YP_791042.1	conserved hypothetical protein
3221908	3223428	+	1521		PA14_36170	YP_791043.1	putative integral membrane protein
3223496	3224443	+	948		PA14_36180	YP_791044.1	putative transcriptional regulator, LysR family
3224525	3225001	+	477		PA14_36190	YP_791045.1	hypothetical protein
3225300	3226106	+	807		PA14_36200	YP_791046.1	putative binding protein component of ABC transporter
3226187	3226903	+	717	*gltJ*	PA14_36220	YP_791047.1	putative amino acid permease
3226905	3227582	+	678	*glnP*	PA14_36230	YP_791048.1	putative amino acid transport system permease
3227598	3228482	-	885		PA14_36250	YP_791049.1	hypothetical protein
3228608	3230203	-	1596		PA14_36260	YP_791050.1	putative signal transduction protein
3230292	3231167	-	876		PA14_36270	YP_791051.1	putative 3-hydroxyisobutyrate dehydrogenase
3231173	3231517	-	345		PA14_36280	YP_791052.1	putative antibiotic biosynthesis monooxygenase
3231514	3232551	-	1038	*ymcB*	PA14_36290	YP_791053.1	putative NADP-dependent oxidoreductase
3232682	3233266	-	585		PA14_36300	YP_791054.1	putative transcriptional regulator, TetR family
3233419	3234672	-	1254	*hcnC*	PA14_36310	YP_791055.1	hydrogen cyanide synthase HcnC
3234675	3236069	-	1395	*hcnB*	PA14_36320	YP_791056.1	hydrogen cyanide synthase HcnB
3236066	3236380	-	315	*hcnA*	PA14_36330	YP_791057.1	hydrogen cyanide synthase HcnA
3236744	3237988	+	1245	*exoY*	PA14_36345	YP_791058.1	adenylate cyclase ExoY
3237985	3238539	-	555		PA14_36350	YP_791059.1	conserved hypothetical protein
3238696	3239118	-	423		PA14_36360	YP_791060.1	putative small intergral membrane protein
3239146	3240360	-	1215		PA14_36370	YP_791061.1	putative ligase
3240498	3241922	+	1425		PA14_36375	YP_791062.1	hypothetical protein
3241906	3242856	+	951		PA14_36390	YP_791063.1	putative methylase
3242840	3243160	-	321		PA14_36400	YP_791064.1	hypothetical protein
3243223	3243831	+	609		PA14_36410	YP_791065.1	conserved hypothetical protein
3243835	3245934	-	2100		PA14_36420	YP_791066.1	putative histidine kinase
3246017	3246607	+	591		PA14_36450	YP_791067.1	conserved hypothetical protein
3246620	3246967	+	348		PA14_36460	YP_791068.1	hypothetical protein
3247252	3247560	+	309		PA14_36470	YP_791069.1	hypothetical protein
3247591	3247812	-	222		PA14_36480	YP_791070.1	hypothetical protein
3247868	3248218	-	351		PA14_36490	YP_791071.1	hypothetical protein
3248245	3249321	-	1077		PA14_36500	YP_791072.1	putative cellulase
3249325	3249795	-	471		PA14_36520	YP_791073.1	conserved hypothetical protein
3249997	3250449	-	453		PA14_36530	YP_791074.1	conserved hypothetical protein
3250575	3251351	-	777		PA14_36540	YP_791075.1	putative hydrolase
3251348	3252445	-	1098		PA14_36550	YP_791076.1	conserved hypothetical protein
3252774	3253139	-	366		PA14_36560	YP_791077.1	hypothetical protein
3253507	3255048	+	1542	*glgA*	PA14_36570	YP_791078.1	glycogen synthase
3255048	3256799	+	1752	*glgB*	PA14_36580	YP_791079.1	putative glycosyl hydrolase
3256792	3258846	+	2055	*malQ*	PA14_36590	YP_791080.1	putative 4-alpha-glucanotransferase
3258839	3261619	+	2781		PA14_36605	YP_791081.1	probable glycosyl hydrolase
3261616	3261921	+	306		PA14_36620	YP_791082.1	conserved hypothetical protein
3261934	3264084	+	2151	*glgX*	PA14_36630	YP_791083.1	putative glycosyl hydrolase
3264184	3264600	+	417		PA14_36650	YP_791084.1	conserved hypothetical protein
3264667	3265914	+	1248		PA14_36660	YP_791085.1	putative Zn-dependent alcohol dehydrogenase
3265918	3266856	+	939		PA14_36670	YP_791086.1	conserved hypothetical protein
3266853	3267590	+	738		PA14_36680	YP_791087.1	putative metal-dependent hydrolase
3267587	3268792	+	1206	*ybhO*	PA14_36690	YP_791088.1	putative phospholipase
3268789	3269784	+	996		PA14_36700	YP_791089.1	putative membrane protein
3269786	3271984	-	2199	*glgB*	PA14_36710	YP_791090.1	1,4-alpha-glucan branching enzyme
3271981	3275283	-	3303		PA14_36730	YP_791091.1	putative trehalose synthase
3275294	3277288	-	1995		PA14_36740	YP_791092.1	putative alpha-amylase family protein
3277432	3278313	-	882		PA14_36760	YP_791093.1	putative KU domain protein
3278336	3278578	-	243		PA14_36770	YP_791094.1	hypothetical protein
3278592	3279083	-	492		PA14_36780	YP_791095.1	putative Mg(2+) transporter
3279080	3279214	-	135		PA14_36790	YP_791096.1	hypothetical protein
3279311	3281440	-	2130	*katE*	PA14_36810	YP_791097.1	catalase HPII
3281521	3281688	-	168		PA14_36820	YP_791098.1	conserved hypothetical protein
3282187	3282585	+	399		PA14_36830	YP_791099.1	hypothetical protein
3282592	3285030	-	2439	*glgP*	PA14_36840	YP_791100.1	glycogen phosphorylase
3285083	3285370	-	288		PA14_36850	YP_791101.1	hypothetical protein
3285614	3285802	+	189		PA14_36860	YP_791102.1	hypothetical protein
3285822	3286682	-	861		PA14_36870	YP_791103.1	putative short-chain dehydrogenase
3286708	3287226	-	519		PA14_36880	YP_791104.1	putative ompetence-damaged protein
3287237	3287476	-	240		PA14_36890	YP_791105.1	putative metallothionein
3287496	3287711	-	216		PA14_36900	YP_791106.1	conserved hypothetical protein
3287787	3290309	-	2523		PA14_36910	YP_791107.1	putative ATP-dependent DNA ligase
3290327	3290863	-	537		PA14_36920	YP_791108.1	putative histidine kinase
3290965	3291489	+	525		PA14_36930	YP_791109.1	hypothetical protein
3291515	3291964	+	450		PA14_36940	YP_791110.1	putative membrane protein
3291942	3293306	-	1365		PA14_36960	YP_791111.1	putative Na+/H+ antiporter
3293335	3293907	-	573		PA14_36980	YP_791112.1	putative outer membrane protein
3294000	3294857	-	858		PA14_36990	YP_791113.1	putative EAL domain protein
3294854	3295567	-	714	*cupA5*	PA14_37000	YP_791114.1	chaperone CupA5
3295557	3296918	-	1362	*cupA4*	PA14_37010	YP_791115.1	fimbrial subunit CupA4
3296915	3299533	-	2619	*cupA3*	PA14_37030	YP_791116.1	usher
3299517	3300263	-	747	*cupA2*	PA14_37040	YP_791117.1	chaperone CupA2
3300351	3300902	-	552	*cupA1*	PA14_37060	YP_791118.1	fimbrial subunit CupA1
3301756	3302982	+	1227		PA14_37070	YP_791119.1	putative phosphoadenosine phosphosulfate sulfotransferase
3303409	3304044	+	636		PA14_37080	YP_791120.1	putative transcriptional regulator
3304080	3305528	-	1449	*gbsA*	PA14_37090	YP_791121.1	putative aldehyde dehydrogenase
3305550	3307187	-	1638		PA14_37100	YP_791122.1	putative dehydrogenase
3307292	3308224	-	933		PA14_37120	YP_791123.1	putative transcriptional regulator, LysR family
3308261	3309397	-	1137		PA14_37130	YP_791124.1	hypothetical protein
3309523	3310428	+	906		PA14_37140	YP_791125.1	putative transcriptional regulator, LysR family
3310576	3311004	+	429		PA14_37150	YP_791126.1	conserved hypothetical protein
3311021	3312133	+	1113		PA14_37170	YP_791127.1	conserved hypothetical protein
3312668	3313744	-	1077	*ada*	PA14_37190	YP_791128.1	O6-methylguanine-DNA methyltransferase
3313936	3314919	+	984		PA14_37200	YP_791129.1	conserved hypothetical protein
3314904	3315701	-	798		PA14_37210	YP_791130.1	conserved hypothetical protein
3315808	3316761	-	954		PA14_37220	YP_791131.1	putative LysR-family transcriptional regulator

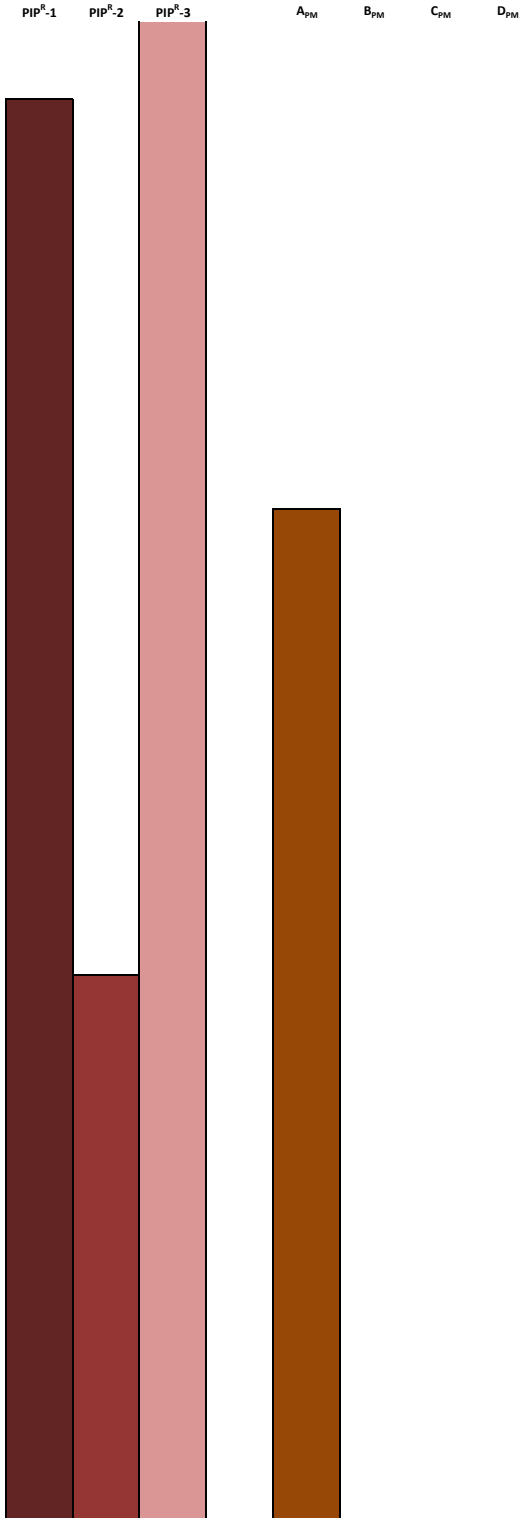

Start	End	Strand	Length	Gene	Locus	Protein Product	Product
3317016	3318287	+	1272		PA14_37250	YP_791132.1	putative major facilitator family transporter
3318312	3319541	+	1230	*opdO*	PA14_37260	YP_791133.1	putative outer membrane porin
3319574	3320317	+	744		PA14_37270	YP_791134.1	putative lactam utilization protein
3320314	3321027	+	714		PA14_37290	YP_791135.1	putative allophanate hydrolase subunit 1
3321024	3321965	+	942		PA14_37310	YP_791136.1	putative allophanate hydrolase subunit 2
3322033	3322509	+	477		PA14_37320	YP_791137.1	putative outer membrane protein
3322528	3324300	-	1773		PA14_37340	YP_791138.1	glyoxylate carboligase
3324471	3324869	+	399		PA14_37350	YP_791139.1	conserved hypothetical protein
3325268	3326026	-	759		PA14_37360	YP_791140.1	putative short-chain dehydrogenase
3326011	3326940	-	930		PA14_37370	YP_791141.1	putative esterase
3326951	3328426	-	1476		PA14_37380	YP_791142.1	putative flavin-binding monooxygenase
3328573	3329607	+	1035		PA14_37400	YP_791143.1	putative transcriptional regulator, AraC family
3329756	3330601	+	846		PA14_37410	YP_791144.1	hypothetical protein
3330603	3331559	-	957		PA14_37420	YP_791145.1	putative transmembrane sensor protein
3331556	3332065	-	510		PA14_37430	YP_791146.1	putative sigma-70 factor, ECF subfamily
3332168	3333364	-	1197		PA14_37440	YP_791147.1	putative MFS transporter
3333351	3334634	-	1284		PA14_37460	YP_791148.1	putative permease
3334631	3335710	-	1080		PA14_37470	YP_791149.1	putative flavin-dependent oxidoreductase
3335723	3338374	-	2652		PA14_37490	YP_791150.1	putative TonB-dependent receptor
3338466	3339314	-	849		PA14_37510	YP_791151.1	conserved hypothetical protein
3339298	3339954	-	657		PA14_37520	YP_791152.1	hypothetical protein
3339951	3340853	-	903		PA14_37530	YP_791153.1	putative hydrolase
3340864	3341373	-	510		PA14_37550	YP_791154.1	putative ring-hydroxylating dioxygenase small subunit
3341401	3343233	-	1833	*asnB*	PA14_37560	YP_791155.1	asparagine synthetase, glutamine-hydrolysing
3343321	3344595	-	1275		PA14_37570	YP_791156.1	ring-hydroxylating dioxygenase, large terminal subunit
3344797	3345273	-	477	*lrp*	PA14_37580	YP_791157.1	putative leucine-responsive regulatory protein
3345406	3346047	+	642	*kynB*	PA14_37590	YP_791158.1	kynurenine formamidase, KynB
3346051	3347301	+	1251		PA14_37610	YP_791159.1	putative kynureninase
3347457	3348863	+	1407		PA14_37630	YP_791160.1	putative amino acid permease
3349149	3351023	+	1875		PA14_37640	YP_791161.1	conserved hypothetical protein
3351063	3352967	+	1905		PA14_37650	YP_791162.1	conserved hypothetical protein
3353004	3353906	-	903		PA14_37660	YP_791163.1	LysR-type transcriptional regulator
3354363	3354629	+	267		PA14_37670	YP_791164.1	hypothetical protein
3354806	3356473	+	1668		PA14_37680	YP_791165.1	conserved hypothetical protein
3356866	3359460	-	2595		PA14_37690	YP_791166.1	putative sensory box protein
3359632	3361740	-	2109	*fusA2*	PA14_37710	YP_791167.1	translation elongation factor G
3362016	3364658	+	2643		PA14_37730	YP_791168.1	putative TonB dependent receptor
3364838	3366562	+	1725		PA14_37745	YP_791169.1	probable carbamoyl transferase
3366606	3367769	+	1164		PA14_37760	YP_791170.1	putative MFS transporter
3367771	3368439	+	669		PA14_37770	YP_791171.1	putative hydrolase
3368436	3369074	+	639		PA14_37780	YP_791172.1	conserved hypothetical protein
3369223	3371043	+	1821	*pcoA*	PA14_37790	YP_791173.1	copper resistance protein A precursor
3371040	3372095	+	1056	*pcoB*	PA14_37810	YP_791174.1	copper resistance protein B precursor
3372115	3373338	-	1224		PA14_37820	YP_791175.1	conserved hypothetical protein
3373541	3374722	-	1182	*iscS*	PA14_37830	YP_791176.1	putative pyridoxal-phosphate dependent enzyme
3374868	3376478	-	1611		PA14_37840	YP_791177.1	putative ATP-binding component of ABC transporter
3376480	3377496	-	1017	*yejE*	PA14_37850	YP_791178.1	putative permease of ABC transporter
3377498	3378571	-	1074		PA14_37870	YP_791179.1	putative peptide ABC transporter, permease protein
3378573	3380381	-	1809		PA14_37880	YP_791180.1	putative binding protein component of ABC transporter
3380385	3382925	-	2541		PA14_37900	YP_791181.1	putative TonB-dependent receptor
3383604	3384506	-	903		PA14_37910	YP_791182.1	putative transcriptional regulator, LysR family
3384617	3386032	+	1416		PA14_37915	YP_791183.1	probable major facilitator superfamily (MFS) transporter
3386039	3386926	-	888	*cynR*	PA14_37940	YP_791184.1	cyn operon transcriptional activator
3387041	3387703	+	663	*cynT*	PA14_37950	YP_791185.1	carbonate dehydratase
3387743	3388213	+	471	*cynS*	PA14_37965	YP_791186.1	cyanate lyase
3388251	3389204	-	954		PA14_37980	YP_791187.1	putative Fe2+-dicitrate sensor, membrane component
3389201	3389707	-	507		PA14_37990	YP_791188.1	putative sigma-70 factor, ECF subfamily
3390035	3390499	+	465		PA14_38000	YP_791189.1	conserved hypothetical protein
3390598	3392031	+	1434		PA14_38010	YP_791190.1	conserved hypothetical protein
3392089	3392496	-	408		PA14_38020	YP_791191.1	putative nitibiotic biosynthesis monooxygenase
3392910	3393899	+	990		PA14_38040	YP_791192.1	putative transcriptional regulator, AraC family
3394935	3395342	+	408		PA14_38050	YP_791193.1	conserved hypothetical protein
3395401	3395661	-	261		PA14_38060	YP_791194.1	conserved hypothetical protein
3395836	3397710	+	1875		PA14_38080	YP_791195.1	putative cysteine proteases
3397868	3398770	-	903		PA14_38090	YP_791196.1	putative pseudouridylate synthase
3398891	3400120	-	1230	*ygjU*	PA14_38110	YP_791197.1	putative transporter, sodium-dicarboxylate symporte
3400608	3401978	-	1371	*ycjJ*	PA14_38130	YP_791198.1	putative lysine-specific permease
3402135	3403511	-	1377		PA14_38140	YP_791199.1	putative glutamine synthetase
3404017	3404775	+	759	*azlC*	PA14_38160	YP_791200.1	putative branched-chain amino acid transport protein AzlC
3404760	3405074	+	315		PA14_38170	YP_791201.1	putative membrane protein
3405199	3406659	-	1461		PA14_38180	YP_791202.1	hypothetical protein
3406799	3407320	-	522		PA14_38190	YP_791203.1	hypothetical protein
3408055	3409713	+	1659	*ilvG*	PA14_38200	YP_791204.1	putative phosphonopyruvate decarboxylase
3409721	3410395	-	675		PA14_38210	YP_791205.1	putative methylase
3410395	3411303	-	909		PA14_38220	YP_791206.1	putative siderophore-interacting protein
3411438	3412862	-	1425	*yjiR*	PA14_38250	YP_791207.1	putative transcriptional regulator, GntR
3413042	3413296	+	255		PA14_38260	YP_791208.1	hypothetical protein
3413293	3413550	+	258		PA14_38270	YP_791209.1	hypothetical protein
3413625	3413924	-	300		PA14_38290	YP_791210.1	conserved hypothetical protein
3413948	3414421	-	474	*grp*	PA14_38300	YP_791211.1	putative glutamate uptake regulatory protein
3414554	3414946	+	393		PA14_38310	YP_791212.1	conserved hypothetical protein
3415099	3416100	+	1002	*yfeH*	PA14_38320	YP_791213.1	putative transporter, bile acid/Na+ symporter family
3416155	3417510	-	1356	*gor*	PA14_38330	YP_791214.1	glutathione reductase
3417655	3418077	+	423		PA14_38340	YP_791215.1	putative ring-cleaving dioxygenase
3418259	3419098	-	840	*galU*	PA14_38350	YP_791216.1	UTP-glucose-1-phosphate uridylyltransferase
3419146	3420507	-	1362	*ugd*	PA14_38360	YP_791217.1	putative UDP-glucose 6-dehydrogenas
3420659	3420883	+	225		PA14_38370	YP_791218.1	conserved hypothetical protein
3420889	3421521	-	633	*amrR*	PA14_38380	YP_791219.1	putative transcriptional regulator
3421686	3422876	+	1191		PA14_38395	YP_791220.1	Resistance-Nodulation-Cell Division (RND) multidrug efflux membrane fusion protein precursor
3422892	3426029	+	3138	*amrB*	PA14_38410	YP_791221.1	RND multidrug efflux transporter
3426271	3427200	-	930		PA14_38420	YP_791222.1	conserved hypothetical protein
3427393	3427797	+	405	*gnyR*	PA14_38430	YP_791223.1	Regulatory gene of gnyRDBHAL cluster, GnyR
3427846	3429009	+	1164	*gnyD*	PA14_38440	YP_791224.1	Citronellolyl-CoA dehydrogenase, GnyD
3429132	3430739	+	1608	*gnyB*	PA14_38460	YP_791225.1	acyl-CoA carboxyltransferase beta chain
3430753	3431550	+	798	*gnyH*	PA14_38470	YP_791226.1	putative enoyl-CoA hydratase
3431547	3433514	+	1968	*gnyA*	PA14_38480	YP_791227.1	alpha subunit of geranoyl-CoA carboxylase, GnyA
3433535	3434437	+	903	*gnyL*	PA14_38490	YP_791228.1	3-hydroxy-gamma-carboxygeranoyl-CoA lyase, GnyL
3434505	3435308	-	804		PA14_38500	YP_791229.1	putative transcriptional regulator, IclR family
3435469	3436767	+	1299	*hmgA*	PA14_38510	YP_791230.1	homogentisate 1,2-dioxygenase
3436772	3438070	+	1299	*fahA*	PA14_38530	YP_791231.1	fumarylacetoacetase
3438067	3438705	+	639	*maiA*	PA14_38550	YP_791232.1	maleylacetoacetate isomerase
3438790	3440142	+	1353	*pcaK*	PA14_38560	YP_791233.1	putative MFS transporter
3440271	3441641	+	1371		PA14_38570	YP_791234.1	putative sigma-54 dependent transcriptional regulator
3441918	3443309	+	1392		PA14_38580	YP_791235.1	putative H+/gluconate symporter
3443343	3444113	+	771	*bdhA*	PA14_38590	YP_791236.1	3-hydroxybutyrate dehydrogenase
3444304	3445728	-	1425		PA14_38610	YP_791237.1	putative short-chain fatty acid transporter
3445941	3447122	-	1182	*atoB*	PA14_38630	YP_791238.1	acetyl-CoA acetyltransferase
3447272	3447928	-	657	*scoB*	PA14_38640	YP_791239.1	putative CoA transferase, subunit B
3447963	3448661	-	699	*scoA*	PA14_38660	YP_791240.1	putative CoA transferase, subunit A
3448793	3449713	+	921		PA14_38680	YP_791241.1	putative transcriptional regulator, LysR family
3449781	3451736	+	1956	*acsA*	PA14_38690	YP_791242.1	putative AMP-(fatty) acid ligase
3451794	3452072	+	279	*ppiC1*	PA14_38700	YP_791243.1	peptidyl-prolyl cis-trans isomerase C1
3452091	3452447	+	357		PA14_38710	YP_791244.1	conserved hypothetical protein
3452444	3453007	+	564		PA14_38720	YP_791245.1	conserved hypothetical protein
3453132	3454340	+	1209	*yhhS*	PA14_38730	YP_791246.1	putative MFS transporter
3454285	3456069	-	1785		PA14_38740	YP_791247.1	putative sensory box histidine kinase/response regulator
3456053	3457216	-	1164		PA14_38750	YP_791248.1	putative iron-containing alcohol dehydrogenase
3457302	3459128	-	1827		PA14_38770	YP_791249.1	putative dipeptidyl aminopeptidase
3459133	3460278	-	1146	*pqqE*	PA14_38780	YP_791250.1	pyrroloquinoline quinone biosynthesis protein E
3460250	3460528	-	279	*pqqD*	PA14_38790	YP_791251.1	pyrroloquinoline quinone biosynthesis protein D
3460525	3461277	-	753	*pqqC*	PA14_38800	YP_791252.1	pyrroloquinoline quinone biosynthesis protein C
3461287	3462201	-	915	*pqqB*	PA14_38820	YP_791253.1	pyrroloquinoline quinone biosynthesis protein B
3462254	3462325	-	72	*pqqA*	PA14_38825	YP_791254.1	pyrroloquinoline quinone biosynthesis protein A
3462683	3464203	-	1521	*exoC*	PA14_38840	YP_791255.1	NAD+ dependent acetaldehyde dehydrogenase
3464290	3464727	-	438	*exoB*	PA14_38850	YP_791256.1	cytochrome c550 precursor
3465040	3466911	+	1872	*exoA*	PA14_38860	YP_791257.1	PQQ-linked alcohol dehydrogenase
3466965	3467612	+	648		PA14_38880	YP_791258.1	conserved hypothetical protein
3467639	3468316	-	678	*exoE*	PA14_38900	YP_791259.1	putative wo-component response regulator
3468329	3468979	-	651	*exoD*	PA14_38910	YP_791260.1	putative sensor kinase
3468988	3469164	-	177		PA14_38920	YP_791261.1	hypothetical protein
3469644	3470309	+	666	*glpR*	PA14_38930	YP_791262.1	putative glycerol regulatory protein
3470319	3471182	+	864		PA14_38950	YP_791263.1	putative transmembrane protein
3471184	3473829	-	2646		PA14_38970	YP_791264.1	putative sensor histidine kinase protein
3473759	3474922	-	1164		PA14_38990	YP_791265.1	conserved hypothetical protein
3475025	3476224	-	1200		PA14_39000	YP_791266.1	conserved hypothetical protein

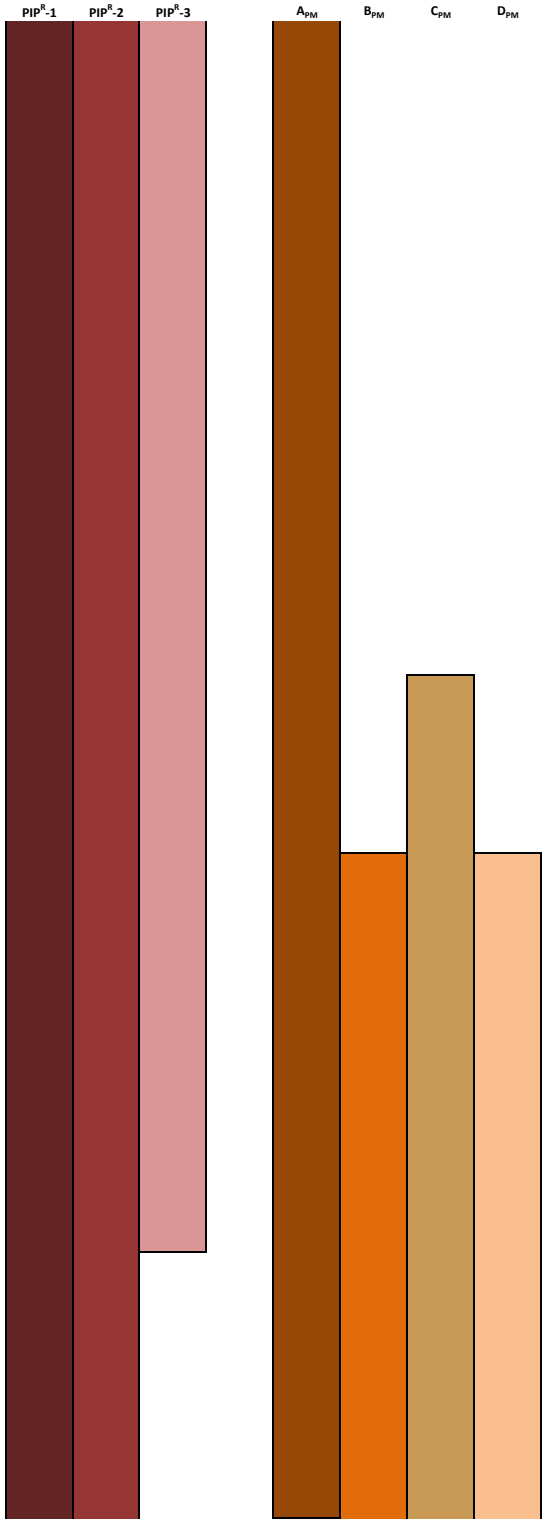

Start	End	Strand	Length	Gene	Locus	Protein Product	Product
3476491	3478818	-	2328	*pqqF*	PA14_39010	YP_791267.1	pyrroloquinoline quinone biosynthesis protein F
3478895	3480598	-	1704		PA14_39020	YP_791268.1	putative membrane protein
3481126	3482439	+	1314	*braZ*	PA14_39050	YP_791269.1	branched-chain amino acid transport carrier
3482675	3482914	+	240		PA14_39060	YP_791270.1	putative lipoprotein
3482981	3483373	-	393		PA14_39070	YP_791271.1	conserved hypothetical protein
3483420	3483653	-	234		PA14_39080	YP_791272.1	hypothetical protein
3483838	3484338	+	501		PA14_39090	YP_791273.1	hypothetical protein
3484359	3484730	-	372		PA14_39100	YP_791274.1	putative 5-carboxymethyl-2-hydroxymuconate isomerase
3485025	3485360	-	336		PA14_39110	YP_791275.1	hypothetical protein
3485688	3487253	+	1566	*ybiT*	PA14_39130	YP_791276.1	putative ATP-binding component of ABC transporter
3487340	3487606	-	267		PA14_39140	YP_791277.1	hypothetical protein
3487713	3488321	-	609	*acpD*	PA14_39150	YP_791278.1	putative acyl carrier protein phosphodiesterase
3488469	3489404	+	936		PA14_39160	YP_791279.1	transcriptional regulator, LysR family
3489415	3489849	-	435		PA14_39180	YP_791280.1	putative membrane protein
3490204	3491037	-	834	*bacA*	PA14_39190	YP_791281.1	bacitracin resistance protein
3491319	3491894	+	576		PA14_39200	YP_791282.1	putative nicotinamide mononucleotide transporter
3491891	3492418	+	528	*nadR*	PA14_39210	YP_791283.1	putative ATPase/kinase
3492721	3493212	+	492		PA14_39220	YP_791284.1	conserved hypothetical protein
3493209	3493778	+	570		PA14_39230	YP_791285.1	conserved hypothetical protein
3493835	3494857	+	1023		PA14_39240	YP_791286.1	conserved hypothetical protein
3494919	3495599	+	681		PA14_39250	YP_791287.1	putative double-glycine peptidase
3495613	3496365	+	753		PA14_39260	YP_791288.1	conserved hypothetical protein
3496426	3497691	+	1266		PA14_39270	YP_791289.1	conserved hypothetical protein
3497825	3498751	-	927	*rbsK*	PA14_39280	YP_791290.1	ribokinase
3498805	3499818	-	1014	*rbsR*	PA14_39300	YP_791291.1	ribose operon repressor RbsR
3499822	3500820	-	999	*rbsC*	PA14_39320	YP_791292.1	ribose ABC transporter, permease protein
3500844	3502376	-	1533	*rbsA*	PA14_39330	YP_791293.1	ribose ABC transporter, ATP-binding protein
3502398	3503357	-	960	*rbsB*	PA14_39350	YP_791294.1	binding protein component precursor of ABC ribose transporter
3503576	3504904	-	1329		PA14_39360	YP_791295.1	putative sigma-54 dependent transcriptional regulator
3505040	3506527	-	1488		PA14_39390	YP_791296.1	ribosomal protein S6 modification enzyme
3506718	3507815	+	1098		PA14_39410	YP_791297.1	putative acetyltransferase
3507877	3508107	+	231		PA14_39420	YP_791298.1	hypothetical protein
3508418	3510313	+	1896		PA14_39440	YP_791299.1	hypothetical protein
3510492	3511631	+	1140		PA14_39460	YP_791300.1	conserved hypothetical protein
3512076	3512852	+	777		PA14_39470	YP_791301.1	hypothetical protein
3513093	3515246	+	2154		PA14_39480	YP_791302.1	conserved hypothetical protein
3516130	3516510	-	381		PA14_39500	YP_791303.1	conserved hypothetical protein
3517005	3519209	-	2205		PA14_39520	YP_791304.1	putative hydroxylase large subunit
3519206	3520195	-	990		PA14_39530	YP_791305.1	putative hydroxylase molybdopterin-containing subunit
3520192	3520704	-	513		PA14_39540	YP_791306.1	putative ferredoxin
3520874	3522169	-	1296		PA14_39560	YP_791307.1	putative chemotaxis transducer
3522478	3522774	+	297		PA14_39570	YP_791308.1	hypothetical protein
3522821	3523390	+	570	*rimJ*	PA14_39580	YP_791309.1	ribosomal protein alanine acetyltransferase
3523452	3525752	-	2301	*metE*	PA14_39590	YP_791310.1	5-methyltetrahydropteroyltriglutamate- homocysteine S-methyltransferase
3525885	3527735	-	1851		PA14_39610	YP_791311.1	conserved hypothetical protein
3528236	3528562	-	327		PA14_39620	YP_791312.1	conserved hypothetical protein
3528562	3529038	-	477		PA14_39630	YP_791313.1	conserved hypothetical protein
3529035	3532880	-	3846		PA14_39640	YP_791314.1	putative CobN/Magnesium chelatase
3532880	3534841	-	1962	*cirA*	PA14_39650	YP_791315.1	putative TonB-dependent receptor
3535009	3535818	+	810		PA14_39660	YP_791316.1	conserved hypothetical protein
3535826	3535948	-	123		PA14_39670	YP_791317.1	hypothetical protein
3535976	3538003	+	2028	*nrdD*	PA14_39690	YP_791318.1	putative ribonucleotide reductase
3538047	3538193	+	147		PA14_39700	YP_791319.1	conserved hypothetical protein
3538190	3538888	+	699	*nrdG*	PA14_39710	YP_791320.1	putative radical-activating enzyme
3539082	3540482	+	1401		PA14_39720	YP_791321.1	putative amino acid oxidase
3540495	3540842	+	348		PA14_39730	YP_791322.1	conserved hypothetical protein
3540887	3542119	+	1233		PA14_39750	YP_791323.1	putative amino acid permease
3542183	3543730	+	1548		PA14_39770	YP_791324.1	putative regulatory protein
3544298	3545524	+	1227	*hvn*	PA14_39780	YP_791325.1	putative haloviprin
3545631	3546311	+	681		PA14_39790	YP_791326.1	conserved hypothetical protein
3546403	3546909	+	507		PA14_39800	YP_791327.1	probable sigma-70 factor, ECF subfamily
3546906	3547856	+	951		PA14_39810	YP_791328.1	putative transmembrane sensor
3548064	3550478	+	2415	*ufrA*	PA14_39820	YP_791329.1	putative TonB-dependent receptor protein
3550519	3551670	+	1152		PA14_39830	YP_791330.1	putative membrane protein
3551857	3553068	+	1212		PA14_39850	YP_791331.1	putative MFS transporter
3553065	3554705	+	1641		PA14_39860	YP_791332.1	putative dienelactone hydrolase
3554748	3555284	+	537	*opaH*	PA14_39870	YP_791333.1	putative hydrolase
3555459	3556106	-	648	*phzG2*	PA14_39880	YP_791334.1	probable pyridoxamine 5'-phosphate oxidase
3556129	3556965	-	837	*phzF2*	PA14_39890	YP_791335.1	probable phenazine biosynthesis protein
3556979	3558862	-	1884	*phzE2*	PA14_39910	YP_791336.1	phenazine biosynthesis protein PhzE
3558859	3559482	-	624	*phzD2*	PA14_39925	YP_791337.1	phenazine biosynthesis protein PhzD
3559479	3560696	-	1218	*phzC2*	PA14_39945	YP_791338.1	phenazine biosynthesis protein PhzC
3560720	3561208	-	489	*phzB2*	PA14_39960	YP_791339.1	probable phenazine biosynthesis protein
3561244	3561732	-	489	*phzA2*	PA14_39970	YP_791340.1	probable phenazine biosynthesis protein
3562214	3562927	-	714	*qscR*	PA14_39980	YP_791341.1	probable transcriptional regulator
3563689	3564456	+	768		PA14_39990	YP_791342.1	putative desaturase
3564462	3565631	+	1170		PA14_40010	YP_791343.1	hypothetical protein
3565650	3566924	+	1275		PA14_40020	YP_791344.1	hypothetical protein
3566872	3567564	+	693		PA14_40030	YP_791345.1	putative enzyme
3567590	3570019	+	2430		PA14_40040	YP_791346.1	putative penicillin acylase
3570016	3570753	+	738		PA14_40050	YP_791347.1	hypothetical protein
3570750	3571139	+	390		PA14_40060	YP_791348.1	conserved hypothetical protein
3571228	3571851	+	624		PA14_40070	YP_791349.1	putative glutathione S-transferase
3571865	3572848	-	984		PA14_40080	YP_791350.1	hypothetical protein
3573078	3574487	+	1410		PA14_40100	YP_791351.1	conserved hypothetical protein
3574471	3575139	+	669		PA14_40110	YP_791352.1	hypothetical protein
3575143	3577506	-	2364	*polB*	PA14_40120	YP_791353.1	DNA polymerase II
3577575	3578108	-	534		PA14_40130	YP_791354.1	putative acetyltransferase
3578194	3578745	+	552		PA14_40150	YP_791355.1	putative transcriptional regulator
3578742	3579140	-	399	*nuoA*	PA14_40160	YP_791356.1	putative NADH-ubiquinone/plastoquinone oxidoreductase
3579153	3579476	-	324	*sugE*	PA14_40170	YP_791357.1	putative transporter
3579807	3580268	+	462		PA14_40180	YP_791358.1	putative oxidoreductase subunit
3580273	3582468	+	2196		PA14_40200	YP_791359.1	putative exported oxidoreductase
3582626	3583180	+	555		PA14_40210	YP_791360.1	putative transcriptional regulator
3583268	3583846	+	579		PA14_40220	YP_791361.1	putative hydrolase
3583955	3585142	-	1188		PA14_40230	YP_791362.1	putative secretion protein
3585132	3587303	-	2172		PA14_40240	YP_791363.1	putative ATP-binding/permease fusion ABC transporter
3587293	3588570	-	1278	*opmL*	PA14_40250	YP_791364.1	putative outer membrane protein precursor
3588570	3595940	-	7371		PA14_40260	YP_791365.1	conserved hypothetical protein
3597214	3598236	+	1023		PA14_40270	YP_791366.1	putative cation transporter
3598297	3599088	+	792		PA14_40280	YP_791367.1	conserved hypothetical protein
3599215	3600471	-	1257	*lasA*	PA14_40290	YP_791368.1	staphylolytic protease preproenzyme LasA
3600755	3601180	-	426		PA14_40300	YP_791369.1	conserved hypothetical protein
3601464	3601703	-	240		PA14_40310	YP_791370.1	putative acyl carrier protein
3601871	3604201	-	2331	*xqhA*	PA14_40320	YP_791371.1	secretion protein XqhA
3604188	3604715	-	528		PA14_40330	YP_791372.1	conserved hypothetical protein
3604857	3605066	-	210		PA14_40340	YP_791373.1	hypothetical protein
3605156	3607432	-	2277		PA14_40350	YP_791374.1	putative DNA helicase
3607425	3609101	-	1677		PA14_40370	YP_791375.1	conserved hypothetical protein
3609235	3609885	+	651		PA14_40380	YP_791376.1	putative transcriptional regulator, TetR family
3610001	3610756	+	756	*modA*	PA14_40390	YP_791377.1	molybdate-binding periplasmic protein precursor modA
3610769	3611455	+	687	*modB*	PA14_40410	YP_791378.1	molybdenum transport protein ModB
3611457	3612542	+	1086	*modC*	PA14_40420	YP_791379.1	molybdenum transport protein ModC
3612564	3613391	-	828		PA14_40430	YP_791380.1	putative O-Methyltransferase
3613477	3614364	+	888		PA14_40440	YP_791381.1	putative transcriptional regulator, LysR family
3614373	3615194	+	822	*str*	PA14_40450	YP_791382.1	streptomycin 3"-phosphotransferase
3615195	3616649	-	1455		PA14_40470	YP_791383.1	putative potassium uptake protein, TrkH family
3616827	3617750	+	924	*yedI*	PA14_40490	YP_791384.1	putative membrane protein
3618097	3619539	+	1443	*ccoN-2*	PA14_40510	YP_791385.1	putative cytochrome c oxidase, cbb3-type, subunit
3619542	3619763	+	222		PA14_40520	YP_791386.1	hypothetical protein
3619855	3621012	+	1158		PA14_40540	YP_791387.1	putative CBS-domain-containing membrane protein
3621000	3621863	-	864		PA14_40550	YP_791388.1	putative transcriptional regulator, LysR family
3622148	3622423	+	276		PA14_40560	YP_791389.1	conserved hypothetical protein
3622472	3623677	-	1206		PA14_40570	YP_791390.1	putative two-component response regulator
3623926	3624930	+	1005		PA14_40600	YP_791391.1	putative transcriptional regulator
3624953	3625195	+	243		PA14_40610	YP_791392.1	conserved hypothetical protein
3625200	3626369	+	1170		PA14_40620	YP_791393.1	putative MFS transporter
3626428	3627012	-	585	*yhgI*	PA14_40630	YP_791394.1	conserved hypothetical protein
3627135	3629423	-	2289	*cti*	PA14_40640	YP_791395.1	fatty acyl cis-trans isomerase
3629785	3630303	+	519		PA14_40650	YP_791396.1	hypothetical protein
3630345	3630809	+	465		PA14_40660	YP_791397.1	conserved hypothetical protein
3631084	3634788	+	3705	*metH*	PA14_40670	YP_791398.1	methionine synthase
3634803	3635165	+	363		PA14_40690	YP_791399.1	conserved hypothetical protein
3635217	3635714	-	498		PA14_40700	YP_791400.1	conserved hypothetical protein
3635728	3636090	-	363		PA14_40710	YP_791401.1	conserved hypothetical protein

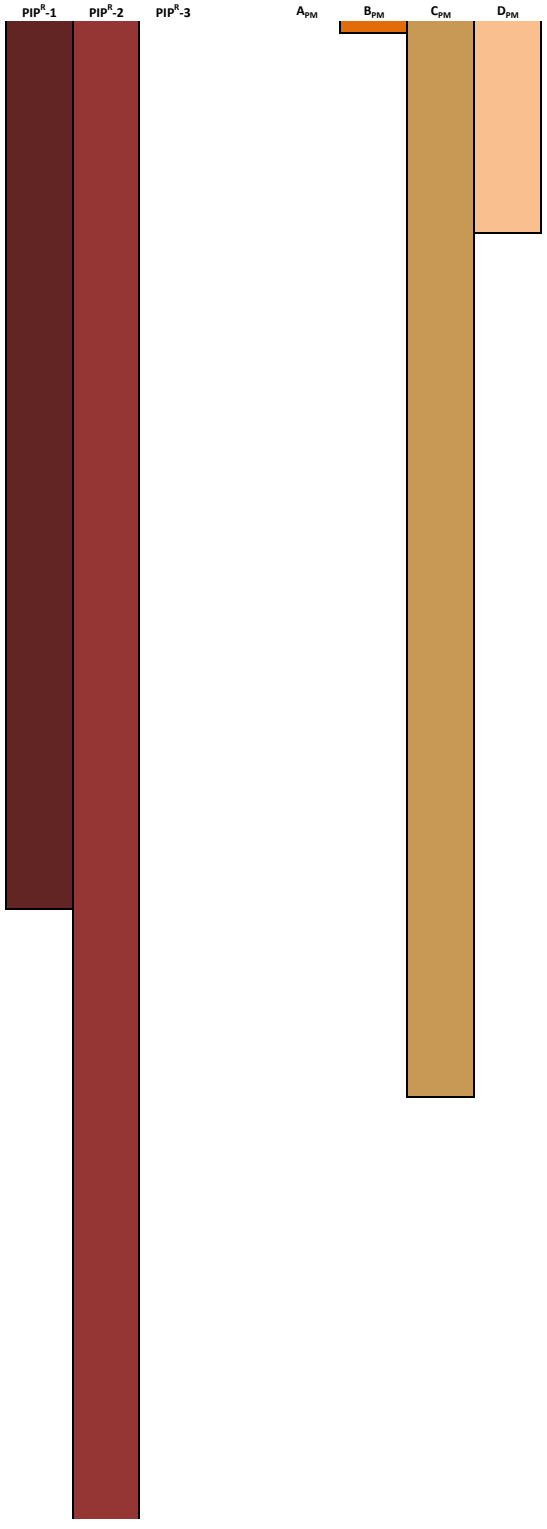

Start	End	Strand	Length	Gene	Locus	Protein Product	Product
3636128	3637168	+	1041		PA14_40730	YP_791402.1	putative Fe-S-cluster redox enzyme
3637233	3637460	+	228		PA14_40740	YP_791403.1	conserved hypothetical protein
3637485	3637640	-	156		PA14_40750	YP_791404.1	hypothetical protein
3637871	3639529	+	1659	*cysI*	PA14_40770	YP_791405.1	sulfite reductase
3639513	3640010	+	498		PA14_40780	YP_791406.1	conserved hypothetical protein
3640075	3640656	-	582		PA14_40790	YP_791407.1	putative transcriptional regulator
3640779	3641216	+	438		PA14_40800	YP_791408.1	conserved hypothetical protein
3641311	3642186	+	876		PA14_40820	YP_791409.1	putative hydrolase
3642173	3643165	-	993	*yhfP*	PA14_40830	YP_791410.1	putative alcohol dehydrogenase, zinc-containing
3643224	3644249	-	1026	*sohB*	PA14_40840	YP_791411.1	putative protease
3644484	3645194	+	711	*gpmA*	PA14_40850	YP_791412.1	putative phosphoglycerate mutase
3645255	3645569	+	315		PA14_40860	YP_791413.1	putative sterol carrier protein
3645827	3646897	+	1071		PA14_40880	YP_791414.1	putative aminoglycoside phosphotransferase
3646922	3647689	+	768		PA14_40890	YP_791415.1	putative short-chain dehydrogenase
3647850	3648611	-	762		PA14_40900	YP_791416.1	putative short-chain dehydrogenase
3648743	3649648	+	906		PA14_40910	YP_791417.1	putative LysR family transcriptional regulatory protein
3649645	3650289	-	645		PA14_40930	YP_791418.1	conserved hypothetical protein
3650390	3651169	+	780		PA14_40940	YP_791419.1	putative membrain protein
3651137	3651973	-	837	*nudC*	PA14_40950	YP_791420.1	putative NADH pyrophosphatase
3651973	3653661	-	1689	*fimL*	PA14_40960	YP_791421.1	pilin biosynthetic protein
3653701	3654513	-	813		PA14_40980	YP_791422.1	putative Enoyl-CoA hydratase
3654737	3656239	+	1503	*nhaB*	PA14_41000	YP_791423.1	sodium/proton antiporter NhaB